BioMed Research International

Redox Signaling in Degenerative Diseases: From Molecular Mechanisms to Health Implications

Guest Editors: Cristina Angeloni, Tullia Maraldi, and David Vauzour

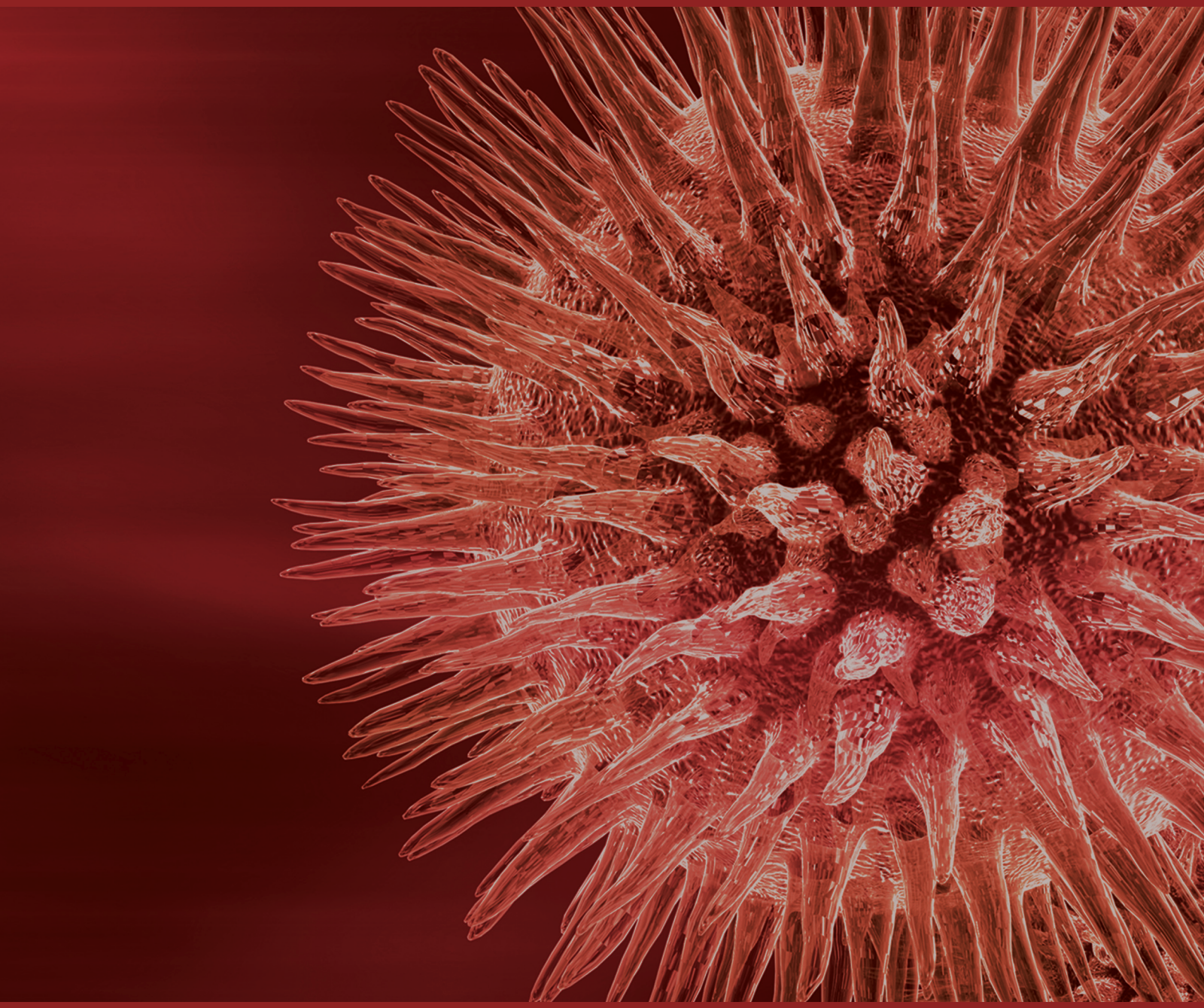

Redox Signaling in Degenerative Diseases: From Molecular Mechanisms to Health Implications

BioMed Research International

Redox Signaling in Degenerative Diseases: From Molecular Mechanisms to Health Implications

Guest Editors: Cristina Angeloni, Tullia Maraldi, and David Vauzour

Contents

Hindawi Publishing Corporation
BioMed Research International
Volume 2014, Article ID 245761, 2 pages
http://dx.doi.org/10.1155/2014/245761

Editorial

Redox Signaling in Degenerative Diseases: From Molecular Mechanisms to Health Implications

Cristina Angeloni,[1] Tullia Maraldi,[2] and David Vauzour[3]

[1] *Department for Life Quality Studies, Alma Mater Studiorum University of Bologna, 47921 Rimini, Italy*
[2] *Department of Surgical, Medical, Dental and Morphological Sciences with Interest in Transplant, Oncology and Regenerative Medicine, University of Modena and Reggio Emilia, 41124 Modena, Italy*
[3] *Norwich Medical School, Faculty of Medicine and Health Sciences, University of East Anglia, Norwich NR4 7TJ, UK*

Correspondence should be addressed to Cristina Angeloni; cristina.angeloni@unibo.it

Received 9 April 2014; Accepted 9 April 2014; Published 25 June 2014

Maintenance of normal intracellular redox status plays an important role in regulating many physiological processes. The cellular oxidation and reduction environment is influenced by the production and removal of reactive oxygen species (ROS). Unbalanced levels of ROS are a common characteristic of many acute and chronic degenerative diseases such as cancer, cardiovascular diseases, type II diabetes, acute liver and renal failure, and neurodegenerative disorders including Parkinson's and Alzheimer's diseases and strokes. On the other hand, in the last years it has been shown that not only are ROS detrimental to cells but at physiological level they regulate a myriad of cellular processes including transcription regulation and cell signaling. Several reports support the hypothesis that cellular ROS levels could function as "second messengers." The second messenger properties of ROS are believed to activate signaling pathways by regulating kinases, phosphatases, transcription factors, or ion channels to coordinate the final response of the cell. Understanding the crosstalk between signaling, ROS, and cell homeostasis is fundamental for understanding redox biology and disease pathogenesis.

This special issue provides a selection of original articles as well as reviews focused on the role of redox signaling in different cell systems and pathological conditions.

A role for intracellular ROS production has been recently implicated in the pathogenesis and progression of a wide variety of neoplasias. ROS sources, such as NAD(P)H oxidase (Nox) complexes, are frequently activated in acute myeloid leukemia blasts and strongly contribute to proliferation, survival, and drug resistance of these cells. M. Guida et al. investigated the role of nuclear Nox-derived ROS in myelodysplastic syndromes (MDS). They reported, in human MDS samples, that Nox4 isoform is localized into the nucleus. Moreover, they demonstrated Nox4 presence in speckle domains proposing that Nox4 could be involved in regulating DNA-mRNA processing machinery by ROS production in specific nuclear area and that Nox4 interacts with Akt and ERK signaling, suggesting a role of nuclear signaling disregulation in MDS progression.

J. K. Kwee explored the paradoxical double effect of antioxidants in solid cancer cells. Antioxidants may hamper the efficacy of chemotherapy by scavenging reactive oxygen species and, on the other hand, alleviate unwanted chemotherapy-induced toxicity, thus allowing for increased chemotherapy doses. From this point of view, the modulation of intracellular antioxidant concentration is a double-edged sword, with both sides exploited for potential therapeutic benefits.

Caveolae/lipid rafts are membrane-rich cholesterol domains endowed with several functions in signal transduction and caveolin-1 (Cav-1) has been reported to be implicated in regulating multiple cancer-associated processes, ranging from tumor growth to multidrug resistance and angiogenesis. As vascular endothelial growth factor receptor-2 (VEGFR-2) and Cav-1 frequently colocalize, C. Caliceti et al. investigated the presence of VEGFR-2 in caveolae/lipid

rafts in a leukemia cell line. Results demonstrated that caveolae/lipid rafts act as platforms for negative modulation of VEGF redox signal transduction cascades leading to glucose uptake and cell proliferation, suggesting therefore novel potential antileukemia targets.

Persistent inflammatory and oxidative stresses are hallmarks of most chronic degenerative diseases such as cardiovascular diseases and CNS pathologies (Alzheimer's, ALS). T. B Kuhn observed that both TNFα and Il-1β impaired morphology and motility of growth cones in spinal cord neuron cultures. Interestingly, inhibiting NADPH oxidase activity rescued loss of neuronal motility and morphology, suggesting that NADPH oxidase serves as a pivotal source of oxidative stress in neurons and, together with a disruption of actin filament reorganization, contributes to the progressive degeneration of neuronal morphology in the diseased or aging CNS.

Mild cognitive impairment (MCI) is regarded as a prodromal phase of late onset Alzheimer's disease (LOAD). It has been proposed that oxidative stress might be implicated in the pathogenesis of LOAD. C. Cervellati et al. investigated whether a redox imbalance, measured as serum level of hydroperoxides and/or serum antioxidant capacity, might be predictive of the clinical progression of MCI to LOAD. Their results suggested that oxidative stress might be precociously involved in LOAD pathogenesis but the two markers are not able to predict the progression from MCI to LOAD.

The review of C. Angeloni et al. focused on the new emerging role of advanced glycation end products (AGEs), induced by high glucose levels or methylglyoxal (MG), in the pathogenesis of Alzheimer's disease (AD). AGEs extensively cross-link proteins in Aβ deposits and neurofilaments exacerbating AD pathological hallmarks. Moreover, AGEs and MG are neurotoxic mediators of oxidative stress in the progression of AD and are capable of activating many redox signaling pathways such as ERK1/2, JNK, and p38 MAPK leading to apoptosis and cellular dysfunction.

Peroxisomes provide glial cells with protective functions against the harmful effects of H_2O_2 on neurons and peroxisome impairment results in nervous lesions. The study of L. D. C. Mannelli et al. highlighted that the PPAR-γ block in astrocytes is strictly related to reduced catalase functionality and expression with a general decrease in antioxidant defenses of the cell. The relevance of the damage induced by PPAR-γ impairment suggests that hypofunctionality of this receptor in glial cells could be present in neurodegenerative diseases and participate in pathological mechanisms through peroxisomal damage.

The review of C. Caliceti et al. describes how ROS regulate Notch and Wnt pathways in the cardiovascular system. Scientific evidences show a sequential and direct link between Notch and Wnt signaling pathways in tuning endothelial cells (ECs), cardiomyocytes functions, and vascular morphogenesis. Understanding the molecular mechanism regulated by ROS could lead to the development of new therapeutic approaches for cardiovascular diseases.

The so-called "glucose spikes," mainly occurring after meals, confer a high cardiovascular risk attributed to acute increases of oxidative stress. The study of I. Russo et al. mimicked "the glucose spikes" in vitro incubating vascular smooth muscle cells (VSMC) with high glucose and demonstrating that high glucose, via oxidative stress, can reduce the cardiovascular protection conferred by the NO/cGMP pathway via phosphorylation of the cytoskeleton protein VASP in VSMC.

The cross-sectional population-based study of C. Cervellati et al. was conducted to investigate the role of oxidative stress in the derangement of bone homeostasis, a hallmark of postmenopausal osteoporosis (PO). They showed an association between increased hydroperoxides serum levels and reduced bone density in postmenopausal women, suggesting that oxidative stress might play a role in the development of PO by enhancing bone resorption rate.

Redox imbalance of luminal pyridine nucleotides in the endoplasmic reticulum (ER) together with oxidative stress results in the activation of autophagy. O. Kapuy and G. Bánhegyi demonstrated that the depletion of ER NADPH in HepG2 cell line, either by the pharmacological agent metyrapone or by silencing the key proteins of luminal NADPH generation, switched on an autophagic mechanism with the incomplete inactivation of the mTOR pathway.

Fibrogenesis is widely considered as the result of a dysregulated wound healing response. In particular, failure of the wave of myofibroblast apoptosis during wound healing combined with an autocrine feed-forward loop of TGF-β production leads to the development and persistence of large numbers of myofibroblasts, a hallmark of fibrotic disorders. The review of N. Sampson et al. summarizes recent in vitro and in vivo data demonstrating that TGF-β-induced myofibroblast differentiation is driven by a prooxidant shift in redox homeostasis.

Collectively, the papers of this special issue provide a better understanding of the role of redox signaling in the pathophysiology of different degenerative diseases and we hope that these contributions could encourage further studies in this important field.

Cristina Angeloni
Tullia Maraldi
David Vauzour

Hindawi Publishing Corporation
BioMed Research International
Volume 2014, Article ID 191767, 20 pages
http://dx.doi.org/10.1155/2014/191767

Research Article

Oxygen Radicals Elicit Paralysis and Collapse of Spinal Cord Neuron Growth Cones upon Exposure to Proinflammatory Cytokines

Thomas B. Kuhn

Department of Chemistry and Biochemistry, University of Alaska Fairbanks, 900 Yukon Drive, Reichardt Building, Room 194, Fairbanks, AK 99775-6150, USA

Correspondence should be addressed to Thomas B. Kuhn; tbkuhn@alaska.edu

Received 16 October 2013; Revised 25 February 2014; Accepted 11 March 2014; Published 23 June 2014

Academic Editor: Tullia Maraldi

A persistent inflammatory and oxidative stress is a hallmark of most chronic CNS pathologies (Alzheimer's (ALS)) as well as the aging CNS orchestrated by the proinflammatory cytokines tumor necrosis factor alpha (TNFα) and interleukin-1 beta (IL-1β). Loss of the integrity and plasticity of neuronal morphology and connectivity comprises an early step in neuronal degeneration and ultimate decline of cognitive function. We examined *in vitro* whether TNFα or IL-1β impaired morphology and motility of growth cones in spinal cord neuron cultures. TNFα and IL-1β paralyzed growth cone motility and induced growth cone collapse in a dose-dependent manner reflected by complete attenuation of neurite outgrowth. Scavenging reactive oxygen species (ROS) or inhibiting NADPH oxidase activity rescued loss of neuronal motility and morphology. TNFα and IL-1β provoked rapid, NOX-mediated generation of ROS in advancing growth cones, which preceded paralysis of motility and collapse of morphology. Increases in ROS intermediates were accompanied by an aberrant, nonproductive reorganization of actin filaments. These findings suggest that NADPH oxidase serves as a pivotal source of oxidative stress in neurons and together with disruption of actin filament reorganization contributes to the progressive degeneration of neuronal morphology in the diseased or aging CNS.

1. Introduction

A spreading inflammatory reaction accompanied by oxidative stress is prevalent in most chronic CNS diseases and acute CNS trauma as well as in the aging CNS [1–3]. The proinflammatory cytokines TNFα (tumor necrosis factor α) and IL-1β (interleukin-1β) exert pleiotropic functions both in CNS development and CNS pathogenesis [4–6]. Persistent high-level expression of TNFα and IL-1β is important to the progressive degeneration of neuronal connectivity and loss of neuronal plasticity ultimately leading to cognitive decline. The role of TNFα and IL-1β as inducers of apoptotic events is well documented, whereas the recognition of their morphogenetic function is more recent [7]. TNFα and IL-1β released from microglia cells inhibited neurite outgrowth, reduced branching, and caused neurite retraction in cultures of Neuro2A cells or primary hippocampal neurons [8, 9]. The intricate pattern of neuronal connectivity innate to cognitive function rests as much on the integrity and stability of the axonal and dendritic architecture as on the plasticity of motile structures to maintain, form, or regenerate connections, which is intimately linked to the dynamic reorganization of the actin cytoskeleton [10, 11]. ROS intermediates greatly affect both the dynamics and organization of actin filaments during oxidative stress of physiological redox signaling [12, 13]. TNFα paralyzed actin filament reorganization in neuroblastoma cells due to oxidative damage, whereas physiological levels of ROS intermediates seem to be necessary for proper growth cone motility [14, 15]. TNFα and IL-1β potently stimulate NADPH oxidase (NOX) activities in neurons and glia cells often localized in coalescing lipid rafts [16, 17]. The members of the NADPH oxidase (NOX) family (NOX1–5, DUOX1/2), defined by the large membrane flavoprotein gp91^{phox} of the phagocyte NAPDH oxidase (NOX2), are ubiquitously expressed in all cell types and have emerged as principal ROS sources both in cellular signaling and disease

progression in response to cytokines, growth factors, and hormones [18, 19]. Functional NOX requires an intricate assembly between two membrane proteins (a NOX isoform, $gp22^{phox}$) and several cytosolic factors ($p47^{phox}$, $p40^{phox}$, $p67^{phox}$) under the regulation of the small GTPases Rac1 or Rac2 [20]. Rho GTPases harbor a dual role in cytokine signaling as regulators of both NOX assembly and the reorganization of actin filament structures [21–23]. In light of these reports, we examined whether ROS intermediates generated by NOX activities in neuronal growth cones are implicated in mediating the neurotoxic effects of TNFα or IL-1β on neurite outgrowth. A mechanistic understanding of the detrimental consequences of TNFα and IL-1β on neuronal connectivity in the CNS neurons is vital to intervene with progressive neurodegeneration in the aging or diseased CNS.

2. Materials and Methods

2.1. Reagents. Unless state otherwise, all reagents were purchased from Sigma (St. Louis, MO). Dulbecco's Modified Eagle Medium (high glucose DMEM), Leibovitz's L-15, and isopropyl β-D-thiogalactopyranoside were obtained from Invitrogen Corporation (Carlsbad, CA). Characterized fetal bovine serum (FBS) was from Hyclone (Logan, UT) and it was heat-inactivated according to the manufacturer. Laminin was from Roche Diagnostics Corporation (Indianapolis, IN). The redox sensitive fluorescent indicators carboxymethyl-2′,7′-dihydrodichlorofluorescein diacetate, 2′,7′-dihydrodichlorofluorescein diacetate, and Calcein Blue were obtained from Molecular Probes (Eugene, OR). Human recombinant tumor necrosis factor α (TNFα) and interleukin-1β (IL-1β), Diphenylene iodonium (DPI), N-acetyl-L-cysteine (NAC), and Manganese(III) tetrakis(4-benzoic acid) porphyrin chloride (MnTBAP) were purchased from Calbiochem (San Diego, CA). Polyclonal rabbit anti-TNF receptor I, polyclonal rabbit anti-TNF receptor II, polyclonal rabbit anti IL-1 receptor type I, polyclonal goat anti-NOX2, polyclonal goat anti-$p47^{phox}$ including respective blocking peptides were all from St. Cruz Biotechnology (St. Cruz, CA). A monoclonal mouse anti-p44/42 MAPK, a monoclonal mouse anti-phospho p44/42 MAPK, and a monoclonal mouse anti-phospho JNK were from Cell Signaling Technologies (Danvers, MA). Fluorescein or rhodamine-labeled goat anti-rabbit and goat anti-mouse IgG (resp.) were from Chemicon (Temecula, CA), whereas rhodamine-conjugated phalloidin was obtained from Cytoskeleton Inc. (Denver, CO). The polyclonal rabbit anti-$p67^{phox}$ was purchased from Abcam (Cambridge, MA).

2.2. Spinal Cord Neuron Cultures. Dissociated, low-density cultures of spinal cord (SC) neurons were established as described [24]. Briefly, spinal cord tissue was dissected from 7 day-old chick embryos (E7) and a single cell suspension obtained after enzymatic digestion (0.5 mg/mL trypsin, 2 mM EDTA, 10 min, 37°C) followed by trituration. After preplating (1 h, 37°C, 5% CO_2 atmosphere, high glucose DMEM, pH 7.3/10% FBS), nonadherent cells (predominantly SC neurons) were collected (3 min, 200 $\times g_{max}$) and resuspended in SC medium (high glucose DMEM pH 7.3, 10% FBS, 12 nM fluorodeoxyuridine, 30 nM uridine, and 1% N3 nutrient supplement) [25]. SC explants were prepared by pushing freshly dissected E7 spinal cord tissue through a wire-mesh (50–75 μm). Dissociated SC neurons (75,000 cells/mL) or SC explants (2 per culture) were plated onto glass cover slips (22 $\times$ 22 mm^2, number 1, Carolina Biological Supply Company, Burlington, NC) mounted over a 1.5 cm hole drilled into the bottom of a 35 mm culture dish. Glass cover slips were treated with poly-D-lysine (100 μg/mL, borate buffer pH 8.4, 30 min, RT) prior to coating with laminin (5 $\mu g/cm^2$, 30 min, RT). These SC neuron cultures contained less than 5% nonneuronal cells with no immunoreactivity against microglia markers.

2.3. Growth Cone Particle Preparations. Preparations of highly enriched growth cone particles were obtained from freshly dissected whole chick embryo brains (E10-12) [26, 27]. After homogenizing (Dounce homogenizer, ice-cold 5 mM HEPES pH 7.3, 1 mM $MgCl_2$, 0.32 M Sucrose, 6–8 volumes per wet weight), homogenates were centrifuged (15 min, 1600 $\times g_{max}$, 4°C). Resulting supernatants were overlaid onto 5 mM HEPES pH 7.3, 1 mM $MgCl_2$, and 0.75 M sucrose and then centrifuged (150,000 $\times g_{max}$, 1 h, 4°C), and material at the interface was collected. After dilution (6-7 times in low sucrose buffer), the suspension was overlaid onto MaxiDense (4-5 sample volumes per volume Maxidense) and centrifuged at 40,000 $\times g_{max}$ (1 h, 4°C), and growth cone particles (GCPs) were collected on top of the MaxiDense cushion. GCPs were resuspended in Kreb's buffer (145 mM NaCl, 5 mM KCl, 1.2 mM $NaH_2PO_4 \times H_2O$, 1.2 mM $MgCl_2$, and 5 mM HEPES pH 7.3) and protein concentration determined (BCA assay, Thermo Scientific, Rockford, IL, USA).

2.4. Measurement of Neurite Lengths. Dissociated SC neurons were grown after the onset of neurite outgrowth indicated by the majority of cells extending at least one process longer than 2 cell body diameters. Cultures were incubated (1 h) with pharmacological agents, followed by bath application (6–8 h) of 100 ng/mL TNFα, 100 ng/mL IL-1β, or 10 μg/mL ovalbumin. After fixation (2% glutaraldehyde), the length of the longest neurite per neuron was measured of at least 50 randomly selected SC neurons only considering processes adhering to the following criteria: (i) emerging from an isolated cell body, (ii) longer than two cell diameters, and (iii) no contact to other neuronal processes or cell bodies. The distribution of neurite length in a population of SC neurons was obtained by plotting the percentage of neurons with neurites longer than a given length against neurite length [28]. As a characteristic for neurite outgrowth under a given condition, the neurite length reached by 50% of neurite-bearing SC neurons (NL_{50}) was calculated as criteria for statistical significance [29]. Purified, recombinant $Rac1^{V12}$-GST, $Rac1^{N17}$-GST, or GST were introduced into freshly dissociated SC neurons (7–10 mg/mL, 500,000 cells, 200 μL 50 mM Tris-Cl pH 7.5, 100 mM NaCl, and 5 mM $MgCl_2$) by trituration loading at the time of plating [26]. Following trituration, SC neurons were immediately transferred in SC medium and plated as described above. For each condition,

measurements were performed in duplicate cultures from two independent dissections.

2.5. Measurement of Growth Cone Advance. Dissociated SC neurons (12 to 16 h in culture) were transferred into observation medium (Leibovitz'L15 without phenol red, pH 7.4, 5 mg/mL ovalbumin, 1% N3), overlaid with light mineral oil to avoid evaporation, and placed onto the microscope stage equilibrated at 37 ± 0.2°C (Nikon TE2000 U). After 15-minute recovery, images of advancing growth cones (20x, phase contrast) were acquired at 3-minute time intervals for a 30 min time period (Coolsnap*fx*, Photometrics, Tuscon, AZ). Cytokines (100 ng/mL TNFα, 100 ng/mL IL-1β) or 10 μg/mL Ovalbumin were bath-applied at t = 8 min. The extension of the growth cone/neurite boundary (μm) was measured as a function of time (min) (Metamorph Software, Meridian Instrument Co, Kent, WA). At least 20 growth cones were monitored for each condition in duplicate cultures from at least two different dissections.

2.6. Recombinant Mutant Rac1 Protein. Recombinant $Rac1^{V12}$-GST or $Rac1^{N17}$-GST protein was induced in *E. coli* DH5α with 0.5 mM isopropyl β-D-thiogalacto-pyranoside (4 h) [30]. After cell lysis (50 mM Tris-Cl pH 7.5, 50 mM NaCl, 5 mM $MgCl_2$, and 1 mM dithiothreitol), a soluble protein fraction was obtained (20,000 $\times g_{max}$, 20 min, 4°C) and subjected to affinity chromatography on glutathione-conjugated agarose. Bound proteins were eluted (5 mM glutathione in lysis buffer), concentrated to 5–7 mg/mL in 50 mM Tris-Cl pH 7.5, 100 mM NaCl, and 5 mM $MgCl_2$ (Centrifugal Devices, Millipore, Bedford, MA), and stored in 100 μL aliquots at −80°C after snap-freezing. Protein preparations showed single bands on Coomassie blue-stained 10% SDS polyacrylamide gels.

2.7. Adenoviral Expression of Rac1 Mutants in SC Neurons. Recombinant, replication deficient adenovirus carrying genes for constitutively active Rac1 ($Rac1^{V12}$ with N-terminal FLAG tag), dominant negative Rac1 ($Rac1^{N17}$ with N-terminal FLAG tag), or lacZ were expressed in E7 chick SC neurons as described previously [31]. At the time of plating, dissociated SC neurons were infected with recombinant adenovirus at 200 moi (multiplicity of infection) in 300 μL SC medium. Cultures were replenished with 200 μL fresh SC medium after 12 h and grown for additional 48 h. At three days after infection, yields of neuronal infections generally exceeded 70% [31, 32]. Amplification of viral stocks was performed in 293 HEK cells and titers greater than 5×10^8 plaque forming units per mL were routinely obtained. Viral stocks were stored at −80°C.

2.8. Quantitative ROS Imaging in SC Neuron Cell Bodies. Dissociated SC neurons were loaded with 10 μM 2′,7′-dihydrodichlorofluorescein diacetate (DCF) or 5 μM dihyroethidium (DMEM/10% FBS) for 30 min (37°C, 5% CO_2 atmosphere), washed, and allowed to recover (15 min, DMEM/10% FBS). Cultures were switched to observation medium, overlaid with light mineral oil, transferred to the heated microscope stage (Zeiss Axiovert125S), and allowed to adapt for 15 min. Images of dissociated SC neurons (random fields of view) were acquired under phase contrast (20x Plan-Apo objective) and FITC illumination (Ex 465–495 nm, DM 505, Em 515–555) using a Peltier cooled CCD camera (Sensys, Photometrics, Tuscon, AZ) after the recovery phase (defined as basal condition), after pharmacological treatments (30 min), and after cytokine exposure (100 ng/mL TNFα or 100 ng/mL IL-1β). Hydrogen peroxide was added to all cultures following treatments to ensure proper loading. As our criteria for SC neurons, we analyzed only cells displaying a large round cell body and one neuronal process at least longer than three cell diameters. Maximum DCF fluorescence intensity per neuronal cell body was determined on a pixel-by-pixel basis following background subtraction (average background of all images at t = 0 min for each condition) followed by erosion (2 pixels) and overlay with the original image (Zeiss imaging analysis software KS 300). All values were normalized to the average DCF fluorescence intensity in control (initial conditions). No morphological changes of neuronal cell bodies were detectable in our assay conditions indicated by constant cell body areas. ROS measurements were performed in duplicate cultures obtained from 3 to 5 independent dissections. At least 50 SC neurons were measured in duplicate cultures of three independent dissections.

2.9. Quantitative ROS Imaging in Advancing SC Neuron Growth Cones. SC explants were incubated (30 min, DMEM/10% FBS) with 20 μM DCF (5′-(and 6′)chloromethyl -dichlorodihydrofluorescein diacetate) and 4 μM Calcein Blue (CB), an oxidation-inert fluorescence indicator. After recovery (15 min, DMEM/10% FBS), cultures were switched to observation medium and overlaid with light mineral oil. Images of advancing growth cones were acquired under phase contrast (40x Plan-Apo), FITC illumination (DCF fluorescence), and DAPI illumination (CB fluorescence) (Coolsnap*fx*) before (pre-stimulus images at t = 0, 2, 4 min) and after (after stimulus images, 2 min time intervals, 16 min time period) bath application of 100 ng/mL TNFα, 100 ng/mL IL-1β, or 10 μg/mL ovalbumin. As our positive loading control, following the observation period, all growth cones were exposed to 100 μM hydrogen peroxide. For image analysis, DCF and CB fluorescence intensities (F_{DCF} and F_{CB}) were integrated (pixel-by-pixel basis) over the growth cone area for each growth cone observed at each time point ($^{Int}F_{DCF,t}$ and $^{Int}F_{CalcB,t}$ with t = time interval) after background subtraction (t = 0 image) and the ratio of integrated DCF and CB fluorescence intensities for each growth cone at each time point was calculated ($R_t = {}^{Int}F_{DCF,t} / {}^{Int}F$ with t = time interval). Next, the average ratio of integrated DCF and CB fluorescence intensities of all growth cones observed at t = 0 min (pre-stimulus) was calculated ($^{av}R_0$) followed by normalization of all ratios for at t = 0 min ($R_t{}^n / {}^{av}R_0$, n = growth cone 1, 2, to n for each condition). At least 15 growth cones were analyzed per condition from three different dissections to provide statistical significance ($^*P < 0.05$).

2.10. ROS Quantification in Growth Cone Particle Preparations. Freshly prepared GCPs (100 μg in Kreb's buffer) were loaded with 20 μM DCF (30 min, 4°C) in the presence of pharmacological reagents (10 μM DPI, 500 μM NAC), washed (14,000 $\times g_{max}$), allowed to recover (10 min, 4°C) with pharmacological reagents present, and then exposed to 100 or 200 ng/mL TNFα (45 min, 4°C). For lysis, GCPs were resuspended in 2% SDS, 10 mM Tris-Cl pH 7.5, 10 mM NaF, 5 mM dithiothreitol, and 2 mM EGTA; sonicated; and cleared by centrifugation (14,000 $\times g_{max}$, 5 min). Total DCF fluorescence intensity was measured (100 μL aliquots, black 96 well plates) using a Beckman Coulter Multimode DTX 880 microplate reader (495 nm excitation filter, 525 emission filter). All data were adjusted to total soluble protein concentration (BCA assay) and normalized to control condition to account for unspecific fluorescence and/or autofluorescence artifact. For all conditions, measurements were obtained in duplicates from three different GCP preparations.

2.11. Indirect Immunocytochemistry. Dissociated SC neurons were fixed (4% paraformaldehyde, 10 mM MES pH 6.1, 138 mM KCl, 3 mM $MgCl_2$, 2 mM EGTA, 15 min, RT) followed by three washes with TBS (20 mM Tris-Cl pH 7.5, 150 mM NaCl). After blocking (30 min), cultures were incubated (2 h, RT) with primary antibodies (4 μg/mL, 2 mg/mL BSA in TBS) against cytokine receptors or MAP kinases, rinsed with TBS (3 times, 15 min each), and incubated with respective secondary antibodies. Cultures were transferred to 60% glycerol/PBS. Images were acquired under FITC illumination on a Radiance 2000 confocal microscope (Bio Rad).

2.12. Actin Filament Quantification. To visualize actin filaments, SC neurons were fixed and permeabilized (0.5% Triton X-100, 15 min). After rinsing (0.1% Triton X-100 in TBS), cultures were incubated (20 min) with rhodamine-conjugated phalloidin (1 : 10 in 1% Triton X-100 in TBS, Cytoskeleton Inc., Denver, CO), washed, and stored in 60% glycerol (4°C) until inspection. Images were acquired (40x oil, Plan Fluor) using a Zeiss LSM 510 confocal microscope equipped with a HeNe laser and an Argon laser. For each condition, 60 randomly selected SC neuron growth cones were scored for the presence of at least one large lamellipodia-like structure (three dissections, $n = 180$) and the percentage of responding growth cones determined.

2.13. Plasma Membrane Translocation of $p67^{phox}$. Freshly prepared GCPs (100 μg per sample) were treated with methyl-β-cyclodextrin (0.1%) or buffer (30 min, 4°C) and then exposed to 200 ng/mL TNFα (1 h, 4°C), whereas cultures of E10 forebrain neurons were subjected to 200 nM PMA (1 h, 37°C). GCPs (centrifugation) or forebrain neurons (scraping) were transferred into a 0.33 M sucrose buffer (20 mM Tris-HCL pH 8.0, 2 mM EDTA, 0.5 EGTA, 2 mM AEBSF, and 25 μg/mL Leupeptin), lysed by sonication, and centrifuged (25,000 $\times g_{max}$, 15 min) to obtain an enriched plasma membrane fraction (pellet). Pellets were resuspended in sucrose buffer containing 1% Triton X-100 and 0.01% saponin (4°C, 15 min) or in 20 mM Tris-HCL pH 8.0, 2 mM EDTA, 0.5 mM EGTA, and 2 mM AEBSF with regard to gel electrophoresis or ELISA analysis, respectively. Suspensions were centrifuged (25,000 $\times g_{max}$, 15 min, 4°C), membrane protein was recovered as the supernatant, and total protein concentration was determined. For ELISA, aliquots of plasma membrane protein (20 μg/mL, TBS/1% Triton-X-100) were incubated (12 h, 25°C) in 96-well high protein absorbent plates (Falcon). After blocking with BSA (5% w/v, TBS, 1% Trition-X-100, 1 h), wells were incubated (overnight, 4°C) with a polyclonal rabbit anti-$p67^{phox}$ (3 μg/mL), rinsed (TBS/1% Triton-X-100), and incubated with a goat anti-rabbit IgG antibody conjugated to HRP (1 : 2000, 45 min, 25°C). After three consecutive washes, wells were supplemented with 100 μL TMB (tetramethylbenzidine) and absorbance at 620 nm was measured 10 min later (Beckman Coulter Multimode DTX 880 microplate reader. All values were adjusted to total membrane protein and normalized to control conditions (duplicates, three independent experiments).

2.14. Gel Electrophoresis and Western Blotting. SC tissue, SC neuron cultures, or GDPs were solubilized in 2% SDS, 10 mM Tris-Cl pH 7.5, 10 mM NaF, 5 mM dithiothreitol, and 2 mM EGTA and sonicated, and a total soluble protein fraction was obtained by centrifugation (supernatant, 14,000 $\times g_{max}$, 5 min). Fractions of total plasma membrane proteins were obtained as described above. Samples containing 20 μg of total soluble protein in Laemmli buffer were subjected to 10% SDS gel electrophoresis followed by western blotting onto PVDF membranes (Bio-Rad, Hercules, CA) [33, 34]. Membranes were blocked (2% nonfat dry milk, TBS pH 8.5, overnight, 4°C), washed (TBS/0.05% Tween 20/2% BSA), and incubated with polyclonal antibodies against cytokine receptor, MAP kinase, phospho MAP kinase, NOX2, $p47^{phox}$, or $p67^{phox}$ (1 h, 4 μg/mL, in TBS/0.05% Tween 20/2% BSA). Membranes were washed (TBS/0.05% Tween 20/2% BSA) and incubated (1 h, RT) with the respective secondary, alkaline phosphatase-conjugated IgG (1 : 10,000, Sigma, St. Louis, MO) followed by colorimetric development (NBT/BCIP one step, Thermo Scientific, Rockford, IL). The specificity of antibodies was verified in lysates of HeLa cells, RAW264 cells, and SH-SY5Y cells (including blocking peptides).

2.15. Statistical Analysis. One-way ANOVA analysis and a Kruskal-Wallis test were employed for comparisons among multiple conditions. Dunnett's t-test was used when comparing the means of multiple conditions with a single control. All statistical values are given as SEM with a significance of $^{*}P < 0.05$ unless indicated otherwise. Measurements were obtained in duplicates from 3 to 5 separate experiments unless stated otherwise.

3. Results

3.1. TNFα and IL-1β Paralyze Growth Cone Motility and Induce Growth Cone Collapse. Recent reports detailed that TNFα exerts morphogenetic functions (rearrangements of the actin cytoskeleton) without induction of apoptosis [7].

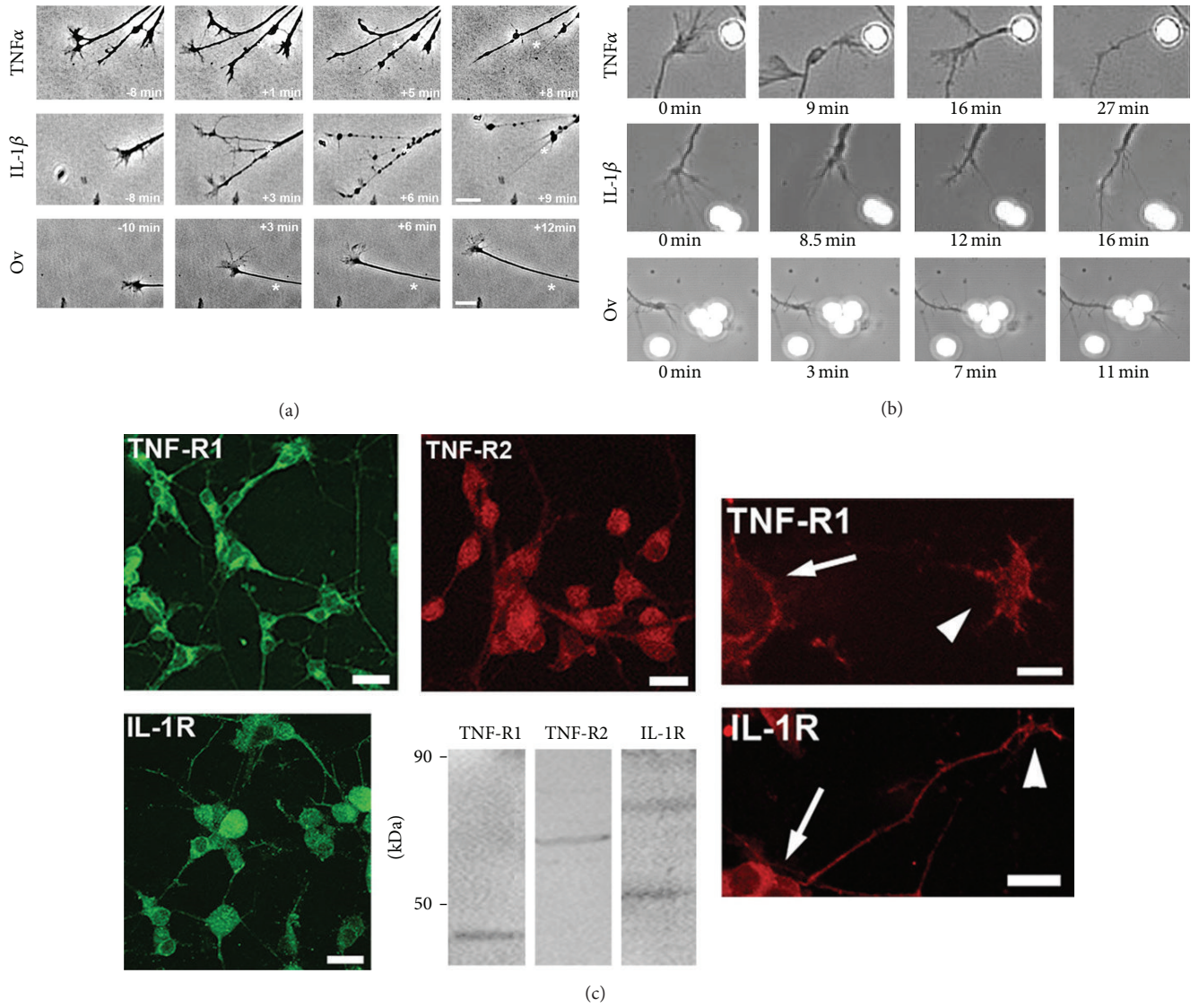

Figure 1: TNFα and IL-1β impair motility and morphology of neuronal growth cones. (a) Acute exposure of dissociated E7 SC neurons (laminin) to 100 ng/mL TNFα (top panel) or IL-1β (middle panel) provoked paralysis of growth cone advance and rapid degeneration of the morphology of growth cones and neurites as opposed to 10 μg/mL ovalbumin (bottom panel). Stars indicate location of the growth cone/neurite border with respect to first image in each panel, respectively (scale bar = 10 μm). (b) To restrict cytokine exposure exclusively to advancing growth cones, polystyrene beads (2.5×10^5 beads/mL, 4 μm in diameter) coated with TNFα or IL-1β were applied to SC neuron cultures and growth cone-bead encounters observed under phase contrast (63x oil, phase contrast). Following physical contact of growth cones to cytokine-coated beads (TNFα—top panel, IL-1β—middle panel), growth cone motility ceased followed by the progressive degeneration of growth cone morphology upon reaching complete collapse. Contact with ovalbumin-coated beads had no influence on growth cone morphology and advance (bottom panel). (c) E7 SC neurons grown on laminin for 2 days were fixed in paraformaldehyde. Cytokine receptors were revealed by indirect immunocytochemistry and analyzed by confocal microscopy (Zeiss LSM510, 40x oil, NA 1.30). TNFα receptor 1 (TNF-R1) and IL-1β receptor (IL-1R) were expressed on cell bodies (arrows) and neurites were expressed as well as on growth cones and filopodia (arrowheads). In contrast, TNFα receptor 2 (TNF-R2) expression was restricted to cell bodies. (Scale bars: upper panel, 20 μm; lower panel 10 μm). Western blots of whole spinal cord (E7 chick) extracts revealed immunoreactivity (stars) against avian cytokine receptors TNF-R1 (48 kDa), TNF-R2 (70 kDa), and IL-1R (76 kDa) as determined in spinal cord lysates (50 μg total protein per lane).

We examined whether TNFα or IL-1β has the potency to alter motility of neuronal growth cones, an actin-cytoskeleton driven mechanism. Live-video, phase contrast microscopy of advancing SC neuron growth cones revealed that an acute exposure to TNFα or IL-1β paralyzed growth cone motility and also caused the collapse of growth cone morphology accompanied by neurite beading and retraction compared to control (ovalbumin) (Figure 1(a)). To demonstrate a direct effect of cytokines on growth cones, we utilized polystyrene beads (4 μm in diameter) covalently coated with TNFα, IL-1β, or ovalbumin (control) to restrict contact between neurons and cytokines exclusively to advancing growth cones

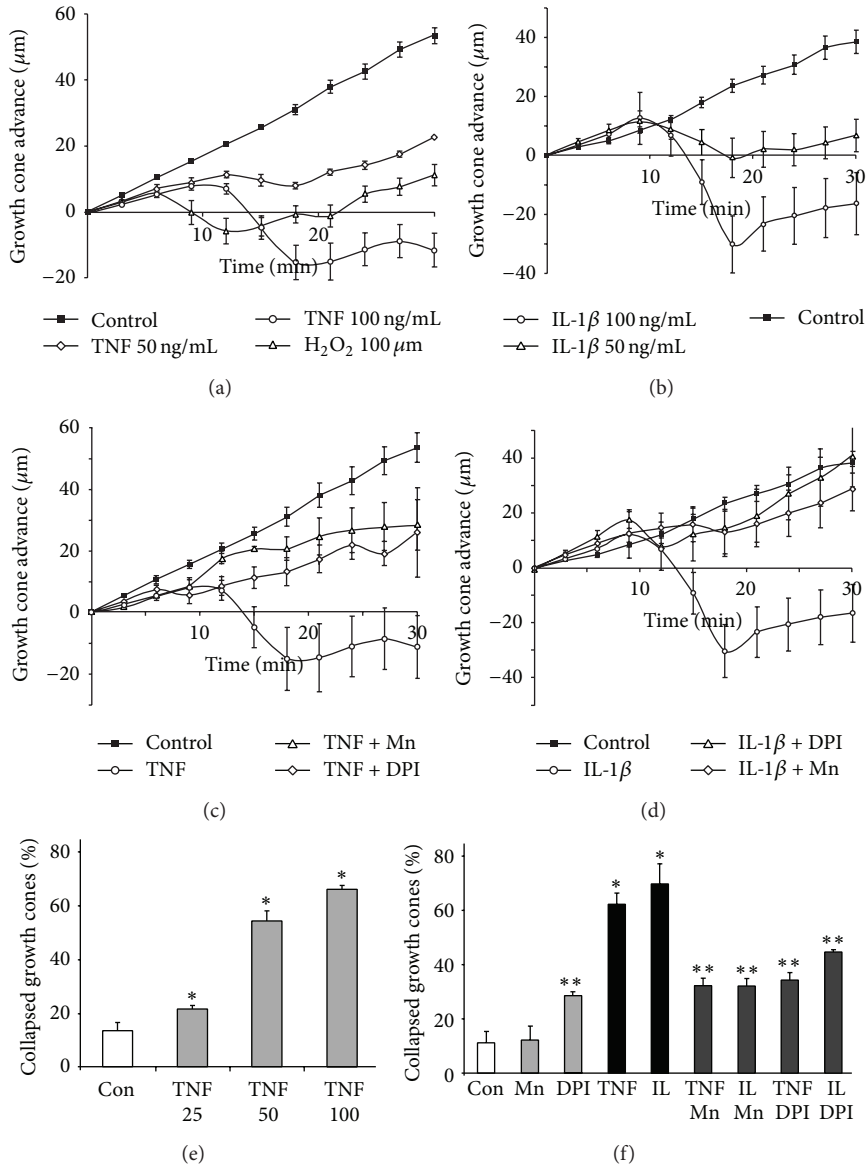

Figure 2: TNFα and IL-1β provoke a redox-sensitive collapse of growth cone motility and morphology. Advancing growth cones in SC neurons cultures (laminin) were randomly selected and images were acquired at 3 min time intervals (20x magnification, phase contrast) in the presence of 10 μM MnTBAP, 2 μM DPI, or PBS (equal volume) before and after acute exposure (t = 6 min) to TNFα (50 or 100 ng/mL), IL-1β (50 or 100 ng/mL), or ovalbumin (10 μg/mL). Growth cone advance was measured as the extension of the growth cone/neurite boundary (μm) per time interval and plotted against time (min) with slopes indicating growth rates. (a and b) Growth cones ceased motility and advance within minutes upon exposure to cytokines (open diamonds, open circles) compared to a steady growth cone advance under control (ovalbumin, closed squares). Growth cones exposed to 100 μM H_2O_2 (open triangles) mostly responded with paralysis, yet slow recovery was measured. In the presence of 50 ng/mL cytokines (open diamonds), growth cones resumed advance after a lag phase however at much slower growth rates, whereas no recovery was detected at concentrations of 100 ng/mL TNFα or IL-1β (open circles). (c and d) ROS scavenging with 5 μM MnTBAP (open triangles) or NOX inhibition with 2 μM DPI (open diamonds) rescued growth cone advance upon acute exposure to 100 ng/mL TNFα (c) or 100 ng/mL IL-1β (d), respectively (open circles). All data were obtained from at least three different dissections (duplicate cultures each, >30 growth cones total) with error bars representing SEM. (e) TNFα elicited a dose-dependent growth cone collapse at concentrations higher than 50 ng/mL. Growth cones with collapsed morphology were quantified (random fields of view) 30 min after application to allow for possible recovery of morphology. (f) Preincubation of SC neuron culture either with 10 μM MnTBAP or with 2 μM DPI provided significant protection against growth cone collapse in the presence of 100 ng/mL TNFα or 100 ng/mL IL-1β (dark grey bars; $^{**}P < 0.05$) as opposed to cytokines alone (black bars), which caused substantial growth cone collapse (dark bar, $^{*}P < 0.05$) compared to control (open bar). A presence of 10 μM MnTBAP (light grey bar, Mn) had no effect on basal levels of collapsed growth cones, whereas 2 μM DPI increased the percentage of collapse growth cones. All data (e and f) were obtained from at least three different dissections (duplicate cultures each). Error bars represent ±SEM.

[35]. Growth cones encountering cytokine-coated beads displayed a series of stereotypic changes in behavior ultimately resulting in growth cone collapse (Figure 1(b)). After establishing long-lasting adhesion contacts with filopodia, growth cones entered a phase characterized by highly mobile, lamellipodia-like structures, which were nonproductive for advance, followed by a collapse of morphology (TNFα: 78 ± 4%, n = 22 and IL-1β: 83 ± 7%, n = 18 of observed growth cones, resp.). None of these growth cone responses occurred upon contact with ovalbumin-coated beads. Cytokine receptors were expressed on SC neurons and their processes (Figure 1(c)). Whole SC tissue extracts (western blotting) exhibited immunoreactivity against TNF receptor 1 (TNF-R1, apparent MW = 48 kDa), TNF receptor 2 (TNF-R2, apparent MW = 70 kDa), and IL-1β receptor type 1 (IL-1R, apparent MW = 76 kDa) in accordance with previous reports [36]. Expression of TNF-R1 and IL-1R was found on neuronal cell bodies, neurites, as well as growth cones; however, TNF-R2 expression was predominantly localized to neuronal cell bodies with virtually no expression on neurites or growth cones.

Next, we quantified growth cones advance (the spatial displacement of the growth cone/neurite boundary over time) in SC explant cultures upon acute exposure to TNFα, IL-1β, or ovalbumin (Ov, control) (Figure 2). Both TNFα and IL-1β caused a rapid, dose-dependent paralysis of growth cone advance and even neurite retraction within less than 10 minutes of addition compared to Ov (Figures 2(a) and 2(b)). Acute bath application of 100 ng/mL TNFα or IL-1β reduced the percentage of advancing growth cones by 83 ± 6% (n = 48, $^{*}P < 0.05$) compared to bath application of 10 μg/mL Ov. In contrast, a considerable fraction of growth cones resumed advance following bath application of 50 ng/mL TNFα or IL-1β (TNFα: 42 ± 14%, n = 24, $^{*}P < 0.05$ and IL-1β: 30 ± 8% n = 20, $^{*}P < 0.05$) however at much slower growth rates (31 ± 6 μm/h and 21 ± 5 μm/h, resp.) compared to growth rates prior to cytokines application (TNFα: 79 ± 8 μm/h, n = 22 and IL-1β: 89 ± 9 μm/h, n = 26). As expected, application of 10 μg/mL Ov had no effect on growth cone advance (before application: 108 ± 10 μm/h and after application: 113 ± 6 μm/h). According to reports and our own findings, we tested whether ROS intermediates were implicated in cytokine-mediated growth cone paralysis and collapse. Scavenging ROS with 10 μM MnTBAP or inhibition of NADPH oxidase (NOX) activities with 2 μM DPI both protected growth cone advance upon exposure to 100 ng/mL TNFα (69 ± 1%, n = 26 and 71 ± 10%, n = 38 of advancing growth cones, resp.) albeit with decreased growth rates (96 ± 9 μm/h, 17% reduction and 82 ± 9 μm/h, 26% reduction, resp.) compared to 10 μg/mL Ov (Figure 2(c)). Growth cone advance was not affected by an addition of MnTBAP (124 ± 10 μm/h) or DPI (98 ± 13 μm/h) in the presence of ovalbumin during the period of observation. Growth cone advance in the presence of 100 ng/mL IL-1β was also rescued by 10 μM MnTBAP or 2 μM DPI (77 ± 12%, n = 38 and 69 ± 6%, n = 50, resp.) (Figure 2(d)). Exogenous addition of ROS to growth cones (100 μM hydrogen peroxide) also reduced the percentage of advancing growth cones (44 ± 2%, n = 42, $^{*}P < 0.05$).

Both cytokines also elicited a dose-dependent growth cone collapse quantified 30 min after addition as shown for TNFα (25 ng/mL: 16 ± 3%, n = 135; 50 ng/mL: 59 ± 4%, $^{*}P < 0.05$, n = 125; 100 ng/mL: 71 ± 8%, $^{*}P < 0.05$, n = 122) compared to 10 μg/mL Ov (13 ± 3%, n = 69) (Figure 2(e)). Moreover, scavenging ROS (10 μM MnTBAP) or inhibiting NOX (2 μM DPI) (32 ± 4%, n = 100 and 34 ± 4%, n = 99, resp., $^{**}P < 0.05$) protected growth cone morphology from the presence of 100 ng/mL TNFα as opposed to the absence of pharmacological agents (63 ± 7%, n = 87, $^{*}P < 0.05$) (Figure 2(f)). Similarly, MnTBAP (31 ± 3%, n = 156) and DPI (44 ± 1%, n = 186) also negated IL-1β-induced growth cone collapse (69 ± 8%, n = 196, $^{*}P < 0.05$). The percentage of collapsed growth cone remained unaltered by the presence of 10 μM MnTBAP (11 ± 6%, n = 99), yet it did significantly increase with 2 μM DPI (27 ± 1%, n = 63). Taken together, these data revealed that TNFα and IL-1β caused rapid degeneration of growth cone morphology and complete loss of motility through a redox-dependent mechanism. The rapid response of growth cones to cytokines together with the expression of cytokines receptors on growth cones strongly suggested a direct mechanism as opposed to indirect effects through neurodegenerative processes originating in neuronal cell bodies.

3.2. A Cytokine-Activated NADPH Oxidase Generates ROS in Growth Cones and Cell Bodies of SC Neurons. To determine the generation of intracellular ROS in advancing growth cones exposed to cytokines, we employed quantitative ratiometric fluorescence analysis utilizing the oxidation-sensitive fluorescent indicator 2′,7′-dihydrodichlorofluorescein (DCF, 10 μM) and the redox inert fluorescence indicator Calcein Blue (CB, 4 μM). Ratiometric analysis distinguishes changes in DCF fluorescence due to ROS formation from dilution/concentration effects simply due to rapid changes in growth cone morphology. Bath application of 100 ng/mL TNFα or 100 ng/mL IL-1β elicited a rise in the relative maximum DCF/CB fluorescence ratio indicative of the formation of ROS (Figure 3). As shown in Figure 3(a) (false colored DCF/CB ratio images), ROS formation was sustained and preceded loss of morphology of the advancing growth cone reflected by atrophy and beading of filopodia, condensation of growth cone body, and retraction. Quantitative analysis demonstrated a significant and sustained ROS formation in advancing growth cones upon exposure to TNFα (100 ng/mL, n = 14), IL-1β (100 ng/mL, n = 10), or 100 μM hydrogen peroxide (positive control, n = 11) compared to 10 μg/mL ovalbumin (negative control, n = 22) (Figure 3(b)). Neither loading with DCF (131 ± 18 μm/h, n > 15) nor loading with CB (118 ± 14 μm/h, n > 15) at the concentrations used affected growth cone advance per se compared to unloaded control (113 ± 9 μm/h).

To examine NOX-dependent ROS production in neuronal growth cones, we utilized freshly isolated growth cone particle preparations (GCPs) obtained from chick E10 forebrain neurons, which are capable of showing complex responses to extrinsic stimuli [37–39]. As shown in Figure 4(a), addition of 100 ng/mL TNFα to laminin-adherent

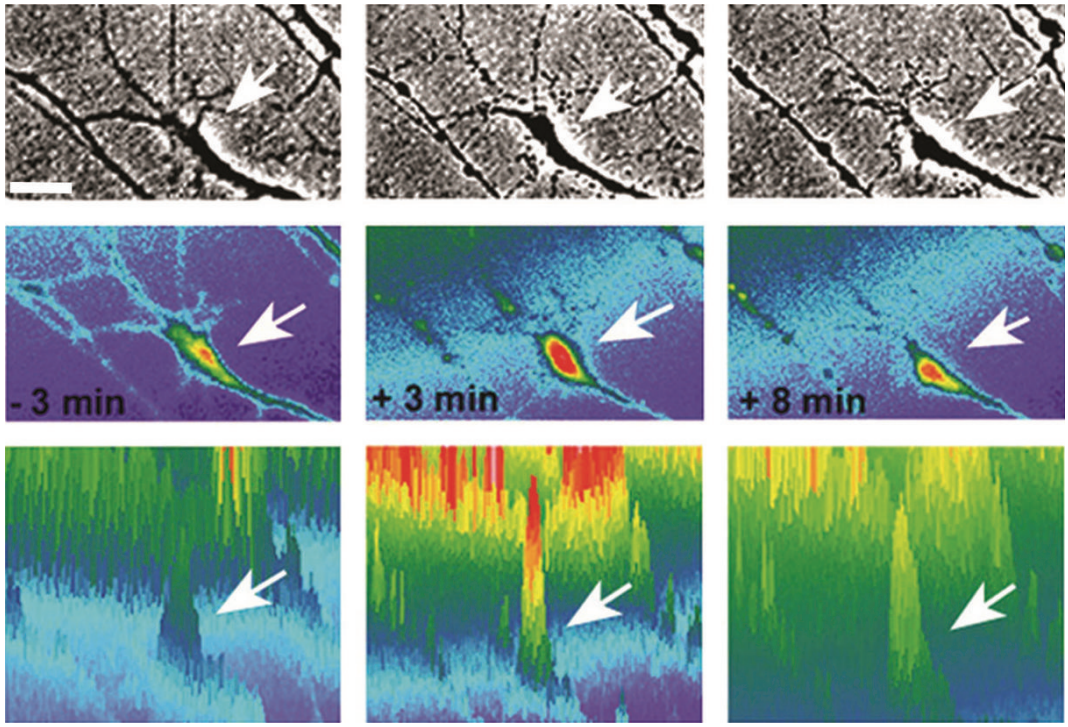

(a)

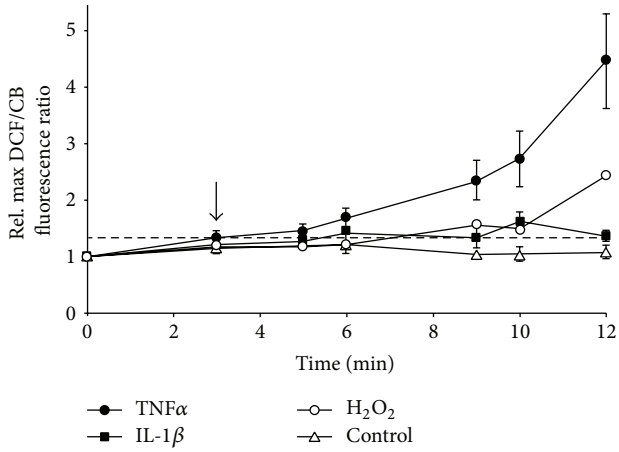

(b)

Figure 3: TNFα stimulates ROS formation in advancing growth cones. ROS formation in advancing SC neuron growth cones was revealed by ratiometric fluorescence imaging. Dissociated E7 chick SC neurons (laminin) were loaded (30 min) with the oxidation-sensitive fluorescent indicator 2′,7′-dihydrodichlorofluorescein (10 μM DCF) and the oxidation-inert fluorescent indicator Calcein blue (4 μM CB). Images of randomly selected growth cones were acquired under FITC fluorescence illumination (DCF), DAPI fluorescence illumination (CB), and phase contrast at short time intervals before and after addition of stimuli (40x, oil, identical parameters). (a) Intracellular ROS formation is represented by a heat spectrum ranging from blue (basal ROS levels) to red (increased ROS levels). Growth cone morphology (arrow) disintegrated over a time period of 11 minutes upon acute exposure to 100 ng/mL TNFα (phase images, upper panel). Ratio imaging (middle panel) revealed a sharp increase in ROS production (t = +3 min) shortly after TNFα exposure that persisted (t = +8 min) compared to basal levels (t = −3 min) further illustrated by profile images of ratiometric images (lower panel) (Scale bar = 5 μm). Note the loss of filopodia and lamellipodia and the contraction of the growth cone body (last panel) were preceded by an increase in ROS. (b) ROS formation in advancing SC neuron growth cones was quantified by ratiometric fluorescence imaging. Maximum DCF and CB fluorescence intensities per growth cone area were determined on a pixel-by-pixel basis and DCF/CB ratios calculated for each condition and time point. All DCF/CB ratios were normalized (average DCF/CB ratio at t = 0 min) and plotted against time. Exposure to 100 ng/mL TNFα (filled circles, n = 14), 100 ng/mL IL-1β (filled squares, n = 10), or 100 μM hydrogen peroxide (positive control, open circles, n = 11) at t = 3 min (arrow) elicited a significant ROS formation (stippled line = significance threshold) in advancing growth cones within less than 5 min upon addition compared to 10 μg/mL ovalbumin (negative control, open triangles, n = 22).

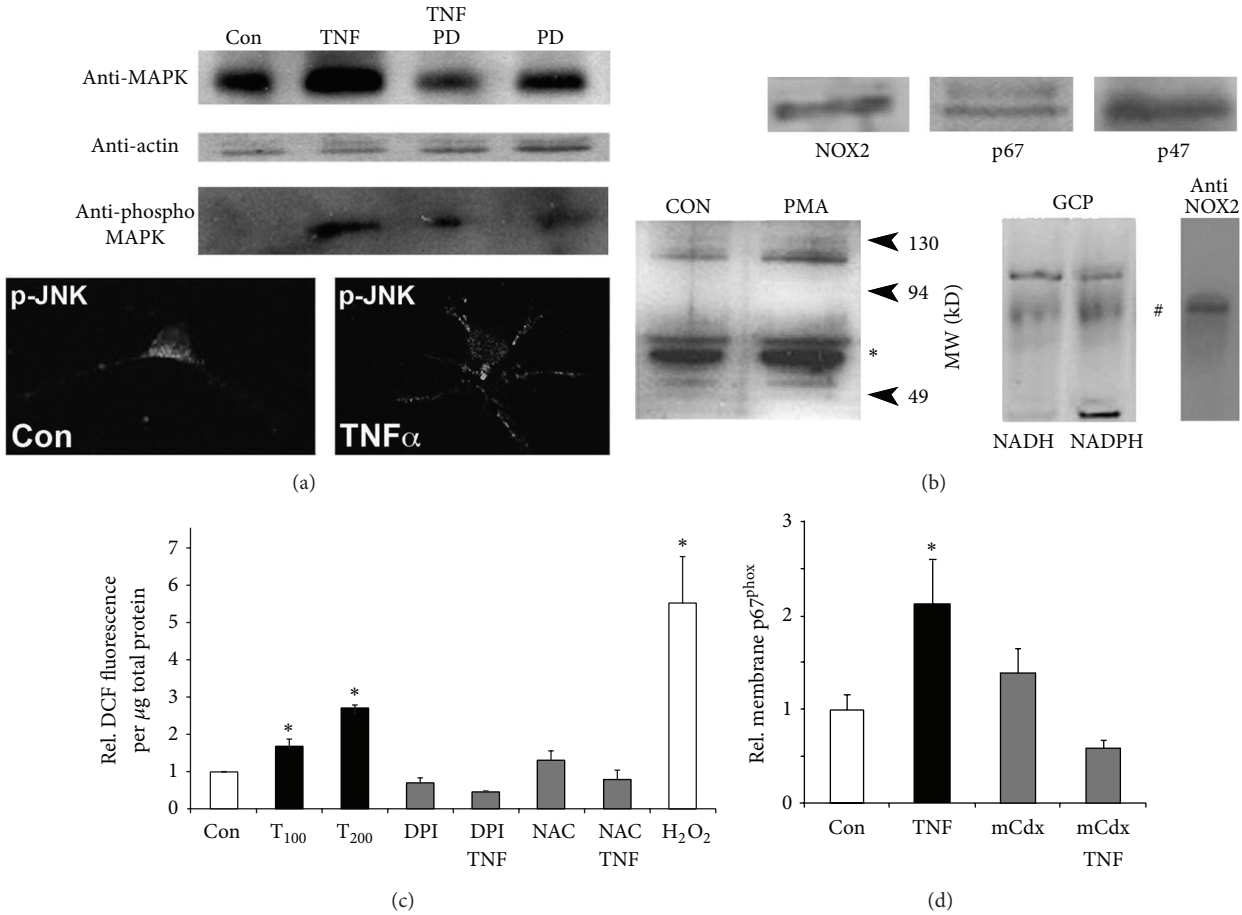

Figure 4: NADPH oxidase mediates ROS formation in growth cones exposed to TNFα. (a) Exposure of freshly isolated growth cone particles (GCPs) to TNFα activates MAP kinase. GCPs were plated on laminin in Krebs buffer (2 h), washed, and incubated with the MAP kinase inhibitors PD98059 (25 μM, 20 min) or PBS (equivalent volume) prior to an addition of 100 ng/mL TNFα. Attached GCPs were lysed and equal amounts of total protein were subjected to SDS gel electrophoresis (10%) followed by western blotting and detection (chemiluminescence) of MAP kinase (top panel) and phospho-MAP kinase immunoreactivity (bottom panel). Actin served as a loading control (middle panel). Exposure of GCPs to TNFα stimulated MAP kinase activity (increased phospho-MAP kinase), which was negated by PD98059. Also, TNFα treatment enhanced expression of MAP kinase (increases in total MAP kinase), a response apparently diminished by a presence of PD98059. Confocal images acquired (63x, oil) of cultured chick forebrain neurons (laminin, 24 h) exposed to 100 ng/mL of TNFα (TNFα) revealed phospho-JNK immunoreactivity (white signal) as a discrete, punctate pattern in cell bodies and neuronal process in contrast to the homogenous appearance in neuronal soma under control conditions (PBS, equivalent volume). Cultures were fixed with 4% paraformaldehyde and immunostained against phospho-JNK. (b) Neuronal growth cones contain a functional NADPH oxidase activity. Lysates obtained from SC neuron cultures revealed immunoreactivity against the large membrane subunit NOX2 and the cytosolic subunits $p67^{phox}$ and $p47^{phox}$. Incubation of chick (E7) forebrain neurons with the NOX activator PMA (400 ng/mL) increased plasma membrane association of the cytosolic subunit $p67^{phox}$ (*) compared to controls (Con) indicative for the formation of the NOX multiprotein complex. Native gel electrophoresis, combined with in-gel NBT staining, of freshly isolated growth cone particles (GCPs) obtained from E10–12 chick forebrain demonstrated one NADPH oxidoreductases activity (#) colocalizing with NOX2 immunoreactivity. (c) GCPs were loaded with 10 μM DCF (30 min) in the presence of 2 μM DPI (NOX inhibitor), 500 μM NAC (antioxidant), or PBS (mock, equivalent volume) prior to addition of TNFα (45 min). DCF fluorescence was determined in GCP lysates, adjusted to total soluble protein, and normalized to control (Con, open bar). TNFα stimulated a significant, dose-dependent ROS formation in GCPs (T_{100} = 100 ng/mL, T_{200} = 200 ng/mL, $^*P < 0.05$), which was abolished by DPI or NAC. Peroxide (H_2O_2) served as a positive control. (d) Plasma membrane association of $p67^{phox}$ normalized to control conditions was quantified (western blotting) using plasma membrane-enriched fractions. Exposure of GCPs to 200 ng/mL TNFα significantly increased the relative plasma membrane association of $p67^{phox}$ (TNF, $^*P < 0.05$) compared to control (Con) indicating the formation of a functional NOX complex. Preincubation of GCPs with methyl-β-cyclodextrin (0.1%) negated plasma membrane translocation of $p67^{phox}$ in the presence of TNFα (mCdx-TNF). All data represent SEM from at least two experiments (triplicate conditions each) with $^*P < 0.05$.

GCPs resulted in MAP kinase and JNK activation, which was corroborated in cultured forebrain neurons. No basal MAP kinase activity (phosphor MAP kinase) was detectable in GCPs under control conditions possibly due a lack of growth factors (serum free plating conditions). Indicative for the formation of a functional NOX multiprotein complex, the NOX activator PMA (200 ng/mL) significantly increased the relative plasma membrane association of $p67^{phox}$ in chick forebrain neurons (Figure 4(b)). Moreover, native gel electrophoresis and NBT staining revealed several NADPH oxidoreductase activities in GCPs, one colocalizing with NOX2 immunoreactivity. The large membrane subunit NOX2 and the cytosolic subunits $p67^{phox}$ and $p47^{phox}$ were also detected in lysates of SC neurons (Figure 4(b)). Addition of TNFα (100 ng/mL) to DCF-loaded GCPs stimulated a significant, dose-dependent increase in ROS formation, which was negated by the NOX inhibitor DPI (5 μM) or the ROS scavenger NAC (1 mM) (Figure 4(c)). The small spatial dimensions of plated GCPs prevented ROS quantification utilizing microscopic imaging. Therefore, we resorted to a protocol involving lysis as previously established [14]. Moreover, plasma membrane association of $p67^{phox}$ in GCPs significantly increased in response to 100 ng/mL TNFα, which was abolished by the lipid raft disrupter methyl-β-cyclodextrin, suggesting that the assembly of NOX occurred predominantly in lipid rafts (Figure 4(d)). The insignificant increase of $p67^{phox}$ in plasma membrane fractions from methyl-β-cyclodextrin-treated cells could result from unspecific adsorption due to the dramatic change in membrane lipid composition. TNFα-coated polystyrene beads or bath application of 100 ng/mL TNFα to DCF-loaded SC neurons stimulated a transient increase in DCF fluorescence intensity in neuronal cell bodies (Figures 5(a) and 5(b)). Cytokine-stimulated ROS formation was dose-dependent with significant stimulation at concentrations higher than 50 ng/mL and saturation at 100 ng/mL (data not shown). Maximum ROS formation (1.62 ± 0.1, $^*P < 0.01$) in SC neuron cell bodies occurred 5.3 ± 0.8 min following bath application of 100 ng/mL TNFα lasting for 6.4 ± 0.6 min (16 ± 2 cells per time interval) (Figure 5(c)). 100 ng/mL IL-1β also increased ROS formation (1.39 ± 0.02, $^*P < 0.01$) within 5 ± 0.7 min upon application and lasted for 7.8 ± 1.4 min ($n = 20 \pm 2$ cells per time interval). Scavenging ROS with 2 mM NAC or 10 μM MnTBAP both suppressed TNFα-stimulated ROS formation (0.75 ± 0.11; $n = 29$ and 0.99 ± 0.05; $n = 65$, resp.) to levels indistinguishable from control (10 μg/mL ovalbumin, 0.99 ± 0.05, $n = 123$) in contrast to TNFα alone (1.53 ± 0.05, $^*P < 0.01$, $n = 184$) (Figure 5(d)). Inhibiting NOX activity (5 μM DPI) also negated ROS formation (1.03 ± 0.07; $n = 70$, $^*P < 0.01$) upon exposure to TNFα. Similar data were obtained upon acute addition of 100 ng/mL IL-1β to SC neurons (data not shown). As our positive control, 200 μM hydrogen peroxide greatly increased relative maximum DCF fluorescence intensity (1.75 ± 0.02; $n = 109$, $^*P < 0.01$), which was abolished in the presence of 10 μM MnTBAP (0.97 ± 0.02; $n = 109$) (Figure 5(d)). Depleting Rac1 activity using adenoviral-mediated expression of FLAG-tagged, dominant-negative $Rac1^{N17}$ completely suppressed TNFα or IL-1β-stimulated ROS formation (1.13 ± 0.05, $n = 93$ and 0.84 ± 0.05, $n = 71$, resp.) as opposed to lacZ expression (TNFα: 1.53 ± 0.05, $^*P < 0.05$, $n = 184$, and IL-1β: 1.30 ± 0.05, $^*P < 0.05$, $n = 117$, resp.) (Figure 6(a)) [31]. In contrast, expression of constitutively active $Rac1^{V12}$ in SC neurons was sufficient to increase ROS formation (1.65 ± 0.04, $n = 450$, $^*P < 0.05$) compared to 200 μM hydrogen peroxide (1.98 ± 0.16, $n = 60$, $^*P < 0.05$) (Figures 6(b) and 6(c)). ROS scavenging with 2 mM NAC or 10 μM MnTBAP as well as NOX inhibition with 10 μM DPI abolished $Rac1^{V12}$-stimulated ROS formation (1.11 ± 0.09, $n = 62$; 0.96 ± 0.09, $n = 109$; and 1.05 ± 0.07, $n = 138$, resp.). Similar results were obtained using purified recombinant GST chimeras of $Rac1^{V12}$ and $Rac1^{N17}$ transfected into E7 SC neurons by trituration loading (data not shown). Expressing $Rac1^{N17}$ alone (1.03 ± 0.04, $n = 247$) or lacZ (0.99 ± 0.03, $n = 105$), our control, had no effect on basal levels of ROS (Figure 6(c)). However addition of 2 mM NAC or 10 μM DPI to $Rac1^{N17}$-expressing SC neurons both reduced ROS formation significantly below basal levels (0.76 ± 0.04, $n = 94$ and 0.55 ± 0.02, $n = 106$, resp., $^*P < 0.05$). These findings revealed that TNFα and IL-1β stimulate a functional assembly of a Rac1-regulated NOX2 complex in the plasma membrane of neuronal growth cones resulting in a transient increase in ROS formation.

3.3. TNFα and IL-1β Attenuate Neurite Outgrowth of SC Neurons in a Redox-Dependent Manner. Next, we examined whether the redox-dependent impairment of growth cone advance is of consequence for neurite outgrowth. Bath application of 100 ng/mL TNFα or IL-1β attenuated neurite outgrowth in SC neuron cultures in a dose-dependent manner indicated by a shift in the distribution to shorter neurite lengths compared to 10 μg/mL ovalbumin (Ov), our control (Figures 7(a) and 7(b), Table 1). Scavenging ROS (10 μM MnTBAP) rescued neurite outgrowth in the presence of TNFα and IL-1β, whereas the NOX inhibitor (2 μM DPI) provided only partial protection of neurite outgrowth (Figures 7(c) and 7(d)). Notably, neurite outgrowth of SC neurons on laminin exhibited inherent redox dependence even in the absence of TNFα or IL-1β (Figures 7(e) and 7(f)). In accordance with previous reports, increasing concentrations of the ROS scavenger N-acetyl-L-cysteine (2 mM NAC, 50% reduction) or 20 μM MnTBAP (10% reduction) inhibited neurite outgrowth compared to control, whereas 10 μM MnTBAP was ineffective [15]. However, we measured a significant increase in neurite outgrowth with 5 μM MnTBAP (25% increase).

To assess the role of Rac1 on neurite outgrowth, $Rac1^{V12}$ (constitutively active Rac1) or $Rac1^{N17}$ (dominant negative Rac1) was introduced as purified recombinant GST chimera into freshly dissected SC neurons by trituration loading [26] (Figure 8). Depletion of Rac1 activity ($Rac1^{N17}$-GST) in SC neurons protected neurite outgrowth upon addition of 100 ng/mL TNFα ($NL_{50} = 81 \pm 5$ μm, $n = 85$, $^{**}P < 0.05$) or 100 ng/mL IL-1β ($NL_{50} = 79 \pm 6$ μm, $n = 68$, $^{**}P < 0.05$) compared to GST-loaded SC neurons ($NL_{50} = 64 \pm 3$ μm, $n = 75$ and $NL_{50} = 69 \pm 2$ μm, $n = 51$), respectively (Figure 8(a)). However, introduction of $Rac1^{N17}$-GST diminished neurite

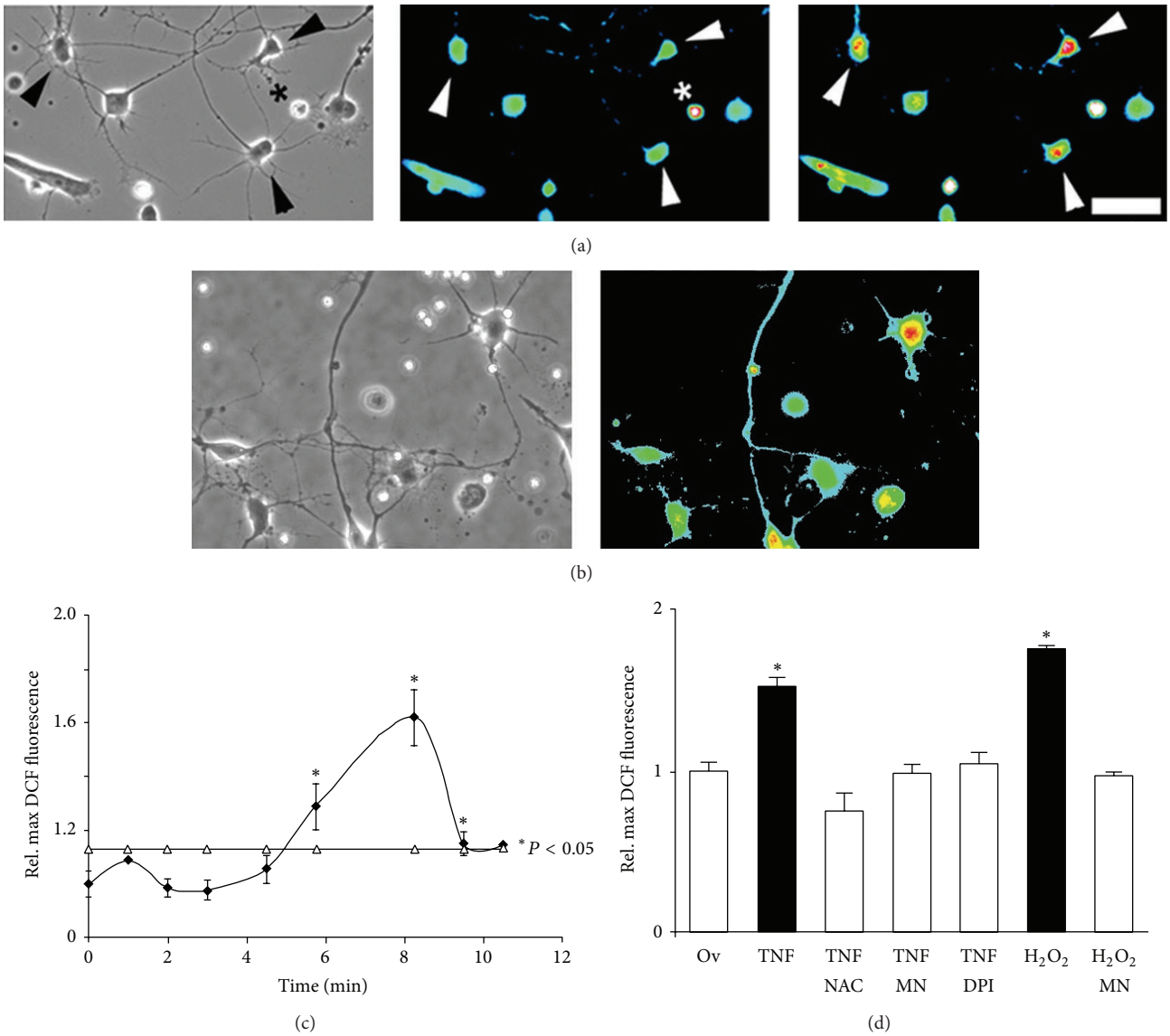

Figure 5: Cytokines elicit ROS formation in cell bodies of SC neurons. Dissociated E7 SC neurons were loaded with 10 μM DCF (30 min), allowed to recover for 15 min, and then incubated (45 min) with NAC, MnTBAP, DPI, or PBS (equal volume) prior to cytokines exposure. Images were acquired at identical parameters (20x). (a) DCF-loaded SC neurons exhibited a distinct neuronal morphology (arrowheads) extending one long and several shorter neuronal processes (left panel, phase contrast image). Note cultures are virtually free of nonneuronal cells. Under control conditions, SC neuron cell bodies displayed basal levels of ROS formation (middle panel, arrowheads). Degenerating cells (star) exhibit very high fluorescence intensity in the absence of any stimuli. Addition of 100 ng/mL TNFα stimulated a robust increase in intracellular ROS (right panel, arrowheads, 8 min after addition). Fluorescence images were false colored (heat spectrum) with fluorescence intensities increasing from blue (basal ROS levels) to red (high ROS levels). (b) TNFα-coated polystyrene beads increased DCF fluorescence intensity in SC neurons indicative of ROS formation. Although qualitative in nature, SC neurons with multiple bead contacts (arrow head) as opposed to single bead contact (asterisk) displayed more intense DCF fluorescence. (c) Maximum DCF fluorescence intensities per neuronal cell body were determined on a pixel-by-pixel basis after background subtraction over time and all values normalized to the average maximum DCF fluorescence intensity under control conditions at $t = 0$ min (relative maximum DCF fluorescence intensity). SC neurons responded with a transient increase in ROS formation in cell bodies (16 ± 2 cells per time interval) upon exposure to 100 ng/mL TNFα (2.5) min (threshold of statistical significance $^*P < 0.01$ shown as open triangles). (d) 100 ng/mL TNFα stimulated a significant increase in ROS formation ($^*P < 0.01$), which was negated by the presence of ROS scavengers (TNFα-NAC 2 mM or TNFα-MnTBAP 10 μM, resp.) or NOX inhibitor (TNFα-DPI 5 μM) to levels indistinguishable from 10 μg/mL ovalbumin (Ov), our control. As a control for DCF loading, 200 μM hydrogen peroxide (H_2O_2) greatly increased relative maximum DCF fluorescence ($^*P < 0.01$), which was suppressed in the presence of 10 μM MnTBAP (H_2O_2-Mn). All measurements were obtained from at least three independent dissections (duplicate cultures each).

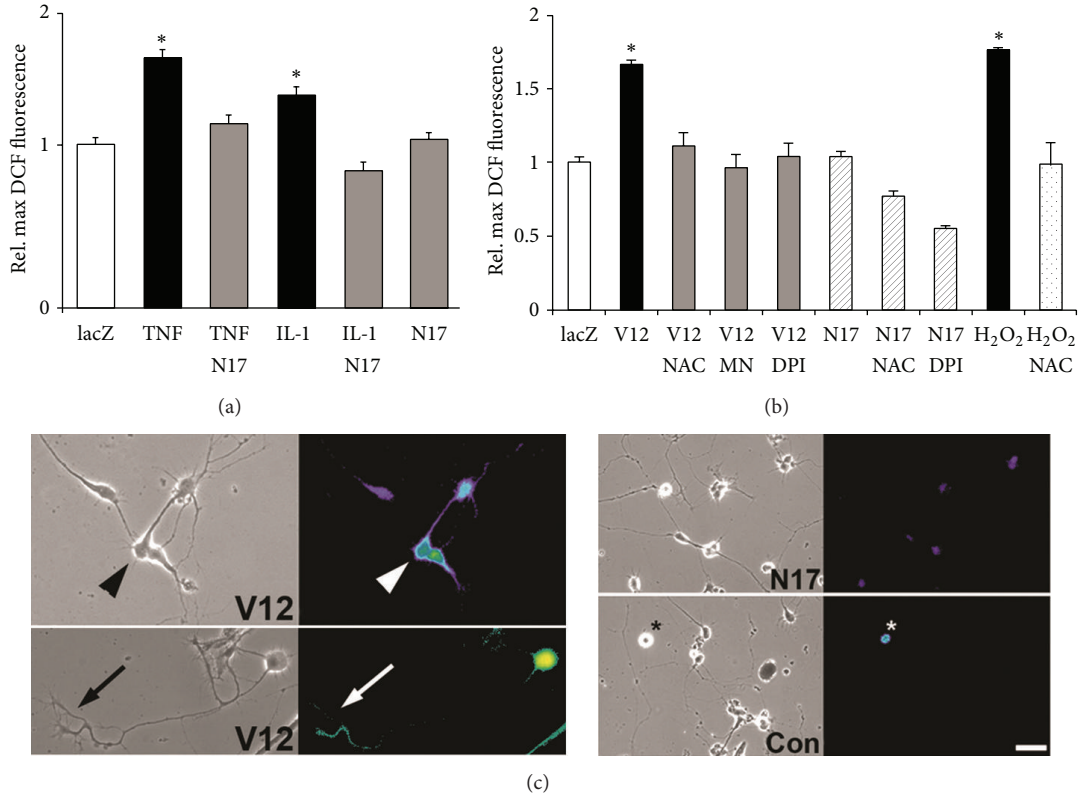

Figure 6: TNFα and IL-1β stimulate a Rac1-mediated ROS formation in SC neurons. Dissociated SC neurons grown on laminin were infected with recombinant, replication deficient adenovirus (200 moi, infection at the time of plating) carrying FLAG-tagged constitutively active $Rac1^{V12}$, FLAG-tagged dominant negative $Rac1^{N17}$, or lacZ. Three days after infection, SC neurons were loaded with 10 μM DCF (30 min), incubated with NAC, MnTBAP, or DPI, and exposed to cytokines (100 ng/mL). Random images were acquired (20x) under FITC fluorescence illumination, relative maximum DCF fluorescence intensity was quantified, and all values normalized to lacZ-expressing SC neurons exposed to 10 μg/mL Ovalbumin (lacZ), our control. (a) Expression of Rac^{N17} completely abolished ROS formation in SC neurons upon exposure to 100 ng/mL TNFα or IL-1β (TNFα-N17 and IL-1β-N17, resp.) compared to lacZ-expressing SC neurons (TNFα and IL-1β, resp., $^{*}P < 0.01$) without altering basal levels of ROS formation (N17). (b) Expression of $Rac1^{V12}$ was sufficient to induce ROS formation in SC neurons, which was negated by 2 mM NAC, 10 μM MnTBAP, or 10 μM DPI. Peroxide (200 μMol/L H_2O_2) served as a DCF loading control. (c) DCF-loaded SC neurons expressing Rac^{V12} (V12) revealed increases in ROS formation both in cell bodies (arrowhead) as well as in neuronal growth cones (arrow) and distal neurites (left panel). In contrast, SC neurons expressing Rac^{N17} (N17) exhibited basal DCF fluorescence intensity compared to lacZ (Con) expressing SC neurons (right panel). Note the intense DCF fluorescence in a degenerating cell (asterisk). A heat spectrum ranging from blue (basal ROS levels) to red (increased ROS levels) indicates ROS production (scale bar = 40 μm).

outgrowth even in the absence of adverse stimuli (NL_{50} = 84 ± 4 μm, n = 132, $^{*}P < 0.05$) compared to GST-loaded SC neurons (NL_{50} = 91 ± 3 μm, n = 99) in accordance with previous findings [26, 40]. Constitutive activation of Rac1 ($Rac1^{V12}$-GST) in SC neurons also resulted in reduction of neurite length (NL_{50} = 83 ± 5 μm, n = 195, $^{*}P < 0.05$) compared to GST-loaded SC neurons (NL_{50} = 98 ± 5 μm, n = 112) (Figure 8(b)). Interestingly, addition of 5 μM MnTBAP restored neurite outgrowth of Rac^{V12}-GST-loaded SC neurons (NL_{50} = 108 ± 6, n = 136, $^{**}P < 0.05$) to levels indistinguishable from GST-loaded SC neurons (NL_{50} = 103±7 μm, n = 103, $^{**}P < 0.05$). This finding implied a role for Rac1 as a regulator of TNFα or IL-1β-stimulated oxidative stress. These findings provided evidence that attenuation of neurite outgrowth in the presence of TNFα or IL-1β required a persistent, Rac1-regulated formation of ROS. Moreover, neurite outgrowth on laminin exhibited an innate redox-sensitivity.

3.4. Cytokines Elicit a Redox-Dependent Reorganization of Actin Filaments in Neuronal Growth Cones. Earlier studies in neuroblastoma cells revealed oxidative damage to actin due to TNFα exposure [14]. We found that growth cones responded rapidly to cytokine exposure with changes in morphology prior to collapse suggesting reorganization of actin filaments. We quantified the percentage of growth cones responding to cytokines with at least one distinct actin filament-rich, lamellipodial structure as a function of both time and pharmacological treatment (Figure 9). Growth cones exhibited a rapid, yet transient increase in actin filament-rich structures within 15 min upon exposure to 100 ng/mL TNFα (65 ± 5%, n = 180, $^{*}P < 0.05$) or 100 ng/mL IL-1β (84 ± 5%, n = 180, $^{*}P < 0.05$) compared to control (23 ± 5%, n = 180, $^{*}P < 0.05$) and persisted up to 30 min (TNFα: 67 ± 5%, n = 180, $^{*}P < 0.05$, and IL-1β: 58 ± 5%, n = 180, $^{*}P < 0.05$) (Figures 9(a) and 9(d)). However, the percentage of growth cones with actin filament-rich structures greatly subsided

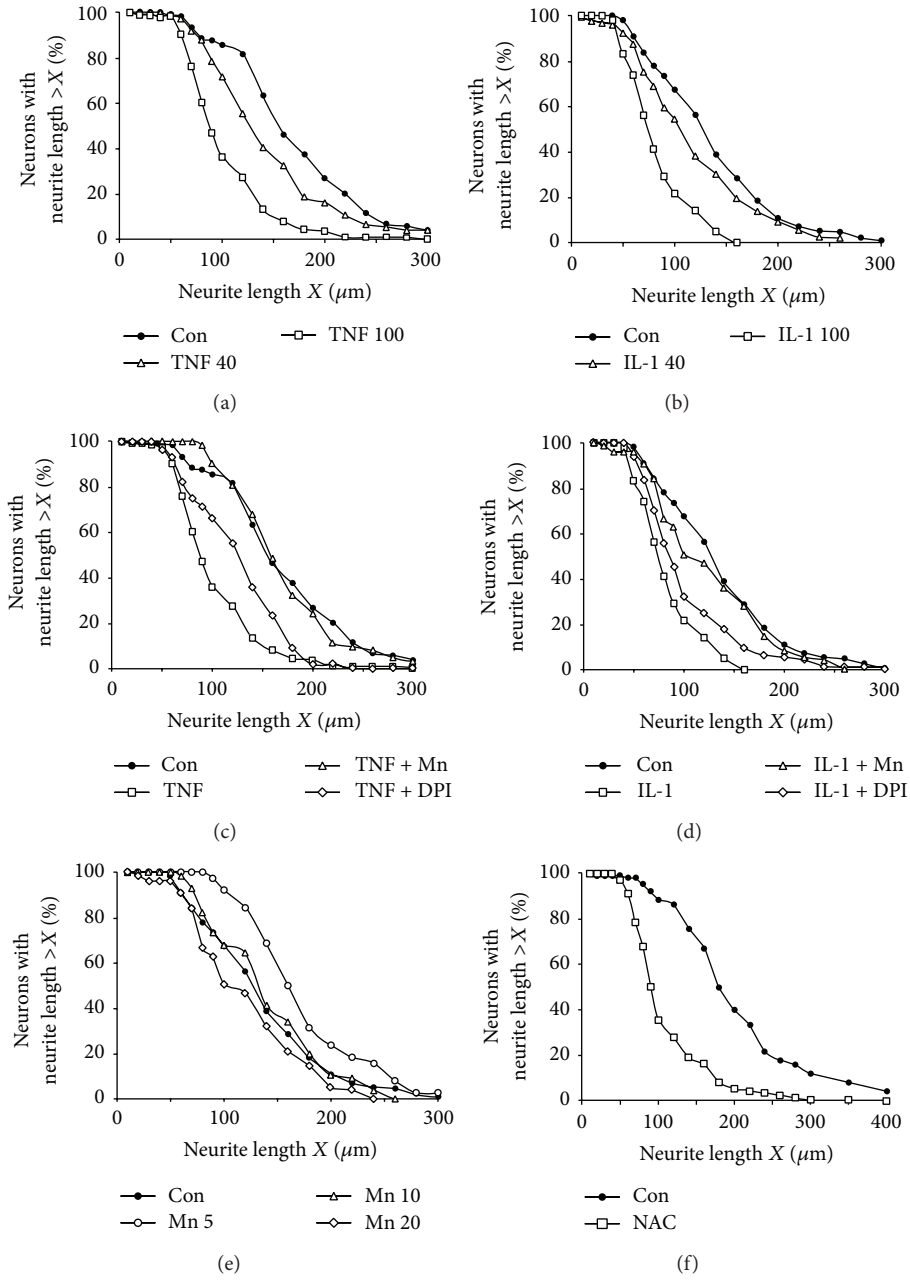

Figure 7: TNFα and IL-1β impede neurite outgrowth in a redox-sensitive manner. Dissociated SC neurons were grown on laminin past the onset of neurite initiation and then incubated with 10 μM MnTBAP, 2 μM DPI, or PBS (10 μL) for 1 h prior to bath application of cytokines or ovalbumin (6 to 8 h) followed by fixation (2% glutaraldehyde). The longest neurite per neuron was measured of randomly selected neurons and the percentage of neurons with a given neurite length was plotted against neurite length. (a and b) Persistent presence of TNFα (a) or IL-1β (b) significantly reduced neurite outgrowth in a dose-dependent manner (40 ng/mL, open triangles; and 100 ng/mL, open squares) indicated by the shift of the neurite length distribution to shorter neurites compared to control (10 μg/mL ovalbumin, filled circles). (c and d) Despite a continuous presence of 100 ng/mL TNFα ((c), open squares) or 100 ng/mL IL-1β ((d), open squares), scavenging ROS with 10 μM MnTBAP (open triangles) rescued neurite outgrowth compared to controls (10 μg/mL ovalbumin, filled circles), whereas inhibiting NOX activity with 2 μM DPI (open diamonds) was only partially protective. (Neurite number measured $\geq$ 60 for each condition, two experiments, and duplicate cultures). (e) In the presence of 20 μM MnTBAP (open diamonds), neurite outgrowth was significantly decreased compared to control (PBS, filled circles). However, concentrations of 10 μM MnTBAP (open triangles) did not significantly alter neurite outgrowth and 5 μM MnTBAP (open circles) on the contrary causes a significant increase in neurite length. (Neurite number measured > 75 for each condition, two experiments, and duplicate cultures). (f) Lastly, an overabundance of the radical scavenger NAC (2 mM, open squares) dramatically reduced neurite outgrowth compared to control (PBS, filled circles) indicated by the shift towards shorter neurites.

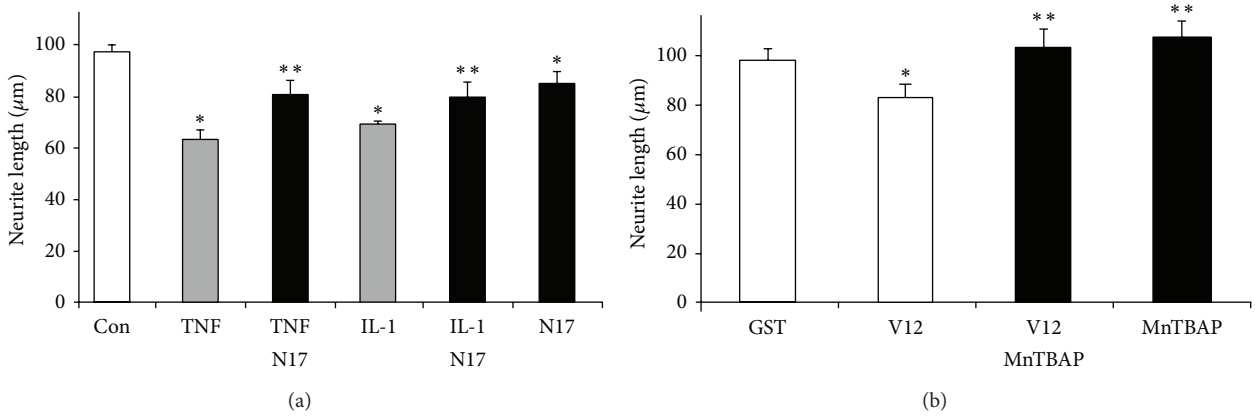

Figure 8: The small GTPase Rac1 mediates redox-dependent neurite outgrowth. Freshly dissected SC neurons were trituration-loaded with purified recombinant $Rac1^{V12}$-GST, $Rac1^{N17}$-GST, or GST only (7 mg/mL each) and grown (laminin) after the onset of neurite initiation. Cultures were supplemented with 100 ng/mL TNFα, 100 ng/mL IL-1β, or 10 μg/mL ovalbumin (8 h) and the average neurite length of the longest neurite reached by 50% of SC neurons (NL_{50}) for each condition quantified ($n > 50$). (a) Introduction of $Rac1^{N17}$-GST (dominant negative mutation, black bars) significantly protected neurite outgrowth in the presence of TNFα (TNFα-N17, $^{**}P < 0.05$) or IL-1β (IL-1β-N17, $^{**}P < 0.05$) compared to SC neurons loaded with GST, which exhibited a great reduction in neurite length in the presence of cytokines (grey bars $^{*}P > 0.05$) compared to control (ovalbumin, open bar). Not unexpected, $Rac1^{N17}$-GST even in the absence of cytokines reduced neurite outgrowth (N17, $^{*}P < 0.05$) compared to control. (b) Similarly, introduction of $Rac1^{V12}$-GST (constitutively active mutation) significantly reduced neurite lengths (V12, $^{*}P < 0.05$) compared to GST-loaded SC neurons (GST). Notably, the presence of 5 μM MnTBAP increased neurite outgrowth of $Rac1^{V12}$-GST-loaded SC neurons (V12-MnTBAP, $^{**}P < 0.05$) to levels indistinguishable from neurite outgrowth of GST-loaded SC neurons treated with 5 μM MnTBAP (MnTBAP, $^{**}P < 0.05$) compared to control. All data were obtained from at least three different dissections (duplicate cultures each) with error bars representing.

Table 1: Redox-sensitive inhibition of neurite outgrowth in response to TNFα and IL-1β.

Condition	NL_{50} ± SEM	n
Control (10 mg/mL Ov)	147 ± 16 μm	104
TNFα 40 ng/mL	118 ± 6 μm*	74
TNFα 100 ng/mL	86 ± 13 μm*	173
TNFα 100 ng/mL + 10 mM MnTBAP	145 ± 13 μm	62
TNFα 100 ng/mL + 2 mM DPI	113 ± 12 μm**	56
Control (10 mg/mL Ov)	128 ± 7 μm	61
IL-1β 40 ng/mL	109 ± 4 μm*	92
IL-1β 100 ng/mL	80 ± 3 μm*	107
IL-1β 100 ng/mL + 10 mM MnTBAP	112 ± 9 μm**	113
IL-1β 100 ng/mL + 2 mM DPI	87 ± 8 μm*	78
PBS	128 ± 12 μm	156
MnTABP 5 mM	161 ± 10 μm*	82
MnTABP 10 mM	133 ± 7 μm	75
MnTABP 20 mM	115 ± 7 μm*	56
PBS	179 ± 7 μm	103
NAC 2 mM	89 ± 7 μm*	102

SC neuron cultures were incubated with pharmacological inhibitors (MnTBAP, DPI) or PBS prior to addition of cytokines for 6–8 hours. After fixation, the average neurite length of the longest neurite per neuron reached by 50% of neurons (NL_{50}) was quantified for each condition. *Significant differences from controls. **Significant difference from cytokine only at $P < 0.05$ by one-way ANOVA and Dunnett's t-test.

45 min after addition (TNFα: 40 ± 4%, $n = 180$, $^{**}P < 0.05$, and IL-1β: 37 ± 5%, $n = 180$, $^{**}P < 0.05$) compared to the initial response. Inhibiting NOX activity (5 μM DPI) greatly diminished the percentage of responding growth cones upon bath application of cytokines (DPI + TNFα: 32 ± 6%, $n = 180$, and DPI + IL-1β: 49 ± 6%, $n = 180$, $^{**}P < 0.05$) compared to absence of DPI (TNFα: 60 ± 6%, $n = 180$, $^{*}P < 0.05$, and IL-1β: 76 ± 6%, $n = 180$, $^{*}P < 0.05$) measured 15 min after addition of cytokines (Figures 9(b) and 9(e)). The percentage of responding growth cones was not altered by DPI treatment alone (18 ± 6%, $n = 180$) compared to control (23 ± 6%, $n = 180$). Similarly, scavenging ROS with 20 μM MnTBAP also negated the formation of actin filament-rich structures in growth cones exposed to cytokines (Mn + TNFα: 24 ± 8%, $n = 180$, and Mn + IL-1β: 18 ± 8%, $n = 180$) to levels indistinguishable from control (18 ± 4%, $n = 180$) compared to cytokines alone (TNFα: 66 ± 8%, $n = 180$, $^{*}P < 0.05$, and IL-1β: 84 ± 8%, $n = 180$, $^{*}P < 0.05$) (Figures 9(c) and 9(f)). A presence of MnTBAP did not alter the percentage of growth cones with actin filament-rich structures (18 ± 3%, $n = 180$). Taken together, these data suggested that TNFα and IL-1β stimulated a redox-dependent, yet transient reorganization of actin filaments in neuronal growth cones prior to collapse of morphology.

4. Discussion

We demonstrated that long-term exposure of SC neurons to the proinflammatory cytokines TNFα and IL-1β provoked the loss of growth cone motility and the subsequent degeneration of growth cone morphology (collapse). These changes in growth cone advance and behavior translated into the impairment of neurite outgrowth and disruption of process architecture of SC neurons, which was rescued either

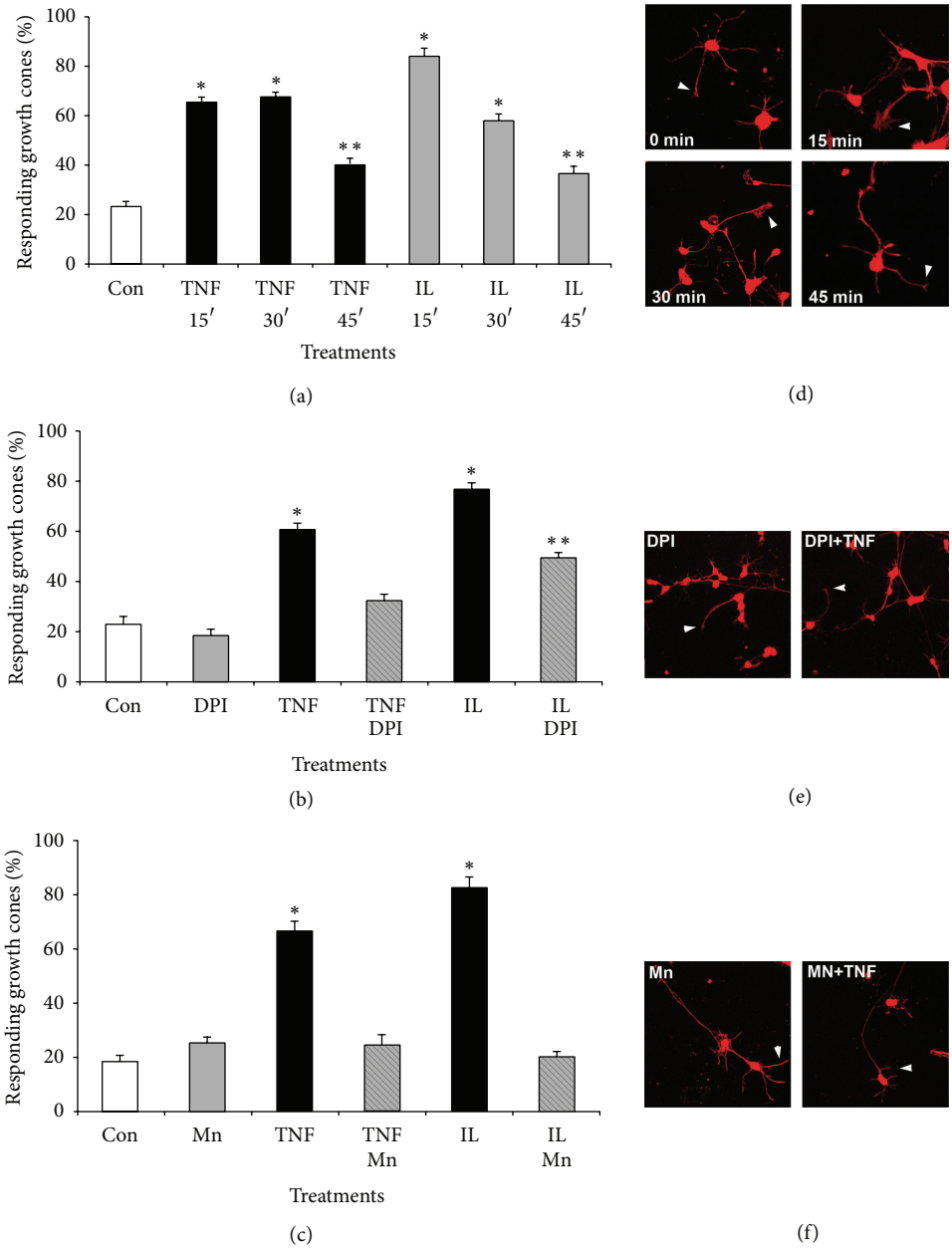

Figure 9: Cytokines elicit redox-dependent reorganization of actin filaments in neuronal growth cones. SC neurons grown on laminin (2 days) were incubated with 40 μM MnTBAP, 5 μM DPI or left untreated prior to addition of TNFα or IL-1β (200 ng/mL) for increasing time periods (15 min, 30 min, and 45 min). Cultures were fixed, permeabilized (Triton-X-100), and stained with rhodamine phalloidin to reveal filamentous actin. Random images were acquired (40x, confocal microscope), growth cones were scored for the presence of at least one, distinct actin filament-rich structure, and all values normalized to control conditions (% responding growth cones). (a) Both TNFα and IL-1β significantly increased the percentage of growth cones with actin-filament rich structures ($^{*}P < 0.01$) at 15 min and 30 min after exposure followed by a significant decrease at 45 min after exposure ($^{**}P < 0.01$ compared to $t = 15$ min) as opposed to control. (b) Inhibition of NOX activity with 2 μM DPI largely negated the formation of actin-filament rich structures upon exposure to TNFα (TNF-DPI) or IL-1β (IL-DPI, $^{**}P < 0.01$) as opposed to TNFα only (TNFα, $^{*}P < 0.01$) or IL-1β only (IL, $^{*}P < 0.01$), respectively. Large actin filament-rich structures were not affected by DPI in the absence of cytokines (DPI) compared to control (Con). (c) Scavenging ROS with 10 μM MnTBAP abolished the formation of actin filament-rich structures in response to TNFα (TNFα-Mn) or IL-1β (IL-Mn) when compared to TNFα only (TNF, $^{*}P < 0.01$) or IL-1β only (IL, $^{*}P < 0.01$). The degree of actin filament-rich structures in the presence of MnTBAP alone (Mn) was indistinguishable from control (Con). *Significant difference from control and **significant difference from respective cytokine treatment at $P < 0.05$ by Kruskal Wallis test and Dunnett's t-test. (d–f) Cultured SC neurons were treated with pharmacological inhibitors prior to bath application of cytokines, fixed with 4% paraformaldehyde, and stained for actin filaments with rhodamine phalloidin (red signal). (d) Representative images of SC neurons with increasing exposure time to TNFα. Actin filament-rich structures in growth cones (lamellipodia) are indicated with arrowheads. (e) Incubation with DPI largely abolished the formation of actin filament-rich structures in SC neurons cultures. (f) Scavenging ROS with MnTBAP effectively negated appearance of actin filament-rich structures in growth cones of SC neurons.

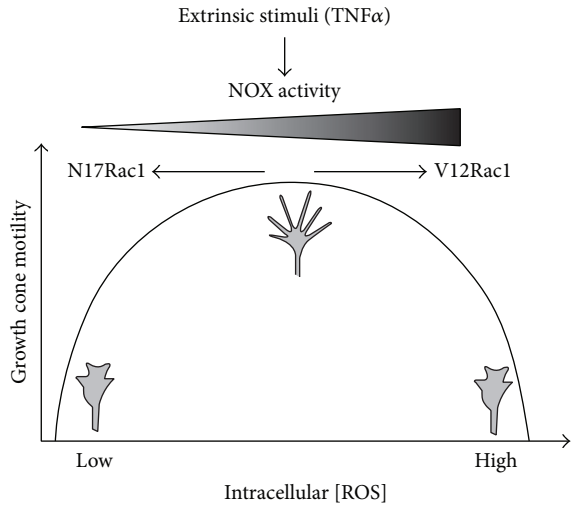

Figure 10: A Rac1-dependent redox rheostat regulates growth cone motility in response to extrinsic stimuli. Exposure of neuronal growth cones either to TNFα or to IL-1β rapidly stimulates ROS generation through NOX activity under the regulation of the small GTPase Rac1 and concomitant paralysis and degeneration of morphology of growth cones. Moreover, growth cone motility is not only sensitive to the overabundance of ROS either via NOX activation or via constitutive Rac1 activity ($Rac1^{V12}$) but is also impaired by a substantial depletion of ROS (antioxidants) or inhibition of Rac1 activity ($Rac1^{N17}$). Consequently, productive growth cone motility requires an optimal concentration of intracellular ROS generated by a Rac1-regulated NOX activity. It is plausible that this Rac1/NOX-redox rheostat is responsive to many extrinsic stimuli including cytokines, growth factors, hormones, and cell adhesion molecules for which redox signaling mechanism has been demonstrated.

by scavenging ROS, inhibiting NOX activity, or depleting Rac1 activity despite a presence of TNFα or IL-1β. Both cytokines stimulated the formation of ROS intermediates and a transient phase of actin filament organization in advancing growth cones. Importantly, ROS intermediates and actin filament reorganization preceded paralysis of growth cone motility and collapse of morphology implying a causative action of this signaling mechanism. Taking into account that exhaustive ROS scavenging (excess of antioxidants) also impaired neurite outgrowth, it is feasible that productive growth cone motility could demand an optimal level of ROS intermediates. We propose that a redox rheostat under the regulation of the Rac1 shapes growth cone motility and hence neurite outgrowth, in response to many extrinsic stimuli other than cytokines (Figure 10).

Prolonged bath application of TNFα or IL-1β (6–8 h) to dissociated SC neurons or SC explants stunted neurite outgrowth in a dose-dependent manner (Figure 7, Table 1) in accordance with previous findings in hippocampal neurons or neuroblastoma cells [8, 9]. In lieu of the well-documented apoptotic potency of TNFα and IL-1β, it was imperative to determine whether inhibition of neurite outgrowth had its origin in neuronal cell bodies (apoptosis, necrosis) or directly in the distal compartment of growth cones. Foremost, cytokines were applied to SC neurons after the onset of neurite outgrowth with the majority of processes longer than two cell diameters. Since the number of neurites per neuron (a measure of neurite initiation) remained unaltered and no measureable neuronal cell death occurred over the time period of cytokine exposure (6–8 h) as determined by a live/dead fluorescence assay (calcein green/propidium iodide counterstaining), neither a decrease in neurite initiation nor a decrease in neuronal cell death could account for the observed reduction in neurite outgrowth. Significant neuronal cell death (>15%) was however apparent 24 hours after cytokine addition and increased to over 40% after 2 days. Evidence for direct action of cytokines on growth cone motility and morphology was obtained by live-video phase microscopy (Figures 1 and 2). Acute exposure to TNFα or IL-1β (bath applied) impaired growth cone motility in a dose-dependent manner within 10 to 15 minutes upon application. Initial paralysis of growth cone advance was followed by degeneration of morphology and subsequent collapse. Restricting cytokine exposure exclusively to advancing growth cones in our bead assay corroborated these findings. In addition, bead assays revealed a transient increase in lamellipodia-like structures or in the vicinity of neuron-bead contacts, which were nonproductive for growth cone advance. This transient increase in actin filaments (Figure 9) was reminiscent of our findings in SH-SY5Y neuroblastoma, yet in the case of primary neurons it revealed a physiological consequence [14]. Direct effects of cytokines on growth cones were further supported by the expression of IL-R1 (IL-1β receptor) and TNF-R1 (high affinity p55 TNFα receptor) on the entire neuronal surface including cell bodies and growth cones (Figure 1). Together these findings provided strong evidence that TNFα and IL-1β directly impaired growth cone motility and morphology as the underlying cause for the attenuation of neurite outgrowth over longer time periods of exposure.

Initial evidence for a role of ROS intermediates was suggested by studies demonstrating that antioxidants (ROS scavenging) or DPI (inhibiting NOX-like activities) largely rescued neurite outgrowth, growth cone motility, growth cone morphology, and lastly actin filament organization in the presence of cytokines. Interestingly, neurite outgrowth of SC neurons on laminin exhibited innate redox dependence. Whereas moderate MnTBAP concentrations (5 μM) significantly increased neurite outgrowth, concentration higher than 10 μM stunted neurite outgrowth corroborating studies in Aplysia neurons [15]. It is plausible that moderate MnTBAP concentration (5 μM) scavenges excessive amounts of superoxide derived from mitochondrial respiration and as byproduct of several enzymatic reactions. Under basal culture conditions, this excessive superoxide might compromise optimal growth cone motility (actin dynamics, tubulin dynamics) and hence the observed enhancement of neurite outgrowth by moderate concentrations of scavenger [41–43]. In contrast, higher MnTBAP concentrations could impair vital redox-dependent mechanism necessary for proper neurite outgrowth [44]. Using the oxidation-sensitive fluorescence indicator DCF, we demonstrated substantial yet transient

generation of ROS (likely superoxide) in growth cones and cell bodies of SC neurons upon exposure to TNFα and IL-1β (Figures 3 and 5). Similar results were obtained using the superoxide-specific fluorescence indicator dihydroethidium, yet investigations suffered from considerable neurotoxicity of dihydroethidium (data not shown). Previous studies in chick cortical neurons and human SH-SY5Y neuroblastoma cells demonstrated superoxide production in response to TNFα utilizing dihydroethidium oxidation or a SOD-inhibitable cytochrome C oxidation as demonstrated [14, 45]. A significant contribution from nonneuronal cells (microglia) was unlikely since (i) SC neuron cultures contained less than 3% nonneuronal cells, (ii) analyzed cells all exhibited distinct neuronal characteristics (i.e., round cell body, one process longer than 2 cell diameters), and (iii) microglia invade and populate the developing CNS at late embryonic or even postnatal stages [46]. Ratiometric imaging demonstrated significant ROS production in advancing growth cones within 3 to 5 min upon exposure to inflammatory stress as opposed to changes in motility and morphology observed 10 to 15 min following exposure. Several findings strongly suggested a NOX2-like activity as the source of ROS in SC neurons, in particular superoxide [14, 47]. SC neurons exhibited immunoreactivity against NOX2 and the cytosolic subunits $p47^{phox}$ and $p67^{phox}$. A presence of other NOX isoforms can however not be excluded, yet antibody quality against NOX1 or NOX3 was insufficient to produce a conclusive finding. TNFα stimulated a dose-dependent increase in ROS intermediates in freshly isolated growth cone particle preparations in conjunction with a presence of NADPH oxidoreductases activity. The phorbol ester PMA as well as TNFα induced translocation of the cytosolic subunit $p67^{phox}$ to plasma membranes. Parallel studies on the translocation of the cytosolic subunit $p47^{phox}$ to plasma membranes were hampered by the considerable variability of immunoreactivity. Expression of NOX-like activities was reported in both primary PNS and CNS neurons [48–51]. Lastly, the antioxidant MnTBAP inhibits the TNFα or IL-1β-stimulated ROS formation. Also, pharmacological inhibition with DPI was effective in blocking TNFα or IL-1β-mediated responses of SC neurons including ROS formation and partial rescue of growth motility, neurite outgrowth, growth cone collapse, and actin filament reorganization (Figures 2, 4, 5, 7, and 9). Notably, all these experiments revealed considerable toxicity of DPI and thus, depending on the duration of DPI application, put restrictions on the usable concentrations of DPI. Mechanistically, DPI blocks single electron transport reactions such as NOX-mediated generation of superoxide. Nevertheless, numerous other enzymatic reactions are also compromised foremost electron transport of complex I in mitochondria, which could account for the observed toxicity. Lastly, depleting Rac1 activity negated cytokine-mediated ROS formation in SC neurons, whereas Rac1 overexpression alone was sufficient to increase ROS formation. The small GTPase Rac1 emerged as a pivotal regulator of cytokine-stimulated ROS formation in SC neurons in accordance with previous reports [22, 52, 53]. In our study, depleting Rac1 activity abolished ROS formation in the presence of TNFα or IL-1β yet without affecting basal ROS levels (Figures 6(b)–6(d)). In contrast, overexpression of constitutively active Rac1 alone was sufficient to stimulated ROS generation in SC neurons and also reduced neurite outgrowth, which was not further exacerbated upon addition of TNFα or IL-1β (data not shown). Effects of Rac1 depletion or overexpression were addressed by trituration loading of purified recombinant Rac1-GST mutant chimeras since adenoviral-mediated expression of Rac1 mutants required a 3-day expression period incompatible with neurite outgrowth analysis [26, 31]. Not unexpectedly, introduction of $Rac1^{N17}$ or $Rac1^{V12}$ resulted in a measurable reduction in neurite outgrowth on laminin even in the absence of cytokines [11, 26, 54, 55]. In support of our findings, numerous reports link Rac1 as a regulator of ROS intermediates in cellular signal transduction. Neurite extension in PC12 cells upon NGF stimulation encompasses increases in Rac1 activity and H_2O_2 formation [56]. A Rac1 mutant lacking residues 124–135 of the insert region blocking ROS generation disrupted membrane ruffling and mitogenesis in fibroblasts and caused a downregulation of RhoA [44, 57–59]. With respect to actin cytoskeleton dynamics, TNFα and IL-1β induced a transient phase of actin filament reorganization (increases in actin filament density) in neuronal growth cones, which was however nonproductive for motility. Interestingly, actin filament reorganization was not repeatable with another addition of cytokines even after wash-out and extensive recover time suggesting permanent or persistent damage to actin filament reorganization by cytokines. Irreversible oxidative damage (carbonylation) to actin was detectable in neuroblastoma cells exposed to TNFα [14]. These findings provided evidence that NOX activation in neuronal growth cones serves as source of ROS intermediates in response to cytokines and that ROS intermediates are likely causative for cytokine-mediated degeneration of neuronal growth cones.

Inflammatory and oxidative stress is a hallmark of neurodegeneration in most chronic, acute, and even some psychiatric CNS pathologies [3, 60, 61]. The proinflammatory cytokines TNFα and IL-1β are important to orchestrate inflammatory and oxidative stress in the disease and aging CNS although pleiotropic actions in the adult and developing CNS are known, hence establishing a complex and delicate balance between neuroprotection and neurotoxicity. Members of the Nox/Duox family have emerged as [46, 62] key sources of oxidative stress in aging and the progression of many pathologies beyond the CNS and have been recognized as key therapeutic targets [63–66]. Our findings provide support for a role of NOX activity in primary neurons as a principal source of oxidative stress triggered by TNFα or IL-1β [16]. Overabundance of ROS intermediates is likely to disrupt proper actin filament dynamics, which is vital for the plasticity and morphology of distal neuronal processes including neurite outgrowth, sprouting, and spine dynamics. Strategies to block NOX activities could thus proof beneficial to blunt inflammatory stress in the diseased and aging CNS and to halt cognitive decline [66, 67].

Abbreviations

DCF: 2′,7′-dichlorofluorescein
DMEM: Dulbecco's Modified Eagle Medium
DPI: Diphenylene iodonium
FBS: Fetal bovine serum
GST: Glutathione-S-transferase
IL-1β: Interleukin-1 beta
MnTBAP: Manganese(III) tetrakis(4-benzoic acid) porphyrin chloride
NAC: N-acetyl-L-cysteine
ROS: Reactive oxygen species
SC: Spinal cord
TBS: Tris-buffered saline
TNFα: Tumor necrosis factor alpha.

Conflict of Interests

The authors declare that there is no conflict of interests regarding the publication of this paper.

Acknowledgments

I would like to extend my appreciation to Drs. Richard Bridges and Mike Kavanaugh (University of Montana) and Dr. Paul Letourneau (University of Minnesota, Minneapolis) for many helpful discussions that were vital in shaping this research. Thanks to Shellie Stewart-Smeets for her contribution on actin filament experiments and Dianne Cabrie for technical assistance. I am indebted to Dr. Mark Wright (University of Alaska, Fairbanks) for his support with native gel electrophoresis and Dr. Kelly Auer (University of Alaska, Fairbanks) for her support with MAP kinase analysis. Support for this work was provided by the Christopher Reeve Paralysis Foundation (KA1-0004-2), NIH/NINDS grant 1U54NS41069, and COBRE The University of Montana.

References

[1] S. Amor, F. Puentes, D. Baker, and P. van der Valk, "Inflammation in neurodegenerative diseases," *Immunology*, vol. 129, no. 2, pp. 154–169, 2010.

[2] M. Cacquevel, N. Lebeurrier, S. Chéenne, and D. Vivien, "Cytokines in neuroinflammation and Alzheimer's disease," *Current Drug Targets*, vol. 5, no. 6, pp. 529–534, 2004.

[3] S.-M. Lucas, N. J. Rothwell, and R. M. Gibson, "The role of inflammation in CNS injury and disease," *British Journal of Pharmacology*, vol. 147, supplement 1, pp. S232–S240, 2006.

[4] M. K. McCoy and M. G. Tansey, "TNF signaling inhibition in the CNS: implications for normal brain function and neurodegenerative disease," *Journal of Neuroinflammation*, vol. 5, article 45, 2008.

[5] R. E. Mrak and W. S. T. Griffin, "Glia and their cytokines in progression of neurodegeneration," *Neurobiology of Aging*, vol. 26, no. 3, pp. 349–354, 2005.

[6] B. Viviani, S. Bartesaghi, E. Corsini, C. L. Galli, and M. Marinovich, "Cytokines role in neurodegenerative events," *Toxicology Letters*, vol. 149, no. 1–3, pp. 85–89, 2004.

[7] S. J. Mathew, D. Haubert, M. Krönke, and M. Leptin, "Looking beyond death: a morphogenetic role for the TNF signalling pathway," *Journal of Cell Science*, vol. 122, no. 12, pp. 1939–1946, 2009.

[8] G. Münch, J. Gasic-Milenkovic, S. Dukic-Stefanovic et al., "Microglial activation induces cell death, inhibits neurite outgrowth and causes neurite retraction of differentiated neuroblastoma cells," *Experimental Brain Research*, vol. 150, no. 1, pp. 1–8, 2003.

[9] H. Neumann, R. Schweigreiter, T. Yamashita, K. Rosenkranz, H. Wekerle, and Y.-A. Barde, "Tumor necrosis factor inhibits neurite outgrowth and branching of hippocampal neurons by a Rho-dependent mechanism," *The Journal of Neuroscience*, vol. 22, no. 3, pp. 854–862, 2002.

[10] R. A. Gungabissoon and J. R. Bamburg, "Regulation of growth cone actin dynamics by ADF/cofilin," *Journal of Histochemistry and Cytochemistry*, vol. 51, no. 4, pp. 411–420, 2003.

[11] L. Luo, "Rho GTPases in neuronal morphogenesis," *Nature Reviews Neuroscience*, vol. 1, no. 3, pp. 173–180, 2000.

[12] L. Moldovan, K. Irani, N. I. Moldovan, T. Finkel, and P. J. Goldschmidt-Clermont, "The actin cytoskeleton reorganization induced by Rac1 requires the production of superoxide," *Antioxidants and Redox Signaling*, vol. 1, no. 1, pp. 29–43, 1999.

[13] V. J. Thannickal and B. L. Fanburg, "Reactive oxygen species in cell signaling," *American Journal of Physiology: Lung Cellular and Molecular Physiology*, vol. 279, no. 6, pp. L1005–L1028, 2000.

[14] B. M. Barth, S. Stewart-Smeets, and T. B. Kuhn, "Proinflammatory cytokines provoke oxidative damage to actin in neuronal cells mediated by Rac1 and NADPH oxidase," *Molecular and Cellular Neuroscience*, vol. 41, no. 2, pp. 274–285, 2009.

[15] V. Munnamalai and D. M. Suter, "Reactive oxygen species regulate F-actin dynamics in neuronal growth cones and neurite outgrowth," *Journal of Neurochemistry*, vol. 108, no. 3, pp. 644–661, 2009.

[16] S. Chakraborty, D. K. Kaushik, M. Gupta, and A. Basu, "Inflammasome signaling at the heart of central nervous system pathology," *Journal of Neuroscience Research*, vol. 88, no. 8, pp. 1615–1631, 2010.

[17] M. J. Morgan, Y.-S. Kim, and Z. Liu, "Lipid rafts and oxidative stress-induced cell death," *Antioxidants and Redox Signaling*, vol. 9, no. 9, pp. 1471–1483, 2007.

[18] B. T. Kawahara, M. T. Quinn, and J. D. Lambeth, "Molecular evolution of the reactive oxygen-generating NADPH oxidase (Nox/Duox) family of enzymes," *BMC Evolutionary Biology*, vol. 7, article 109, 2007.

[19] J. D. Lambeth, "NOX enzymes and the biology of reactive oxygen," *Nature Reviews Immunology*, vol. 4, no. 3, pp. 181–189, 2004.

[20] Y. Groemping and K. Rittinger, "Activation and assembly of the NADPH oxidase: a structural perspective," *Biochemical Journal*, vol. 386, no. 3, pp. 401–416, 2005.

[21] A. Leonardi, H. Ellinger-Ziegelbauer, G. Franzoso, K. Brown, and U. Siebenlist, "Physical and functional interaction of filamin (actin-binding protein-280) and tumor necrosis factor receptor-associated factor 2," *The Journal of Biological Chemistry*, vol. 275, no. 1, pp. 271–278, 2000.

[22] M. Peppelenbosch, E. Boone, G. E. Jones et al., "Multiple signal transduction pathways regulate TNF-induced actin reorganization in macrophages: inhibition of Cdc42-mediated filopodium formation by TNF," *Journal of Immunology*, vol. 162, no. 2, pp. 837–845, 1999.

[23] R. Singh, B. Wang, A. Shirvaikar et al., "The IL-1 receptor and rho directly associate to drive cell activation in inflammation,"

Journal of Clinical Investigation, vol. 103, no. 11, pp. 1561–1570, 1999.

[24] T. B. Kuhn, "Growing and working with spinal motor neurons," *Methods in Cell Biology*, vol. 71, pp. 67–87, 2003.

[25] J. E. Bottenstein and G. H. Sato, "Growth of a rat neuroblastoma cell line in serum free supplemented medium," *Proceedings of the National Academy of Sciences of the United States of America*, vol. 76, no. 1, pp. 514–517, 1979.

[26] T. B. Kuhn, M. D. Brown, and J. R. Bamburg, "Rac1-dependent actin filament organization in growth cones is necessary for b1-integrin-mediated advance but not for growth on poly-D-lysine," *Journal of Neurobiology*, vol. 37, pp. 524–540, 1998.

[27] R. Owen Lockerbie, V. E. Miller, and K. H. Pfenninger, "Regulated plasmalemmal expansion in nerve growth cones," *The Journal of Cell Biology*, vol. 112, no. 6, pp. 1215–1227, 1991.

[28] S. Chang, F. G. Rathjen, and J. A. Raper, "Extension of neurites on axons is impaired by antibodies against specific neural cell surface glycoproteins," *The Journal of Cell Biology*, vol. 104, no. 2, pp. 355–362, 1987.

[29] E. T. Stoeckli, T. B. Kuhn, C. O. Duc, M. A. Ruegg, and P. Sonderegger, "The axonally secreted protein axonin-1 is a potent substratum for neurite growth," *The Journal of Cell Biology*, vol. 112, no. 3, pp. 449–455, 1991.

[30] A. Hall, "Rho GTpases and the actin cytoskeleton," *Science*, vol. 279, no. 5350, pp. 509–514, 1998.

[31] T. B. Kuhn, M. D. Brown, C. L. Wilcox, J. A. Raper, and J. R. Bamburg, "Myelin and collapsin-1 induce motor neuron growth cone collapse through different pathways: inhibition of collapse by opposing mutants of rac1," *The Journal of Neuroscience*, vol. 19, no. 6, pp. 1965–1975, 1999.

[32] M. Brown, B. Cornejo, T. Kuhn, and J. Bamburg, "Cdc42 stimulates neurite outgrowth and formation of growth cone filopdia and lamellipodia," *Journal of Neurobiology*, vol. 43, pp. 352–364, 2000.

[33] U. K. Laemmli, "Cleavage of structural proteins during the assembly of the head of bacteriophage T4," *Nature*, vol. 227, no. 5259, pp. 680–685, 1970.

[34] H. Towbin, T. Staehelin, and J. Gordon, "Electrophoretic transfer of proteins from polyacrylamide gels to nitrocellulose sheets: procedure and some applications," *Proceedings of the National Academy of Sciences of the United States of America*, vol. 76, no. 9, pp. 4350–4354, 1979.

[35] T. B. Kuhn, M. F. Schmidt, and S. B. Kater, "Laminin and fibronectin guideposts signal sustained but opposite effects to passing growth cones," *Neuron*, vol. 14, no. 2, pp. 275–285, 1995.

[36] M. A. Wride and E. J. Sanders, "Expression of tumor necrosis factor-α (TNFα)-cross-reactive proteins during early chick embryo development," *Developmental Dynamics*, vol. 198, no. 3, pp. 225–239, 1993.

[37] C. Cypher and P. C. Letourneau, "Identification of cytoskeletal, focal adhesion, and cell adhesion proteins in growth cone particles isolated from developing chick brain," *Journal of Neuroscience Research*, vol. 30, no. 1, pp. 259–265, 1991.

[38] S. Helmke and K. H. Pfenninger, "Growth cone enrichment and cytoskeletal association of non-receptor tyrosine kinases," *Cell Motility and the Cytoskeleton*, vol. 30, no. 3, pp. 194–207, 1995.

[39] P. Negre-Aminou and K. H. Pfenninger, "Arachidonic acid turnover and phospholipase A2 activity in neuronal growth cones," *Journal of Neurochemistry*, vol. 60, no. 3, pp. 1126–1136, 1993.

[40] Z. Jin and S. M. Strittmatter, "Rac1 mediates collapsin-1-induced growth cone collapse," *The Journal of Neuroscience*, vol. 17, no. 16, pp. 6256–6263, 1997.

[41] C. E. Cooper, R. P. Patel, P. S. Brookes, and V. M. Darley-Usmar, "Nanotransducers in cellular redox signaling: modification of thiols by reactive oxygen and nitrogen species," *Trends in Biochemical Sciences*, vol. 27, no. 10, pp. 489–492, 2002.

[42] I. Dalle-Donne, R. Rossi, A. Milzani, P. di Simplicio, and R. Colombo, "The actin cytoskeleton response to oxidants: from small heat shock protein phosphorylation to changes in the redox state of actin itself," *Free Radical Biology and Medicine*, vol. 31, no. 12, pp. 1624–1632, 2001.

[43] I. Lassing, F. Schmitzberger, M. Björnstedt et al., "Molecular and structural basis for redox regulation of β-actin," *Journal of Molecular Biology*, vol. 370, no. 2, pp. 331–348, 2007.

[44] A. S. Nimnual, L. J. Taylor, and D. Bar-Sagi, "Redox-dependent downregulation of Rho by Rac," *Nature Cell Biology*, vol. 5, no. 3, pp. 236–241, 2003.

[45] S. J. Gustafson, K. L. Dunlap, C. M. McGill, and T. B. Kuhn, "A nonpolar blueberry fraction blunts NADPH oxidase activation in neuronal cells exposed to tumor necrosis factor-α," *Oxidative Medicine and Cellular Longevity*, vol. 2012, Article ID 768101, 12 pages, 2012.

[46] J. E. Merrill, "Tumor necrosis factor alpha, interleukin 1 and related cytokines in brain development: normal and pathological," *Developmental Neuroscience*, vol. 14, no. 1, pp. 1–10, 1992.

[47] P. L. Hordijk, "Regulation of NADPH oxidases: the role of Rac proteins," *Circulation Research*, vol. 98, no. 4, pp. 453–462, 2006.

[48] K. M. Noh and J. Y. Koh, "Induction and activation by zinc of NADPH oxidase in cultured cortical neurons and astrocytes," *The Journal of Neuroscience*, vol. 20, no. 23, article RC111, 2000.

[49] P. Vallet, Y. Charnay, K. Steger et al., "Neuronal expression of the NADPH oxidase NOX4, and its regulation in mouse experimental brain ischemia," *Neuroscience*, vol. 132, no. 2, pp. 233–238, 2005.

[50] M. Dvorakova, B. Höhler, E. Richter, J. B. Burritt, and W. Kummer, "Rat sensory neurons contain cytochrome b558 large subunit immunoreactivity," *NeuroReport*, vol. 10, no. 12, pp. 2615–2617, 1999.

[51] S. P. Tammariello, M. T. Quinn, and S. Estus, "NADPH oxidase contributes directly to oxidative stress and apoptosis in nerve growth factor-deprived sympathetic neurons," *The Journal of Neuroscience*, vol. 20, no. 1, article RC53, 2000.

[52] A. Puls, A. G. Eliopoulos, C. D. Nobes, T. Bridges, L. S. Young, and A. Hall, "Activation of the small GTPase Cdc42 by the inflammatory cytokines TNFα and IL-1, and by the Epstein-Barr virus transforming protein LMP1," *Journal of Cell Science*, vol. 112, no. 17, pp. 2983–2992, 1999.

[53] B. Wojciak-Stothard, A. Entwistle, R. Garg, and A. Ridley, "Regulation of TNF alpha-induced reorganization of the actin cytoskeleton and cell-cell junctions by rho, rac, and cdc42 in human endothelial cells," *Journal of Cell Physiology*, vol. 176, pp. 150–165, 1998.

[54] A. Hall and C. D. Nobes, "Rho GTPases: molecular switches that control the organization and dynamics of the actin cytoskeleton," *Philosophical Transactions of the Royal Society B: Biological Sciences*, vol. 355, no. 1399, pp. 965–970, 2000.

[55] G. Meyer and E. L. Feldman, "Signaling mechanisms that regulate actin-based motility processes in the nervous system," *Journal of Neurochemistry*, vol. 83, no. 3, pp. 490–503, 2002.

[56] K. Suzukawa, K. Miura, J. Mitsushita et al., "Nerve growth factor-induced neuronal differentiation requires generation of rac1-regulated reactive oxygen species," *The Journal of Biological Chemistry*, vol. 275, no. 18, pp. 13175–13178, 2000.

[57] J. L. Freeman, A. Abo, and J. D. Lambeth, "Rac "insert region" is a novel effector region that is implicated in the activation of NADPH oxidase, but not PAK65," *The Journal of Biological Chemistry*, vol. 271, no. 33, pp. 19794–19801, 1996.

[58] T. Joneson and D. Bar-Sagi, "A Rac1 effector site controlling mitogenesis through superoxide production," *The Journal of Biological Chemistry*, vol. 273, no. 29, pp. 17991–17994, 1998.

[59] A. E. Karnoub, C. J. Der, and S. L. Campbell, "The insert region of Rac1 is essential for membrane ruffling but not cellular transformation," *Molecular and Cellular Biology*, vol. 21, no. 8, pp. 2847–2857, 2001.

[60] S. M. Allan and N. J. Rothwell, "Cytokines and acute neurodegeneration," *Nature Reviews Neuroscience*, vol. 2, no. 10, pp. 734–744, 2001.

[61] Y. Sei, L. Vitkovic, and M. M. Yokoyama, "Cytokines in the central nervous system: regulatory roles in neuronal function, cell death and repair," *Neuroimmunomodulation*, vol. 2, no. 3, pp. 121–133, 1995.

[62] L. Vitkovic, J. Bockaert, and C. Jacque, ""Inflammatory" cytokines: neuromodulators in normal brain?" *Journal of Neurochemistry*, vol. 74, no. 2, pp. 457–471, 2000.

[63] K. Bedard and K.-H. Krause, "The NOX family of ROS-generating NADPH oxidases: physiology and pathophysiology," *Physiological Reviews*, vol. 87, no. 1, pp. 245–313, 2007.

[64] T. Kawahara and J. D. Lambeth, "Molecular evolution of Phox-related regulatory subunits for NADPH oxidase enzymes," *BMC Evolutionary Biology*, vol. 7, article 178, 2007.

[65] K.-H. Krause, D. Lambeth, and M. Krönke, "NOX enzymes as drug targets," *Cellular and Molecular Life Sciences*, vol. 69, no. 14, pp. 2279–2282, 2012.

[66] J. D. Lambeth, K.-H. Krause, and R. A. Clark, "NOX enzymes as novel targets for drug development," *Seminars in Immunopathology*, vol. 30, no. 3, pp. 339–363, 2008.

[67] H.-M. Gao, H. Zhou, and J.-S. Hong, "NADPH oxidases: novel therapeutic targets for neurodegenerative diseases," *Trends in Pharmacological Sciences*, vol. 33, no. 6, pp. 295–303, 2012.

Hindawi Publishing Corporation
BioMed Research International
Volume 2014, Article ID 209845, 9 pages
http://dx.doi.org/10.1155/2014/209845

Review Article

A Paradoxical Chemoresistance and Tumor Suppressive Role of Antioxidant in Solid Cancer Cells: A Strange Case of Dr. Jekyll and Mr. Hyde

Jolie Kiemlian Kwee

Coordenação de Pesquisa, Instituto Nacional de Câncer, Rua André Cavalcante 37, 20231-050, Rio de Janeiro, RJ, Brazil

Correspondence should be addressed to Jolie Kiemlian Kwee; jkwee@inca.gov.br

Received 5 December 2013; Revised 16 March 2014; Accepted 17 March 2014; Published 3 April 2014

Academic Editor: David Vauzour

Modulation of intracellular antioxidant concentration is a double-edged sword, with both sides exploited for potential therapeutic benefits. While antioxidants may hamper the efficacy of chemotherapy by scavenging reactive oxygen species and free radicals, it is also possible that antioxidants alleviate unwanted chemotherapy-induced toxicity, thus allowing for increased chemotherapy doses. Under normoxic environment, antioxidants neutralize toxic oxidants, such as reactive oxygen species (ROS), maintaining them within narrow boundaries level. This redox balance is achieved by various scavenging systems such as enzymatic system (e.g., superoxide dismutases, catalase, and peroxiredoxins), nonenzymatic systems (e.g., glutathione, cysteine, and thioredoxin), and metal-binding proteins (e.g., ferritin, metallothionein, and ceruloplasmin) that sequester prooxidant metals inhibiting their participation in redox reactions. On the other hand, therapeutic strategies that promote oxidative stress and eventually tumor cells apoptosis have been explored based on availability of chemotherapy agents that inhibit ROS-scavenging systems. These contradictory assertions suggest that antioxidant supplementation during chemotherapy treatment can have varied outcomes depending on the tumor cellular context. Therefore, understanding the antioxidant-driven molecular pathways might be crucial to design new therapeutic strategies to fight cancer progression.

1. Introduction

Reactive oxygen and nitrogen species (ROS/RNS) are oxidants natural products formed during cell vital metabolism activity that orchestrate the transmission of regulatory signals for proliferation, migration, defence, vasorelaxation, autophagy, and apoptosis signals (Figure 1(a)) [1–12]. Progress in redox biochemistry study has revealed an oxygen adaptation, whereby the cell has acquired the capability to initiate changes to the local redox environment as a means of regulating signaling pathways [1–4, 6–11]. This has changed the way cellular oxidant production is viewed, from a simplistic model where all oxidant production is inherently damaging to a more complex scenario where a regulated small increase in oxidant production can be essential for optimal cellular function (Figure 1) [1–12]. In this model ROS and RNS act as second messengers, forming an integral part of the signal transduction network [1–4, 9, 11, 12]. Reactive nitrogen species are produced by the endothelium inducing vascular relaxation when vascular smooth muscle cells were stimulated with vasodilators such as acetylcholine, histamine, and bradykinin. Nitric oxide synthase catalyzes a five-electron oxidation of a guanidine nitrogen of L-arginine in the formation of citrulline and nitric oxide [7–9, 11, 12]. On the other hand, ROS are heterogeneous group diatomic oxygen derived of free and nonfree radicals species with a wide range of reactivity [10–12]. Their formation begins with the univalent reduction of oxygen to produce superoxide radical ($O_2^{\bullet -}$), a free radical that gives rise to many highly reactive species such as hydroperoxyl radical ($HO_2^{\bullet}$), hydrogen peroxide (H_2O_2), and hydroxyl radical ($^{\bullet}OH$) (Figure 2) [10–12]. For example, superoxide can dismutate to form hydrogen peroxide (H_2O_2), a membrane-permeable, mildly prooxidant molecule which in turn can lead to formation of several highly oxidizing derivatives such as hydroxyl radicals (Figure 2). Also, $O_2^{\bullet -}$ can react with nitric oxide ($NO^{\bullet}$) resulting in peroxynitrite ($OONOO^-$), a high RNS (Figure 2) [11, 12]. Mitochondria

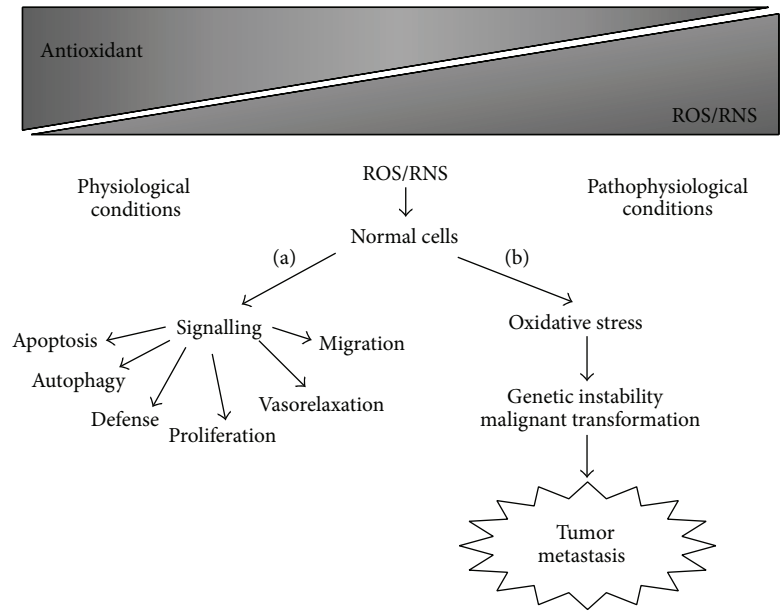

Figure 1: Schematic representation of reactive oxygen and nitrogen species (ROS/RNS) inductions in physiological (a) and pathophysiological (b) conditions.

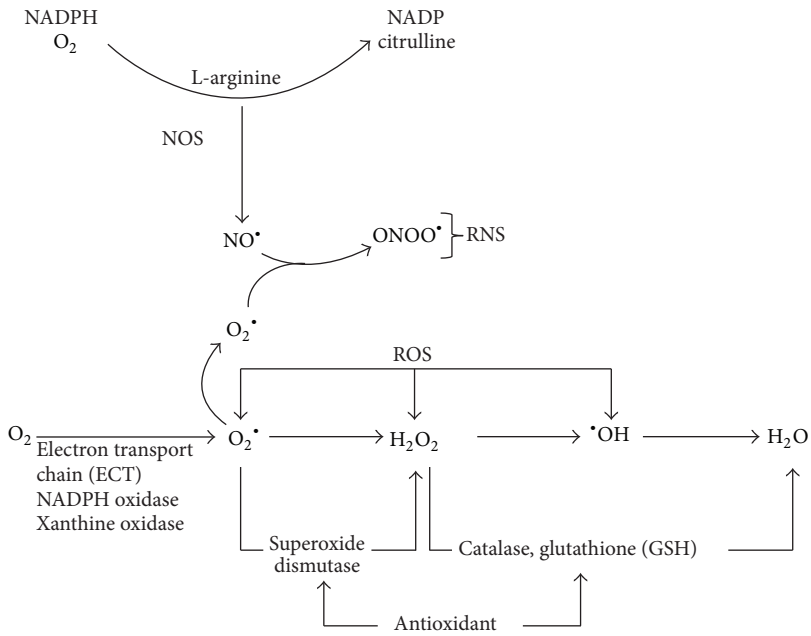

Figure 2: Sources of reactive oxygen (ROS) and nitrogen (RNS) species production. Enzymatic and nonenzymatic antioxidants counterbalance it.

form the major powerhouse of ROS production; they are generated in association with the activity of the respiratory chain such as NADH dehydrogenase enzyme complexes in aerobic ATP production [13–15]. In addition, two classic phagocytic ROS-generating enzymes use molecular oxygen as a substrate, including the multisubunit NADPH oxidase and its homologue NOX/Duox family and myeloperoxidase in various tissues in response to extracellular influences [16, 17]. Other sources of ROS production include the cytochrome P450 (CYP450) system, which is involved mainly in removing or detoxifying toxic substances in the liver [13] and xanthine oxidase which catalyzes the oxidation of hypoxanthine to xanthine with the formation of H_2O_2 [18]. The imbalance of this cellular redox state is characteristic of many diseases where abnormal oxidant production causes extensive tissue damage (Figure 1(b)) [3, 6, 19]. Antioxidant has been defined as any substance that significantly delays or prevents oxidative damage of an oxidizable substrate (Figure 2). Due to their high reactivity, the ROS production levels are tightly controlled by antioxidants to avoid oxidative

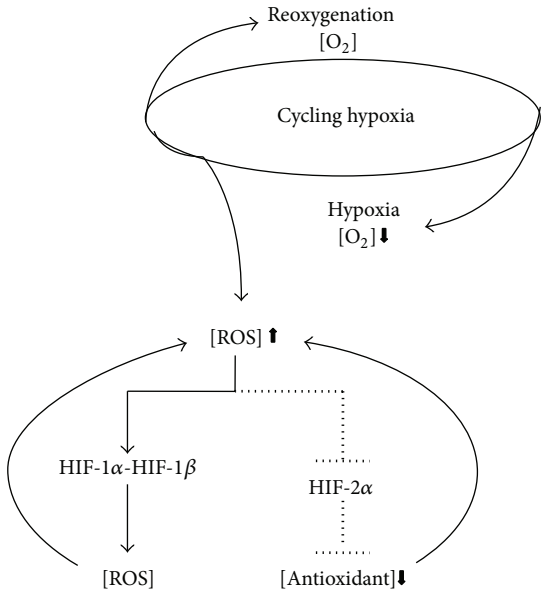

Figure 3: Schematic representation of cycling hypoxia effects on ROS production through activities modulations of HIF-1α and HIF-2α.

stress and, eventually, oxidative damage which is frequently linked to genetic instability, tumor promotion, and metastasis (Figure 1) [20]. On the other hand, the primary mechanism of many chemotherapy drugs and ionizing radiation, widely used against cancer cells, is the formation of ROS [11, 21]. At this point, questions arise whether reduction of oxidative stress in tumor cell environment with antioxidant treatment would be beneficial or not [22]. Moreover, it should be stressed that the antioxidants cannot distinguish between the radicals that play a beneficial role and those that cause carcinogenesis. Understanding the biological redox system for the development of more effective and less toxic chemotherapy ROS induction strategies for cancer cells is deserved [21, 22]. Therefore, the modulation of intracellular antioxidant concentration is a double-edged sword, with both sides exploited for potential therapeutic benefits.

2. ROS and Hypoxia in Solid Tumors

Solid tumors are known to have a poor microvascular network and high interstitial fluid pressure resulting in hypoxic environment conferring chemo and radiotherapy resistance [22]. There are three major forms of hypoxia that varies with the duration: acute, chronic, and intermittent. Acute hypoxia occurs when tumor vessels become temporarily hypoxic for a period of seconds or a few hours. Chronic hypoxia is a progressive and severe reduction in oxygen (hours to days) [22]. Intermittent hypoxia, also referred to as cycling hypoxia, is characterized by cyclic periods of hypoxia and reoxygenation and plays the main role in resistance of solid tumor treatments (Figure 3) [23–26]. Hypoxic microenvironments are characterized by extreme heterogeneities in tumor cells oxygenation that arise as a result of the increased oxygen diffusion distance due to tumor expansion and poorly developed vascular networks [22, 27]. Gradients in oxygen are frequently found surrounding perfused vessels, ranging from normal values near the blood vessel to complete anoxia adjacent to necrosis [27, 28]. The balanced proportion of hypoxic cells in cancer is driven by the tolerance of individual cells to these different types of hypoxia and varies remarkably among different tumors with otherwise similar clinical features [29]. These differences are important, because the fraction of viable hypoxic cells is a major determinant of prognosis, as hypoxic cells are highly resistant to chemotherapy and radiation therapy (Figure 3). Reducing cellular tolerance to hypoxia is therefore a strategy to reduce the proportion of hypoxic cells in tumors to improve current cancer therapy [27–33]. Tumor cells can adapt to hypoxic conditions by employing a variety of survival tools, which result in the promotion of cancer cell growth and metastasis [22, 32]. This adaptation is mainly mediated by hypoxia-inducible factor-1 (HIF-1) (Figure 3). HIF-1 is a heterodimeric transcription factor consisting of an oxygen-regulated subunit (HIF-1α) and a stable nuclear factor, HIF-1β aryl hydrocarbon receptor nuclear translocator (ARNT). Under normoxic conditions, HIF-1α is hydroxylated by prolyl hydroxylase (PHD) at proline 402 and proline 564, and the hydroxylated HIF-1α recruits von Hippel-Lindau (pVHL), an E3 ubiquitin protein ligase, and is rapidly degraded by the proteasome after being targeted for ubiquitination (Figure 3). Under hypoxic conditions, cytosolic HIF-1α is stabilized by inhibition of the oxygen- and PHD-dependent enzymatic hydroxylation of proline residues and subsequently translocated to the nucleus, where it binds HIF-1β [30, 34, 35]. The complex binds to the hypoxia-response element in its targets, which results in the transactivation of numerous genes encoding proteins necessary for the blood supply, energy production, growth/survival, invasion/metastasis, and chemo/radioresistance (Figure 4) [30, 35]. An association of HIF-1α overexpression with cell proliferation and poor prognosis has been observed in many kinds of human cancers [30, 34, 35]. It is well known that hypoxic conditions increase intracellular ROS levels [14] and recent studies provide important insights into the molecular mechanisms by which cycling hypoxia increases the oxidative stress [24]. This constant generation of ROS through intensive cycling hypoxia stabilizes HIF-1α by preventing its degradation and induces HIF-2α degradation (Figure 3). Since HIF-1α regulates genes encoding prooxidant enzymes and HIF-2α is a potent regulator of the genes encoding antioxidant enzymes, it was proposed that both HIFs contribute in part to the oxidative stress caused by cycling hypoxia. [36–39]. Ironically the main mechanism of ionizing irradiation and many anticancer drugs to induce apoptosis is through ROS which activate HIF-1α [11, 30].

3. ROS and Chemotherapeutic Drugs

Despite great improvements in screening strategies and adjuvant therapies, current treatments still rely heavily on conventional chemotherapy for most cancers. Additionally, most of these conventional chemotherapies agents such as taxanes, anthracyclines, and platinum coordination complexes induce ROS [11, 40–42] and are somehow cardiotoxic [43, 44].

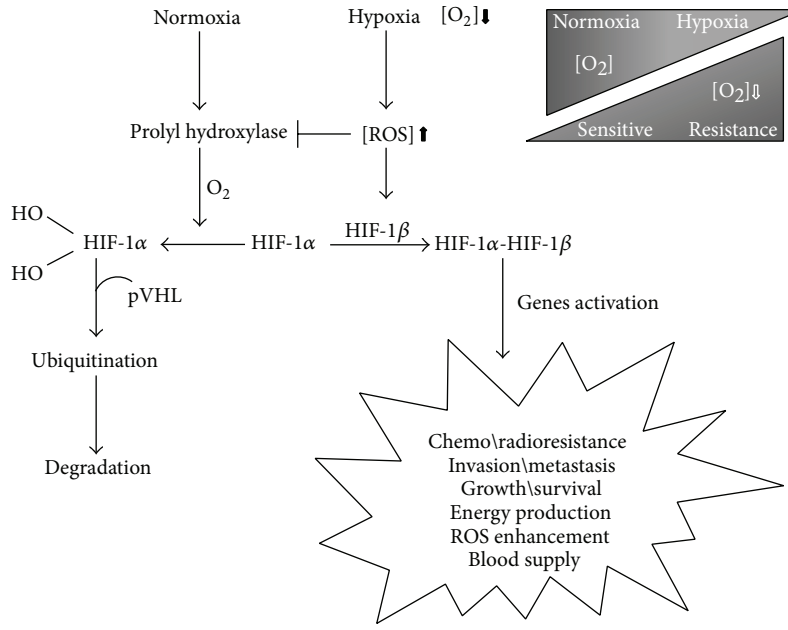

Figure 4: Role of ROS in hypoxia and normoxia.

Hence, the efficacy of these prooxidant chemotherapeutic agents is dose-dependent, which is limited by toxicity to nontumor tissues, as a result of its poor tumor selectivity. Modulation of ROS levels by antioxidants may be effective in protecting nontumor tissues especially the heart from oxidative damage but they may also reduce the efficacy of these anticancer drugs [43]. Nevertheless, the mechanism by which these chemotherapeutic agents inducers exhibit antitumor effects is likely multifactorial. Consequently, to improve survival length and preserve quality of life, the challenge is to develop approaches aimed at increasing chemotherapy toxicity to tumor tissue while not affecting nontumor tissues [43, 44]. Therefore, the degree to which ROS contribute to the antineoplastic effects of these chemotherapeutic drugs should be evaluated.

4. Antioxidants Playing Hyde and Jekyll

4.1. Exogenous Antioxidant. In order to maintain an appropriate level of ROS and regulate their action, the body's natural defense against oxidative stress consists of several antioxidative systems. Therefore, mammalian cells have developed many enzymatic and nonenzymatic antioxidative systems [20, 45, 46] as well as transfer proteins that sequester prooxidant metals inhibiting their participation in redox reactions (Table 1) [47]. Components of the endogenous antioxidant defense system work together and in concert with dietary antioxidants (Table 2) [20, 21, 46] to prevent and reduce oxidative stress. In addition, the antioxidant activity of many of these enzymes and compounds is reliant upon minerals derived from the diet such as selenium, copper, manganese, and zinc (Table 2) [48]. Much debate has focused on the use of antioxidant supplements by patients undergoing chemotherapy due to concerns that the antioxidants may interfere with the mechanism of action of the therapeutic agent and subsequently decrease its efficacy [21, 49]. On the other hand, others argue that antioxidant supplements are beneficial to patients undergoing chemotherapy because they enhance the efficacy of the chemotherapy as well as alleviate toxic side effects, allowing patients to tolerate chemotherapy for the full course of treatment and lessen the need for dose reduction [20, 43]. Despite convincing

Table 1: Endogenous antioxidants.

Endogenous antioxidants	Examples
Enzymes	Superoxide dismutase
	Catalase
	Peroxiredoxins
GSH enzyme-linked system	Glutathione peroxidase
	Glutathione S-transferase
	Glutathione reductase
Nonenzymes	Glutathione
	Cysteine
	Thioredoxin
Metal-binding proteins	Ferritin
	Metallothionein
	Ceruloplasmin

Table 2: Exogenous antioxidants.

Example of exogenous antioxidants		
Vitamin C	⟶	Ascorbate/ascorbic acid
Vitamin E	⟶	Tocopherols, tocotrienols
Carotenoids	⟶	α-carotene, β-carotene, lycopene
Polyphenols	⟶	Flavonols, flavanols, anthocyanins, isoflavones, phenolic acid
Trace elements	⟶	Selenium, copper, manganese, zinc

evidence from preclinical experiments, clinical trials that tested dietary antioxidant nutrients and micronutrients as cancer chemoprevention agents have been unsuccessful or even resulted in harm [49, 50]. The lack of success in clinical trials and the discrepancies with preclinical experiments can be explained by factors, such as (i) lack of biological rationale for selecting the specific agents of interest, (ii) limited number of agents tested to date, and (iii) insufficient duration of the interventions and follow-up. Moreover, this high level of heterogeneity within epidemiological data may support the existence of other factors that could modulate the relationship between antioxidant and cancer development, explaining contrasted results across different populations [21, 49].

4.2. Endogenous Antioxidants. Modulation of endogenous antioxidants is among other strategies to balance the intracellular redox levels. Among the various ROS metabolically generated, H_2O_2, the nonradical two-electron reduction product of oxygen, emerged as central hub in redox signaling and oxidative stress. Processes such as proliferation, differentiation, inflammation, and apoptosis use H_2O_2 as signaling compound. Metabolic sinks of this low-molecular-weight include the peroxidatic reaction carried out by catalase and numerous peroxidases [51]. However, due to the high affinity of H_2O_2 for thiol residues, the new and expanding family of thiol-specific antioxidant enzymes, peroxiredoxins, has received considerable attention. Indeed, under physiological conditions, eukaryotic peroxiredoxins are responsible for the reduction of 90% of intracellular H_2O_2. On the other hand, peroxiredoxins can be easily inactivated by H_2O_2, disabling peroxidase activity and therefore limiting their ability to act as antioxidant, particularly in an oxidative environment like inflammation and intermittent hypoxia [52]. Notably, enhancement of GSH levels was described in hypoxic intracellular environment [53, 54]. Glutathione (GSH) is considered to be the major thiol-disulfide redox buffer of the cell. On average, the GSH intracellular concentration is 0.5–10 mM [55]. This is far higher than most redox active compounds making GSH an important intracellular antioxidant and redox potential regulator that plays a vital role in drug detoxification and cellular protection from damage by free radicals, peroxides, and toxins [56]. Given the range of critical cellular functions involving GSH, it has long been considered that the modulation of intracellular GSH levels would be of great clinical benefits. Enhancement of GSH levels for cytoprotection is available by the administration of its precursor N-Acetyl cysteine, since direct administration of reduced GSH has physical and chemical limitations [56, 57]. Contrastingly, these cytoprotective effects of GSH and its associated enzymes in many types of cancer lead to an increased tumor cell survival and chemotherapy drug resistance [58].

4.2.1. Glutathione and Chemoresistance. Preclinical studies of chemosensitization through antioxidant modulation have been reported in different tumor cells [44, 58–60]. However, chemoresistance is a complex system with multiple and heterogeneous mechanisms of action which are orchestrated not only by the tumor microenvironments but also by the biology of the tumor [61, 62]. Although most of the chemotherapeutic drugs are prooxidants, not all the cancer cell death induction pathways are ROS-dependent [43]. Nevertheless, chemoresistance is not caused by a single factor but rather contributed by combinations of many drug-resistant factors such as (1) reduced intracellular drug accumulation which may result from changes in drug transportation (increased efflux and decreased influx of anticancer drugs) and/or enhancement of detoxification activity; (2) increased DNA repair involving increased nucleotide excision repair, interstrand crosslink repair, or loss mismatch repair; (3) changes in the apoptotic cell death pathways; and (4) intracellular elevated antioxidant levels [63]. Among the antioxidants involved in the maintenance of intracellular redox balance, a main role is played by glutathione (GSH) [57]. GSH and its related enzymes participate not only in the antioxidant defense systems, but also in some drug-resistance metabolic processes such as detoxification and efflux of xenobiotics and blockage of the apoptosis tumor cell death pathway [58]. GSH is a major contributing factor to drug resistance by interacting with chemotherapeutic drugs such as cisplatin and trisenox [64, 65]. In fact, there are clinical evidences supporting a role of the GSH system in overcoming drug resistance and/or toxicity in solid tumors (e.g., lung cancers and bladder) treatments outcome [60, 63]. Therefore, much effort has been directed at depleting cellular GSH levels in order to sensitize tumor cells to the cytotoxic effects of anticancer drugs. The use of buthionine sulfoximine (BSO), an inhibitor of GSH synthesis [66], was performed in clinical trials [67–70]. However, the approach was limited by BSO availability and lack of selectivity of this drug for tumor versus normal cells [56]. But it is notable that GSH plays an important role in drug resistance and its depletion demonstrated to be effective in the sensitization of different types of cancer patients to cytotoxic chemotherapy [67–70]. Another alternative in progress is the development and optimization of GSH analogues that inhibit the enzyme glutathione-S-transferase (GST) responsible for the detoxification overcoming, therefore, chemoresistance [56, 71]. Among the GSH analogues developed, one (TLK 286), which is in clinical trial phase 3 settings for non-small-cell lung and ovarian cancer, appears to sensitize these tumors to cytotoxic chemotherapies [56]. However, the lack of tumor specificity is still a potential problem.

4.3. Antioxidant and Possible Clinical Benefits. Altogether, it should be recognized that understanding the redox biochemistry differences between normal and cancer cells is essential for the design and development of strategies to overcome oxidative damage or prooxidant chemoresistance [61, 62]. Even within a specific cancer type, the malignant cell populations are heterogeneous and intracellular oxidative levels may change as the disease progress [61]. Consequently, studying intra- and intertumor heterogeneous distribution of antioxidants levels may be an important factor to overcome tumor progression. Additionally, it is known that alterations in cellular redox metabolism play a crucial role in the activation or loss of tumor suppressor proteins activities such as breast cancer susceptibility gene breast cancer 1 (BRCA1) and phosphatase and tensin homolog deleted on chromosome 10

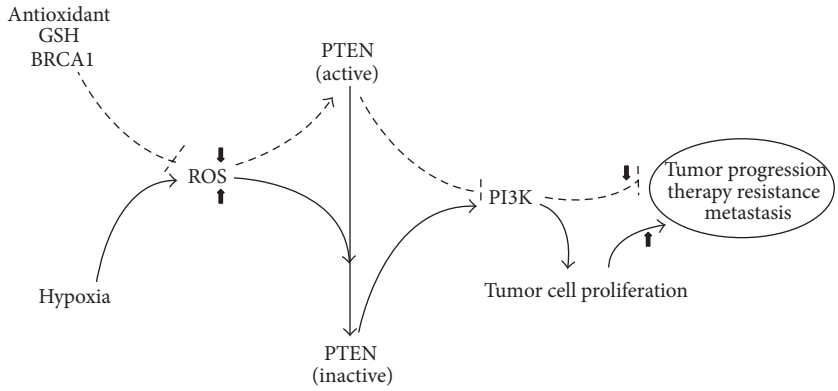

Figure 5: Possible clinical benefits of antioxidant in tumor progression.

(PTEN) [3, 72–78]. The BRCA1 is an oncosuppressor gene with a relatively broad cellular role such as DNA repair (including nucleotide excision repair, NER, and double-strand break repair, DSBR), transcriptional regulation, and chromatin remodeling [79–83]. Notably, BRCA1 has also an antioxidant role in response to oxidative stress in which ROS cause DNA damage due to oxidation [73–75]. Loss or mutation of the BRCA1 gene was firstly described to be associated with increased risk of breast and ovarian cancers [80, 82–86]. Moreover, BRCA1 expression has been correlated with cancer aggressiveness and chemotherapy sensitivity in other solid tumors such as prostate [87–89], non-small-cell lung cancer [90–94], and pancreas [95, 96]. The superfamily of protein tyrosine phosphatase (PTP) enzymes functions in a coordinated pattern with protein tyrosine kinases to control the cellular regulatory signal processes such as cell growth, proliferation, and differentiation [97–100]. PTEN, a class 2 VH1-like (poxvirus vaccinia) DUSP (dual specificity phosphatase) [100] and likewise a member of phosphatase protein family, is modulated by ROS [98, 101]. The oxidation of the active site Cys by ROS abrogates PTEN catalytic activity and, thereby, switching on the phosphatidylinositol-3-kinase (PI3K) proliferation pathway [72, 75–77, 100, 101]. The tumor suppressor PTEN is one of the most frequently mutated genes in human cancer and is generally associated with advanced cancers and metastases [72]. A recent study reveals that PTEN loss activity is the most important alteration for cellular malignant transformation in mammary epithelial cells [102]. A recent study reveals that PTEN loss activity is a common event in breast cancers caused by BRCA1 deficiency [103] due to ROS enhancement. Recently, the modulation of other tumor suppressor genes was described to be ROS-dependent [78, 104, 105]. Therefore, the use of antioxidant might protect the biomarkers ROS-dependent tumorigenesis like BRCA1 and PTEN (Figure 5).

5. Conclusions

Enhancing the capacity of antioxidant in order to protect cells from redox-related changes or environmental toxins represents a persistent aim in the search for cytoprotective strategies against cancer. On the contrary, the strategy of depleting antioxidant is aimed at sensitizing cancer cells to chemotherapy, the so-called chemosensitization. In this context, it has been reported that antioxidant may be a determining factor for the sensitivity of some tumors to various chemotherapeutic agents. In particular, GSH and GSH enzyme-linked system are a relevant parameter for chemotherapy response, and it may be utilized as a useful biomarker for selecting tumors potentially responsive to chemotherapeutic regiments. The involvement of antioxidant in the carcinogenesis and in the drug resistance of tumor cell is clear, but further studies, aimed at understanding the antioxidant-driven molecular pathways and the biology of the tumor cells, are crucial to design new therapeutic strategies to fight cancer progression and overcome chemoresistance.

Conflict of Interests

The author declares that there is no conflict of interests regarding the publication of this paper.

Acknowledgments

The author would like to express the deepest gratitude to A. C. S. Ferreira, B. M. Bomfim, L. F. R. Silva, and R. A. Fernandes, who believed in their project from the start and, in particular, to D. F. Baptista to whom this paper is dedicated. This work was supported by grants from Fundação do Câncer (FAF).

References

[1] J. P. Fruehauf and F. L. Meyskens Jr., "Reactive oxygen species: a breath of life or death?" *Clinical Cancer Research*, vol. 13, no. 3, pp. 789–794, 2007.

[2] M. L. Circu and T. Y. Aw, "Reactive oxygen species, cellular redox systems, and apoptosis," *Free Radical Biology and Medicine*, vol. 48, no. 6, pp. 749–762, 2010.

[3] T. Finkel, "Signal transduction by reactive oxygen species," *Journal of Cell Biology*, vol. 194, no. 1, pp. 7–15, 2011.

[4] M. Dodson, V. Darley-Usmar, and J. Zhang, "Cellular metabolic and autophagic pathways: traffic control by redox signaling," *Free Radical Biology and Medicine*, vol. 63, pp. 207–221, 2013.

[5] M. Jimenez-Del-Rio and C. Velez-Pardo, "The bad, the good, and the ugly about oxidative stress," *Oxidative Medicine and Cellular Longevity*, vol. 2012, Article ID 163913, 13 pages, 2012.

[6] V. A. Kobliakov, "Mechanisms of tumor promotion by reactive oxygen species," *Biochemistry (Moscow)*, vol. 75, no. 6, pp. 675–685, 2010.

[7] J. S. Beckman and W. H. Koppenol, "Nitric oxide, superoxide, and peroxynitrite: the good, the bad, and the ugly," *American Journal of Physiology: Cell Physiology*, vol. 271, no. 5, pp. C1424–C1437, 1996.

[8] J. S. Stamler, D. J. Singel, and J. Loscalzo, "Biochemistry of nitric oxide and its redox-activated forms," *Science*, vol. 258, no. 5090, pp. 1898–1902, 1992.

[9] J. Loscalzo, "The identification of nitric oxide as endothelium-derived relaxing factor," *Circulation Research*, vol. 113, no. 2, pp. 100–103, 2013.

[10] I. Fridovich, "Oxygen toxicity: a radical explanation," *The Journal of Experimental Biology*, vol. 201, no. 8, pp. 1203–1209, 1998.

[11] B. Kalyanaraman, "Teaching the basics of redox biology to medical and graduate students: oxidants, antioxidants and disease mechanisms," *Redox Biology*, vol. 1, no. 1, pp. 244–257, 2013.

[12] L. F. Olsen, O. G. Issinger, and B. Guerra, "The yin and yang of redox regulation," *Redox Report*, vol. 18, no. 6, pp. 245–252, 2013.

[13] P. Ježek and L. Hlavatá, "Mitochondria in homeostasis of reactive oxygen species in cell, tissues, and organism," *The International Journal of Biochemistry and Cell Biology*, vol. 37, no. 12, pp. 2478–2503, 2005.

[14] R. O. Poyton, K. A. Ball, and P. R. Castello, "Mitochondrial generation of free radicals and hypoxic signaling," *Trends in Endocrinology and Metabolism*, vol. 20, no. 7, pp. 332–340, 2009.

[15] C. L. Quinlan, I. V. Perevoshchikova, M. Hey-Mogensen et al., "Sites of reactive oxygen species generation by mitochondria oxidizing different substrates," *Redox Biology*, vol. 1, no. 1, pp. 304–312, 2013.

[16] J. D. Lambeth, T. Kawahara, and B. Diebold, "Regulation of Nox and Duox enzymatic activity and expression," *Free Radical Biology and Medicine*, vol. 43, no. 3, pp. 319–331, 2007.

[17] R. P. Brandes, N. Weissmann, and K. Schröder, "Nox family NADPH oxidases in mechano-transduction: mechanisms and consequences," *Antioxidants and Redox Signaling*, vol. 20, no. 6, pp. 887–898, 2014.

[18] N. Cantu-Medellin and E. E. Kelley, "Xanthine oxidoreductase-catalyzed reactive species generation: a process in critical need of reevaluation," *Redox Biology*, vol. 1, no. 1, pp. 353–358, 2013.

[19] J. Lugrin, N. Rosenblatt-Velin, R. Parapanov et al., "The role of oxidative stress during inflammatory processes," *Biological Chemistry*, vol. 395, no. 2, pp. 203–230, 2014.

[20] V. Fuchs-Tarlovsky, "Role of antioxidants in cancer therapy," *Nutrition*, vol. 29, no. 1, pp. 15–29, 2012.

[21] K. I. Block, A. C. Koch, M. N. Mead, P. K. Tothy, R. A. Newman, and C. Gyllenhaal, "Impact of antioxidant supplementation on chemotherapeutic toxicity: a systematic review of the evidence from randomized controlled trials," *International Journal of Cancer*, vol. 123, no. 6, pp. 1227–1239, 2008.

[22] J. Denekamp, A. Daşu, and A. Waites, "Vasculature and microenvironmental gradients: the missing links in novel approaches to cancer therapy?" *Advances in Enzyme Regulation*, vol. 38, no. 1, pp. 281–299, 1998.

[23] C. Cooper, G.-Y. Liu, Y.-L. Niu, S. Santos, L. C. Murphy, and P. H. Watson, "Intermittent hypoxia induces proteasome-dependent down-regulation of estrogen receptor α in human breast carcinoma," *Clinical Cancer Research*, vol. 10, no. 24, pp. 8720–8727, 2004.

[24] C.-H. Hsieh, C.-H. Lee, J.-A. Liang, C.-Y. Yu, and W.-C. Shyu, "Cycling hypoxia increases U87 glioma cell radioresistance via ROS induced higher and long-term HIF-1 signal transduction activity," *Oncology Reports*, vol. 24, no. 6, pp. 1629–1636, 2010.

[25] Y. Liu, X. Song, X. Wang et al., "Effect of chronic intermittent hypoxia on biological behavior and hypoxia-associated gene expression in lung cancer cells," *Journal of Cellular Biochemistry*, vol. 111, no. 3, pp. 554–563, 2010.

[26] V. K. Bhaskara, I. Mohanam, J. S. Rao, and S. Mohanam, "Intermittent hypoxia regulates stem-like characteristics and differentiation of neuroblastoma cells," *PLoS ONE*, vol. 7, no. 2, Article ID e30905, 2012.

[27] K. A. Whelan and M. J. Reginato, "Surviving without oxygen: hypoxia regulation of mammary morphogenesis and anoikis," *Cell Cycle*, vol. 10, no. 14, pp. 2287–2294, 2011.

[28] S. E. Rademakers, P. N. Span, J. H. A. M. Kaanders, F. C. G. J. Sweep, A. J. van der Kogel, and J. Bussink, "Molecular aspects of tumour hypoxia," *Molecular Oncology*, vol. 2, no. 1, pp. 41–53, 2008.

[29] S. Strese, M. Fryknäs, R. Larsson et al., "Effects of hypoxia on human cancer cell line chemosensitivity," *BMC Cancer*, vol. 13, no. 331, pp. 1–11, 2013.

[30] Y. Yang, S. Karakhanova, J. Werner et al., "Reactive oxygen species in cancer biology and anticancer therapy," *Current Medicinal Chemistry*, vol. 20, no. 30, pp. 3677–3692, 2013.

[31] C. H. Hsieh, C. P. Wu, H. T. Lee et al., "NADPH oxidase subunit 4 mediates cycling hypoxia-promoted radiation resistance in glioblastoma multiforme," *Free Radical Biology and Medicine*, vol. 53, no. 4, pp. 649–658, 2012.

[32] L. Flamant, E. Roegiers, M. Pierre et al., "TMEM45A is essential for hypoxia-induced chemoresistance in breast and liver cancer cells," *BMC Cancer*, vol. 12, no. 391, pp. 1–16, 2012.

[33] T. Rhim, D. Y. Lee, and M. Lee, "Hypoxia as target for tissue specific gene therapy," *Journal of Controlled Release*, vol. 172, no. 2, pp. 484–494, 2013.

[34] T. Miyata, S. Takizawa, and C. van Ypersele de Strihou, "Hypoxia. 1. Intracellular sensors for oxygen and oxidative stress: novel therapeutic targets," *American Journal of Physiology: Cell Physiology*, vol. 300, no. 2, pp. C226–C231, 2011.

[35] J.-W. Kim, P. Gao, and C. V. Dang, "Effects of hypoxia on tumor metabolism," *Cancer and Metastasis Reviews*, vol. 26, no. 2, pp. 291–298, 2007.

[36] J. Nanduri, N. Wang, G. Yuan et al., "Intermittent hypoxia degrades HIF-2α via calpains resulting in oxidative stress: implications for recurrent apnea-induced morbidities," *Proceedings of the National Academy of Sciences of the United States of America*, vol. 106, no. 4, pp. 1199–1204, 2009.

[37] B. Keith, R. S. Johnson, and M. C. Simon, "HIF1 α and HIF2 α: sibling rivalry in hypoxic tumour growth and progression," *Nature Reviews Cancer*, vol. 12, no. 1, pp. 9–22, 2012.

[38] J. Nanduri, D. R. Vaddi, S. A. Khan et al., "Xanthine oxidase mediates hypoxia-inducible factor-2α degradation by intermittent hypoxia," *PLoS ONE*, vol. 8, no. 10, Article ID e75838, 2013.

[39] H. Rundqvist and R. S. Johnson, "Tumour oxygenation: implications for breast cancer prognosis," *Journal of Internal Medicine*, vol. 274, no. 2, pp. 105–112, 2013.

[40] B. Ramanathan, K.-Y. Jan, C.-H. Chen, T.-C. Hour, H.-J. Yu, and Y.-S. Pu, "Resistance to paclitaxel is proportional to cellular total

antioxidant capacity," *Cancer Research*, vol. 65, no. 18, pp. 8455–8460, 2005.

[41] C. M. Woolston, L. Zhang, S. J. Storr et al., "The prognostic and predictive power of redox protein expression for anthracycline-based chemotherapy response in locally advanced breast cancer," *Modern Pathology*, vol. 25, no. 8, pp. 1106–1116, 2012.

[42] A. Brozovic, A. Ambriović-Ristov, and M. Osmak, "The relationship between cisplatin-Induced reactive oxygen species, glutathione, and BCL-2 and resistance to cisplatin," *Critical Reviews in Toxicology*, vol. 40, no. 4, pp. 347–359, 2010.

[43] D. T. Vincent, Y. F. Ibrahim, M. G. Espey et al., "The role of antioxidant in the era of cardio-oncology," *Cancer Chemotherapy and Pharmacology*, vol. 72, no. 6, pp. 1157–1168, 2013.

[44] C. Glorieux, N. Dejeans, B. Sid, R. Beck, P. B. Calderon, and J. Verrax, "Catalase overexpression in mammary cancer cells leads to a less aggressive phenotype and an altered response to chemotherapy," *Biochemical Pharmacology*, vol. 82, no. 10, pp. 1384–1390, 2011.

[45] E. M. Hanschmann, J. R. Godoy, C. Berndt et al., "Thioredoxins, glutaredoxins, and peroxiredoxins—molecular mechanisms and health significance: from cofactors to antioxidants to redox signaling," *Antioxidants and Redox Signaling*, vol. 19, no. 13, pp. 1539–1605, 2013.

[46] D. D. Rio, A. R. Mateos, J. P. E. Spencer et al., "Dietary (poly) phenolics in human health: structures, bioavailability, and evidence of protective effects against chronic diseases," *Antioxidants and Redox Signaling*, vol. 18, no. 14, pp. 1818–1892, 2013.

[47] M. Zalewska, J. Trefon, and H. Milnorowicz, "The role of metallothionein interactions with other proteins," *Proteomics*, 2014.

[48] I. Romero-Canelón and P. J. Sadler, "Next-generation metal anticancer complexes: multitargeting via redox modulation," *Inorganic Chemistry*, vol. 52, no. 21, pp. 12276–12291, 2013.

[49] M. Goodman, R. M. Bostick, O. Kucuk, and D. P. Jones, "Clinical trials of antioxidants as cancer prevention agents: past, present, and future," *Free Radical Biology and Medicine*, vol. 51, no. 5, pp. 1068–1084, 2011.

[50] G. Bjelakovic, D. Nikolova, and C. Gluud, "Antioxidant supplements and mortality," *Current Opinion in Clinical Nutrition and Metabolic Care*, vol. 17, no. 1, pp. 40–44, 2014.

[51] H. Sies, "Role of metabolic H_2O_2 generation: redox signaling and oxidative stress," *The Journal Biological Chemistry*, 2014.

[52] R. A. Poynton and M. B. Hampton, "Peroxiredoxins as biomarkers of oxidative stress.," *Biochimica et Biophysica Acta*, vol. 1840, no. 2, pp. 906–912, 2014.

[53] J. J. Merino, C. Roncero, M. J. Oset-Gasque et al., "Antioxidant and protective mechanisms against hypoxia and hypoglycaemia in cortical neurons *in vitro*," *International Journal of Molecular Sciences*, vol. 15, no. 2, pp. 2475–2493, 2014.

[54] V. V. Khramtsov and R. J. Gillies, "Janus-faced tumor microenvironment and redox," *Antioxidant and Redox Signaling*, 2014.

[55] V. I. Lushchak, "Glutathione homeostasis and fuctions: potential targets for medical interventions," *Journal of Amino Acids*, vol. 2012, Article ID 736837, 26 pages, 2012.

[56] J. H. Wu and G. Batist, "Glutathione and glutathione analogues, therapeutic potentials," *Biochimica et Biophysica Acta*, vol. 1830, no. 5, pp. 3350–3353, 2013.

[57] D. M. Townsend, K. D. Tew, and H. Tapiero, "The importance of glutathione in human disease," *Biomedicine and Pharmacotherapy*, vol. 57, no. 3, pp. 145–155, 2003.

[58] N. Traverso, R. Ricciarelli, M. Nitti et al., "Role of glutathione in cancer progression and chemoresistance," *Oxidative Medicine and Cellular Longevity*, vol. 2013, Article ID 972913, 10 pages, 2013.

[59] J. K. Kwee, D. G. Luque, A. C. D. S. Ferreira et al., "Modulation of reactive oxygen species by antioxidants in chronic myeloid leukemia cells enhances imatinib sensitivity through survivin downregulation," *Anti-Cancer Drugs*, vol. 19, no. 10, pp. 975–981, 2008.

[60] P. Yang, J. O. Ebbert, Z. Sun, and R. M. Weinshilboum, "Role of the glutathione metabolic pathway in lung cancer treatment and prognosis: a review," *Journal of Clinical Oncology*, vol. 24, no. 11, pp. 1761–1769, 2006.

[61] D. Hanahan and R. A. Weinberg, "Hallmarks of cancer: the next generation," *Cell*, vol. 144, no. 5, pp. 646–674, 2011.

[62] T. Fiaschi and P. Chiarugi, "Oxidative stress, tumor microenvironment, and metabolic reprogramming: a diabolic liaison," *International Journal of Cell Biology*, vol. 2012, Article ID 762825, 8 pages, 2012.

[63] X. Hu and Y. Xuan, "Bypassing cancer drug resistance by activating multiple death pathways—a proposal from the study of circumventing cancer drug resistance by induction of necroptosis," *Cancer Letters*, vol. 259, no. 2, pp. 127–137, 2008.

[64] B. Köberle, M. T. Tomicic, S. Usanova, and B. Kaina, "Cisplatin resistance: preclinical findings and clinical implications," *Biochimica et Biophysica Acta*, vol. 1806, no. 2, pp. 172–182, 2010.

[65] P.-S. Ong, S.-Y. Chan, and P. C. Ho, "Differential augmentative effects of buthionine sulfoximine and ascorbic acid in As_2O_3-induced ovarian cancer cell death: Oxidative stress-independent and -dependent cytotoxic potentiation," *International Journal of Oncology*, vol. 38, no. 6, pp. 1731–1739, 2011.

[66] M. Jozefczak, T. Remans, J. Vangronsveld, and A. Cuypers, "Glutathione is a key player in metal-induced oxidative stress defenses," *International Journal of Molecular Sciences*, vol. 13, no. 3, pp. 3145–3175, 2012.

[67] H. H. Bailey, R. T. Mulcahy, K. D. Tutsch et al., "Phase I clinical trial of intravenous L-buthionine sulfoximine and melphalan: an attempt at modulation of glutathione," *Journal of Clinical Oncology*, vol. 12, no. 1, pp. 194–205, 1994.

[68] P. J. O'Dwyer, T. C. Hamilton, F. P. LaCreta et al., "Phase I trial of buthionine sulfoximine in combination with melphalan in patients with cancer," *Journal of Clinical Oncology*, vol. 14, no. 1, pp. 249–256, 1996.

[69] H. H. Bailey, G. Ripple, K. D. Tutsch et al., "Phase I study of continuous-infusion L-S,R-buthionine sulfoximine with intravenous melphalan," *Journal of the National Cancer Institute*, vol. 89, no. 23, pp. 1789–1796, 1997.

[70] H. H. Bailey, "L-S,R-buthionine sulfoximine: historical development and clinical issues," *Chemico-Biological Interactions*, vol. 111-112, pp. 239–254, 1998.

[71] D. Hamilton and G. Batist, "Glutathione analogues in cancer treatment," *Current Oncology Reports*, vol. 6, no. 2, pp. 116–122, 2004.

[72] L. Salmena, A. Carracedo, and P. P. Pandolfi, "Tenets of PTEN tumor suppression," *Cell*, vol. 133, no. 3, pp. 403–414, 2008.

[73] T. Saha, J. K. Rih, and E. M. Rosen, "BRCA1 down-regulates cellular levels of reactive oxygen species," *The FEBS Letters*, vol. 583, no. 9, pp. 1535–1543, 2009.

[74] Z. Huang, L. Zuo, Z. Zhang et al., "3,3′-Diindolylmethane decreases VCAM-1 expression and alleviates experimental colitis via a BRCA1-dependent antioxidant pathway," *Free Radical Biology and Medicine*, vol. 50, no. 2, pp. 228–236, 2011.

[75] B. Vurusaner, G. Poli, and H. Basaga, "Tumor suppressor genes and ROS: complex networks of interactions," *Free Radical Biology and Medicine*, vol. 52, no. 1, pp. 7–18, 2012.

[76] H. Luo, Y. Yang, J. Duan et al., "PTEN-regulated AKT/FoxO3a/Bim signaling contributes to reactive oxygen species-mediated apoptosis in selenite-treated colorectal cancer cells," *Cell Death and Disease*, vol. 4, article e481, 2013.

[77] F. G. Meng and Z. Y. Zhang, "Redox regulation of protein tyrosine phosphatase activity by hydroxyl radical," *Biochimica et Biophysica Acta*, vol. 1834, no. 1, pp. 464–469, 2013.

[78] S. J. Kim, H. J. Jung, and C. J. Lim, "Reactive oxygen species-dependent down-regulation of tumor suppressor genes PTEN, USP28, DRAM, TIGAR, and CYLD under oxidative stress," *Biochemical Genetics*, vol. 51, no. 11-12, pp. 901–915, 2013.

[79] A. Tutt and A. Ashworth, "The relationship between the roles of BRCA genes in DNA repair and cancer predisposition," *Trends in Molecular Medicine*, vol. 8, no. 12, pp. 571–576, 2002.

[80] N. Turner, A. Tutt, and A. Ashworth, "Hallmarks of 'BRCAness' in sporadic cancers," *Nature Reviews Cancer*, vol. 4, no. 10, pp. 814–819, 2004.

[81] R. Roy, J. Chun, and S. N. Powell, "BRCA1 and BRCA2: different roles in a common pathway of genome protection," *Nature Reviews Cancer*, vol. 12, no. 1, pp. 68–78, 2012.

[82] M. L. Li and R. A. Greenberg, "Links between genome integrity and BRCA1 tumor suppression," *Trends in Biochemical Sciences*, vol. 37, no. 10, pp. 418–424, 2012.

[83] W. D. Foulkes and A. Y. Shuen, "In brief: BRCA1 and BRCA2," *Journal of Pathology*, vol. 230, no. 4, pp. 347–349, 2013.

[84] Y. Miki, J. Swensen, D. Shattuck-Eidens et al., "A strong candidate for the breast and ovarian cancer susceptibility gene BRCA1," *Science*, vol. 266, no. 5182, pp. 66–71, 1994.

[85] P. A. Futreal, Q. Liu, D. Shattuck-Eidens et al., "BRCA1 mutations in primary breast and ovarian carcinomas," *Science*, vol. 266, no. 5182, pp. 120–122, 1994.

[86] N. J. Birkbak, B. Kochupurakkai, J. M. G. Izarzugaza et al., "Tumor mutation burden forecasts outcome in ovarian cancer with BRCA1 or BRCA2 mutations," *PLos ONE*, vol. 08, no. 11, Article ID e80023, 2013.

[87] S. Fan, J.-A. Wang, R.-Q. Yuan et al., "BRCA1 as a potential human prostate tumor suppressor: modulation of proliferation, damage responses and expression of cell regulatory proteins," *Oncogene*, vol. 16, no. 23, pp. 3069–3082, 1998.

[88] E. Castro, C. Goh, D. Olmos et al., "Germline BRCA mutations are associated with higher risk of nodal involvement, distant metastasis, and poor survival outcomes in prostate cancer," *Journal of Clinical Oncology*, vol. 31, no. 14, pp. 1748–1757, 2013.

[89] P. de Luca, C. P. Moiola, F. Zalazar et al., "BRCA1 and p53 regulate critical prostate cancer pathways," *Prostate Cancer and Prostatic Diseases*, vol. 16, no. 3, pp. 233–238, 2013.

[90] A. Passaro, A. Palazzo, P. Trenta et al., "Molecular and clinical analysis of predictive biomarkers in non-small-cell lung cancer," *Current Medicinal Chemistry*, vol. 19, no. 22, pp. 3689–3700, 2012.

[91] M. Pesta, V. Kulda, O. Fiala et al., "Prognostic significance of ERCC1, RRM1 and BRCA1 in surgically-treated patients with non-small cell lung cancer," *Anticancer Research*, vol. 32, no. 11, pp. 5003–5010, 2012.

[92] H. Harada, K. Miyamoto, Y. Yamashita et al., "Methylation of breast cancer susceptibility gene 1 (BRCA1) predicts recurrence in patients with curatively resected stage I non-small cell lung cancer," *Cancer*, vol. 119, no. 4, pp. 792–798, 2013.

[93] M. Tiseo, P. Bordi, B. Bortesi et al., "ERCC1/BRCA1 expression and gene polymorphisms as prognostic and predictive factors in advanced NSCLC treated with or without cisplatin," *British Journal of Cancer*, vol. 108, no. 8, pp. 1695–1703, 2013.

[94] M. Sung and P. Giannakakou, "BRCA1 regulates microtubule dynamics and taxane-induced apoptotic cell signaling," *Oncogene*, vol. 33, no. 11, pp. 1418–1428, 2014.

[95] J. E. Axilbund and E. A. Wiley, "Genetic testing by cancer site: pancreas," *Cancer Journal*, vol. 18, no. 4, pp. 350–354, 2012.

[96] T. Wang, S. C. Wentz, N. L. Ausborn et al., "Pattern of breast cancer susceptibility gene 1 expression is a potential prognostic biomarker in resectable pancreatic ductal adenocarcinoma," *Pancreas*, vol. 42, no. 6, pp. 977–982, 2013.

[97] E. B. Fauman and M. A. Saper, "Structure and function of the protein tyrosine phosphatases," *Trends in Biochemical Sciences*, vol. 21, no. 11, pp. 413–417, 1996.

[98] N. K. Tonks, "Protein tyrosine phosphatases: from genes, to function, to disease," *Nature Reviews Molecular Cell Biology*, vol. 7, no. 11, pp. 833–846, 2006.

[99] T. Hunter, "Tyrosine phosphorylation: thirty years and counting," *Current Opinion in Cell Biology*, vol. 21, no. 2, pp. 140–146, 2009.

[100] L. Tautz, D. A. Critton, and S. Grotegut, "Protein tyrosine phosphatases: structure, function, and implication in human disease," *Methods in Molecular Biology*, vol. 1053, pp. 179–221, 2013.

[101] N. K. Tonks, "Redox redux: revisiting PTPs and the control of cell signaling," *Cell*, vol. 121, no. 5, pp. 667–670, 2005.

[102] M. M. Pires, B. D. Hopkins, L. H. Saal et al., "Alterations of EGFR, p53 and PTEN that mimic changes found in basal-like breast cancer promote transformation of human mammary epithelial cells," *Cancer Biology and Therapy*, vol. 14, no. 3, pp. 246–253, 2013.

[103] L. H. Saal, S. K. Gruvberger-Saal, C. Persson et al., "Recurrent gross mutations of the PTEN tumor suppressor gene in breast cancers with deficient DSB repair," *Nature Genetics*, vol. 40, no. 1, pp. 102–107, 2008.

[104] K. Bensaad, A. Tsuruta, M. A. Selak et al., "TIGAR, a p53-inducible regulator of glycolysis and apoptosis," *Cell*, vol. 126, no. 1, pp. 107–120, 2006.

[105] K. Bensaad, E. C. Cheung, and K. H. Vousden, "Modulation of intracellular ROS levels by TIGAR controls autophagy," *The EMBO Journal*, vol. 28, no. 19, pp. 3015–3026, 2009.

Hindawi Publishing Corporation
BioMed Research International
Volume 2014, Article ID 328959, 9 pages
http://dx.doi.org/10.1155/2014/328959

Research Article

A Short-Term Incubation with High Glucose Impairs VASP Phosphorylation at Serine 239 in response to the Nitric Oxide/cGMP Pathway in Vascular Smooth Muscle Cells: Role of Oxidative Stress

Isabella Russo, Michela Viretto, Gabriella Doronzo, Cristina Barale, Luigi Mattiello, Giovanni Anfossi, and Mariella Trovati

Internal Medicine and Metabolic Disease Unit, Department of Clinical and Biological Sciences, School of Medicine of the Turin University, San Luigi Gonzaga Hospital, Orbassano, 10043 Turin, Italy

Correspondence should be addressed to Mariella Trovati; mariella.trovati@unito.it

Received 15 November 2013; Revised 31 January 2014; Accepted 15 February 2014; Published 23 March 2014

Academic Editor: David Vauzour

A reduction of the nitric oxide (NO) action in vascular smooth muscle cells (VSMC) could play a role in the vascular damage induced by the glycaemic excursions occurring in diabetic patients; in this study, we aimed to clarify whether a short-term incubation of cultured VSMC with high glucose reduces the NO ability to increase cGMP and the cGMP ability to phosphorylate VASP at Ser-239. We observed that a 180 min incubation of rat VSMC with 25 mmol/L glucose does not impair the NO-induced cGMP increase but reduces VASP phosphorylation in response to both NO and cGMP with a mechanism blunted by antioxidants. We further demonstrated that high glucose increases radical oxygen species (ROS) production and that this phenomenon is prevented by the PKC inhibitor chelerythrine and the NADPH oxidase inhibitor apocynin. The following sequence of events is supported by these results: (i) in VSMC high glucose activates PKC; (ii) PKC activates NADPH oxidase; (iii) NADPH oxidase induces oxidative stress; (iv) ROS impair the signalling of cGMP, which is involved in the antiatherogenic actions of NO. Thus, high glucose, via oxidative stress, can reduce the cardiovascular protection conferred by the NO/cGMP pathway via phosphorylation of the cytoskeleton protein VASP in VSMC.

1. Introduction

Among the factors involved in the huge increase of cardiovascular risk occurring in diabetes mellitus, a pivotal role is played by a reduced synthesis and action of nitric oxide (NO) [1], a substance exerting a major role in vascular biology by a wide array of antihypertensive and antiatherogenic properties [2–4]. As it is widely recognized, in diabetes mellitus there is a reduced synthesis of NO by vascular endothelium, mirrored by a reduction of the so-called "endothelial-dependent relaxation," that is, the "in vivo" vasodilation induced by agents able to stimulate the endothelial synthesis of NO [5, 6]. More controversial is the impairment of the NO action in diabetic patients: for instance, in some studies the so-called "endothelium-independent" relaxation (i.e. the vasodilation induced by exogenous administration of NO donors) is preserved in the presence of an impaired "endothelial-dependent relaxation" [7–9], whereas in other studies both the endothelial and the non-endothelial-dependent relaxation are impaired [10–14].

Therefore, since the endothelial-independent vasodilation mirrors the response of vascular smooth muscle cells (VSMCs) to NO, it has not been completely clarified as yet whether in the presence of diabetes mellitus these cells show a normal or an impaired response to NO, at least as far as vasodilation is concerned.

One of the main actions of NO is to activate the soluble guanylate cyclase (sGC), with the consequent biosynthesis of cyclic guanosine $3'$,$5'$-monophosphate (cGMP), an ubiquitous intracellular second messenger which mediates a large spectrum of biological processes, such as cell contractility, mobility, growth, and apoptosis: the relevance of cGMP

signalling in cardiovascular pathophysiology and therapeutics has been exhaustively reviewed [4, 15]. In particular, cGMP deeply influences VSMC contractility, proliferation, and switch from the contractile "differentiated" to the synthetic/secretory "de-differentiated" phenotype [16]. The influence of cGMP on the cardiovascular system is exerted by activating cGMP-dependent protein kinases and phosphatases [15, 17].

The main cGMP-dependent protein kinase in VSMC is PKG type I [15]: the sequential activation of sGC and PKG plays a crucial role in NO action. In particular, downregulation of both enzymes impairs the NO ability to modulate VSMC functions, leading to excessive proliferation, constriction, and secretory activity, as observed in vascular disorders, and ablation of the PKG gene deeply interferes with NO/cGMP-dependent VSMC relaxation both "in vivo" and "in vitro" [18].

One of the PKG-I actions is the phosphorylation, mainly at serine 239, of the vasodilatory-stimulated phosphoprotein (VASP): VASP is a thin filament-actin binding cytoskeletal protein playing a pivotal role in cell adhesion, motility, and migration and—by binding to actin filaments and stress fibers—in cell contraction [19–23]. Thus, VASP phosphorylation at serine 239 is not only a marker of PKG activation but also a mediator of relevant biological actions exerted by the NO/cGMP/PKG pathway, such as modulation of actin polymerization, cell-cell contacts, and relaxation [19–23].

Dysfunction of the cGMP signalling at any level occurs in many cardiovascular diseases, such as arterial and pulmonary hypertension, atherosclerosis, cardiac hypertrophy, vascular remodelling, myocardial ischemia, and heart failure [15]. The dysfunction of the cGMP signalling in diabetes mellitus needs to be further elucidated, as previously mentioned.

Since hyperglycaemia is the main biochemical feature of diabetes mellitus, we aimed to clarify in this study whether high glucose impairs in VSMC the ability of NO to increase the synthesis of cGMP and to activate the downstream cascade of events leading to VASP phosphorylation; furthermore, we aimed to clarify the mechanisms involved in this putative impairment, with a peculiar emphasis for the oxidative stress, which is deeply involved in the pathogenesis of diabetes vascular complications and mediates the vascular damage induced by hyperglycaemia [24, 25].

In particular, we aimed at investigating the role of a short-term VSMC incubation with high glucose: the rationale of our experimental design "in vitro" is the fact that in the last years it has been observed that acute increases of blood glucose concentrations "in vivo," the so-called "glucose spikes," mainly occurring after meals, confer a high cardiovascular risk attributed to acute increases of oxidative stress [26].

Interestingly, in a prospective study carried out in our diabetes clinic, we demonstrated that postprandial blood glucose is a stronger predictor of cardiovascular events and death than fasting blood glucose even after the correction for the long-term glucose control marker haemoglobin A1C [27, 28].

In the light of these clinical observations, we decided to evaluate the influence of short-term incubations with high glucose on the NO/cGMP pathway in VSMC and the potential role of oxidative stress.

We also aimed at evaluating the role of protein kinase C (PKC) in the putative glucose-induced, oxidative stress-mediated impairment of the NO-cGMP signalling in VSMC, since one of the main mechanisms linking high glucose and oxidative stress is the glucose-induced activation of PKC, which in turn activates the superoxide anion generating enzyme nicotinamide adenine dinucleotide phosphate (NADPH) oxidase [29].

2. Materials and Methods

2.1. Research Design. The study has been carried out in cultured rat aortic VSMC.

(a) To evaluate whether high glucose reduces the NO ability to increase the VASP phosphorylation at serine 239, aortic VSMCs were incubated for 60 min with the NO donor SNP (100 μmol/L) with or without a 120 min preincubation of 25 mmol/L glucose to measure VASP phosphorylation at serine 239: in the following part of the paper, we will indicate this kind of phosphorylation simply as "VASP phosphorylation."

(b) To evaluate whether the glucose-induced impairment of the NO ability to phosphorylate VASP is attributable to a reduction of the NO ability to increase cGMP, cGMP concentrations have been measured in aortic VSMC incubated for 60 min with the NO donor SNP (100 μmol/L) with or without a 120 min preincubation with 25 mmol/L glucose.

(c) To evaluate whether high glucose reduces the cGMP ability to phosphorylate VASP, VASP phosphorylation has been measured in aortic VSMC incubated for 60 min with the cell-permeable cGMP analog 8-Br-cGMP (500 μmol/L) with or without a 120 min preincubation with 25 mmol/L glucose.

(d) To evaluate the involvement of oxidative stress on the high glucose-induced impairment of the NO- and cGMP-induced VASP phosphorylation, the experiments described at points (a) and (c) were repeated in the presence of a 20 min preincubation with the ROS scavenging enzymes SOD (300 U/mL) + catalase (250 U/mL).

(e) To evaluate whether high glucose increases radical oxygen species (ROS) production in VSMC and whether this increase is attributable to a PKC-induced activation of NADPH oxidase, ROS concentrations were measured in VSMC with or without a 180 min incubation with 25 mmol/L glucose, in the absence or in the presence of a 20 min preincubation with the PKC inhibitor chelerythrine (2.5 μmol/L) and the NADPH oxidase inhibitor apocynin (10 μmol/L). To evaluate the putative influence on ROS production of two other ROS sources, that is, the mitochondrial electron transport chain complex and xanthine oxidase, experiments with 25 mmol/L glucose were

also repeated in the presence of a 20 min preincubation with their specific inhibitors, that is, rotenone (10 μmol/L) and allopurinol (50 μmol/L), respectively. Finally, as a control experiment for the methods employed, experiments with 25 mmol/L glucose were repeated in the presence of a 20 min preincubation with 300 U/mL SOD + 250 U/mL catalase when hydrogen peroxide was measured and 300 U/mL SOD when superoxide anion was measured.

(f) To evaluate whether high glucose increases PKC alpha-beta phosphorylation, the phosphorylation of PKC α/βII was measured in VSMC with or without a 180 min incubation with 25 mmol/L glucose.

(g) To evaluate whether activation of PKC and NADPH oxidase mediates the influence of high glucose on the VASP phosphorylation in response to cGMP, experiments described at point (c) were repeated in the presence of a 20 min preincubation with 2.5 μmol/L chelerythrine and 10 μmol/L apocynin. Experiments have been also repeated in the presence of 10 μmol/L rotenone, to exclude the influence of the mitochondrial electron transport chain complex.

2.2. Chemicals. Minimum essential medium (MEM), bovine serum albumin (BSA), sodium nitroprusside (SNP), 8-Br-cGMP, lucigenin, $CaCl_2$, $MgCl_2$, 4β-phorbol 12-myristate 13-acetate (PMA), superoxide dismutase (SOD), catalase, chelerythrine, apocynin, rotenone, and allopurinol were from Sigma-Aldrich (St. Louis, MO, USA). Dihydrodichlorofluorescin diacetate was from Invitrogen Molecular Probes (Paisley, UK). Compounds used for western blots are detailed in the specific paragraphs.

2.3. Animals and VSMC Culture. Experiments have been carried out in VSMC derived from aorta of lean Zucker rats isolated and cultured in our laboratory. In particular, male and age-matched rats ($n = 4$), purchased from Charles River Laboratories (Calco, Italy), were fed with standard rodent chow and water ad libitumuntil 14 weeks old and killed with CO_2 after 12-hour fasting. Aorta was processed for VSMC isolation, culture, and characterization. Cells were characterized by phenotype and checked for the presence of smooth muscle cell α-actin and the absence of factor VIII (staining with a fluorescein isothiocyanate-conjugated antibody specific for factor VIII antigen). Cells were cultured using MEM (containing 5 mmol/L glucose) supplemented with 10% fetal calf serum (FCS), 10 mM glutamine, and antibiotics, and buffered with 10 mM N-Tris (hydroxymethyl) methyl-2-aminoethane-sulphonic acid (TES) and 10 mM N-(2-hydroxyethyl) piperazine-N1-(2-ethanesulphonic acid) (HEPES). For the experiments, cells were used at 3th-4th passage and cultured until 70% confluence was achieved. Then, medium with serum was removed and cells were made quiescent by serum starvation and cultured in MEM containing 0.1% BSA. Experiments have been carried out following the National Institutes of Health Guide for the Care and Use of Laboratory Animals 1996 (7th ed.; Washington, DC: National Academy Press, National Research Council Guide) and approved by our Institution.

2.4. Intracellular cGMP Measurement. For intracellular cGMP measurementcells were cultured into 6-well plates with medium containing 10% FCS until 70% confluence was achieved; the medium was then removed and replaced overnight with medium containing 0.1% BSA. At the end of the different incubation periods, medium was removed from each well and 300 μL absolute ethanol was added. A complete evaporation of ethanol was obtained under shaking. Then, the precipitated was dissolved in 300 μL acetate buffer and kept at −70°C until the assays. cGMP was measured by RIA kits (Immuno Biological Laboratories, Hamburg, Germany). The sensitivity of assay was less than 0.3 fmol per 0.1 mL, the specificity was 100% for cGMP, 0.0004% for cAMP, and 0.0001% for guanosine monophosphate (GMP), guanosine diphosphate (GDP), adenosine triphosphate (ATP), and guanosine triphosphate (GTP), and intra-assay coefficient of variation was 4.4%. Results were expressed as picomoles cGMP per milligram cell proteins.

2.5. Protein Expression and Extent of Protein Phosphorylation by Western Blot. To evaluate the protein expression and the extent of protein phosphorylation by western blot, VSMC extracts (20 μg) were separated by 10% SDS-PAGE and transferred to Immobilon-P Transfer Membranes (Millipore Co, Bedford, MA, USA). Membranes were incubated with the following primary antibodies: rabbit polyclonal anti-total VASP (1 : 15000) and mouse monoclonal anti-VASP phosphorylation at Ser 239 (1 : 1000) (Santa Cruz Biotecnology Inc., CA, USA); rabbit polyclonal anti-PKC ($\alpha/\beta/\gamma$) (1 : 1000) (Upstate, USA) and rabbit polyclonal phospho-PKC α/βII (Thr 638/641) (1 : 1000) (Cell Signalling, USA). We used as secondary antibodies anti-rabbit (1 : 10000) or anti-mouse (1 : 50000) conjugated to horseradish peroxidase. All the antibodies were diluted in PBS containing 0.1% Tween-20 (Sigma-Aldrich). Blots were scanned and analyzed densitometrically by the image analyzer 1D Image Analysis software (Kodak, Rochester, NY).

2.6. Determination of Cellular Reactive Oxygen Species (ROS). ROS were measured by using the DCF-DA assay, more specific for detection of hydrogen peroxide, and the lucigenin assay, more specific for the detection of superoxide anion.

2.6.1. The DCF-DA Assay. This assay was carried out by using the sensitive fluorescent indicator 2′,7′-dihydrodichlorofluorescin diacetate (DCF-DA), a diacetylated fluorescence probe which diffuses into the cells, where intracellular esterases cleave the acetyl groups, and is oxidized by H_2O_2 to the highly fluorescent 2′,7′-dichlorodihydrofluorescein (DCF) [30].

In particular, VSMCs cultured in 96-multiwell plates (1×10^5 mL^{-1}) were incubated with MEM with BSA 0.1% containing 5 or 25 mmol/L glucose for 3 h at 37°C. Positive control cells were incubated with 5 mmol/L glucose in the presence of 4β-phorbol 12-myristate 13-acetate (PMA)

(10 μmol/L) for 1 h, washed, and loaded with DCF-DA. After treatment, the medium was aspirated and cells were washed with PBS containing 1 mM $CaCl_2$ and 1 mM $MgCl_2$ (PBS^+) and incubated in the dark for 60 min at 37°C in the presence of 10 μM of DCF-DA. After that, cells were washed with PBS^+ and the emitted DCF fluorescence was collected and measured using a plate fluorometer (GloMax-Multi Detection System, Promega Corporation, Madison, WI, USA) fitted with 490 nm excitation and 520 nm emission filters. Each assay was carried out with six replicates and the fluorescence measure for each treatment was the average value of at least three independent experiments. ROS intracellular levels were expressed as fold increase from values with 5 mmol/L glucose.

2.6.2. The Lucigenin Assay. O_2^- levels were measured by lucigenin-enhanced chemiluminescence method based on light emission from reaction between reduced lucigenin and O_2^- as previously described [31]. Briefly, VSMCs, after a 24 h serum starvation, were resuspended at 5×10^5 cells/mL into a luminometer cuvette containing phosphate buffer and maintained at 37°C for 10 min. After a 5 sec dark adaptation, lucigenin (final concentration 25 μmol/L) was added into the cuvette and chemiluminescence was recorded 3 sec after the last injection over a 60 min period at 1 min intervals by the luminescence reader (GloMax-Multi Detection System, Promega Corporation, Madison, WI, USA). Specificity of reaction for O_2^- was demonstrated by preincubating cells with extracellular SOD (300 U/mL). Chemiluminescence activity unit is the relative light unit and O_2^- intracellular levels were expressed as relative light unit per cell.

2.7. Statistical Analysis. Data are expressed as means ± standard error of the mean (S.E.M). Statistical analysis was performed by means of analysis of variance (ANOVA) to determine the statistical significance of dose-response effects and by unpaired Student's t-test when only two values were compared.

3. Results

3.1. High Glucose Reduces the SNP-Induced VASP Phosphorylation at Ser 239. As shown in Figure 1, (i) high glucose did not modify VASP expression and phosphorylation in the absence of SNP; (ii) SNP did not modify total VASP expression neither in the absence nor in the presence of high glucose; (iii) SNP induced a significant VASP phosphorylation in the presence of both 5 mmol/L ($n = 6$, $P < 0.0001$) and 25 mmol/L glucose ($n = 6$, $P = 0.003$), the percent values on baseline being 602.4 ± 17% and 165.7 ± 10.9%, respectively. In the presence of 25 mmol/L glucose, values were significant lower than in the presence of 5 mmol/L glucose ($P < 0.0001$).

3.2. High Glucose Does Not Modify the SNP-Induced Increase of cGMP. As shown in Figure 2, SNP induced a significant increase of cGMP concentrations in the presence of both 5 mmol/L glucose ($n = 6$, $P < 0.0001$) and 25 mmol/L glucose ($n = 6$, $P < 0.0001$), without significant differences between the two glucose concentrations.

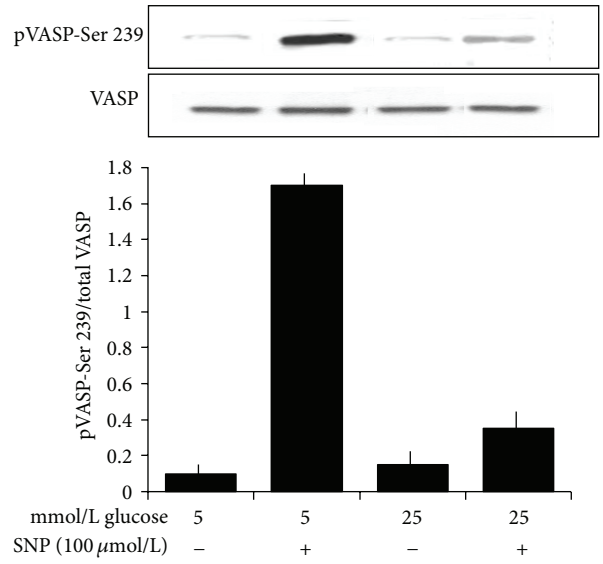

Figure 1: Effects of a 120 min preincubation with 5 and 25 mmol/L glucose on total VASP expression and VASP phosphorylation at Ser 239 in the absence or in the presence of a 60 min incubation with the NO donor SNP (100 μmol/L). Blots are representative of six different experiments. The increase induced by SNP on VASP phosphorylation at both 5 and 25 mmol/L ($P < 0.0001$ and $P = 0.003$, respectively) was lower at 25 than at 5 mmol/L ($P < 0.0001$). SNP did not modify total VASP expression neither in the absence nor in the presence of high glucose.

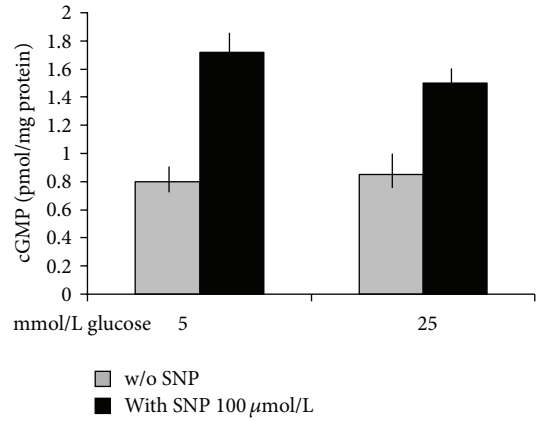

Figure 2: Effects of a 120 min preincubation with 5 and 25 mmol/L glucose on cGMP production in the absence or in the presence of a 60 min incubation with the NO donor SNP (100 μmol/L). The increase induced by SNP at both 5 and 25 mmol/L ($n = 6$, $P < 0.0001$ for both) was similar for both glucose concentrations (P = ns).

3.3. High Glucose Reduces the cGMP-Induced VASP Phosphorylation at Ser 239. As shown in Figure 3, 8-Br-cGMP induced a significant VASP phosphorylation in the presence of 5 mmol/L ($n = 6$, $P < 0.0001$), 15 mmol/L ($n = 6$, $P < 0.0001$), and 25 mmol/L glucose ($n = 6$, $P < 0.0001$). When values are expressed as percent of baseline values at glucose 5 mmol/L, the extent of VASP phosphorylation induced by 8-Br-cGMP dose dependently decreased (ANOVA: $P < 0.0001$).

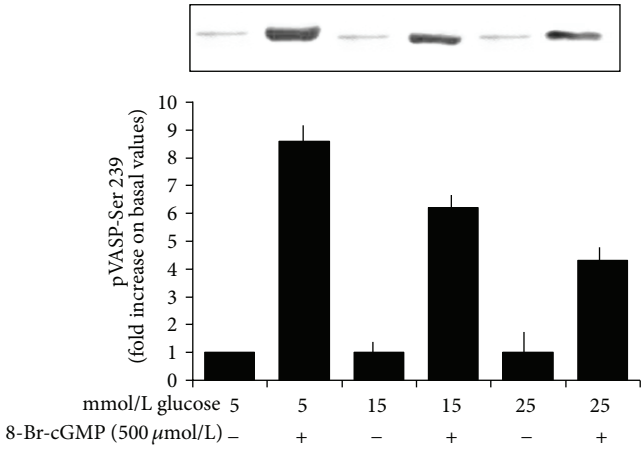

Figure 3: Effects of a 120 min preincubation with 5, 15, and 25 mmol/L glucose on VASP phosphorylation at Ser 239 in the absence or in the presence of a 60 min incubation with the cell-permeable cGMP analog 8-Br-cGMP (500 μmol/L). Blots are representative of six different experiments. 8-Br-cGMP induced a significant VASP phosphorylation at the three glucose concentrations ($P < 0.0001$ for each of them). When values are expressed as percent of values at glucose 5 mmol/L, the extent of VASP phosphorylation induced by 8-Br-cGMP dose dependently decreased (ANOVA: $P < 0.0001$).

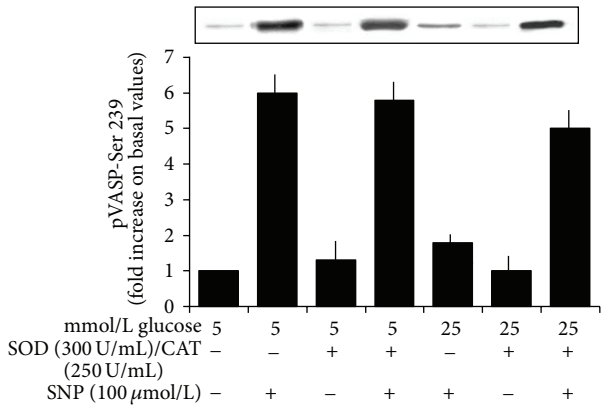

Figure 4: Effects of a 20 min preincubation with the antioxidant mixture SOD (300 U/mL) + catalase (250 U/mL) on the SNP-induced VASP phosphorylation at Ser 239 in the presence of 5 and 25 mmol/L glucose. Blots are representative of six different experiments. SOD and catalase did not modify the significant increase of VASP phosphorylation induced by SNP in the presence of 5 mmol/L glucose but significantly increased the extent of the SNP-induced VASP phosphorylation in the presence of glucose 25 mmol/L ($P < 0.0001$).

3.4. The Antioxidant Mixture SOD + Catalase Prevents the Inhibitory Effects Exerted by High Glucose on the VASP Phosphorylation Induced by SNP and by 8-Br-cGMP. As shown in Figures 4 and 5, the antioxidant mixture SOD + catalase did not modify the extent of VASP phosphorylation induced by SNP or 8-Br-cGMP in the presence of 5 mmol/L glucose but restored the inhibitory effects induced by 25 mmol/L glucose ($n = 6$, $P < 0.0001$ for both).

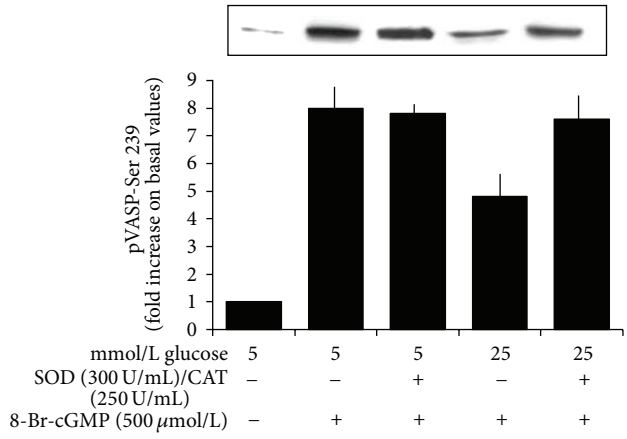

Figure 5: Effects of a 20 min preincubation with the antioxidant mixture SOD (300 U/mL) + catalase (250 U/mL) on the 8-Br-cGMP-induced VASP phosphorylation at Ser 239 in the presence of 5 and 25 mmol/L glucose. Blots are representative of six different experiments. SOD and catalase did not modify the significant increase of VASP phosphorylation induced by 8-Br-cGMP in the presence of 5 mmol/L glucose but significantly increased the extent of 8-Br-cGMP-induced VASP phosphorylation in the presence of glucose 25 mmol/L ($P < 0.0001$).

3.5. The High Glucose-Induced Increase of ROS Production Is Prevented by PKC and NADPH Oxidase Inhibitors. As shown in Figure 6, a 180 min incubation with 25 mmol/L glucose increased ROS production, measured by the DCF-DA assay specific for H_2O_2 ($n = 6$, $P < 0.0001$). This increase was inhibited by preincubation with the PKC inhibitor chelerythrine (2.5 μmol/L) ($n = 6$, $P < 0.0001$), the NADPH-oxidase inhibitor apocynin (10 μmol/L) ($n = 6$, $P < 0.0001$), and, as expected, by SOD (300 U/mL) + catalase (250 U/mL) ($n = 6$, $P < 0.0001$). With the three inhibitors, ROS values were similar to those measured in the presence of 5 mmol/L glucose (P = ns). ROS production was unaffected by incubation with 10 μmol/L rotenone and 50 μmol/L allopurinol (P = ns versus 25 mmol/L glucose for both).

Similar results have been obtained by the lucigenin assay, specific for O_2^-. In particular, when values are expressed as percent of baseline values at 5 mmol/L glucose, in the presence of 180 min incubation with 25 mmol/L glucose the O_2^- production was 144.7 ± 22.5% ($n = 6$, $P < 0.0001$): this increase was completely inhibited by preincubation with the PKC inhibitor chelerythrine (2.5 μmol/L) ($n = 6$, $P < 0.0001$), the NADPH-oxidase inhibitor apocynin (10 μmol/L) ($n = 6$, $P < 0.0001$), and, as expected, by SOD (300 U/mL) ($n = 6$, $P < 0.0001$). With the three inhibitors, O_2^- values were similar to those measured in the presence of 5 mmol/L glucose (P = ns).

3.6. High Glucose Increases PKC Alpha/Beta Phosphorylation. As shown in Figure 7, 25 mmol/L glucose induces a PKC α/βII activating phosphorylation without modifying

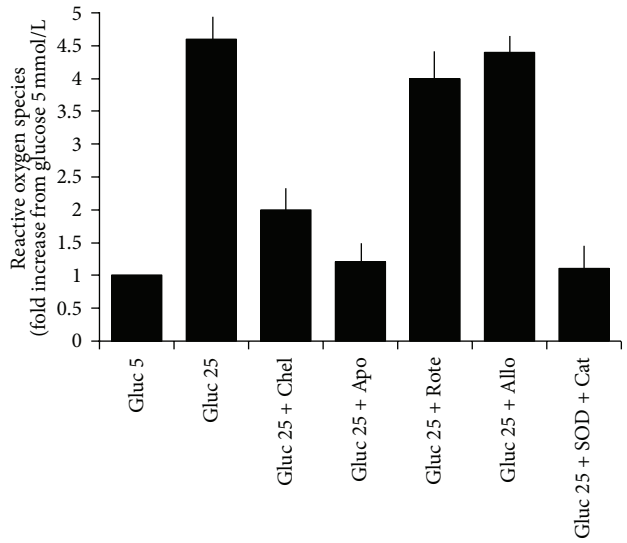

Figure 6: Effects of a 180 min incubation with 5 and 25 mmol/L glucose on ROS concentrations in the absence or in the presence of a 20 min preincubation with the PKC inhibitor chelerythrine (2.5 μmol/L), the NADPH-oxidase inhibitor apocynin (10 μmol/L), the mitochondrial electron transport chain complex inhibitor rotenone (10 μmol/L), the xanthine oxidase inhibitor allopurinol (50 μmol/L), and a mixture of SOD and catalase (300 U/mL/250 U/mL) ($n = 6$). ROS values in the presence of 25 mmol/L glucose were significantly higher than in the presence of 5 mmol/L glucose ($n = 6$, $P < 0.0001$). SOD + catalase, chelerythrine, and apocynin blunted the effects of glucose 25 mmol/L ($P < 0.0001$ for each), whereas rotenone and allopurinol did not modify the high glucose effects (P = ns).

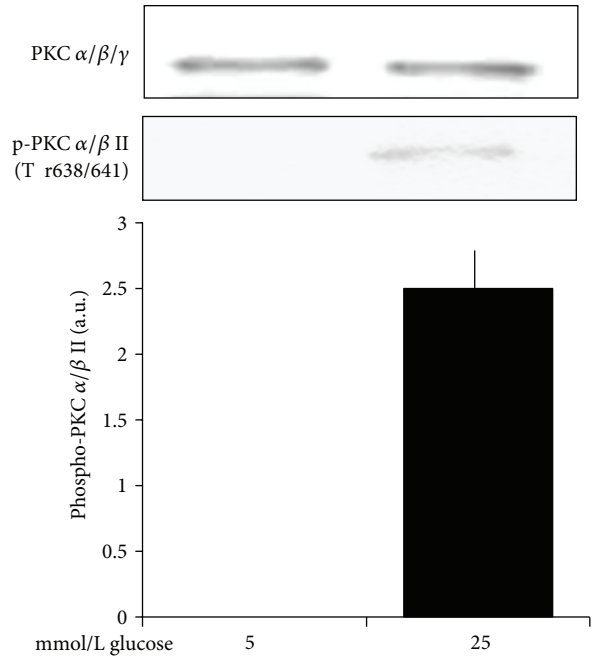

Figure 7: Effects of a 180 min incubation with 5 and 25 mmol/L glucose on nonphosphorylated PKC $\alpha/\beta/\gamma$ isoforms and on PKC α/βII phosphorylated at Thr 638/641. Blots are representative of four different experiments. Glucose 25 mmol/L did not modify the expression of nonphosphorylated PKC $\alpha/\beta/\gamma$ isoforms and increased PKC α/βII phosphorylation ($P < 0.0001$).

protein expression. In particular, a 180 min incubation with 25 mmol/L glucose in comparison to 5 mmol/L glucose (i) did not modify the expression of total PKC $\alpha/\beta/\gamma$ ($n = 4$, P = ns); (ii) increased the phosphorylation of PKC α/βII at Thr 638/641 ($n = 4$, $P < 0.0001$).

3.7. In the Presence of High Glucose, the cGMP-Induced VASP Phosphorylation Is Increased by PKC and NADPH Oxidase Inhibitors. As shown in Figure 8, the VASP phosphorylation induced by 8-Br-cGMP in the presence of 25 mmol/L glucose was significantly enhanced by both 2.5 μmol/L chelerythrine and 10 μmol/L apocynin ($n = 4$, $P < 0.0001$ for both) and was unaffected by 10 μmol/L rotenone.

4. Discussion

This study shows that, in cultured rat aortic VSMC, a short-term incubation with high glucose impairs the NO-induced VASP phosphorylation at serine 239 and that this effect is not due to a reduced cGMP synthesis but due to a reduced cGMP action and involves oxidative stress. The proposed mechanism is the following sequence of events: (i) high glucose activates PKC; (ii) PKC activates NADPH oxidase; (iii) NADPH oxidase increases the production of superoxide anion, and, consequently, of hydrogen peroxide; (iv) ROS impair the cGMP ability to phosphorylate VASP at serine 239.

As far as we know, this study provides the first evidence of the high glucose ability to reduce the NO/cGMP-induced VASP phosphorylation in cultured VSMC: a previous study, carried out with a long-term incubation with high glucose, demonstrated a similar inhibition in cultured human lung microvascular endothelial cells [32]. A reduced VASP phosphorylation was also observed in endothelial progenitor cells derived from two diabetic patients and therefore exposed to high glucose "in vivo" [32].

Our study also shows that oxidative stress plays a pivotal role in the high glucose-induced impairment of the NO/cGMP signalling in VSMC, since this impairment is completely prevented by the antioxidant mixture SOD + catalase.

As it is well known, during the physiological cellular metabolism oxygen undergoes a cascade of reductions, leading to the sequential production of superoxide anion, which is dismutated by superoxide dismutases (SOD) to hydrogen peroxide, which is catalyzed to H_2O by catalase; superoxide anion and hydrogen peroxide belong to the class of the "Reactive Oxygen Species" (ROS); excessive increases of ROS lead to the so-called "oxidative stress," a common phenomenon in many vascular diseases, such as diabetes mellitus, arterial hypertension, hypercholesterolemia, and heart failure, as reviewed [33–35].

In our study, SOD and catalase completely prevented the inhibiting influence exerted by high glucose on the VASP

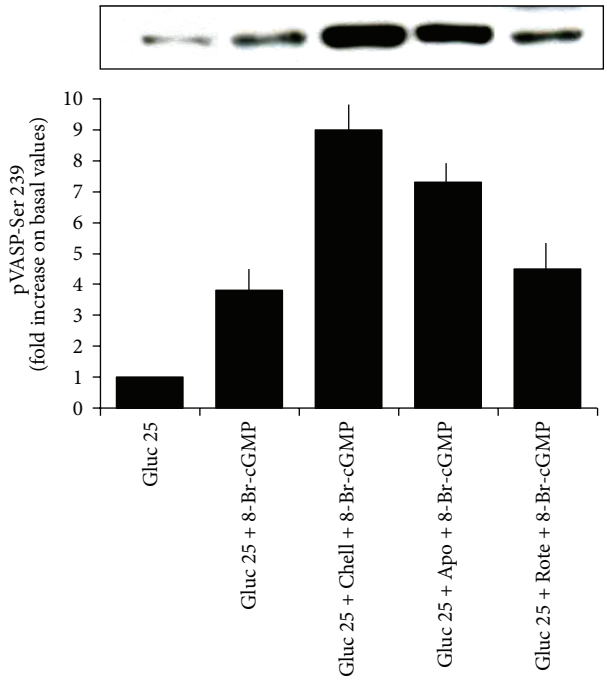

Figure 8: Effects of a 20 min preincubation with the PKC inhibitor chelerythrine (2.5 μmol/L), the NADPH-oxidase inhibitor apocynin (10 μmol/L), and the mitochondrial electron transport chain complex inhibitor rotenone (10 μmol/L), on the 8-Br-cGMP-induced VASP phosphorylation at Ser 239 in the presence of 25 mmol/L glucose. Blots are representative of four different experiments. Chelerythrine and apocynin significantly increased the extent of 8-Br-cGMP-induced VASP phosphorylation in the presence of glucose 25 mmol/L ($P < 0.0001$ for both), which was not modified by rotenone (P = ns).

phosphorylation induced by the NO/cGMP signalling, underlining the role of oxidative stress in this phenomenon.

Our working hypothesis was that high glucose increases in a short-term oxidative stress by a PKC-induced activation of NADPH oxidase; this hypothesis has been confirmed by the experiments carried out by measuring ROS concentrations, in which both PKC and NADPH oxidase inhibition impaired the stimulating effect of high glucose, whereas inhibitors of other potential ROS sources, such as mitochondrial respiratory chain complex and xanthine oxidase, did not modify the high glucose effects. Interestingly, PKC and NADPH oxidase inhibitors were also able to restore the extent of the cGMP-induced VASP phosphorylation impaired by high glucose. As it is well known, NADPH oxidase is the major source of ROS in VSMC [36]. We recently demonstrated that also oleic acid increases oxidative stress in VSMC by a mechanism involving both PKC and NADPH oxidase [37]. Previous observations carried out in our laboratory demonstrated that a 24 h incubation of rat VSMC with hydrogen peroxide reduces the cGMP-induced VASP phosphorylation, indicating a peculiar role of oxidative stress in the impairment of cGMP signalling [31].

In rat aortic VSMC, it has been demonstrated that a long-term (24–48 h) incubation with high glucose in the absence of exposure to NO donors or cGMP reduces the constitutive PKG-1 synthesis and, consequently, the PKG-induced VASP phosphorylation; also in this case the phenomenon is prevented by NADPH oxidase and PKC inhibitors [38]. The same authors demonstrated that a 3 h incubation with high glucose failed to modify PKG-1 expression [38]; thus, the results we obtained in the present study cannot be attributed to a reduced synthesis of PKG.

Independently of high glucose, a ROS-mediated reduction of PKG activity without any change in PKG expression has been observed in cultured VSMC from ovine fetal intrapulmonary veins exposed for 30 min to hypoxia and attributed to posttranslational, ROS-induced PKG nitration in tyrosine residues [39]; interestingly, the ROS-mediated downregulation of PKG activity was more evident in the presence of cGMP, suggesting that one or more residues within the cGMP-binding region of PKG are susceptible to ROS-induced posttranslational modifications [39]. In agreement with this observation, in our experimental conditions the extent of VASP phosphorylation—a reliable marker of PKG activity in vascular tissue [19]—was reduced by high glucose via oxidative stress only in the presence of NO or cGMP.

In conclusion, our study originally demonstrates the ability of high glucose to influence the NO/cGMP/PKG/VASP pathway in isolated, cultured VSMC by a mechanism involving the increase of oxidative stress mediated by a PKC-induced enhancement of the NADPH oxidase activity. It therefore provides some new information to further explain the interesting results of previous investigations carried out in aortas from rats sacrificed weeks after a streptozotocin injection, representing a classical animal model of "in vivo" hyperglycaemia [40, 41]. Obviously, when hyperglycaemia occurs "in vivo," high glucose affects many different tissues with the occurrence of the well-known intercellular interplay mediated by the release of different molecules, a phenomenon prevented by the "in vitro" incubation with high glucose of isolated cells. In any case, in these "in vivo" studies it has been demonstrated that streptozotocin-induced diabetes causes an impairment of endothelium-dependent [40, 41] and endothelium-independent vasodilation [41] and increases NADPH oxidase activity and expression and superoxide production in aorta [40, 41], the last phenomenon being prevented by the incubation of aortic rings with PKC inhibitors and by their "in vivo" administration [40]. Interestingly, "in vivo" administration of a PKC inhibitor markedly decreased superoxide anion production both in the endothelial and in the media layers of the aorta, indicating the occurrence of a PKC-mediated increase of oxidative stress in VSMC, the main component of the media [40].

Furthermore, acetylcholine induced an increase of VASP phosphorylation at serine 239 in aortic tissue of control rats, but not in that of rats with streptozotocin-induced diabetes; owing to the experimental design, this phenomenon has been attributed to the marked reduction of the acetylcholine-induced NO production in the vascular endothelium [41].

Our study, carried out in isolated cultured VSMC, adds a further piece of information on the mechanisms of glucose-induced impairment of VASP phosphorylation in vascular tissues, since it clarifies that in VSMC this impairment is due

to a defect of the cGMP signalling and therefore occurs also independently of the reduced NO synthesis and bioavailability caused by the glucose effects on vascular endothelium.

Finally, our present study provides the first demonstration of the ability of high glucose to rapidly reduce the NO/cGMP signalling in VSMC; this fact could be relevant to explain one of the possible mechanisms by which the so-called "glucose spikes" occurring "in vivo" in diabetic patients negatively influence vascular function [26].

5. Conclusions

In conclusion, in cultured aortic VSMC a short-term incubation with high glucose reduces the ability of both NO and cGMP to phosphorylate VASP at Ser 239 with a mechanism mediated by oxidative stress. As described in the Introduction, VASP phosphorylation is deeply involved in many antihypertensive and antiatherogenic biological actions exerted by the NO/cGMP/PKG pathway, such as modulation of cell adhesion, motility, migration, and contraction. Since the impairment of the NO pathway plays a pivotal role in the pathogenesis of the atherothrombotic vascular complications of diabetes, our results, by identifying a potential mechanism involved in the reduced NO action in VSMC, could have a clinical relevance. In particular, the results of our study can clarify another mechanism of the harmful vascular consequences of the so-called "glucose spikes" occurring "in vivo" in diabetic patients, which have been attributed to acute increases of oxidative stress, indicating an involvement of VSMC beyond the previously described involvement of vascular endothelium.

Conflict of Interests

The authors declare that there is no conflict of interests regarding the publication of this paper.

Acknowledgment

The study has been supported by a grant of the Turin University to Mariella Trovati. Professor Giovanni Anfossi is deceased.

References

[1] D. H. Endemann and E. L. Schiffrin, "Nitric oxide, oxidative excess, and vascular complications of diabetes mellitus," *Current Hypertension Reports*, vol. 6, no. 2, pp. 85–89, 2004.

[2] S. Moncada and E. A. Higgs, "The discovery of nitric oxide and its role in vascular biology," *British Journal of Pharmacology*, vol. 147, pp. S193–S201, 2006.

[3] P. Pacher, J. S. Beckman, and L. Liaudet, "Nitric oxide and peroxynitrite in health and disease," *Physiological Reviews*, vol. 87, no. 1, pp. 315–424, 2007.

[4] F. Murad, "Nitric oxide and cyclic GMP in cell signaling and drug development," *The New England Journal of Medicine*, vol. 355, no. 19, pp. 2003–2011, 2006.

[5] R. M. A. Henry, I. Ferreira, P. J. Kostense et al., "Type 2 diabetes is associated with impaired endothelium-dependent, flow-mediated dilation, but impaired glucose metabolism is not: the Hoorn Study," *Atherosclerosis*, vol. 174, no. 1, pp. 49–56, 2004.

[6] Y. Su, X. Liu, Y. Sun, Y. Wang, Y. Luan, and Y. Wu, "Endothelial dysfunction in impaired fasting glycemia, impaired glucose tolerance, and type 2 diabetes mellitus," *American Journal of Cardiology*, vol. 102, no. 4, pp. 497–498, 2008.

[7] H. O. Steinberg, H. Chaker, R. Leaming, A. Johnson, G. Brechtel, and A. D. Baron, "Obesity/insulin resistance is associated with endothelial dysfunction: implications for the syndrome of insulin resistance," *The Journal of Clinical Investigation*, vol. 97, no. 11, pp. 2601–2610, 1996.

[8] R. V. Hogikyan, A. T. Galecki, B. Pitt, J. B. Halter, D. A. Greene, and M. A. Supiano, "Specific impairment of endothelium-dependent vasodilation in subjects with type 2 diabetes independent of obesity," *Journal of Clinical Endocrinology and Metabolism*, vol. 83, no. 6, pp. 1946–1952, 1998.

[9] C. Scheede-Bergdahl, D. B. Olsen, D. Reving, R. Boushel, and F. Dela, "Insulin and non-insulin mediated vasodilation and glucose uptake in patients with type 2 diabetes," *Diabetes Research and Clinical Practice*, vol. 85, no. 3, pp. 243–251, 2009.

[10] G. E. McVeigh, G. M. Brennan, G. D. Johnston et al., "Impaired endothelium-dependent and independent vasodilation in patients with Type 2 (non-insulin-dependent) diabetes mellitus," *Diabetologia*, vol. 35, no. 8, pp. 771–776, 1992.

[11] G. F. Watts, S. F. O'Brien, W. Silvester, and J. A. Millar, "Impaired endothelium-dependent and independent dilatation of forearm resistance arteries in men with diet-treated non-insulin-dependent diabetes: role of dyslipidaemia," *Clinical Science*, vol. 91, no. 5, pp. 567–573, 1996.

[12] S. B. Williams, J. A. Cusco, M. Roddy, M. T. Johnstone, and M. A. Creager, "Impaired nitric oxide-mediated vasodilation in patients with non-insulin-dependent diabetes mellitus," *Journal of the American College of Cardiology*, vol. 27, no. 3, pp. 567–574, 1996.

[13] A. Avogaro, F. Piarulli, A. Valerio et al., "Forearm nitric oxide balance, vascular relaxation, and glucose metabolism in NIDDM patients," *Diabetes*, vol. 46, no. 6, pp. 1040–1046, 1997.

[14] A. Natali, E. Toschi, S. Baldeweg et al., "Clustering of insulin resistance with vascular dysfunction and low-grade inflammation in type 2 diabetes," *Diabetes*, vol. 55, no. 4, pp. 1133–1140, 2006.

[15] E. J. Tsai and D. A. Kass, "Cyclic GMP signaling in cardiovascular pathophysiology and therapeutics," *Pharmacology and Therapeutics*, vol. 122, no. 3, pp. 216–238, 2009.

[16] T. Münzel, R. Feil, A. Mülsch, S. M. Lohmann, F. Hofmann, and U. Walter, "Physiology and pathophysiology of vascular signaling controlled by guanosine 3′, 5′-cyclic monophosphate-dependent protein kinase," *Circulation*, vol. 108, no. 18, pp. 2172–2183, 2003.

[17] J. Schlossmann, R. Feil, and F. Hofmann, "Insights into cGMP signalling derived from cGMP kinase knockout mice," *Frontiers in Bioscience*, vol. 10, pp. 1279–1289, 2005.

[18] A. Pfeifer, P. Klatt, S. Massberg et al., "Defective smooth muscle regulation in cGMP kinase I-deficient mice," *The EMBO Journal*, vol. 17, no. 11, pp. 3045–3051, 1998.

[19] M. Oelze, H. Mollnau, N. Hoffmann et al., "Vasodilator-stimulated phosphoprotein serine 239 phosphorylation as a sensitive monitor of defective nitric oxide/cGMP signaling and endothelial dysfunction," *Circulation Research*, vol. 87, no. 11, pp. 999–1005, 2000.

[20] D. A. Calderwood, S. J. Shattil, and M. H. Ginsberg, "Integrins and actin filaments: reciprocal regulation of cell adhesion and signaling," *The Journal of Biological Chemistry*, vol. 275, no. 30, pp. 22607–22610, 2000.

[21] A. V. Kwiatkowski, F. B. Gertler, and J. J. Loureiro, "Function and regulation of Ena/VASP proteins," *Trends in Cell Biology*, vol. 13, no. 7, pp. 386–392, 2003.

[22] A. Schäfer, M. Burkhardt, T. Vollkommer et al., "Endothelium-dependent and -independent relaxation and VASP serines 157/239 phosphorylation by cyclic nucleotide-elevating vasodilators in rat aorta," *Biochemical Pharmacology*, vol. 65, no. 3, pp. 397–405, 2003.

[23] H. R. Kim, P. Graceffa, F. Ferron et al., "Actin polymerization in differentiated vascular smooth muscle cells requires vasodilator-stimulated phosphoprotein," *American Journal of Physiology—Cell Physiology*, vol. 298, no. 3, pp. C559–C571, 2010.

[24] T. Mazzone, A. Chait, and J. Plutzky, "Cardiovascular disease risk in type 2 diabetes mellitus: insights from mechanistic studies," *The Lancet*, vol. 371, no. 9626, pp. 1800–1809, 2008.

[25] F. Giacco and M. Brownlee, "Oxidative stress and diabetic complications," *Circulation Research*, vol. 107, no. 9, pp. 1058–1070, 2010.

[26] A. Ceriello, K. Esposito, L. Piconi et al., "Glucose "peak" and glucose "spike": impact on endothelial function and oxidative stress," *Diabetes Research and Clinical Practice*, vol. 82, no. 2, pp. 262–267, 2008.

[27] F. Cavalot, A. Petrelli, M. Traversa et al., "Postprandial blood glucose is a stronger predictor of cardiovascular events than fasting blood glucose in type 2 diabetes mellitus, particularly in women: lessons from the San Luigi Gonzaga diabetes study," *Journal of Clinical Endocrinology and Metabolism*, vol. 91, no. 3, pp. 813–819, 2006.

[28] F. Cavalot, A. Pagliarino, M. Valle et al., "Postprandial blood glucose predicts cardiovascular events and all-cause mortality in type 2 diabetes in a 14-year follow-up: lessons from the San Luigi Gonzaga Diabetes Study," *Diabetes Care*, vol. 34, pp. 2237–2243, 2011.

[29] T. Inoguchi, T. Sonta, H. Tsubouchi et al., "Protein kinase C-dependent increase in reactive oxygen species (ROS) production in vascular tissues of diabetes: role of vascular NAD(P)H oxidase," *Journal of the American Society of Nephrology*, vol. 14, pp. S227–S232, 2003.

[30] C. P. LeBel, H. Ischiropoulos, and S. C. Bondy, "Evaluation of the probe $2'$,$7'$-dichlorofluorescin as an indicator of reactive oxygen species formation and oxidative stress," *Chemical Research in Toxicology*, vol. 5, no. 2, pp. 227–231, 1992.

[31] I. Russo, P. del Mese, G. Doronzo et al., "Resistance to the nitric oxide/cyclic guanosine $5'$-monophosphate/ protein kinase G pathway in vascular smooth muscle cells from the obese zucker rat, a classical animal model of insulin resistance: role of oxidative stress," *Endocrinology*, vol. 149, no. 4, pp. 1480–1489, 2008.

[32] S. L. Calzi, D. L. Purich, K. H. Chang et al., "Carbon monoxide and nitric oxide mediate cytoskeletal reorganization in microvascular cells via vasodilator-stimulated phosphoprotein phosphorylation: evidence for blunted responsiveness in diabetes," *Diabetes*, vol. 57, no. 9, pp. 2488–2494, 2008.

[33] R. M. Touyz and E. L. Schiffrin, "Reactive oxygen species in vascular biology: implications in hypertension," *Histochemistry and Cell Biology*, vol. 122, no. 4, pp. 339–352, 2004.

[34] T. Fukai and M. Ushio-Fukai, "Superoxide dismutases: role in redox signaling, vascular function, and diseases," *Antioxidants and Redox Signaling*, vol. 15, no. 6, pp. 1583–1606, 2011.

[35] A. Schramm, P. Matusik, G. Osmenda, and T. J. Guzik, "Targeting NADPH oxidases in vascular pharmacology," *Vascular Pharmacology*, vol. 56, pp. 216–231, 2012.

[36] B. Lassègue and R. E. Clempus, "Vascular NAD(P)H oxidases: specific features, expression, and regulation," *American Journal of Physiology—Regulatory Integrative and Comparative Physiology*, vol. 285, no. 2, pp. R277–R297, 2003.

[37] G. Doronzo, M. Viretto, C. Barale et al., "Oleic acid increases synthesis and secretion of VEGF in rat vascular smooth muscle cells: role of oxidative stress and impairment in obesity," *International Journal of Molecular Sciences*, vol. 14, pp. 18861–18880, 2013.

[38] S. Liu, X. Ma, M. Gong, L. Shi, T. Lincoln, and S. Wang, "Glucose down-regulation of cGMP-dependent protein kinase I expression in vascular smooth muscle cells involves NAD(P)H oxidase-derived reactive oxygen species," *Free Radical Biology and Medicine*, vol. 42, no. 6, pp. 852–863, 2007.

[39] S. Negash, Y. Gao, W. Zhou, J. Liu, S. Chinta, and J. U. Raj, "Regulation of cGMP-dependent protein kinase-mediated vasodilation by hypoxia-induced reactive species in ovine fetal pulmonary veins," *American Journal of Physiology—Lung Cellular and Molecular Physiology*, vol. 293, no. 4, pp. L1012–L1020, 2007.

[40] U. Hink, H. Li, H. Mollnau et al., "Mechanisms underlying endothelial dysfunction in diabetes mellitus," *Circulation Research*, vol. 88, no. 2, pp. E14–E22, 2001.

[41] M. C. Wendt, A. Daiber, A. L. Kleschyov et al., "Differential effects of diabetes on the expression of the gp91 phox homologues nox1 and nox4," *Free Radical Biology and Medicine*, vol. 39, no. 3, pp. 381–391, 2005.

Hindawi Publishing Corporation
BioMed Research International
Volume 2014, Article ID 857504, 13 pages
http://dx.doi.org/10.1155/2014/857504

Research Article

Role of Plasma Membrane Caveolae/Lipid Rafts in VEGF-Induced Redox Signaling in Human Leukemia Cells

Cristiana Caliceti,[1] Laura Zambonin,[2] Benedetta Rizzo,[3] Diana Fiorentini,[2] Francesco Vieceli Dalla Sega,[2] Silvana Hrelia,[3] and Cecilia Prata[2]

[1] *Department of Clinical and Experimental Medicine, University of Ferrara, Via Fossato di Mortara 66, 44121 Ferrara, Italy*
[2] *Department of Pharmacy and Biotechnology, Alma Mater Studiorum-University of Bologna, Via Irnerio 48, 40126 Bologna, Italy*
[3] *Department for Life Quality Studies, Alma Mater Studiorum-University of Bologna, C.so Augusto 237, 47921 Rimini, Italy*

Correspondence should be addressed to Cecilia Prata; cecilia.prata@unibo.it

Received 15 November 2013; Accepted 21 January 2014; Published 11 March 2014

Academic Editor: Cristina Angeloni

Caveolae/lipid rafts are membrane-rich cholesterol domains endowed with several functions in signal transduction and caveolin-1 (Cav-1) has been reported to be implicated in regulating multiple cancer-associated processes, ranging from tumor growth to multidrug resistance and angiogenesis. Vascular endothelial growth factor receptor-2 (VEGFR-2) and Cav-1 are frequently colocalized, suggesting an important role played by this interaction on cancer cell survival and proliferation. Thus, our attention was directed to a leukemia cell line (B1647) that constitutively produces VEGF and expresses the tyrosine-kinase receptor VEGFR-2. We investigated the presence of VEGFR-2 in caveolae/lipid rafts, focusing on the correlation between reactive oxygen species (ROS) production and glucose transport modulation induced by VEGF, peculiar features of tumor proliferation. In order to better understand the involvement of VEGF/VEGFR-2 in the redox signal transduction, we evaluated the effect of different compounds able to inhibit VEGF interaction with its receptor by different mechanisms, corroborating the obtained results by immunoprecipitation and fluorescence techniques. Results here reported showed that, in B1647 leukemia cells, VEGFR-2 is present in caveolae through association with Cav-1, demonstrating that caveolae/lipid rafts act as platforms for negative modulation of VEGF redox signal transduction cascades leading to glucose uptake and cell proliferation, suggesting therefore novel potential targets.

1. Introduction

Caveolae and lipid rafts are ordered structures of membrane microdomains, characterized by high concentration of cholesterol and glycosphingolipids, which are involved in fundamental cellular functions such as endocytosis, protein trafficking, and signal transduction [1–4]. Several different mechanisms probably underlie the lipid raft-controlled cell signaling. For example, rafts may contain incomplete signaling pathways that are activated when a receptor and/or other required molecules are recruited into the raft. Otherwise, rafts may be important in limiting signaling, either by physical sequestration of signaling components to block nonspecific interactions or by suppressing the intrinsic activity of signaling proteins present within rafts [5, 6].

The maintenance of cholesterol levels is essential for functional caveolae and depends, in part, on the interaction of cholesterol with caveolin-1 (Cav-1), the major structural component of caveolae [7]. Various receptors and signaling molecules are localized in these membrane regions and are negatively regulated by Cav-1 through its scaffolding domain. In cancers, it is increasingly clear that Cav-1 is implicated in regulating multiple cancer-associated processes, ranging from cellular transformation, tumor growth, invasion, and metastasis to multidrug resistance and angiogenesis [8, 9].

Recent experimental evidence shows also that Vascular Endothelial Growth Factors (VEGF) promote the release of Vascular Endothelial Growth Factors Receptor 2 (VEGFR-2 or KDR) from caveolae/lipid rafts and its consequent activation, possibly stimulating NAD(P)H oxidases (Nox) in

endothelial cells [10]. In these cells, VEGFR-2 is present in caveolae through association with Cav-1, which negatively regulates receptor activity in basal state. Dissociation of VEGFR-2 from caveolae/Cav-1 seems to be essential for VEGFR-2 autophosphorylation and activation of downstream signaling events [7].

There is now a consensus that VEGF family is crucial for vascular development and neovascularisation in both physiologic and pathologic processes. Although both VEGFR-1 and VEGFR-2 are expressed in the vascular endothelium, the angiogenic activities of VEGFs (in particular, VEGF-A) are transduced mainly through VEGFR-2 [11]. VEGF receptors, indeed, are not exclusively expressed by endothelial cells but are also present in hematopoietic cells. This is not a surprising event because during embryonic development, hematopoietic and early endothelial cells (angioblasts) originate from a common precursor known as hemangioblast. Given this common root, several pathways are shared by hematopoietic and vascular cells [12, 13]. Moreover, leukemia cells have been associated with angiogenesis, upon the demonstration that leukemia progression is accompanied by an increase in bone marrow vascularization [14]. In many leukemia cells, VEGF/VEGFR interactions may stimulate proliferation, migration, and survival by autocrine and paracrine loops [15]. In recent studies, the expression of VEGF/VEGFR in acute myeloid leukemia (AML) patients has been detected and the increased levels of plasma VEGF have been correlated with reduced survival and lower remission rates [16, 17].

Therefore, the elucidation of the mechanisms underlying VEGF/VEGFR activity in leukemia cells is necessary for the development of agents to be used in combination with/instead of standard chemotherapy. To achieve this goal, it must be taken into consideration also the strong role played by the redox environment in leukemia survival, growth, progression, relapse, and drug resistance. Reactive oxygen species (ROS), indeed, play both positive and negative roles in cellular proliferation and survival; this feature has been exploited by leukemia cells to promote the hallmarks of cancer phenotype, either through phosphorylation events or transcriptional alteration [18].

In this context, our attention has been focused on the study of the correlation between caveolae/lipid rafts and redox signaling in the human erythromegakaryocytic cell line, B1647, a model of acute myeloid leukemia (AML) constitutively producing VEGF and expressing its tyrosine-kinase receptor VEGFR-2 [19]. We previously showed that Nox-derived ROS are involved in sustaining the high glucose uptake observed in B1647 cells [20]; subsequently, we demonstrated that VEGF-induced ROS derived from Nox2 and Nox4 play a prosurvival role in the leukemia cell line [21].

In the present work, we investigated the potential involvement of plasma membrane caveolae/lipid rafts in VEGF-mediated redox signaling in the human leukemia cell line.

To this purpose, we evaluated the effect of methyl-β-cyclodextrin (CD), the most efficient compound used to induce cholesterol depletion from plasma membrane thus disrupting caveolae/lipid rafts [22] on VEGFR-2 distribution in the plasma membrane and on VEGF/VEGFR-2 interaction. Subsequently, the modulation of ROS generation and glucose transporter 1 (Glut1) activity in B1647 cells was investigated.

2. Materials and Methods

2.1. Chemicals. Iscove's modified Dulbecco's medium (IMDM) was purchased from BioWhittaker (Walkersville, MD, USA), and human serum (HS) was from CambrexBioscience. VEGF was from BioVision (Mountain View, CA, USA). Methyl-β-cyclodextrin (CD), diphenyleneiodonium chloride (DPI), phloretin, 2-deoxy-D-glucose (DOG), cholesterol, phenylmethylsulfonyl fluoride (PMSF), N-tosyl-L-lysine chloromethyl ketone (TLCK), N-tosyl-L-phenylalanine chloromethyl ketone (TPCK), sodium orthovanadate, protease inhibitor cocktail, Trypan blue solution (0,4%), 3-(4,5-dimethylthiazol-2-yl)-2,5-diphenyl tetrazolium bromide (MTT), Igepal, Triton X-100, sucrose, Semaxinib (SU5416), mouse monoclonal antiserum against tubulin (no. T7816), and rabbit antibody against flotillin-2 (no. F1805) were from Sigma-Aldrich (St. Louis, MO, USA). 2-Deoxy-D-[2,6-^{3}H]-glucose and [1,2-^{3}H(N)]-cholesterol were from PerkinElmer (Massachusetts, USA); nitrocellulose paper and ECL Plus Western Blotting Detection Reagents were from GE Healthcare (UK). Bevacizumab was provided by Roche. Triton X-100 and sucrose were from Merck (Whitehouse Station, NJ, USA). DC Protein Assay Kit was from Bio-Rad (USA). Anti-caveolin-1 (no. 610059) and anti-transferrin receptor (CD71) (no. 612124) were provided by BD Biosciences (San Jose, CA, USA); anti-Lyn antibody (no. ab1890) was from Abcam (Cambridge, UK). Anti-Glut1 (no. CBL242), anti-VEGF receptor-2 (no. 05-554), and anti-P-tyrosine (no. 06-427) were from Millipore (Temecula, CA, USA). Anti-Glut1 (N-20) (no. sc-1603) and fluorescent FITC-conjugated anti-goat IgG (no. sc-2024) were from Santa Cruz Biotechnology (Santa Cruz, CA, USA). Sulfosuccinimidyl 6-(biotinamido) hexanoate (NHS-LC-biotin) and streptavidin-agarose beads were purchased from Pierce (Rockford, IL, USA).

All the other chemicals and solvents were of the highest analytical grade.

2.2. Cell Culture. B1647 is a humane acute myeloid leukemia (AML) cell line cultured in IMDM supplemented with 5% human serum (HS).

The experimental model employed 16–18 h serum-depleted cells, as these conditions were more apt for focusing experiments on self-produced VEGF and cholesterol roles, ruling out other growth factor effects.

2.3. Cell Viability Evaluation. Viable cells were evaluated by the Trypan blue exclusion test. Cell viability was also assayed by the MTT assay [23], since the reduction of tetrazolium salts is widely accepted as a reliable way to examine cell viability/proliferation. Cells were incubated with 0.5 mg/mL

MTT for 4 h at 37°C. At the end of the incubation, purple formazan salt crystals were formed and dissolved by adding the solubilization solution (10% SDS, 0.01 M HCl) and then the plates were incubated overnight in humidified atmosphere (37°C, 5% CO_2). The absorption at 570 nm was measured on a multiwell plate reader (Wallac Victor^2, PerkinElmer).

2.4. Cholesterol Depletion. B1647 cells suspended in culture medium were incubated overnight with [^{3}H]-cholesterol (0.5 μCi/mL) and then washed, suspended in PBS, and exposed to different concentrations of CD (5 mM) for different time points (0–30 min). To measure the relative cholesterol content, cells were washed twice in PBS and pelleted at 4.000 g for 1 min and sample radioactivity was quantified by liquid-scintillation counting [24].

2.5. Isolation of Membrane Caveolae/Lipid Rafts. Caveolae/lipid rafts and detergent-soluble proteins were separated by flotation assays adapted from previously described methods [24, 25]. 200 × 10^6 B1647 cells (approximately 6 mg of protein) were washed twice with PBS, pelleted at 300 g for 7 min, and left on ice for 10 min. The cell pellet was incubated at 4°C in 1.2 mL of lysis buffer (1% Triton X-100, 150 mM NaCl, 50 mM TRIS, and 5 mM EDTA supplemented with 0.1 mM PMSF, 0.1 mM TLCK, 0.1 mM TPCK, 1 mM orthovanadate, and protease inhibitor cocktail, pH 8.0). In all subsequent steps, solutions and samples were kept at 4°C. The lysates were then spun for 10 min at 6.000 g in an Eppendorf Microfuge and supernatants were homogenized in a Potter homogenizer with 20 strokes. For sucrose gradient separations, 1.0 mL of 80% sucrose prepared in PBS was mixed with an equal volume of homogenized sample and then overlaid with a 5–40% sucrose linear step gradient (1.3 mL each of 5%, 30%, and 40% sucrose in PBS). After centrifugation in a SW50.1 Beckman rotor at 160.000 g for 18 h at 4°C, nine 500 μL fractions were collected from the top of the gradient. Same volume aliquots of each fraction were added with Laemmli buffer containing both mercaptoethanol and bromophenol blue and boiled for 3 min. Samples were then subjected to SDS-PAGE and immunoblotting.

To measure the relative cholesterol content along the sucrose gradient fractionation, B1647 cells were preincubated at 37°C for 16 hours with [^{3}H]-cholesterol (0.1 μCi/mL) in cell culture medium. Cells exposed (or not) to 5 mM CD for 20 min were lysed with TX-100 at 4°C and subjected to sucrose gradient centrifugation as previously described. [^{3}H]-cholesterol content of each of the nine fractions collected was quantified by liquid scintillation counting.

2.6. Protein Assay. Protein concentration was usually determined by the Bradford method with BSA as standard [26]. The protein content of fractions obtained from sucrose gradient was determined by a Bio-Rad DC protein assay kit, using BSA in the presence of appropriate concentration of Triton X-100 or SDS as a standard.

2.7. Measurement of Intracellular ROS Levels. ROS intracellular level was evaluated using a fluorescent method, implying the probe, 2′,7′-dichlorofluorescin diacetate (DCFH-DA). Briefly, cells were incubated with 5 μM DCFH-DA for 30 min at 37°C and analyzed spectrofluorimetrically at $\lambda_{Ex/Em}$ 485/535 nm in a multiwell plate reader (Wallac Victor^2, PerkinElmer). Fluorescence values represent the percentage of inhibition of intracellular ROS with respect to controls.

2.8. Glucose Transport Assay. The measurement of glucose transport rate was performed according to [20]. In brief, 4 × 10^6 cells/mL were suspended in PBS, incubated with different *stimuli* and/or inhibitors at 37°C and then treated with a mixture of 2-deoxy-D-[2,6-^{3}H] glucose (0.4 μCi/assay) and 1 mM unlabelled glucose analogue (DOG mixture) for 2 min at 37°C under conditions where the uptake was linear at least for 20 min. After this time, the uptake was stopped by adding phloretin (final concentration, 0.2 mM), a potent inhibitor of glucose transport activity. Sample radioactivity was measured by liquid scintillation counting.

Transported 2-deoxy-D-glucose was less than 20% of the extracellular-sugar concentration; therefore, glucose transport assay could be considered in *zero-trans* conditions [27]. B1647 cells deprived of medium components and suspended in PBS during glucose transport measurements maintained their viability up to 2 hours at 37°C; thus, the number of viable cells during time intervals of experiments was considered constant (data not shown).

To test the effect of CD on the glucose transport activity, cells were incubated at 37°C with 5 mM CD for 20 min, washed, resuspended in 0.5 mL of PBS, and added with DOG mixture for the measurement of glucose uptake as previously described.

2.9. SDS-PAGE and Western Blot Analysis. Cells were lysed with buffer (1% Igepal, 150 mM NaCl, 50 mM Tris-HCl, 5 mM EDTA, 0,1 mM PMSF, 0,1 mM TLCK, 0,1 mM TPCK, 1 mM orthovanadate, and protease inhibitor cocktail, pH 8.0) in ice for 15 min. Cell lysates or fractions obtained after sucrose gradient centrifugation were separated on 10% SDS-polyacrylamide gel using a Mini-Protean II apparatus (BioRad Laboratories) and then transferred electrophoretically to nitrocellulose membranes. Nonspecific binding to membrane was blocked by incubating in Tris-buffered saline (TBS)/Tween, pH 8.0, containing 5% nonfat dried milk for 1 hour at room temperature. Blots were probed overnight at 4°C with primary antibodies, washed with TBS/Tween, and then incubated for 1 hour at room temperature with secondary horseradish peroxidase conjugates antibodies. Membranes were washed and the antigens were then visualized by addition of ECL Plus Western Blotting Detection Reagents.

2.10. Immunoprecipitation. B1647 cells maintained in the presence or absence of serum (+HS, −HS) for 16 h were lysates as described above for Western Blot. Lysates containing equal protein amounts were incubated overnight with anti-VEGFR-2 or anti-caveolin-1 antibodies. Then, samples were incubated

with protein A-Sepharose beads for 1.5 h at 4°C and then pelleted. Pellets were washed four times with lysis buffer, treated with reducing buffer containing 4% 2-mercaptoethanol, and then boiled for 3 min. Samples were then subjected to SDS-PAGE and immunoblotting with primary antibodies (anti-caveolin-1, anti-P-tyrosine, anti-VEGFR-2, and anti-Nox2) washed with TBS/Tween and then incubated for 1 hour at room temperature with the proper secondary horseradish peroxidase conjugate antibodies. Membranes were washed and the antigens were then visualized by addition of ECL Plus Western Blotting Detection Reagents.

2.11. Immunofluorescence. B1647 cells (2×10^6) were incubated for 20 min with or without 10 mM CD and then pelleted and fixed in 3% (w/v) paraformaldehyde for 15 min. Cells were washed twice with HBSS, blocked with PBS/BSA 1% (w/v) for 1 hour, and then incubated for 1 hour with 20 μg/mL of anti-Glut1 raised against a peptide within an extracellular domain of the human transporter protein. Cells were then treated for 1 hour with fluorescent FITC-conjugated rabbit anti-goat IgG, mounted on slides, and visualized using an Olympus IX50 microscope.

2.12. Statistical Analysis. Results are expressed as means with standard deviation. Differences between the means were determined by two-tailed Student's t-test or by Newman-Keuls multiple comparison test following one-way ANOVA and were considered significant at $P < 0.05$.

3. Results

3.1. Plasma Membrane Cholesterol Depletion by Means of Methyl-β-cyclodextrin (CD): Setting of Conditions. Cyclodextrins are cyclic oligomers of glucose that have the capacity to sequester lipophilic molecules in their hydrophobic core [28]. It has been shown that β-cyclodextrins remove cholesterol from cultured cells [29–31], and, among the different dextrin derivatives, methyl-β-cyclodextrin (CD) was shown to be the most efficient as acceptor of cellular cholesterol and the most commonly used [22, 31]. Therefore, we chose methyl-β-cyclodextrin to induce cholesterol depletion from plasma membrane of B1647 cell line and performed experiments to set the desired conditions, as the degree of cholesterol depletion is a function of the β-cyclodextrin derivative concentration, incubation time, temperature, and cell type subjected to the treatment [32].

First of all, B1647 cells suspended in culture medium were incubated overnight with [^{3}H]-cholesterol (0.5 mCi/mL) and then washed and exposed to different concentrations of CD (2.5–25 mM) for 20–40 min in order to find the best working conditions (not shown). Figure 1(a) represents the time course of CD effect on cholesterol level, evidencing that 5 mM CD for 20 min was able to remove about 60% cholesterol, keeping cell viability only about 10% decreased, as resulted by Trypan Blue exclusion test (Figure 1(b)). MTT assay was performed under the same conditions, confirming these results (not shown). These conditions, establishing a lipid environment alteration associated with membrane integrity, were selected for the following experiments.

3.2. Isolation and Identification of Membrane Caveolae/Lipid Rafts by Detergent Extraction and Sucrose Gradient Centrifugation in B1647 Cell Line. The isolation of membrane caveolae/lipid rafts relies on the relative insolubility in Triton X-100 (TX-100) detergent of membrane regions enriched in cholesterol and glycosphingolipids.

Thus, B1647 cells were lysed using TX-100 and centrifuged and the supernatant was collected and subsequently subjected to sucrose density-gradient (5–40%) centrifugation as described in Section 2. Nine fractions were collected and analyzed by SDS-PAGE followed by Western blotting using antiflotillin-2 (48 kDa), anti-caveolin-1 (24 kDa), and anti-Lyn (58 kDa) antibodies as protein markers for detergent resistant membrane fractions. Indeed, flotillin-2 and Lyn are known to be associated with caveolae/lipid rafts in different cell lines [33], as well as Cav-1, the major structural component of caveolae. The transferrin receptor (CD71), an integral membrane protein, was selected as a marker for nonraft membrane fractions.

As reported in Figure 2(a), flotillin-2, Lyn, and Cav-1 are localized in the low-density region of the gradient (fractions 2–6), between approximately the 10% and 25% sucrose layers, where caveolae/lipid rafts are supposed to be; instead, CD71 is located in the fractions 6–9.

The protein content of the different gradient fractions is reported in Figure 2(b), showing that the bulk of B1647 proteins was found in the high-density region at the bottom of the sucrose gradient.

Moreover, since it has been shown that CD is capable of removing cholesterol from both raft and nonraft fractions [34], the effect of CD treatment on cholesterol distribution in sucrose gradient fractionation was investigated. B1647 cells were labeled with [^{3}H]-cholesterol as described in Section 2. Cells were then exposed (or not) to 5 mM CD for 20 min, lysed with Triton X-100, and subjected to sucrose gradient centrifugation. As reported in Figure 2(c), fractions 2–6, where caveolae/lipid rafts are localized, exhibited the highest cholesterol content. Moreover, the cholesterol distribution profile of the samples treated with CD shows that, in our experimental conditions, fractions 2 and 3 exhibited a higher cholesterol depletion, evidencing a more efficient cholesterol removal from detergent resistant membranes, that is, caveolae/lipid rafts, compared to the other fractions.

3.3. Effect of Cholesterol Depletion from Plasma Membrane on VEGFR-2 Localization, ROS Generation, and Glucose Transport Activity in B1647 Cells. Since we previously demonstrated that a VEGF-mediated redox signaling pathway, creating a loop, is responsible for maintaining high intracellular ROS level, glucose uptake, and consequently B1647 cell proliferation [20, 21], we performed an experiment in order to understand the importance of caveolae/lipid rafts in the VEGFR-2 activation, stimulated by the autocrine VEGF production, characteristic of B1647 cells [19]. To investigate the functional role of caveolae/lipid rafts in the regulation of

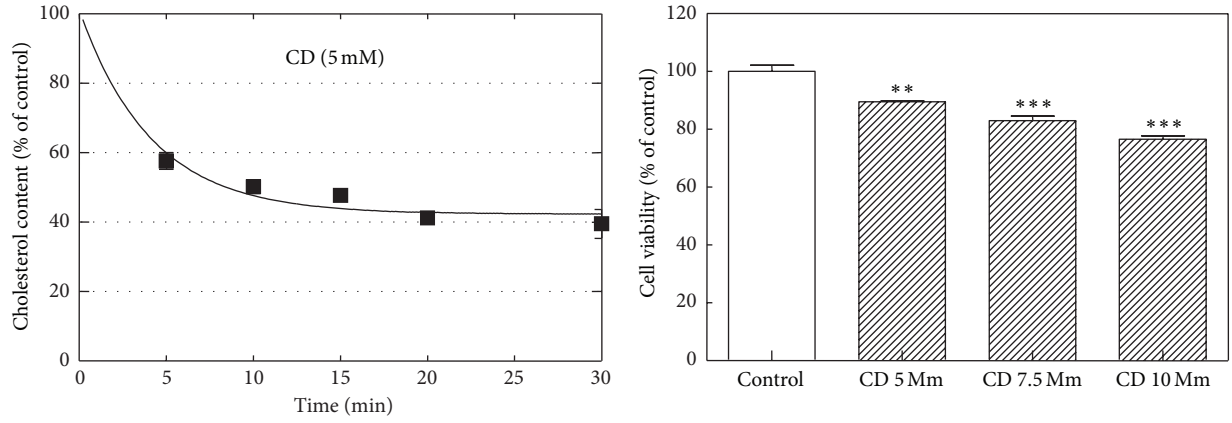

(a) (b)

Figure 1: *Effect of incubation time of CD on cholesterol content and cell viability in B1647 cells.* (a) Cells were incubated with [^{3}H]-cholesterol (0.5 μCi/mL) in cell culture medium for 16 h at 37°C, washed, resuspended in PBS, and treated with 5 mM CD for different time periods (0–30 min). Cell suspensions were washed with PBS and then [^{3}H]-cholesterol content was estimated by liquid scintillation counting. (b) The viability of the cells treated at different CD concentrations (5–10 mM) for 20 min was evaluated by Trypan Blue exclusion test as described in Section 2. Results are expressed as means ± SD of three independent experiments, each performed in triplicate. $^{**}P < 0.005$: significantly different from control cells; $^{***}P < 0.0005$: significantly different from control cells.

these activities, CD, a well-established cholesterol depleting reagent was used to cause their disruption.

B1647 cells, in the presence or absence of human serum (HS) and/or CD, were lysed by TX-100, centrifuged, and the supernatants were collected then separated by sucrose density-gradient (5–40%) centrifugation as described in Section 2. Nine fractions were collected and SDS-PAGE followed by Western blotting was performed to observe the localization of VEGFR-2.

As reported in Figure 3(a), cell treatment with CD resulted in the redistribution of VEGFR-2 from caveolae/lipid rafts to noncaveolar fractions both in the presence and in the absence of HS. Moreover, the distribution of VEGFR-2 is slightly different between cells in the presence of HS or starved, suggesting that the VEGF autoproduced by cells in the presence of human serum (normal condition) is able to link to its receptor causing a shift of the VEGF-VEGFR-2 complex towards noncaveolar membrane regions.

Parallel experiments were performed in order to examine the effect of CD in the presence or absence of HS on intracellular ROS level by means of a fluorimetric analysis implying DCFH-DA (Figure 3(b)) and on glucose uptake by using ^{3}H-DOG, a labeled glucose analogue (Figure 3(c)): both parameters increased after cholesterol depletion from plasma membrane by CD treatment, according to Western blotting results reported in Figure 3(a). These results suggest that VEGF-VEGFR-2 interaction, facilitated by the partial caveolae/lipid raft disruption, triggers a signal transduction pathway leading to an increase in ROS generation and glucose uptake.

Moreover, analyses of the images obtained by immunofluorescence microscopy of cells labelled with an anti-Glut1 antibody against an extracellular domain of Glut1 revealed that incubation with CD greatly enhances the staining for the transporter at the cell surface (Figure 3(d)). These results indicate that CD treatment increases glucose uptake through Glut1 recruitment into the plasma membrane from intracellular pool.

As previously shown [21], the absence of human serum caused a slight decrease both in DCF fluorescence and DOG uptake, indicating that VEGF self-production decreases in respect to normal conditions (i.e., in the presence of human serum) and/or that different agents modulate ROS production and glucose transport.

Thus, in order to better evaluate the role of VEGF, ruling out other effect due to other serum components, the following experiments were performed also on serum-depleted cells in the presence or absence of exogenous VEGF.

3.4. Association of VEGFR-2 with Caveolin-1. To better understand the relationship between caveolae/lipid rafts and VEGF receptor activation, the interaction/colocalization between VEGFR-2 and Cav-1 was investigated.

Therefore, B1647 cells were serum starved for 18 h and the colocalization of VEGFR-2 and Cav-1 was evaluated by immunoprecipitation experiments. As reported in Figure 4, in serum starved condition Cav-1 and VEGFR-2 colocalize and VEGFR-2 phosphorylation significantly decreases. These results indicate that the presence of VEGF could modulate the activation as well as the localization of VEGFR-2.

3.5. Importance of VEGF/VEGFR-2 Interaction for ROS Generation and Glucose Uptake. In order to corroborate the obtained results, we evaluated the effect of different compounds able to inhibit VEGF interaction with its receptor by different mechanisms.

In particular, B1647 cells in the presence or absence of serum (HS) were incubated for 2 hours with 3.4 nM

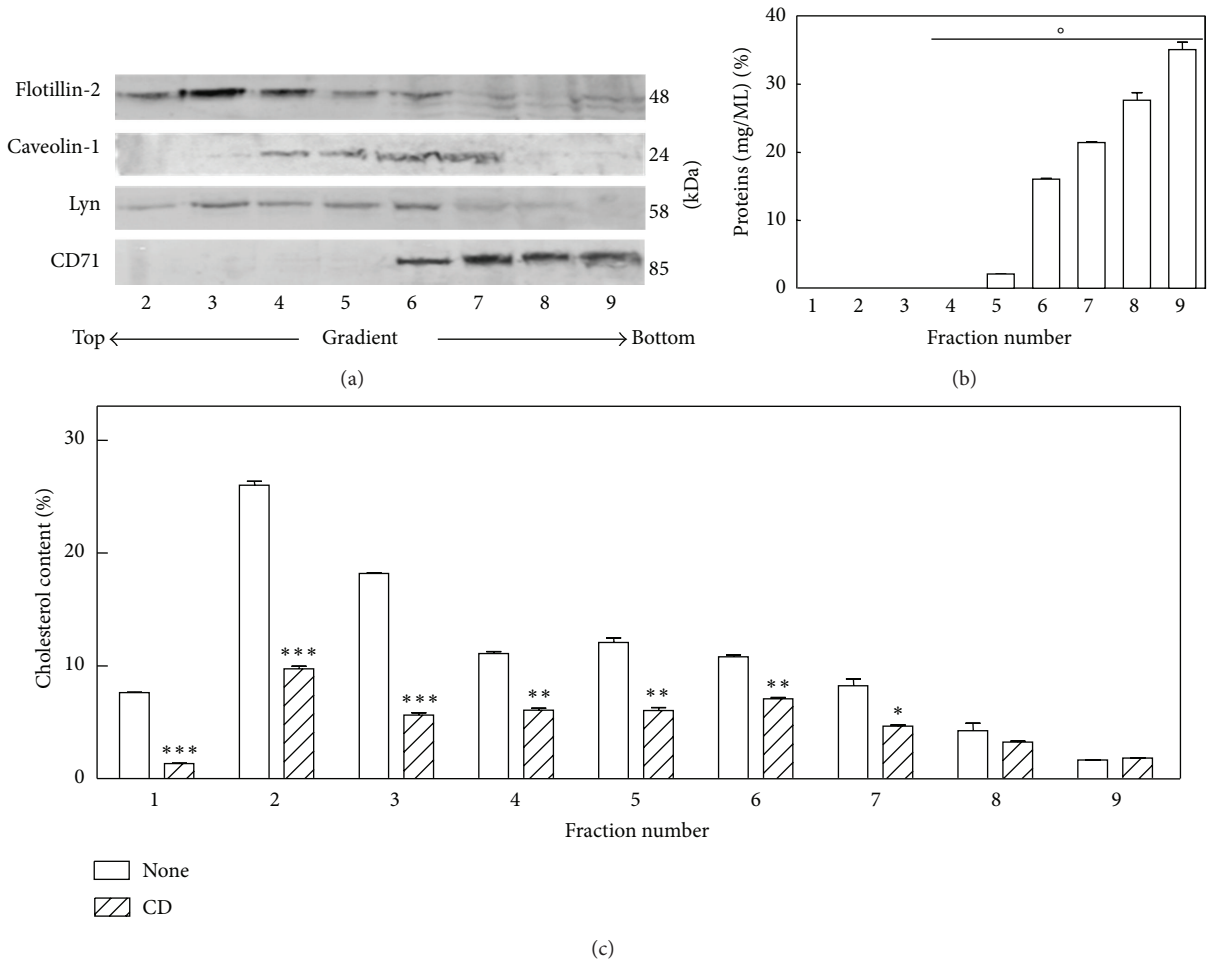

Figure 2: Isolation and identification of membrane caveolae/lipid rafts by detergent extraction and sucrose gradient centrifugation in B1647 cell line. (a) Cells were lysed with 1% Triton X-100 at 4°C and separated by sucrose density-gradient ultracentrifugation as described in Section 2. Equal aliquots of each fraction were subjected to SDS-PAGE and Western blotting. Flotillin-2, caveolin-1, and Lyn were used as markers for caveolae/lipid raft fractions and CD71 for nonlipid raft fractions. (b) Typical profile of protein concentrations in gradient fractions after ultracentrifugation. Protein content was determined as described in Section 2. (c) Cells were preincubated at 37°C for 16 hours with [^{3}H]-cholesterol (0.1 μCi/mL) in cell culture medium then exposed (or not) to 10 mM CD for 20 min, lysed with 1% Triton X-100 at 4°C, and subjected to sucrose density gradient ultracentrifugation as previously described. [^{3}H]-cholesterol content of each fraction collected was quantified by liquid scintillation counting. Results are expressed as means ± SD of three independent experiments, each performed in triplicate. $^{\circ}P < 0.01$: significantly different from each other; $^{*}P < 0.01$: significantly different from untreated cells; $^{**}P < 0.005$: significantly different from untreated cells; $^{***}P < 0.001$: significantly different from untreated cells.

Bevacizumab, a monoclonal anti-VEGF antibody [35], for 30 minutes or with 5 μM Cav-1 scaffolding domain (CSD) that represents the essential portion (residues 82 to 101) for Cav-1 interaction with other proteins [36].

Results showed that both Bevacizumab and CSD caused a decrease of intracellular ROS level in the presence or absence of HS (Figure 5).

50 ng/mL VEGF treatment, in the presence of inhibitors, was unable to induce ROS generation; on the contrary, it increased the intracellular ROS level in serum-depleted cells reaching the ROS content of control cells, confirming previously reported data [21].

Subsequently, cells were subjected to the same treatments and analyzed for glucose transport, (Figure 6), obtaining results very similar to that reported in Figure 5.

Semaxinib (SU5416), one of the most frequently used inhibitor of VEGFR-tyrosine activity, was also utilized (20 μM for 2 hours), obtaining a trend of response comparable to Bevacizumab and CSD effects. Semaxinib was not suitable for the detection of its effect on ROS intracellular level due to its autofluorescence [37].

Survival experiments performed by MTT assay demonstrated that cell viability did not change in these experimental conditions (data not shown).

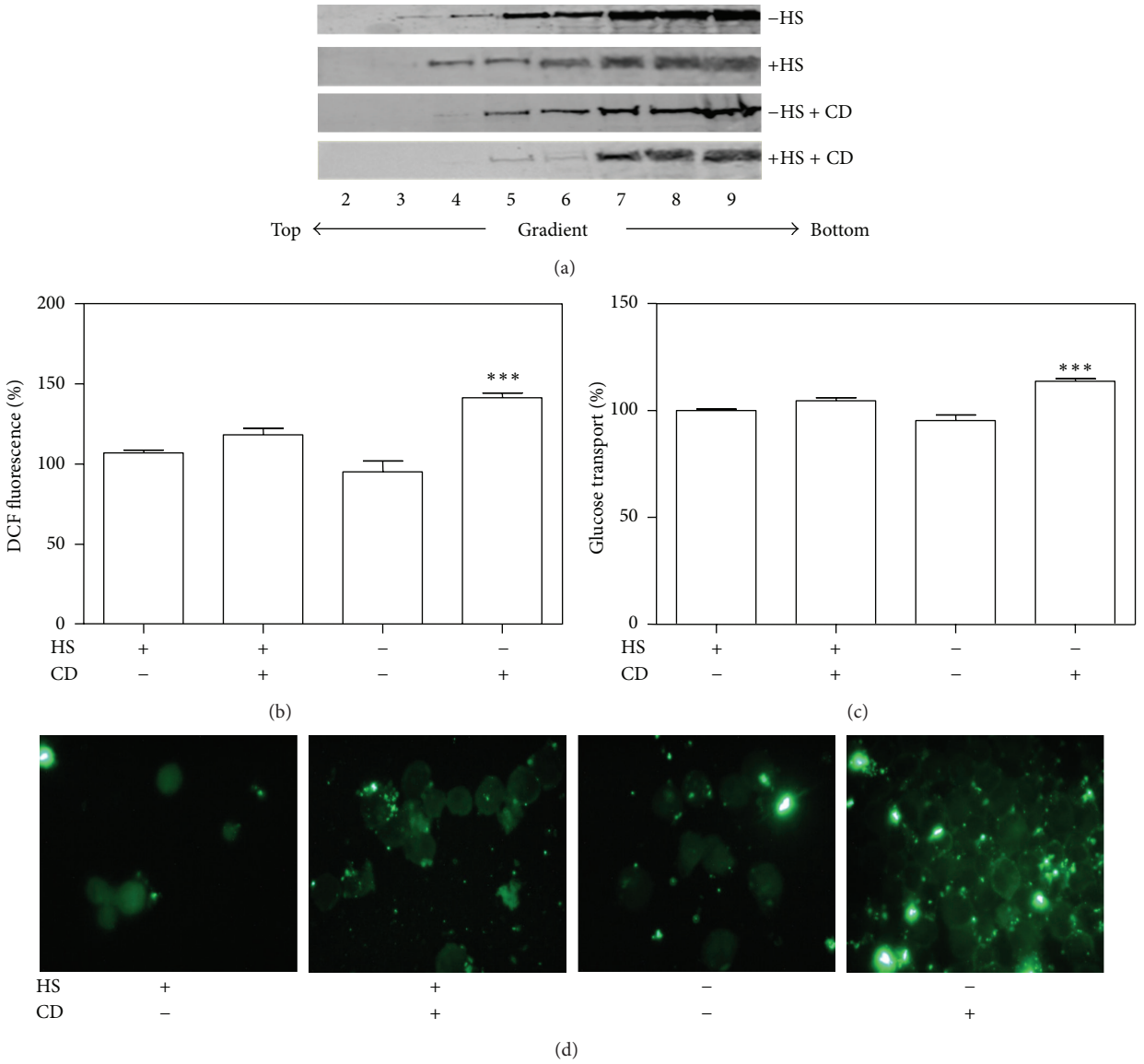

Figure 3: Effect of cholesterol depletion from plasma membrane on VEGFR-2 localization, ROS generation, and glucose transport activity in B1647 cells. (a) Cells in the presence or absence of human serum (HS) and/or pretreated with 5 mM CD for 20 min were lysed with 1% Triton X-100 at 4°C and separated by sucrose density-gradient ultracentrifugation as described in Section 2. Equal aliquots of each fraction were subjected to SDS-PAGE, Western blotting, and revealed for anti-VEGFR-2 (210 kDa). A representative blot is shown. (b) Cells in the presence or absence of human serum (HS) and/or pretreated with 5 mM CD for 20 min were incubated with 5 μM DCFH-DA and ROS intracellular level was measured spectrofluorimetrically as described in Section 2. (c) Cells in the presence or absence of human serum (HS) and/or pretreated with 5 mM CD for 20 min were incubated with DOG mixture and glucose uptake was assayed by liquid scintillation counting as described in Section 2. (d) Cells in the presence or absence of human serum (HS) and incubated (or not) in PBS at 37°C with 5 mM CD for 20 min were fixed in 3% (w/v) paraformaldehyde for 15 min. Cells were then immunolabelled with anti-Glut1 (N-20) antibody (raised against an extracellular domain of Glut1, therefore, evidencing that Glut1 is present on the cell surface), treated with fluorescent FITC-conjugated secondary antibody, and visualized using immunofluorescence microscopy.

3.6. Caveolin-1 Interaction with Nox2 and VEGFR-2 in the Presence or Absence of VEGF in B1647 Cells. It has already been reported that Nox2 is present in caveolae/lipid rafts in association with Cav-1 in vascular smooth muscle cells [38] and that Nox4 is mainly located in nonraft region of the plasma membrane [39].

Figure 7(a) shows that in absence of VEGF (−HS) Nox2 colocalizes with Cav-1 in B1647 cells. CD and VEGF treatment significantly decreases Cav-1/Nox2 association, demonstrating that in absence of VEGF, Nox2 colocalizes with Cav-1, presumably into caveolae/lipid raft compartments.

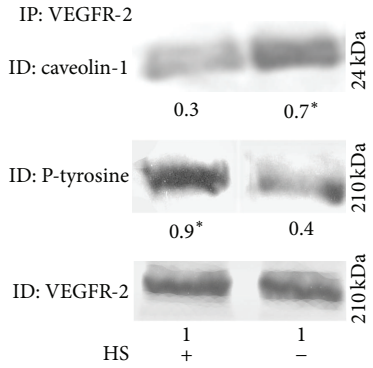

Figure 4: *Association of VEGFR-2 with caveolin-1 in B1647 cells.* Cells deprived or not of serum (±HS) were subjected to immunoprecipitation with anti-VEGFR-2 as described in Section 2. Samples were electrophoresed, immunoblotted, and revealed for anti-caveolin-1, for antiphosphotyrosine, or with anti-VEGFR-2. A representative blot is shown. Results were obtained considering three independent Western blot experiments. Relative amounts determined by scanning densitometry are expressed in arbitrary units. $^*P < 0.05$: significantly different from control cells (+HS).

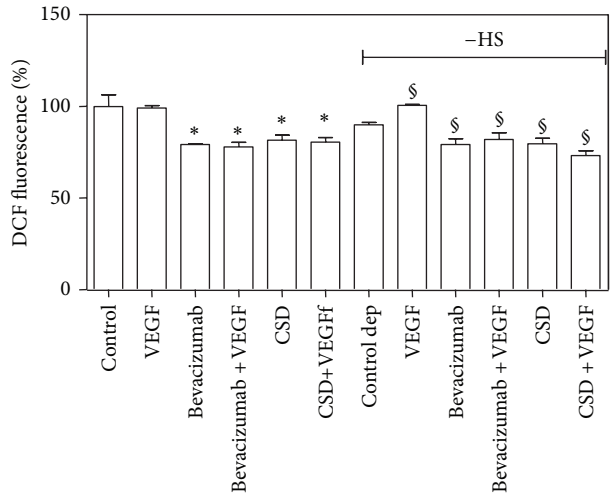

Figure 5: *Effect of different inhibitors of VEGF/VEGFR-2 interaction on intracellular ROS level in B1647 cells.* Cells, control, and serum starved (–HS, "Control dep") were treated with 500 μg/mL Bevacizumab for 30 min or 5 μM Cav-1 scaffolding domain (CSD) for 2 h, in the presence or absence of 50 ng/mL VEGF; then, the intracellular ROS level was spectrofluorimetrically measured by means of DCFH-DA, as described in Section 2. $^*P < 0.05$: significantly different from control cells; $^{\S}P < 0.05$: significantly different from serum deprived control cells (–HS).

After CD and VEGF treatment, VEGFR-2 association with Cav-1 significantly decreases and this effect is partially counteracted by HS starvation (absence of VEGF) (Figure 7(c)). Additionally, we did not observe a colocalization between p-VEGFR-2 and Cav-1 suggesting that the activation of VEGFR-2 occurs in noncaveolar compartments (data not shown).

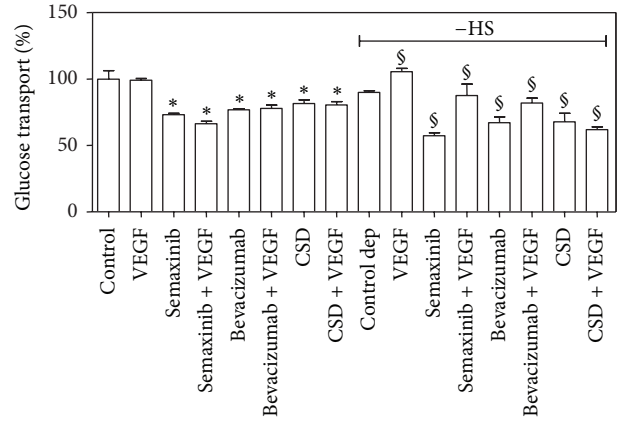

Figure 6: *Effect of different inhibitors of VEGF/VEGFR-2 interaction on glucose transport in B1647 cells.* Cells, control, and serum starved (–HS, "Control dep") were treated with 20 μM Semaxinib for 2 h, 500 μg/mL Bevacizumab for 30 min, or 5 μM Cav-1 scaffolding domain (CSD) for 2 h, in the presence or absence of 50 ng/mL VEGF; then, glucose uptake was assayed by liquid scintillation counting as described in Section 2. $^*P < 0.05$: significantly different from control cells; $^{\S}P < 0.05$: significantly different from serum deprived control cells (–HS).

4. Discussion

Caveolae/lipid rafts function as signaling organizing centers and platforms by exploiting multiple protein-lipid and protein-protein interactions to link the cytoplasmic tail of trans-membrane receptors with other protein scaffolds to assemble kinases, phosphatases, and other catalytically active molecules, consequently modulating specific signals that are temporally and spatially controlled [40, 41]. This concept is peculiar for redox signaling: in order to act as signal molecules, ROS must be generated in discrete compartments and following certain *stimuli* thus produced in a controlled manner from the standpoint of the space/time [42–44].

Regarding this context, we have been intrigued by recent reports showing the involvement of caveolae in the regulation of redox signal transduction mediated by VEGF in endothelial cells [10, 45–48]. VEGFR-2 signal transduction seems to follow the scheme for the activation of receptor tyrosine kinases, following receptor dimerization induced by VEGF binding. Dissociation of VEGFR-2 from caveolae has been shown to be essential for its autophosphorylation and activation of downstream signaling events [7, 47]. Moreover, VEGF and its receptors have been shown to be critical players in the embryonic development of endothelial and blood cells [49] and the evidence that angiogenesis plays a pathophysiological role in leukemia has been well documented [50].

Since endothelial cells share signal transduction pathways with hematopoietic cells [51], we investigated the potential role played by caveolae/lipid rafts in the modulation of redox signaling induced by VEGF, in a model of human acute leukemia: B1647 cell line.

We previously demonstrated that B1647 cells possess high level of Nox-derived ROS that sustain cellular growth and

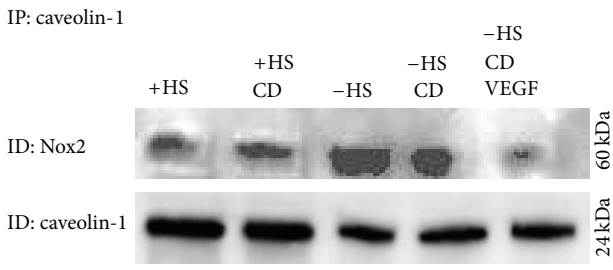

(a)

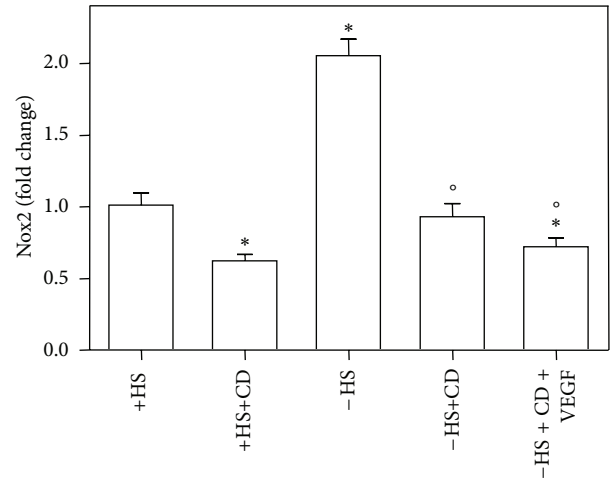

(b)

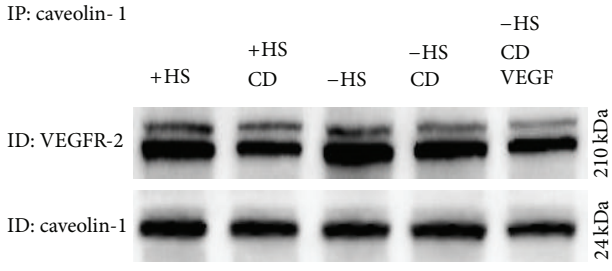

(c)

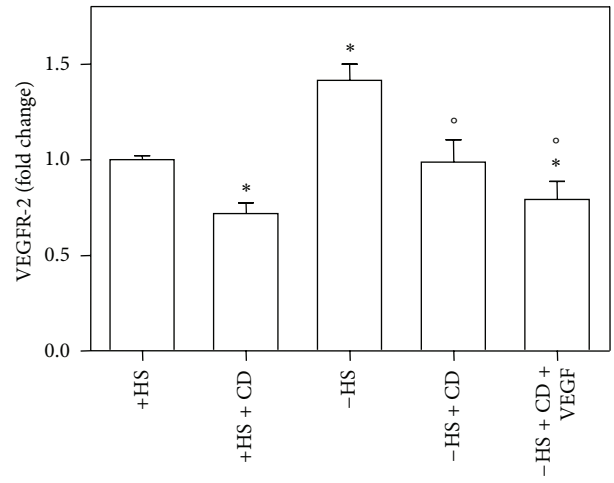

(d)

Figure 7: *Caveolin-1 interaction with Nox2 and VEGFR-2 in the presence or absence of VEGF in B1647 cells.* Cells deprived or not of serum (±HS) were subjected to immunoprecipitation with anti-caveolin-1 as described in Section 2. (a) Samples were electrophoresed, immunoblotted, and revealed for anti-Nox2 and anti-caveolin-1; a representative blot is shown. (b) Densitometric analysis normalized for caveolin-1 content and expressed as fold change in Nox2 expression with respect to control (+HS). (c) Samples were electrophoresed, immunoblotted, and revealed for anti-VEGFR-2 and anti-caveolin-1; a representative blot is shown. (d) Densitometric analysis normalized for caveolin-1 content and expressed as fold change in VEGFR-2 expression with respect to control (+HS). Results were obtained considering three independent Western blot experiments. $^{*}P < 0.05$: significantly different from control cells (+HS); $^{\circ}P < 0.05$: significantly different from control serum starved cells (−HS).

glucose uptake, creating a loop signal transduction suggested to be maintained by autocrine VEGF production [20, 21].

Frequently, leukemia cells contain relatively elevated intracellular ROS level and it has been previously established that Nox-generated ROS can trigger genomic instability and different downstream prosurvival pathways [52], even if the mechanisms involved are not completely understood. Their elucidation could have important therapeutic implications.

Several studies have shown that AML cells release angiogenic growth factors such as VEGF within the bone marrow and that subsets of acute leukemias also express VEGF receptors; thus, autocrine stimulation of leukemia cells by VEGF may result in proliferation, migration, and resistance to chemotherapy [53]; VEGF exerts indeed its trophic effect on malignant myeloid progenitors via either paracrine or autocrine interaction [54].

In the present work we report that VEGFR-2 is partially localized in caveolae/lipid rafts, and after the binding with VEGF a shift to nonraft portions of membrane occurs, causing the trigger of phosphorylation cascade by the activation of tyrosine kinase VEGFR-2 and leading to increase of glucose transport marker of cell proliferation.

The first step was the setting of the optimal conditions for obtaining a caveolae/lipid raft disruption by considerable cholesterol depletion from membrane without affecting cell viability during the time of the experiment. As tools to achieve this goal we used CD, reported to have the highest affinity for cholesterol inclusion and to be the most efficient in extracting cholesterol from membranes [22]; nevertheless, the CD efficiency may vary significantly depending on its concentration, duration of the exposure, and cell model. In our conditions, cell treatment with 5 mM CD for 20 min was able to remove 60% of cholesterol from plasma membrane without seriously affecting cell viability.

Because of the lack of a standardized method to detect and isolate caveolae/lipid rafts [43], here the experimental evidence of their existence is given by their resistance to solubilization by the nonionic detergent TX-100 1% at 4°C followed by density-gradient centrifugation [55]. In order to exclude the hypothesis of artifacts, we used an alternative method to isolate raft-like membranes with a detergent-free medium containing a high sodium carbonate concentration, obtaining similar results (data not shown).

Even if several studies revealed that β-cyclodextrins are capable of removing cholesterol from both raft and nonraft fractions [22], the efficiency of cholesterol removal preferentially from lipid rafts is obtained by using short time exposures or very low CD concentration [34]. Figure 2(c) demonstrated that although the cholesterol content of all membrane fractions was significantly reduced, in our experimental conditions CD was able to remove cholesterol more efficiently from detergent resistant membrane, representing the fractions containing caveolae/lipid rafts.

Our results show that in sucrose gradient fractionations of lysed B1647 cells (+HS), VEGFR-2 is present both in raft and nonraft regions. When cells are deprived of serum (−HS), VEGFR-2 content increases in the caveolae/raft fraction and when CD was added to the cells VEGFR-2 is mainly present in nonraft fraction. These results compared to data on the ROS intracellular level and glucose uptake (Figures 3(b) and 3(c)) of cells subjected to the same treatments (i.e., in the presence or absence of serum and in the presence or absence of CD) suggests that when VEGF, normally autoproduced by B1647 cells, binds to its receptor it causes its activation, displacing it from raft to nonraft regions. The disruption of rafts allows more interaction between VEGF and its VEGFR-2 receptor, increasing its phosphorylation and modulating the derived signal transduction pathways leading to glucose uptake. Images reported in Figure 3(d) confirm the increase in Glut1 isoform on the plasma membrane of cells in the presence of CD.

Moreover, we demonstrated that VEGFR-2 in the absence of serum is more linked to Cav-1, a major caveolae component [7]; instead, in normal condition (+HS) where VEGF autocrine production is *bona fide* high, VEGFR-2 binding to Cav-1 significantly decreases promoting its activation, as demonstrated by the higher level of phosphorylation observed. These data are in accordance with those obtained in endothelial cells, where Cav-1 acts as negative regulator of VEGFR-2 activity [7].

To deeply analyze the importance of VEGF/VEGFR-2 interaction to induce ROS production and related glucose uptake [21] and the downregulation exerted by VEGFR-2 localization in caveolae/lipid rafts, we tested, in control and serum starved cells, different compounds able to inhibit the binding of VEGF to its receptors. In particular, Bevacizumab was selected as a monoclonal anti-VEGF antibody highly active against several cancers [56]. Today, it is the most commonly used anti-VEGF drug against tumor-derived VEGF [35, 57], validating Folkman's early prediction on the importance of inhibit tumor angiogenesis [58]. Nevertheless, the wide adverse effects induced by anti-VEGF agents demonstrate that these drugs have a broad impact on vasculatures in multiple healthy tissues and organs.

As previously cited, caveolae are coated with a 24 kDa protein, Cav-1. This protein regulates multiple cancer-associated processes including cellular transformation, tumor growth, cell migration and metastasis, cell death and survival, multidrug resistance, and angiogenesis. However, Cav-1 has been reported to influence both positively and negatively various aspects of tumor progression and to act as tumor suppressor or poor prognostic factor in many human cancers [8].

To clarify the role of Cav-1 in our model, we incubated the cells with the Cav-1 scaffolding domain (CSD), representing the portion of the protein (residues 82 to 101) essential for both Cav-1 oligomerization and the interaction with other proteins [36]. Associations with other proteins through the CSD provide coordinated and efficient signal transduction [59]. CSD binds many signaling molecules, including endothelial nitric-oxide synthase (eNOS), Src-like kinases, Ha-Ras, and heterotrimeric G-proteins [60]. Binding of these proteins to CSD in many cases negatively regulates their function [61]. Moreover, acute vascular inflammation in mice was prevented by systemic administration of cell-permeable CSD peptide [62].

Our results suggest that Cav-1 or VEGFR-2 localization in caveolae may act as negative regulators of the receptor activity. Similarly, the treatment of HUVEC with CSD caused significant reduction in the VEGF-stimulated phosphorylation of VEGFR-2, suggesting that CSD inhibits Cav-1-mediated angiogenic signaling [47].

Last but not least, Semaxinib, a reversible, ATP-competitive, oxindole-based inhibitor of VEGFR-2 tyrosine kinase, inhibits VEGF-dependent phosphorylation of the VEGFR-2 overexpressed in NIH 3T3 cells with an IC_{50} of 1.04 μM. In an ELISA-based assay, Semaxinib inhibits autophosphorylation of the VEGFR-2 at an IC_{50} of 1.23 μM [63]. The results obtained with the three compounds able to inhibit VEGF/VEGFR-2 interaction confirm the importance of this molecular complex in maintaining the redox loop leading to high intracellular ROS level and glucose uptake of B1647 cells.

We previously reported that, in B1647 cells expressing Nox2 and Nox4, VEGF signaling and Nox activity are coupled [20, 21]; moreover, it has been recently demonstrated that inhibitors of both Nox and VEGF receptors are able to induce apoptosis in leukemia cell lines and that lipid rafts play a role in this process [40]. Thus, we performed experiments to evaluate the involvement of caveolae/lipid rafts in the

coordination of VEGFR-2 activation and ROS production by Nox2. Nox4, indeed, is a constitutive active isoform [64] reported to be mainly present in nonraft region of the plasma membrane [39]. Figure 7 suggests that VEGF promotes the dissociation of both Nox2 and VEGFR-2 from Cav-1 and the consequently activation of Nox2–VEGFR-2 axis in nonraft fractions. Our results are in accordance with those by Han and colleagues [65], demonstrating that in human renal proximal tubule cells the majority of p22phox and Rac1 is distributed in lipid rafts, whereas Nox4 is excluded from them. Cholesterol depletion increased NAD(P)H oxidase activity by redistributing NAD(P)H oxidase subunits in nonlipid raft membrane, suggesting that in human nonphagocytic cells, lipid rafts keep NAD(P)H oxidase (Nox2) in the inactive state.

Our data support recent findings reporting that the recruitment of specific receptors, transporters, and isoforms of NAD(P)H oxidase within membrane microdomains generates redox signaling platforms, recently defined as "redoxosomes," which could be the missing link between receptor activation and enzymatic generation of ROS [48, 66].

Moreover, results here reported suggest emerging targets for new pharmaceutical application and clinical translation.

5. Conclusions

In this study we evaluated the potential involvement of caveolae/lipid rafts in the modulation of VEGF-induced redox signal transduction in leukemia cells.

We demonstrated, for the first time to our knowledge, that the colocalization of VEGFR-2 and Nox2 in caveolae/lipid rafts is involved in the negative modulation of glucose uptake, necessary to the deregulated proliferation of B1647 leukemia cell line.

Studies of how the redox system is controlled and balanced towards/against a proliferative advantage in leukemia cells suggest new therapeutic targets and may hold the key to unlocking therapeutic resistance in leukemia.

Abbreviations

AML: Acute myeloid leukemia
B1647: Human erythromegakaryocytic leukemia cell line
Cav-1: Caveolin-1
CD: Methyl-β-cyclodextrin
CD71: Transferrin receptor
CSD: Cav-1 scaffolding domain
DCF: Dichlorofluorescein
DCFH-DA: Dichlorofluorescin diacetate
DOG: 2-deoxy-D-glucose
DPI: Diphenyleneiodonium chloride
Glut1: Glucose transporter-1
HS: Human serum
Nox: NAD(P)H oxidase
ROS: Reactive oxygen species
VEGF: Vascular endothelial cell growth factor
VEGFR-1: Vascular endothelial growth factor receptor-1
VEGFR-2: Vascular endothelial growth factor receptor-2 (also known as KDR).

Conflict of Interests

The authors declare that there is no conflict of interests regarding the publication of this paper.

Authors' Contribution

Cristiana Caliceti and Laura Zambonin contributed equally to this paper. Silvana Hrelia and Cecilia Prata are co-last authors.

Acknowledgments

The authors are grateful to Professor Laura Landi for scientific suggestions, guidance, and constructive discussion of this research; they immensely appreciate her strong support and mentorship in regard to their research endeavors. The authors would like to thank Professor Laura Bonsi who kindly provided B1647 cell line used in this study and Dr. Emanuela Leoncini for her help in the preparation of this paper. This work was supported by grants from Italian Ministry for Education, University and Research (MIUR), and Fondazione del Monte di Bologna e Ravenna, Italy. The funders had no role in study design, data collection and analysis, decision to publish, or paper preparation.

References

[1] K. Simons and R. Ehehalt, "Cholesterol, lipid rafts, and disease," *Journal of Clinical Investigation*, vol. 110, no. 5, pp. 597–603, 2002.

[2] J. A. Allen, R. A. Halverson-Tamboli, and M. M. Rasenick, "Lipid raft microdomains and neurotransmitter signalling," *Nature Reviews Neuroscience*, vol. 8, no. 2, pp. 128–140, 2007.

[3] P. A. Insel, B. P. Head, R. S. Ostrom et al., "Caveolae and lipid rafts: G protein-coupled receptor signaling microdomains in cardiac myocytes," *Annals of the New York Academy of Sciences*, vol. 1047, pp. 166–172, 2005.

[4] E. J. Smart and R. G. W. Anderson, "Alterations in membrane cholesterol that affect structure and function of caveolae," *Methods in Enzymology*, vol. 353, pp. 131–139, 2002.

[5] L. J. Pike, "Lipid rafts: bringing order to chaos," *Journal of Lipid Research*, vol. 44, no. 4, pp. 655–667, 2003.

[6] R. G. Parton and M. A. del Pozo, "Caveolae as plasma membrane sensors, protectors and organizers," *Nature Reviews Molecular Cell Biology*, vol. 14, no. 2, pp. 98–112, 2013.

[7] L. Labrecque, I. Royal, D. S. Surprenant, C. Patterson, D. Gingras, and R. Béliveau, "Regulation of vascular endothelial growth factor receptor-2 activity by caveolin-1 and plasma membrane cholesterol," *Molecular Biology of the Cell*, vol. 14, no. 1, pp. 334–347, 2003.

[8] J. G. Goetz, P. Lajoie, S. M. Wiseman, and I. R. Nabi, "Caveolin-1 in tumor progression: the good, the bad and the ugly," *Cancer and Metastasis Reviews*, vol. 27, no. 4, pp. 715–735, 2008.

[9] X. . Zhao, Y. He, J. Gao et al., "Caveolin-1 expression level in cancer associated fibroblasts predicts outcome in gastric cancer," *PLoS One*, vol. 8, no. 3, Article ID e59102, 2013.

[10] M. Ushio-Fukai, "VEGF signaling through NADPH oxidase-derived ROS," *Antioxidants and Redox Signaling*, vol. 9, no. 6, pp. 731–739, 2007.

[11] T. Matsumoto and H. Mugishima, "Signal transduction via vascular endothelial growth factor (VEGF) receptors and their roles in atherogenesis," *Journal of Atherosclerosis and Thrombosis*, vol. 13, no. 3, pp. 130–135, 2006.

[12] K. Choi, M. Kennedy, A. Kazarov, J. C. Papadimitriou, and G. Keller, "A common precursor for hematopoietic and endothelial cells," *Development*, vol. 125, no. 4, pp. 725–732, 1998.

[13] T. S. Park, L. Zimmerlin, and E. T. Zambidis, "Efficient and simultaneous generation of hematopoietic and vascular progenitors from human induced pluripotent stem cells," *Cytometry A*, vol. 83, no. 1, pp. 114–126, 2012.

[14] A. R. Perez-Atayde, S. E. Sallan, U. Tedrow, S. Connors, E. Allred, and J. Folkman, "Spectrum of tumor angiogenesis in the bone marrow of children with acute lymphoblastic leukemia," *American Journal of Pathology*, vol. 150, no. 3, pp. 815–821, 1997.

[15] A. Tzankov, M. Medinger, and N. Fischer, "Vascular endothelial growth factor-related pathways in hemato-lymphoid malignancies," *Journal of Oncology*, vol. 2013, Article ID 729725, 13 pages, 2010.

[16] A. Aguayo, H. M. Kantarjian, E. H. Estey et al., "Plasma vascular endothelial growth factor levels have prognostic significance in patients with acute myeloid leukemia but not in patients with myelodysplastic syndromes," *Cancer*, vol. 95, no. 9, pp. 1923–1930, 2002.

[17] G. Song, Y. Li, and G. Jiang, "Role of VEGF/VEGFR in the pathogenesis of leukemias and as treatment targets (review)," *Oncology Reports*, vol. 28, no. 6, pp. 1935–1944, 2012.

[18] M. E. . Irwin, N. Rivera-Del Valle, and J. Chandra, "Redox control of leukemia: from molecular mechanisms to therapeutic opportunities," *Antioxidants & Redox Signaling*, vol. 18, no. 11, pp. 1349–1383, 2012.

[19] L. Bonsi, L. Pierdomenico, M. Biscardi et al., "Constitutive and stimulated production of VEGF by human megakaryoblastic cell lines: effect on proliferation and signaling pathway," *International Journal of Immunopathology and Pharmacology*, vol. 18, no. 3, pp. 445–455, 2005.

[20] C. Prata, T. Maraldi, D. Fiorentini, L. Zambonin, G. Hakim, and L. Landi, "Nox-generated ROS modulate glucose uptake in a leukaemic cell line," *Free Radical Research*, vol. 42, no. 5, pp. 405–414, 2008.

[21] T. Maraldi, C. Prata, C. Caliceti et al., "VEGF-induced ROS generation from NAD(P)H oxidases protects human leukemic cells from apoptosis," *International Journal of Oncology*, vol. 36, no. 6, pp. 1581–1589, 2010.

[22] R. Zidovetzki and I. Levitan, "Use of cyclodextrins to manipulate plasma membrane cholesterol content: evidence, misconceptions and control strategies," *Biochimica et Biophysica Acta*, vol. 1768, no. 6, pp. 1311–1324, 2007.

[23] T. Maraldi, D. Fiorentini, C. Prata, L. Landi, and G. Hakim, "Glucose-transport regulation in leukemic cells: How can H_2O_2 mimic stem cell factor effects?" *Antioxidants and Redox Signaling*, vol. 9, no. 2, pp. 271–279, 2007.

[24] C. Caliceti, L. Zambonin, C. Prata et al., "Effect of plasma membrane cholesterol depletion on glucose transport regulation in leukemia cells," *PLoS One*, vol. 7, no. 7, Article ID e41246, 2012.

[25] D. A. Brown, "Analysis of raft affinity of membrane proteins by detergent-insolubility," *Methods in Molecular Biology*, vol. 398, pp. 9–20, 2007.

[26] M. M. Bradford, "A rapid and sensitive method for the quantitation of microgram quantities of protein utilizing the principle of protein dye binding," *Analytical Biochemistry*, vol. 72, no. 1-2, pp. 248–254, 1976.

[27] T. Maraldi, M. Rugolo, D. Fiorentini, L. Landi, and G. Hakim, "Glucose transport activation in human hematopoietic cells M07e is modulated by cytosolic calcium and calmodulin," *Cell Calcium*, vol. 40, no. 4, pp. 373–381, 2006.

[28] J. Pitha, T. Irie, P. B. Sklar, and J. S. Nye, "Drug solubilizers to aid pharmacologists: amorphous cyclodextrin derivatives," *Life Sciences*, vol. 43, no. 6, pp. 493–502, 1988.

[29] Y. Ohtani, T. Irie, K. Uekama, K. Fukunaga, and J. Pitha, "Differential effects of α-, β- and γ-cyclodextrins on human erythrocytes," *European Journal of Biochemistry*, vol. 186, no. 1-2, pp. 17–22, 1989.

[30] E. P. C. Kilsdonk, P. G. Yancey, G. W. Stoudt et al., "Cellular cholesterol efflux mediated by cyclodextrins," *The Journal of Biological Chemistry*, vol. 270, no. 29, pp. 17250–17256, 1995.

[31] U. Klein, G. Gimpl, and F. Fahrenholz, "Alteration of the myometrial plasma membrane cholesterol content with β-cyclodextrin modulates the binding affinity of the oxytocin receptor," *Biochemistry*, vol. 34, no. 42, pp. 13784–13793, 1995.

[32] A. E. Christian, M. P. Haynes, M. C. Phillips, and G. H. Rothblat, "Use of cyclodextrins for manipulating cellular cholesterol content," *Journal of Lipid Research*, vol. 38, no. 11, pp. 2264–2272, 1997.

[33] K. Barnes, J. C. Ingram, M. D. M. Bennett, G. W. Stewart, and S. A. Baldwin, "Methyl-β-cyclodextrin stimulates glucose uptake in Clone 9 cells: a possible role for lipid rafts," *Biochemical Journal*, vol. 378, part 2, pp. 343–351, 2004.

[34] K. Gaus, E. Chklovskaia, B. Fazekas De St. Groth, W. Jessup, and T. Harder, "Condensation of the plasma membrane at the site of T lymphocyte activation," *Journal of Cell Biology*, vol. 171, no. 1, pp. 121–131, 2005.

[35] Y. . Yang, Y. Zhang, Z. Cao et al., "Anti-VEGF- and anti-VEGF receptor-induced vascular alteration in mouse healthy tissues," *Proceedings of the National Academy of Sciences of the United States of America*, vol. 110, no. 29, pp. 12018–12023, 2013.

[36] J. Couet, S. Li, T. Okamoto, T. Ikezu, and M. P. Lisanti, "Identification of peptide and protein ligands for the caveolin- scaffolding domain. Implications for the interaction of caveolin with caveolae-associated proteins," *The Journal of Biological Chemistry*, vol. 272, no. 10, pp. 6525–6533, 1997.

[37] P. Vajkoczy, M. D. Menger, B. Vollmar et al., "Inhibition of tumor growth, angiogenesis, and microcirculation by the novel Flk-1 inhibitor SU5416 as assessed by intravital multifluorescence videomicroscopy," *Neoplasia*, vol. 1, no. 1, pp. 31–41, 1999.

[38] M. Ushio-Fukai, L. Zuo, S. Ikeda, T. Tojo, N. A. Patrushev, and R. W. Alexander, "cAbl tyrosine kinase mediates reactive oxygen species- and caveolin-dependent AT1 receptor signaling in vascular smooth muscle: role in vascular hypertrophy," *Circulation Research*, vol. 97, no. 8, pp. 829–836, 2005.

[39] L. L. Hilenski, R. E. Clempus, M. T. Quinn, J. D. Lambeth, and K. K. Griendling, "Distinct Subcellular Localizations of Nox1 and Nox4 in Vascular Smooth Muscle Cells," *Arteriosclerosis, Thrombosis, and Vascular Biology*, vol. 24, no. 4, pp. 677–683, 2004.

[40] M. Ushio-Fukai and Y. Nakamura, "Reactive oxygen species and angiogenesis: NADPH oxidase as target for cancer therapy," *Cancer Letters*, vol. 266, no. 1, pp. 37–52, 2008.

[41] K. S. George and S. Wu, "Lipid raft: a floating island of death or survival," *Toxicology and Applied Pharmacology*, vol. 259, no. 3, pp. 311–319, 2012.

[42] P.-L. Li and E. Gulbins, "Lipid rafts and redox signaling," *Antioxidants and Redox Signaling*, vol. 9, no. 9, pp. 1411–1415, 2007.

[43] H. H. Patel and P. A. Insel, "Lipid rafts and caveolae and their role in compartmentation of redox signaling," *Antioxidants and Redox Signaling*, vol. 11, no. 6, pp. 1357–1372, 2009.

[44] B. Yang, T. N. Oo, and V. Rizzo, "Lipid rafts mediate H_2O_2 prosurvival effects in cultured endothelial cells," *The FASEB Journal*, vol. 20, no. 9, pp. E688–E697, 2006.

[45] J. Oshikawa, S.-J. Kim, E. Furuta et al., "Novel role of p66shc in ROS-dependent VEGF signaling and angiogenesis in endothelial cells," *American Journal of Physiology: Heart and Circulatory Physiology*, vol. 302, no. 3, pp. H724–H732, 2012.

[46] J. Oshikawa, N. Urao, H. W. Kim et al., "Extracellular SOD-derived H_2O_2 promotes VEGF signaling in caveolae/lipid rafts and post-ischemic angiogenesis in mice," *PLoS ONE*, vol. 5, no. 4, Article ID e10189, 2010.

[47] S. A. Tahir, S. Park, and T. C. Thompson, "Caveolin-1 regulates VEGF-stimulated angiogenic activities in prostate cancer and endothelial cells," *Cancer Biology and Therapy*, vol. 8, no. 23, pp. 2286–2296, 2009.

[48] M. Ushio-Fukai, "Compartmentalization of redox signaling through NaDPH oxidase-derived ROS," *Antioxidants and Redox Signaling*, vol. 11, no. 6, pp. 1289–1299, 2009.

[49] E. Saulle, R. Riccioni, S. Coppola et al., "Colocalization of the VEGF-R2 and the common IL-3/GM-CSF receptor beta chain to lipid rafts leads to enhanced p38 activation," *British Journal of Haematology*, vol. 145, no. 3, pp. 399–411, 2009.

[50] W. W. Li, M. Hutnik, and G. Gehr, "Antiangiogenesis in haematological malignancies," *British Journal of Haematology*, vol. 143, no. 5, pp. 622–631, 2008.

[51] N. Cao and Z.-X. Yao, "The Hemangioblast: from Concept to Authentication," *Anatomical Record*, vol. 294, no. 4, pp. 580–588, 2011.

[52] P. S. Hole, R. L. Darley, and A. Tonks, "Do reactive oxygen species play a role in myeloid leukemias?" *Blood*, vol. 117, no. 22, pp. 5816–5826, 2011.

[53] C. Casalou, R. Fragoso, J. F. M. Nunes, and S. Dias, "VEGF/PLGF induces leukemia cell migration via P38/ERK1/2 kinase pathway, resulting in Rho GTPases activation and caveolae formation," *Leukemia*, vol. 21, no. 7, pp. 1590–1594, 2007.

[54] A. F. List, B. Glinsmann-Gibson, C. Stadheim, E. J. Meuillet, W. Bellamy, and G. Powis, "Vascular endothelial growth factor receptor-1 and receptor-2 initiate a phosphatidylinositide 3-kinase-dependent clonogenic response in acute myeloid leukemia cells," *Experimental Hematology*, vol. 32, no. 6, pp. 526–535, 2004.

[55] J. Oshikawa, S.-J. Kim, E. Furuta et al., "Novel role of p66shc in ROS-dependent VEGF signaling and angiogenesis in endothelial cells," *American Journal of Physiology: Heart and Circulatory Physiology*, vol. 302, no. 3, pp. H724–H732, 2012.

[56] N. Ferrara, K. J. Hillan, H.-P. Gerber, and W. Novotny, "Discovery and development of bevacizumab, an anti-VEGF antibody for treating cancer," *Nature Reviews Drug Discovery*, vol. 3, no. 5, pp. 391–400, 2004.

[57] H. Hurwitz, L. Fehrenbacher, W. Novotny et al., "Bevacizumab plus irinotecan, fluorouracil, and leucovorin for metastatic colorectal cancer," *The New England Journal of Medicine*, vol. 350, no. 23, pp. 2335–2342, 2004.

[58] J. Folkman, "Tumor angiogenesis: therapeutic implications," *The New England Journal of Medicine*, vol. 285, no. 21, pp. 1182–1186, 1971.

[59] A. F. G. Quest, L. Leyton, and M. Párraga, "Caveolins, caveolae, and lipid rafts in cellular transport, signaling, and disease," *Biochemistry and Cell Biology*, vol. 82, no. 1, pp. 129–144, 2004.

[60] A. Schlegel and M. P. Lisanti, "The caveolin triad: caveolae biogenesis, cholesterol trafficking, and signal transduction," *Cytokine and Growth Factor Reviews*, vol. 12, no. 1, pp. 41–51, 2001.

[61] M. Drab, P. Verkade, M. Elger et al., "Loss of caveolae, vascular dysfunction, and pulmonary defects in caveolin-1 gene-disrupted mice," *Science*, vol. 293, no. 5539, pp. 2449–2452, 2001.

[62] A. M. Kwiatek, R. D. Minshall, D. R. Cool, R. A. Skidgel, A. B. Malik, and C. Tiruppathi, "Caveolin-1 regulates store-operated Ca^{2+} influx by binding of its scaffolding domain to transient receptor potential channel-1 in endothelial cells," *Molecular Pharmacology*, vol. 70, no. 4, pp. 1174–1183, 2006.

[63] T. A. T. Fong, L. K. Shawver, L. Sun et al., "SU5416 is a potent and selective inhibitor of the vascular endothelial growth factor receptor (Flk-1/KDR) that inhibits tyrosine kinase catalysis, tumor vascularization, and growth of multiple tumor types," *Cancer Research*, vol. 59, no. 1, pp. 99–106, 1999.

[64] K. Bedard and K.-H. Krause, "The NOX family of ROS-generating NADPH oxidases: physiology and pathophysiology," *Physiological Reviews*, vol. 87, no. 1, pp. 245–313, 2007.

[65] W. Han, H. Li, V. A. M. Villar et al., "Lipid rafts keep NADPH oxidase in the inactive state in human renal proximal tubule cells," *Hypertension*, vol. 51, no. 2, pp. 481–487, 2008.

[66] F. O. Oakley, R. L. Smith, and J. F. Engelhardt, "Lipid rafts and caveolin-1 coordinate interleukin-1β (IL-1β)-dependent activation of NFκB by controlling endocytosis of Nox2 and IL-1β receptor 1 from the plasma membrane," *The Journal of Biological Chemistry*, vol. 284, no. 48, pp. 33255–33264, 2009.

Hindawi Publishing Corporation
BioMed Research International
Volume 2014, Article ID 238485, 12 pages
http://dx.doi.org/10.1155/2014/238485

Review Article

Role of Methylglyoxal in Alzheimer's Disease

Cristina Angeloni,[1] Laura Zambonin,[2] and Silvana Hrelia[1]

[1] *Department for Life Quality Studies, Alma Mater Studiorum, University of Bologna, Corso d'Augusto 237, 47900 Rimini, Italy*
[2] *Department of Pharmacy and Biotechnology, Alma Mater Studiorum, University of Bologna, Via Irnerio 48, 40126 Bologna, Italy*

Correspondence should be addressed to Cristina Angeloni; cristina.angeloni@unibo.it

Received 13 December 2013; Revised 28 January 2014; Accepted 30 January 2014; Published 9 March 2014

Academic Editor: Tullia Maraldi

Alzheimer's disease is the most common and lethal neurodegenerative disorder. The major hallmarks of Alzheimer's disease are extracellular aggregation of amyloid β peptides and, the presence of intracellular neurofibrillary tangles formed by precipitation/aggregation of hyperphosphorylated tau protein. The etiology of Alzheimer's disease is multifactorial and a full understanding of its pathogenesis remains elusive. Some years ago, it has been suggested that glycation may contribute to both extensive protein cross-linking and oxidative stress in Alzheimer's disease. Glycation is an endogenous process that leads to the production of a class of compounds known as advanced glycation end products (AGEs). Interestingly, increased levels of AGEs have been observed in brains of Alzheimer's disease patients. Methylglyoxal, a reactive intermediate of cellular metabolism, is the most potent precursor of AGEs and is strictly correlated with an increase of oxidative stress in Alzheimer's disease. Many studies are showing that methylglyoxal and methylglyoxal-derived AGEs play a key role in the etiopathogenesis of Alzheimer's disease.

1. Introduction

Alzheimer's disease (AD) is the most common and lethal neurodegenerative disorder characterized by progressive neuronal loss and neuroinflammation in the brain and associated with progressive cognitive decline, memory impairment, and changes in behavior and personality, with rising incidence among elderly people. One of the pathological hallmarks of AD is neuritic plaques in the cerebral cortex and hippocampus. Amyloid β (Aβ), a 40–42 amino-acid peptide generated by proteolytic cleavages of the amyloid-β protein precursor (APP) [1], is one of the main components of neuritic plaques. Aβ is cytotoxic and capable of inducing oxidative stress and neurodegeneration [2, 3]. Another distinctive feature of AD is neurofibrillary tangles (NFTs), composed of bundles of paired helical filaments (PHFs) [4], mainly containing hyperphosphorylated microtubule-associated tau protein (MAP-tau) [5]. Under normal physiological conditions, tau promotes assembly and stability of microtubules and is thus involved in axonal transport [6, 7]. In AD, tau proteins aggregate forming fibrillar insoluble intracellular inclusions. The main processes involved in the etiology and pathogenesis of AD are reported in Figure 1.

The full understanding of the etiology and pathogenesis of AD has remained elusive, and more and more evidences are confirming that AD is a disease with numerous genetic and environmental contributing factors. Some years ago, it has been proposed that a chemical process known as glycation may contribute to both extensive protein cross-linking and oxidative stress in AD [8]. Nonenzymatic protein glycation is an endogenous process in which reducing sugars react with amino groups in proteins through a series of Maillard reactions forming reversible Schiff base and Amadori compounds, producing a heterogeneous class of molecules, collectively termed advanced glycation end products (AGEs) [9]. The α-ketoaldehyde methylglyoxal (MG), formed endogenously as a by-product of the glycolytic pathway, by degradation of triosephosphates or nonenzymatically by sugar fragmentation reactions, is the most potent precursor of AGE formation [10]. MG is able to induce cellular damage, cross-linking of proteins, and glycation [11] playing an important role in the pathogenesis of many neurodegenerative diseases

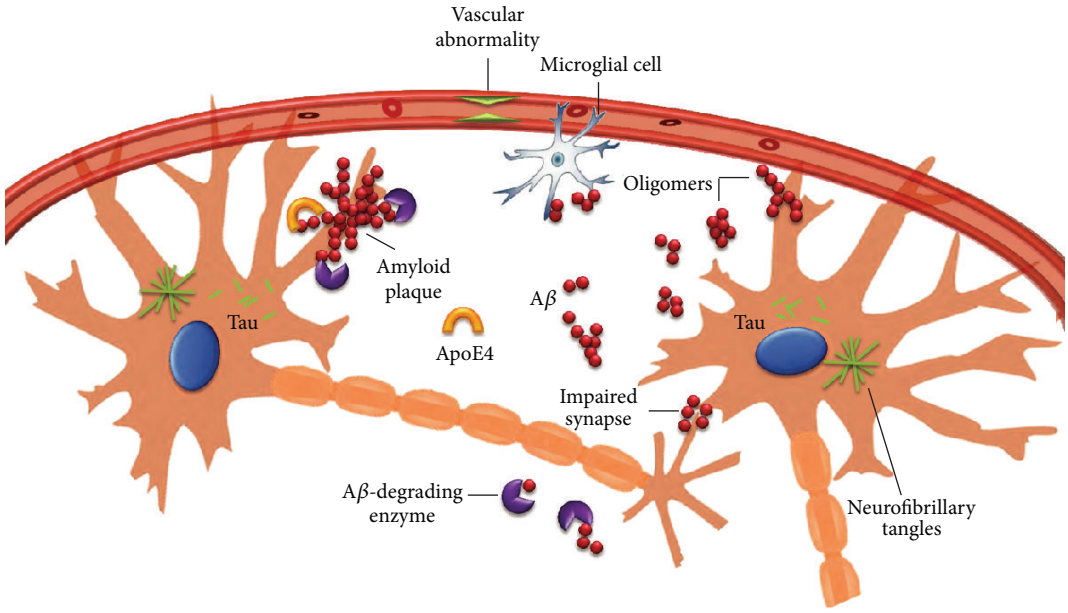

Figure 1: Classical processes participating in the etiology and pathogenesis of AD (modified from [131]).

[12]. In AD, AGEs accumulate in neurons and astroglia and are also found associated with neuritic amyloid plaques and NFTs [13–16]. MG may also contribute to neurodegeneration triggering oxidative stress [17–19]. Oxidative stress is characterized by an imbalance between reactive oxygen species (ROS) production and the detoxifying endogenous system. There is accumulating evidence suggesting a key role of oxidative stress in the pathophysiology of AD [20–23]. A central role for oxidative stress by the activation of NADPH oxidase in astrocytes has been demonstrated as the cause of Aβ-induced neuronal death [24] and of alterations in astrocyte mitochondrial bioenergetics that may in turn affect neuronal functioning and/or survival [25].

As oxidative stress and MG are closely interlinked, the role of MG and MG-induced production of AGEs and ROS in the development of AD is reviewed in this paper. In addition, the ability of MG to modulate detrimental redox signaling in AD has been considered.

2. Methylglyoxal Production

MG is a reactive intermediate of cellular metabolism, present ubiquitously in all cells. It is produced under both normal and pathological conditions via several different pathways, involving both enzymatic and nonenzymatic reactions [26]. The rate of MG formation depends on the organism, tissue, cell metabolism, and physiological conditions; therefore, MG plasma concentration reflects these factors. Plasmatic MG can be derived from exogenous sources, such as coffee, alcoholic beverages, and food [27, 28] and from endogenous sources: in situ formation in the plasma, release from cells, and loss from injured cells [29].

Since MG is ubiquitously present in living cells, almost all foods and beverages contain MG, as reviewed by Vistoli et al. [30]. The main sources of MG are represented by mono-, oligo-, and polysaccharides and lipids [31]. Several reactions and processes are involved in the accumulation of MG: autoxidation, photodegradation, and heating and prolonged storage are the main sources of MG as a degradation product in foodstuff [32–35]. Moreover, many microorganisms produce and release MG: fermentation can be a critical process increasing MG levels in alcoholic drinks and fermented foods [36]. MG is reported to originate also from environmental sources. Cigarette smoke is one of the combustion processes that can generate MG [37]; drinking water can contain MG due to the purification treatments [38]; rainwater can absorb MG from polluted air and transmits it to the soil [39].

Endogenously derived MG is formed during carbohydrate and lipid and amino acid metabolisms and involves both enzymatic and nonenzymatic reactions [40–43]. The enzymes that catalyze the reactions of MG synthesis are MG synthase, cytochrome P450 2E1, myeloperoxidase, and amino oxidase, participating in glycolytic bypass, acetone metabolism, and amino acid breakdown, respectively; nonenzymatic pathways include the spontaneous decomposition of dihydroxyacetone phosphate, the Maillard reaction, the oxidation of acetol, and lipid peroxidation [42].

The main pathway leading to MG is linked to carbohydrate metabolism and involves enzymatic and nonenzymatic degradation of the triosephosphate intermediates glyceraldehyde 3-phosphate and dihydroxyacetone-phosphate deriving from glycolysis [40, 44, 45]. It should be noted that triosephosphates originate not only from glycolytic processes but also from other routes of glucose metabolism (Entner-Doudoroff pathway, hexose monophosphate route) and from xylitol metabolism or the activity of glycerophosphate dehydrogenase, linking glycerol breakdown to MG production [40]. Dihydroxyacetone phosphate can be converted to MG by either spontaneous nonenzymatic elimination of the phosphate group or by the enzymatic contribution of MG

synthase, an enzyme found in prokaryotic and mammalian systems [36, 46]. MG can also derive via the Maillard reaction in vivo under physiological conditions, similar to what is observed during food cooking and through the glycation of macromolecules and the autoxidation of carbohydrates [43].

MG production deriving from lipid metabolism is mainly linked to the acetone metabolism [47]. Acetone is derived from acetoacetate by myeloperoxidase activity and is converted to MG by the cytochrome P450 2E1 via acetol as intermediate [48]. In pathological conditions like ketosis and diabetic ketoacidosis, the oxidation of ketone bodies is likely to be an important source of MG [49]. In addition, triacylglycerol hydrolysis produces glycerol that can be transformed into MG through glycerolphosphate produced by a specific glycerol kinase [50]. Lipoperoxidation is another nonenzymatic process leading to MG formation [51, 52].

The catabolism of the aminoacids threonine and glycine (and partially tyrosine) can also generate MG through the aminoacetone intermediate [53–55]. This metabolic oxidative pathway is mediated by the enzyme semicarbazide sensitive amine oxidase (SSAO) and appears to be exacerbated in low coenzyme A states [56, 57].

3. Methylglyoxal Induced AGE Production

MG is able to induce protein glycation leading to the formation of AGEs [11] and is believed to be the most important source of AGEs. Glycation of proteins is a complex series of parallel and sequential reactions known as Maillard reaction [58]. Glycation starts with the reaction of glucose with lysine and leads to the formation of fructosyllysine (FL) and N-terminal amino acid residue-derived fructosamines while later stage reactions produce stable adducts [58]. It has been observed that FL degrades slowly to form AGEs [59] while MG reacts relatively rapidly with proteins to form AGEs [58], in particular MG is up to 20,000 times more reactive than glucose in glycation reactions [11]. MG reacts almost exclusively with arginine residues and to a lesser extent with lysine, cysteine, and tryptophan residues. The reaction of MG with arginine leads to the formation of cyclic imidazolone adducts (MG-H) [60] and other related structural isomers. MG-H is formed as three structural isomers: Nδ-(5-hydro-5-methyl-4-imidazolon-2-yl)-ornithine (MG-H1), 2-amino-5-(2-amino-5-hydro-5-methyl-4-imidazolon-1-yl)pentanoic acid (MG-H2), and 2-amino-5-(2-amino-4-hydro-4-methyl-5-imidazolon-1-yl) pentanoic acid (MG-H3) [61]. These adducts can undergo other reactions; they can add a second MG molecule yielding either Nδ-(4-carboxy-4,6-dimethyl-5,6-dihydroxy-1,4,5,6-tetrahydropyrimidine-2-yl)-L-ornithine (THP) [62] or argpyrimidine (Nδ-(5-hydroxy-4,6-dimethylpyrimidine-2-yl)-l-ornithine) [63]. MG also reacts with lysine residues to form the N_ε-(1-carboxyethyl)-L-lysine (CEL) and N_ε-(1-carboxymethyl)-L-lysine (CML) adducts and the lysine dimer 1,3-di(N_ε-lysino)-4-methyl-imidazolium (MOLD) [64]. With one lysine and one arginine residue, MG forms 2-ammonio-6-(2-[(4-ammonio-5-oxido-5-oxopentyl) amino]-4-methyl-4,5-dihydro-1H-imidazol-5-ylidene amino) hexanoate (MODIC) [65]. MG can react also with cysteine residues giving reversible hemithioacetal adducts [66] and could spontaneously modify tryptophan residues yielding β carboline derivatives [33].

In human serum albumin, the following concentrations of MG-derived AGEs were detected: MG-H1 2493 ± 87 mmol/mol protein; argpyrimidine 200 ± 40 mmol/mol protein; CEL 29.7 ± 1.8 mmol/mol protein; and MOL 5 ± 1 mmol/mol protein [67]. In cerebrospinal fluid of patients with amyotrophic lateral sclerosis, elevated levels of CML were reported [68], and the tissue levels of CML in cortical neurons and cerebral vessels were related to the severity of cognitive impairment in patients with cerebrovascular disease [69]. It has been demonstrated that MG is involved in the increased levels of AGEs observed in AD [70] and MG-derived AGEs such as CEL and MOLD and MG-derived hydroimidazolone have each been identified in intracellular protein deposits in neurofibrillary tangles [71] and cerebrospinal fluid [72].

4. Methylglyoxal Induced ROS Production

The production of ROS and reactive nitrogen species (RNS) during MG metabolism have been extensively depicted in some reviews [43, 73, 74] and a large body of literature describes the correlation among MG, AGEs, oxidative stress, and pathologies [40] such as diabetes [75], hypertension [76], aging [74, 77, 78], and neurodegeneration [13, 79].

Although the link between MG and free radicals has been investigated since the 1960s mainly by Szent-Gyorgyi [80, 81], only in 1993, the generation of ROS in a cellular system was described [82].

Free radicals and/or ROS and RNS can be produced during both the formation of MG and its degradation; the reactions involved in these processes could be summarized as follows. The enzymatic formation of MG from aminoacetone (catalyzed by SSAO) or from acetol (catalyzed by galactose oxidase) is coupled to hydrogen peroxide production [83, 84]; hydrogen peroxide is produced also when MG is converted to pyruvate by the action of the enzyme glyoxal oxidase [85, 86]. The autoxidation of aminoacetone to MG, mediated by metal ions such as Fe^{2+} and Cu^{2+}, is considered a source of carbon-centered radicals and superoxide [87, 88]; similarly, the nonenzymatic reaction from acetoacetate to MG produces ROS, in the presence of myoglobin, hemoglobin, manganese, cytochrome c, or peroxidase [89, 90].

MG, likewise for monosaccharide, undergoes autoxidation [91–93] and photolysis [94], resulting in ROS generation; these reactions involve superoxide, hydrogen peroxide, and hydroxyl radical [95].

As reported in [43] and [77], ROS production related to MG has been identified in a very wide range of cellular systems, for example, vascular smooth muscle cells (VSMCs), endothelial cells, rat hepatocytes, platelet, neurons, and so forth. We have recently demonstrated that MG induces ROS production in primary culture of rat cardiomyocytes [96].

Moreover, MG is able to increase the activity of prooxidant enzymes [97–99] and to reduce antioxidants, in particular glutathione (GSH) and its enzymes [17, 100, 101]. Since the glyoxalase system that degrades MG uses reduced glutathione

as a cofactor [102], decreased antioxidants in turn impair the detoxification of MG, leading to further oxidative damage.

It has been reported, furthermore, that MG can modify Cu,Zn superoxide dismutase (SOD) by covalent cross-linking, releasing copper ions from the enzyme and inactivating it [103]. Other studies indicate that MG increases mitochondrial superoxide production [104, 105].

The correlation between ROS levels and MG concentration has been reported both in animals and cultured cells [43, 76, 77]. Commonly, in cell models, the administration of MG to the medium is followed by ROS level determination, that is often obtained by the 2′,7′-dichlorodihydrofluorescein diacetate (DCFH-DA) assay or, seldom, by other tests such as lucigenin-linked chemiluminescence assay [106].

As previously reported, MG is the most reactive endogenous carbonyl able to generate AGEs. AGEs also induce oxidative stress through several mechanisms. AGEs stimulate production of cytokines and growth factors [62, 66, 107–111]. Moreover, AGEs bind to the AGE receptor (RAGE) and scavenger receptors to induce oxidative stress in various cells including VSMCs, endothelial cells, and mononuclear phagocytes [112]. In endothelial cells, AGEs increase expression of vascular cell adhesion molecule-1 (VCAM-1), intercellular adhesion molecule-1 (ICAM-1), and increase activity of nuclear factor kappa light chain enhancer of activated B cells (NF-κB) to increase oxidative stress [109, 113].

5. Methylglyoxal and Methylglyoxal-Derived AGE Deposits in AD

As both the extracellular Aβ deposits and the intracellular NFTs have elevated stability and are long-lived proteins, they represent an ideal substrate for glycation [70]. It has been suggested that the insolubility and protease resistance of β-amyloid plaques are caused by extensive AGE-covalent protein cross-linking [4, 16]. In 1994, Vitek et al. observed, for the first time, that plaque fractions of AD brains contained about 3-fold more AGE adducts than preparations from healthy, age-matched controls. They showed that the in vivo half-life of β-amyloid is prolonged in AD, resulting in greater accumulation of AGE modifications which in turn may act to promote accumulation of additional amyloid [114]. An immunohistochemical study using a monoclonal antibody specific for AGE proteins showed extracellular AGE immunoreactivity in amyloid plaques in different cortical areas, in particular, primitive plaques, coronas of classic plaques and some glial cells in AD cortex were positive for AGEs [115]. More recently, Fawver et al. [14] stained AD brain tissue for AGEs, and similar to the previous findings, AGEs were colocalized with amyloid plaques. In addition, Ko et al. [116] showed that APP was upregulated by AGEs in vitro and in vivo, and AGEs modulate APP expression through ROS. To explore whether glycated Aβ is more toxic than authentic Aβ, Li et al. [117] treated 8-DIV embryonic hippocampal neurons with Aβ or Aβ-AGE for 24 h. They found that Aβ-AGE was more toxic than Aβ in decreasing cell viability, increasing cell apoptosis, inducing tau hyperphosphorylation, and reducing synaptic proteins. It has also been observed that MG is not only capable of increasing the rate of production of β-amyloid β-sheets, oligomers and protofibrils but also of increasing the size of the aggregates [13].

The ε4 allele of the apolipoprotein E (ApoE) is known as an important susceptibility gene for AD [118, 119]. It has been demonstrated that ApoE is codeposited in senile plaques in brains of patients with AD [120] and ApoE4 carriers present a higher Aβ deposition in the form of senile plaques than noncarriers [121, 122]. Interestingly, AGEs colocalized to a very high degree with ApoE and ApoE4 exhibited a 3-fold greater AGE-binding activity than the ApoE3 isoform [123]. The authors suggested that ApoE may participate in aggregate formation in the AD brain by binding to AGE-modified plaque components, which may explain why ApoE4 is associated with increased risk of AD.

As discussed above, AGEs can be localized intracellularly. Evidences have been provided that AGEs may accumulate in pyramidal neurons exhibiting a granular perikaryonal distribution in human brain whereas animals show a nuclear staining pattern [124]. It has been shown that AGEs accumulate in endosomal and lysosomal vesicles of pyramidal neurons in the hippocampus, the dentate gyrus, cortical layers III, V, and VI, and in entorhinal cortical layers II, III, V, and VI [125]. Interestingly, Wong et al. [126] observed colocalization of AGEs and inducible nitric oxide synthase (iNOS) in a few astrocytes in the upper neuronal layers in the early stage AD brains, while, in late AD brains, there was a much denser accumulation of astrocytes colocalized with AGEs and iNOS in the deeper and particularly upper neuronal layers. An immunohistochemical study showed that, in AD patients, the percentage of AGE-positive neurons (and astroglia) increases with the progression of the disease and those neurons which show diffuse cytosolic AGE immunoreactivity also contain hyperphosphorylated tau, suggesting a link between AGE accumulation and the formation of early neurofibrillary tangles [16]. Using specific AGE antibodies directed against CML, pyrraline, and hexitol-lysine it has been demonstrated that AGEs are colocalized with NFTs [15, 127, 128].

In AD patients, AGEs accumulate also in the cerebrospinal fluid (CSF), which is in close contact with the brain. An increased accumulation of Amadori products in all major proteins of CSF of AD patients including albumin, apolipoprotein E, and transthyretin has been observed [129]. Bär et al. [130] measured significantly elevated levels of CML in CSF of AD patients when compared to controls. In CSF protein, Ahmed et al. [72] observed an increased levels of CML residues in subjects with AD and in CSF ultrafiltrate; the concentrations of MG-derived hydroimidazolone free adducts were also increased.

6. Role of Methylglyoxal and Methylglyoxal-Derived AGEs in the Progression of AD

The process underlying AD is complex and involves many different features such as mitochondrial dysfunction, abnormal protein aggregation, inflammation, and excitotoxicity. Beeri et al. [132] conducted an interesting clinical study on 267 subjects, at least 75 years old, and cognitively intact at

the beginning of the project. They demonstrated that the subjects with higher serum levels of MG had a faster rate of cognitive decline. Several potential mechanisms have been suggested to explain MG and MG-derived AGE neurotoxicity. Krautwald and Münch [70] suggested that AGEs contribute to the pathogenesis of AD in two different ways: cross-linking cytoskeletal proteins inducing neuronal dysfunction and death and accumulating on Aβ deposits chronically activating micro- and astroglial cells, as widely underlined in the previous paragraph. Moreover, it has been observed that MG is a neurotoxic mediator of oxidative damage in the progression of AD and other neurodegenerative diseases [133]. The brain is highly susceptible to oxidative stress due to its high energy demand, high oxygen consumption, large amounts of peroxidizable polyunsaturated fatty acids, and low levels of antioxidant enzymes [134]. It is no wonder that ROS induced damage to biomolecules is widely reported in AD and increasing evidences suggest that oxidative stress plays a critical role in the disease [135]. As the impairment of mitochondrial function is the main source of ROS generation and also a major target of oxidative damage, mitochondrial dysfunction has been implicated in AD [136, 137]. de Arriba et al. [138] demonstrated that MG may seriously affect mitochondrial respiration and the energetic status of cells. In particular, they observed that MG increases intracellular ROS and lactate production in SH-SY5Y neuroblastoma cells and decreases mitochondrial membrane potential and intracellular ATP levels. SH-SY5Y neuroblastoma cells have been extensively used to study the effect of MG as they show greater sensitivity to MG challenge, due to a defective antioxidant and detoxifying ability [17]. Huang et al. [139] observed that MG induced Neuro-2A neuroblastoma cell line apoptosis via alternation of mitochondrial membrane potential and Bax/Bcl-2 ratio, activation of caspase-3, and cleavage of poly(ADP-ribose) polymerase (PARP). Moreover, they investigated the mechanisms behind MG-induced neuronal cell apoptosis demonstrating that MG activates proapoptotic mitogen-activated protein kinase (MAPK) signaling pathways (JNK and p38). This data is in agreement with the results of Chen et al. [140] that, using primary cultures of rat hippocampal neurons, demonstrated that MG increases the expression level of cleaved caspase-3 and decreases Bcl-2/Bax ratio. As activated caspase-3 immunoreactivity is elevated in AD and exhibits a high degree of colocalization with NFTs and senile plaque in AD brain, it has been suggested that activated caspase-3 may be a factor in functional decline [63].

AGEs exert direct toxicity to cells through predominantly apoptotic mechanisms. Yin et al. [141] investigated the effects of AGEs in SH-SY5Y cells and rat cortical neurons. They observed that AGEs induce cell death increasing intracellular ROS through the increase of NADPH oxidase activity. Moreover, endoplasmic reticulum stress was triggered by AGE-induced oxidative stress, resulting in the activation of C/EBP homologous protein (CHOP) and caspase-12 that consequently initiates cell death. Tau phosphorylation is strictly controlled by the coordinated activities of tau phosphatase(s) and tau kinase(s), and the hyperphosphorylation of tau in the AD brain might be due to the overactive protein kinases and/or inactivation of protein phosphatases [142, 143]. Tau can be phosphorylated by different protein kinases such as the members of the MAPK family (JNK, p38 and Erk1/2), GSK-3β, and cyclin-dependent kinase 5 (cdk5), while protein phosphatase (PP) 2A plays a major role in regulating dephosphorylating of the hyperphosphorylated tau isolated from the AD brains [143–147]. Using wild-type mouse N2a cells, Li et al. [148] observed that MG induces tau hyperphosphorylation and activates GSK-3β and p38, while the simultaneous inhibition of GSK-3β or p38 could attenuate MG-induced tau hyperphosphorylation, suggesting an important roles of GSK-3β and p38 in the MG-induced NTFs formation. On the other hand, an interesting proteomic study demonstrated a decreased level of PP2 in SH-SY5Y cells subjected to MG-induced oxidative stress. Thus, it could be speculated that MG has a double role in inducing tau hyperphosphorylation: enhancing kinase activities and reducing phosphatase level. Besides hyperphosphorylation, it has been suggested that carbonyl-derived posttranslational modifications of neurofilaments may account for the biochemical properties of NFTs, likely as a result of extensive cross-links [149, 150]. Kuhla et al. [151], in an in vitro experiment, incubated wild-type and seven pseudophosphorylated mutant tau proteins with MG and observed the formation of PHF-like structures. Interestingly, MG formed PHFs in a concentration-dependent manner and this process could be accelerated by hyperphosphorylation.

7. Redox Signaling Modulated by Methylglyoxal in AD

As previously highlighted, MG cytotoxicity to tissue or cells is mainly mediated through an increase of oxidative stress and an induction of apoptosis. Oxidative stress is thought to play a causative role in the development of AD [152, 153]. Such stress is a typical activator of two important MAPK pathways in AD: the JNK and the p38 signaling pathways [154]. It has been suggested that the activation of the MAPK signaling pathways contributes to AD pathogenesis through different mechanisms including induction of apoptosis in neurons [155–158], activation of β- and γ-secretases, [159, 160] and phosphorylation and stabilization of APP [161, 162]. Different studies have associated MG with MAPK pathways. In RAW 264.7 cells, MG stimulated the simultaneous activation of p44/42 and p38 MAPK and also stimulates the translocation to the cell membranes of another important protein kinase involved in cellular signaling: protein kinase C (PKC) [163]. Moreover, Pal et al. [164] indicated that MG stimulates iNOS activation by p38 MAPK-NF-$\kappa\beta$-dependent pathway and ROS production by ERK and JNK activation in sarcoma-180 tumor bearing mice.

Regarding the implications of MAPK signaling pathway in oxidative damage leading to apoptosis, it has been observed that MG is able to induce apoptosis in PC12 cells through the phosphatidylinositol-3 kinase/Akt/mammalian target of rapamycin/gamma-glutamylcysteine ligase catalytic subunit (PI3K/Akt/mTOR/GCLc)/redox signaling pathway. Huang et al. [165] indicated that MG-induced Neuro-2A cell apoptosis was mediated through activation of the MAPK signaling

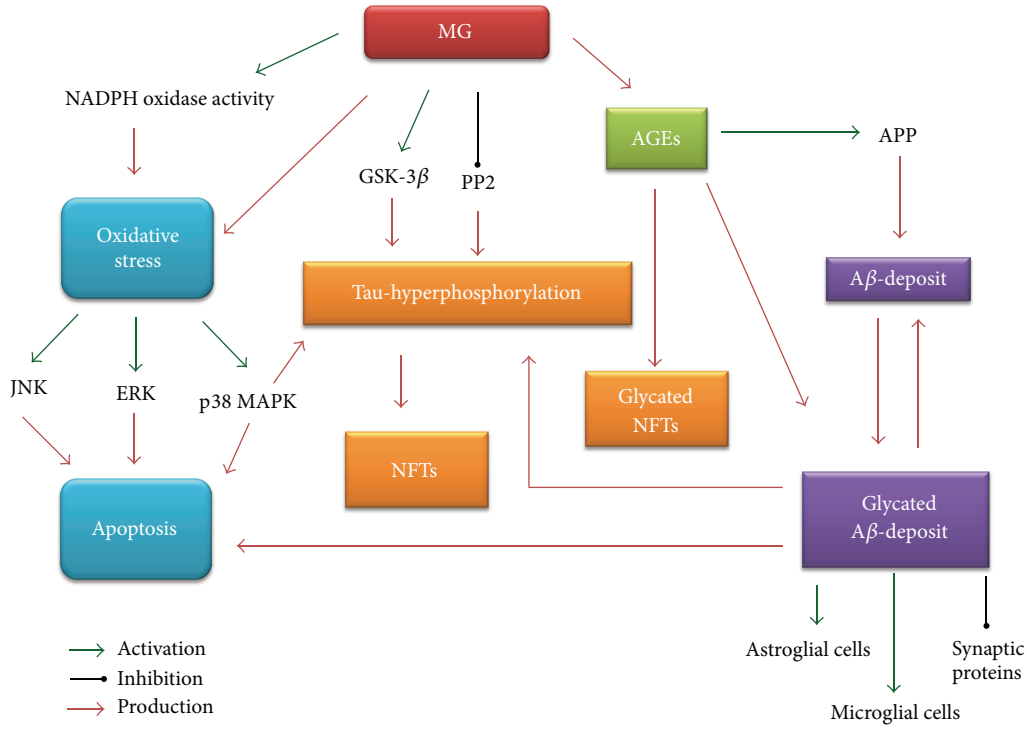

Figure 2: Role of MG and MG-derived AGEs in AD.

pathway mediated by p38 and JNK. Recently, Heimfarth et al. [166] demonstrated that the exposure of slices of cerebral cortex and hippocampus of new born rats to mM MG induced ROS production and cytotoxicity. In particular, they showed that the signaling pathway mediated by ERK is totally implicated in the ROS-mediated cytotoxic damage as the initial blockage of MEK/ERK signaling pathway might be useful for the protection of cells from the high ROS levels. Additionally, they observed that p38MAPK and JNK pathway activation is related with ROS-independent mechanisms leading to reduced cell viability and apoptotic cell death.

Moreover, as it has been underlined in the previous paragraph, the MG activation of GSK-3β and p38 MAPK induces AD tau hyperphosphorylation [148].

8. Conclusions

Many scientific evidences revealed different important actions of MG on signal transduction, redox balance, and cell energetic status as well as homeostatic control of cellular function. Elevated MG levels induce AGEs and ROS production playing a role in AD by several mechanisms (Figure 2). AGEs extensively cross-link proteins in Aβ deposits and neurofilaments exacerbating AD pathological hallmarks. In particular, AGEs cross-link proteins in Aβ deposits making them more insoluble, protease resistant, and more toxic. MG induces tau hyperphosphorylation by enhancing kinase activities and reducing phosphatase level. Moreover, MG is a neurotoxic mediators of oxidative stress in the progression of AD and is capable of activating many redox signaling pathways leading to apoptosis and cellular dysfunction. Accumulation of AGEs further magnifies ROS production by inducing the glycation of important antioxidant enzymes and by providing precursor of oxidative stress. In conclusion, it can be reasonably supposed that cognitive decline associated with AD might be strongly linked to an increase in MG levels due to an oxoaldehyde detoxification impairment or an altered endogenous oxoaldehyde production. From a clinical point of view, the reduction of risk factors for pathologies such as diabetes, characterized by MG accumulation due to hyperglycemic conditions and impaired glucose metabolism [167], and the enhancement of MG scavenging system may provide new therapeutic opportunities to reduce the pathophysiological modifications associated with carbonyl stress in AD.

Abbreviation List

AD:	Alzheimer's disease
AGEs:	Advanced glycation end products
ApoE:	Apolipoprotein E
APP:	Amyloid-β protein precursor
Argpyrimidine:	Nδ-(5-Hydroxy-4,6-dimethylpyrimidine-2-yl)-l-ornithine
Aβ:	Amyloid β
cdk5:	Cyclin-dependent kinase 5
CEL:	Nε-(1-Carboxyethyl)-L-lysine
CHOP:	C/EBP homologous protein
CML:	Nε-(1-Carboxymethyl)-L-lysine
CSF:	Cerebrospinal fluid

DCFH-DA:	2′,7′-Dichlorodihydrofluorescein diacetate
FL:	Fructosyl-lysine
GSH:	Glutathione
ICAM-1:	Intercellular adhesion molecule-1
iNOS:	Inducible nitric oxide synthase
MAP-tau:	Microtubule-associated tau protein
MAPK:	Mitogen activated protein kinase
MG-H:	Imidazolone adducts (methylglyoxal-derived hydroimidazolone)
MG-H1:	Nδ-(5-Hydro-5-methyl-4-imidazolon-2-yl)-ornithine
MG-H2:	2-Amino-5-(2-amino-5-hydro-5-methyl-4-imidazolon-1-yl) pentanoic acid
MG-H3:	2-Amino-5-(2-amino-4-hydro-4-methyl-5-imidazolon-1-yl) pentanoic acid
MG:	Methylglyoxal
MODIC:	2-Ammonio-6-(2-[(4-ammonio-5-oxido-5-oxopentyl) amino]-4-methyl-4, 5-dihydro-1H-imidazol-5-ylidene amino) hexanoate
MOLD:	1,3-Di(Nε-lysino)-4-methyl-imidazolium
NADPH:	Nicotinamide adenine dinucleotide phosphate
NF-κB:	Nuclear factor kappa light chain enhancer of activated B cells
NFTs:	Neurofibrillary tangles
PARP:	Poly (ADP-ribose) polymerase
PHFs:	Paired helical filaments
PI3K/Akt/mTOR/GCLc:	Phosphatidylinositol-3 kinase/Akt/mammalian target of rapamycin/gamma-glutamylcysteine ligase catalytic subunit
PKC:	Protein kinase C
PP:	Protein phosphatase
RAGE:	Receptor for AGEs
RNS:	Reactive nitrogen species
ROS:	Reactive oxygen species
SOD:	Superoxide dismutase
SSAO:	Semicarbazide sensitive amine oxidase
THP:	Nδ-(4-Carboxy-4,6-dimethyl-5,6-dihydroxy-1,4,5,6-tetrahydropyrimidine-2-yl)-L-ornithine
VCAM-1:	Vascular cell adhesion molecule-1
VSMCs:	Vascular smooth muscle cells.

Conflict of Interests

The authors declare that there is no conflict of interests regarding the publication of this paper.

Acknowledgments

This work was supported by MIUR-FIRB (Project RBAP11-HSZS) and "Fondazione del Monte di Bologna e Ravenna" (Italy) (Cristina Angeloni and Silvana Hrelia).

References

[1] H. Zheng and E. H. Koo, "Biology and pathophysiology of the amyloid precursor protein," *Molecular Neurodegeneration*, vol. 6, no. 1, article 27, 2011.

[2] D. M. Walsh, I. Klyubin, J. V. Fadeeva, M. J. Rowan, and D. J. Selkoe, "Amyloid-β oligomers: their production, toxicity and therapeutic inhibition," *Biochemical Society Transactions*, vol. 30, no. 4, pp. 552–557, 2002.

[3] D. T. Loo, A. Copani, C. J. Pike, E. R. Whittemore, A. J. Walencewicz, and C. W. Cotman, "Apoptosis is induced by β-amyloid in cultured central nervous system neurons," *Proceedings of the National Academy of Sciences of the United States of America*, vol. 90, no. 17, pp. 7951–7955, 1993.

[4] A.-L. Bulteau, P. Verbeke, I. Petropoulos, A.-F. Chaffotte, and B. Friguet, "Proteasome inhibition in glyoxal-treated fibroblasts and resistance of glycated glucose-6-phosphate dehydrogenase to 20 S proteasome degradation in vitro," *The Journal of Biological Chemistry*, vol. 276, no. 49, pp. 45662–45668, 2001.

[5] P. S. Sachdev, L. Zhuang, N. Braidy, and W. Wen, "Is Alzheimer's a disease of the white matter?" *Current Opinion in Psychiatry*, vol. 26, no. 3, pp. 244–251, 2013.

[6] D. W. Cleveland, S. Y. Hwo, and M. W. Kirschner, "Purification of tau, a microtubule associated protein that induces assembly of microtubules from purified tubulin," *Journal of Molecular Biology*, vol. 116, no. 2, pp. 207–225, 1977.

[7] R. Brandt and G. Lee, "Functional organization of microtubule-associated protein tau. Identification of regions which affect microtubule growth, nucleation, and bundle formation in vitro," *The Journal of Biological Chemistry*, vol. 268, no. 5, pp. 3414–3419, 1993.

[8] G. Münch, J. Thome, P. Foley, R. Schinzel, and P. Riederer, "Advanced glycation endproducts in ageing and Alzheimer's disease," *Brain Research Reviews*, vol. 23, no. 1-2, pp. 134–143, 1997.

[9] P. Ulrich and A. Cerami, "Protein glycation, diabetes, and aging," *Recent Progress in Hormone Research*, vol. 56, pp. 1–21, 2001.

[10] P. J. Thornalley, "Pharmacology of methylglyoxal: formation, modification of proteins and nucleic acids, and enzymatic detoxification—a role in pathogenesis and antiproliferative chemotherapy," *General Pharmacology*, vol. 27, no. 4, pp. 565–573, 1996.

[11] P. J. Thornalley, "Dicarbonyl intermediates in the Maillard reaction," *Annals of the New York Academy of Sciences*, vol. 1043, pp. 111–117, 2005.

[12] R. Ramasamy, S. J. Vannucci, S. S. D. Yan, K. Herold, S. F. Yan, and A. M. Schmidt, "Advanced glycation end products and RAGE: a common thread in aging, diabetes, neurodegeneration, and inflammation," *Glycobiology*, vol. 15, no. 7, pp. 16R–28R, 2005.

[13] K. Chen, J. Maley, and P. H. Yu, "Potential implications of endogenous aldehydes in β-amyloid misfolding, oligomerization and fibrillogenesis," *Journal of Neurochemistry*, vol. 99, no. 5, pp. 1413–1424, 2006.

[14] J. N. Fawver, H. E. Schall, R. D. P. Chapa, X. Zhu, and I. V. Murray, "Amyloid-beta metabolite sensing: biochemical linking of glycation modification and misfolding," *Journal of Alzheimer's Disease*, vol. 30, no. 1, pp. 63–73, 2012.

[15] R. J. Castellani, P. L. R. Harris, L. M. Sayre et al., "Active glycation in neurofibrillary pathology of Alzheimer disease: Nε-(Carboxymethyl) lysine and hexitol-lysine," *Free Radical Biology and Medicine*, vol. 31, no. 2, pp. 175–180, 2001.

[16] H.-J. Lüth, V. Ogunlade, B. Kuhla et al., "Age- and stage-dependent accumulation of advanced glycation end products in intracellular deposits in normal and Alzheimer's disease brains," *Cerebral Cortex*, vol. 15, no. 2, pp. 211–220, 2005.

[17] F. Amicarelli, S. Colafarina, F. Cattani et al., "Scavenging system efficiency is crucial for cell resistance to ROS-mediated methylglyoxal injury," *Free Radical Biology and Medicine*, vol. 35, no. 8, pp. 856–871, 2003.

[18] S. Kikuchi, K. Shinpo, F. Moriwaka, Z. Makita, T. Miyata, and K. Tashiro, "Neurotoxicity of methylglyoxal and 3-deoxyglucosone on cultured cortical neurons: synergism between glycation and oxidative stress, possibly involved in neurodegenerative diseases," *Journal of Neuroscience Research*, vol. 57, no. 2, pp. 280–289, 1999.

[19] K. Shinpo, S. Kikuchi, H. Sasaki, A. Ogata, F. Moriwaka, and K. Tashiro, "Selective vulnerability of spinal motor neurons to reactive dicarbonyl compounds, intermediate products of glycation, in vitro: implication of inefficient glutathione system in spinal motor neurons," *Brain Research*, vol. 861, no. 1, pp. 151–159, 2000.

[20] D. A. Butterfield and C. M. Lauderback, "Lipid peroxidation and protein oxidation in Alzheimer's disease brain: potential causes and consequences involving amyloid β-peptide-associated free radical oxidative stress," *Free Radical Biology and Medicine*, vol. 32, no. 11, pp. 1050–1060, 2002.

[21] C. E. Cross, B. Halliwell, E. T. Borish et al., "Oxygen radicals and human disease. Davis conference," *Annals of Internal Medicine*, vol. 107, no. 4, pp. 526–545, 1987.

[22] W. R. Markesbery, "Oxidative stress hypothesis in Alzheimer's disease," *Free Radical Biology and Medicine*, vol. 23, no. 1, pp. 134–147, 1997.

[23] A. Tarozzi, C. Angeloni, M. Malaguti, F. Morroni, S. Hrelia, and P. Hrelia, "Sulforaphane as a potential protective phytochemical against neurodegenerative diseases," *Oxidative Medicine and Cellular Longevity*, vol. 2013, Article ID 415078, 10 pages, 2013.

[24] A. Y. Abramov, L. Canevari, and M. R. Duchen, "β-amyloid peptides induce mitochondrial dysfunction and oxidative stress in astrocytes and death of neurons through activation of NADPH oxidase," *Journal of Neuroscience*, vol. 24, no. 2, pp. 565–575, 2004.

[25] E. Motori, J. Puyal, N. Toni et al., "Inflammation-induced alteration of astrocyte mitochondrial dynamics requires autophagy for mitochondrial network maintenance," *Cell Metabolism*, vol. 18, no. 6, pp. 844–859, 2013.

[26] M. S. Silva, R. A. Gomes, A. E. Ferreira, A. P. Freire, and C. Cordeiro, "The glyoxalase pathway: the first hundred years... and beyond," *The Biochemical Journal*, vol. 453, no. 1, pp. 1–15, 2013.

[27] I. Nemet, L. Varga-Defterdarović, and Z. Turk, "Methylglyoxal in food and living organisms," *Molecular Nutrition and Food Research*, vol. 50, no. 12, pp. 1105–1117, 2006.

[28] J. Wang and T. Chang, "Methylglyoxal content in drinking coffee as a cytotoxic factor," *Journal of Food Science*, vol. 75, no. 6, pp. H167–H171, 2010.

[29] M. P. Kalapos, "Where does plasma methylglyoxal originate from?" *Diabetes Research and Clinical Practice*, vol. 99, no. 3, pp. 260–271, 2013.

[30] G. Vistoli, D. De Maddis, A. Cipak, N. Zarkovic, M. Carini, and G. Aldini, "Advanced glycoxidation and lipoxidation end products (AGEs and ALEs): an overview of their mechanisms of formation," *Free Radical Research*, vol. 47, no. S1, pp. 3–27, 2013.

[31] J. Degen, M. Hellwig, and T. Henle, "1,2-dicarbonyl compounds in commonly consumed foods," *Journal of Agricultural and Food Chemistry*, vol. 60, no. 28, pp. 7071–7079, 2012.

[32] Y. V. Pfeifer, P. T. Haase, and L. W. Kroh, "Reactivity of thermally treated alpha-dicarbonyl compounds," *Journal of Agricultural and Food Chemistry*, vol. 61, no. 12, pp. 3090–3096, 2013.

[33] I. Nemet and L. Varga-Defterdarović, "Methylglyoxal-derived β-carbolines formed from tryptophan and its derivates in the Maillard reaction," *Amino Acids*, vol. 32, no. 2, pp. 291–293, 2007.

[34] S. Kuntz, S. Rudloff, J. Ehl, R. G. Bretzel, and C. Kunz, "Food derived carbonyl compounds affect basal and stimulated secretion of interleukin-6 and -8 in Caco-2 cells," *European Journal of Nutrition*, vol. 48, no. 8, pp. 499–503, 2009.

[35] J. P. Casazza, M. E. Felver, and R. L. Veech, "The metabolism of acetone in rat," *The Journal of Biological Chemistry*, vol. 259, no. 1, pp. 231–236, 1984.

[36] R. A. Cooper, "Metabolism of methylglyoxal in microorganisms," *Annual Review of Microbiology*, vol. 38, pp. 49–68, 1984.

[37] K. Fujioka and T. Shibamoto, "Determination of toxic carbonyl compounds in cigarette smoke," *Environmental Toxicology*, vol. 21, no. 1, pp. 47–54, 2006.

[38] V. Camel and A. Bermond, "The use of ozone and associated oxidation processes in drinking water treatment," *Water Research*, vol. 32, no. 11, pp. 3208–3222, 1998.

[39] T.-M. Fu, D. J. Jacob, F. Wittrock, J. P. Burrows, M. Vrekoussis, and D. K. Henze, "Global budgets of atmospheric glyoxal and methylglyoxal, and implications for formation of secondary organic aerosols," *Journal of Geophysical Research D*, vol. 113, no. 15, Article ID D15303, 2008.

[40] M. P. Kalapos, "Methylglyoxal in living organisms—chemistry, biochemistry, toxicology and biological implications," *Toxicology Letters*, vol. 110, no. 3, pp. 145–175, 1999.

[41] P. J. Beisswenger, S. K. Howell, R. G. Nelson, M. Mauer, and B. S. Szwergold, "α-oxoaldehyde metabolism and diabetic complications," *Biochemical Society Transactions*, vol. 31, part 6, pp. 1358–1363, 2003.

[42] M. P. Kalapos, "Methylglyoxal and glucose metabolism: a historical perspective and future avenues for research," *Drug Metabolism and Drug Interactions*, vol. 23, no. 1-2, pp. 69–91, 2008.

[43] M. P. Kalapos, "The tandem of free radicals and methylglyoxal," *Chemico-Biological Interactions*, vol. 171, no. 3, pp. 251–271, 2008.

[44] Q. Cui and M. Karplus, "Catalysis and specificity in enzymes: a study of triosephosphate isomerase and comparison with methyl glyoxal synthase," *Advances in Protein Chemistry*, vol. 66, pp. 315–372, 2003.

[45] J. P. Richard, "Mechanism for the formation of methylglyoxal from triosephosphates," *Biochemical Society Transactions*, vol. 21, no. 2, pp. 549–553, 1993.

[46] R. A. Cooper, "[104] Methylglyoxal synthase," *Methods in Enzymology*, vol. 41, pp. 502–508, 1975.

[47] A. Dhar, K. Desai, M. Kazachmov, P. Yu, and L. Wu, "Methylglyoxal production in vascular smooth muscle cells from different metabolic precursors," *Metabolism: Clinical and Experimental*, vol. 57, no. 9, pp. 1211–1220, 2008.

[48] F. Y. Bondoc, Z. Bao, W.-Y. Hu et al., "Acetone catabolism by cytochrome P450 2E1: studies with CYP2E1-null mice," *Biochemical Pharmacology*, vol. 58, no. 3, pp. 461–463, 1999.

[49] Z. Turk, I. Nemet, L. Varga-Defteardarovic, and N. Car, "Elevated level of methylglyoxal during diabetic ketoacidosis and its recovery phase," *Diabetes and Metabolism*, vol. 32, no. 2, pp. 176–180, 2006.

[50] J.-Y. Jung, H. S. Yun, J. Lee, and M.-K. Oh, "Production of 1,2-propanediol from glycerol in saccharomyces cerevisiae," *Journal of Microbiology and Biotechnology*, vol. 21, no. 8, pp. 846–853, 2011.

[51] T. Shibamoto, "Analytical methods for trace levels of reactive carbonyl compounds formed in lipid peroxidation systems," *Journal of Pharmaceutical and Biomedical Analysis*, vol. 41, no. 1, pp. 12–25, 2006.

[52] H. Esterbauer, K. H. Cheeseman, and M. U. Dianzani, "Separation and characterization of the aldehydic products of lipid peroxidation stimulated by ADP-Fe^{2+} in rat liver microsomes," *The Biochemical Journal*, vol. 208, no. 1, pp. 129–140, 1982.

[53] P. J. Thornalley, "The glyoxalase system in health and disease," *Molecular Aspects of Medicine*, vol. 14, no. 4, pp. 287–371, 1993.

[54] G. A. Lyles and J. Chalmers, "The metabolism of aminoacetone to methylglyoxal by semicarbazide-sensitive amine oxidase in human umbilical artery," *Biochemical Pharmacology*, vol. 43, no. 7, pp. 1409–1414, 1992.

[55] E. J. H. Bechara, F. Dutra, V. E. S. Cardoso et al., "The dual face of endogenous α-aminoketones: pro-oxidizing metabolic weapons," *Comparative Biochemistry and Physiology C*, vol. 146, no. 1-2, pp. 88–110, 2007.

[56] B. A. Callingham, A. E. Crosbie, and B. A. Rous, "Some aspects of the pathophysiology of semicarbazide-sensitive amine oxidase enzymes," *Progress in Brain Research*, vol. 106, pp. 305–321, 1995.

[57] G. A. Lyles, "Mammalian plasma and tissue-bound semicarbazide-sensitive amine oxidases: biochemical, pharmacological and toxicological aspects," *International Journal of Biochemistry and Cell Biology*, vol. 28, no. 3, pp. 259–274, 1996.

[58] P. J. Thornalley, "Protein and nucleotide damage by glyoxal and methylglyoxal in physiological systems—role in ageing and disease," *Drug Metabolism and Drug Interactions*, vol. 23, no. 1-2, pp. 125–150, 2008.

[59] P. J. Thornalley, A. Langborg, and H. S. Minhas, "Formation of glyoxal, methylglyoxal and 8-deoxyglucosone in the glycation of proteins by glucose," *The Biochemical Journal*, vol. 344, part 1, pp. 109–116, 1999.

[60] P. J. Thornalley, S. Battah, N. Ahmed et al., "Quantitative screening of advanced glycation endproducts in cellular and extracellular proteins by tandem mass spectrometry," *The Biochemical Journal*, vol. 375, part 3, pp. 581–592, 2003.

[61] N. Ahmed, P. J. Thornalley, J. Dawczynski et al., "Methylglyoxal-derived hydroimidazolone advanced glycation end-products of human lens proteins," *Investigative Ophthalmology and Visual Science*, vol. 44, no. 12, pp. 5287–5292, 2003.

[62] T. Oya, N. Hattori, Y. Mizuno et al., "Methylglyoxal modification of protein. Chemical and immunochemical characterization of methylglyoxal-arginine adducts," *The Journal of Biological Chemistry*, vol. 274, no. 26, pp. 18492–18502, 1999.

[63] I. N. Shipanova, M. A. Glomb, and R. H. Nagaraj, "Protein modification by methylglyoxal: chemical nature and synthetic mechanism of a major fluorescent adduct," *Archives of Biochemistry and Biophysics*, vol. 344, no. 1, pp. 29–36, 1997.

[64] E. B. Frye, T. P. Degenhardt, S. R. Thorpe, and J. W. Baynes, "Role of the Maillard reaction in aging of tissue proteins: advanced glycation end product-dependent increase in imidazolium cross-links in human lens proteins," *The Journal of Biological Chemistry*, vol. 273, no. 30, pp. 18714–18719, 1998.

[65] K. M. Bieme, D. Alexander Fried, and M. O. Lederer, "Identification and quantification of major maillard cross-links in human serum albumin and lens protein: evidence for glucosepane as the dominant compound," *The Journal of Biological Chemistry*, vol. 277, no. 28, pp. 24907–24915, 2002.

[66] T. W. C. Lo, M. E. Westwood, A. C. McLellan, T. Selwood, and P. J. Thornalley, "Binding and modification of proteins by methylglyoxal under physiological conditions: a kinetic and mechanistic study with Nα-acetylarginine, Nα- acetylcysteine, and Nα-acetyllysine, and bovine serum albumin," *The Journal of Biological Chemistry*, vol. 269, no. 51, pp. 32299–32305, 1994.

[67] N. Ahmed, D. Dobler, M. Dean, and P. J. Thornalley, "Peptide mapping identifies hotspot site of modification in human serum albumin by methylglyoxal involved in ligand binding and esterase activity," *The Journal of Biological Chemistry*, vol. 280, no. 7, pp. 5724–5732, 2005.

[68] E. Kaufmann, B. O. Boehm, S. D. Süssmuth et al., "The advanced glycation end-product Nε-(carboxymethyl)lysine level is elevated in cerebrospinal fluid of patients with amyotrophic lateral sclerosis," *Neuroscience Letters*, vol. 371, no. 2-3, pp. 226–229, 2004.

[69] L. Southern, J. Williams, and M. M. Esiri, "Immunohistochemical study of N-epsilon-carboxymethyl lysine (CML) in human brain: relation to vascular dementia," *BMC Neurology*, vol. 7, article 35, 2007.

[70] M. Krautwald and G. Münch, "Advanced glycation end products as biomarkers and gerontotoxins—a basis to explore methylglyoxal-lowering agents for Alzheimer's disease?" *Experimental Gerontology*, vol. 45, no. 10, pp. 744–751, 2010.

[71] T. Jono, T. Kimura, J. Takamatsu et al., "Accumulation of imidazolone, pentosidine and Nε-(carboxymethyl)lysine in hippocampal CA4 pyramidal neurons of aged human brain," *Pathology International*, vol. 52, no. 9, pp. 563–571, 2002.

[72] N. Ahmed, U. Ahmed, P. J. Thornalley, K. Hager, G. Fleischer, and G. Münch, "Protein glycation, oxidation and nitration adduct residues and free adducts of cerebrospinal fluid in Alzheimer's disease and link to cognitive impairment," *Journal of Neurochemistry*, vol. 92, no. 2, pp. 255–263, 2005.

[73] N. Taniguchi, M. Takahashi, H. Sakiyama et al., "A common pathway for intracellular reactive oxygen species production by glycoxidative and nitroxidative stress in vascular endothelial cells and smooth muscle cells," *Annals of the New York Academy of Sciences*, vol. 1043, pp. 521–528, 2005.

[74] K. M. Desai and L. Wu, "Free radical generation by methylglyoxal in tissues," *Drug Metabolism and Drug Interactions*, vol. 23, no. 1-2, pp. 151–173, 2008.

[75] L. F. Dmitriev and V. N. Titov, "Lipid peroxidation in relation to ageing and the role of endogenous aldehydes in diabetes and other age-related diseases," *Ageing Research Reviews*, vol. 9, no. 2, pp. 200–210, 2010.

[76] T. Chang and L. Wu, "Methylglyoxal, oxidative stress, and hypertension," *Canadian Journal of Physiology and Pharmacology*, vol. 84, no. 12, pp. 1229–1238, 2006.

[77] I. Dhar and K. Desai, "Chapter 30. Aging: drugs to eliminate methylglyoxal, a reactive glucose metabolite, and advanced glycation endproducts," in *Pharmacology*, L. Gallelli, Ed., 2012.

[78] M. P. Kalapos, K. M. Desai, and L. Wu, "Methylglyoxal, oxidative stress, and aging," in *Aging and Age-Related Disorders*, Oxidative Stress in Applied Basic Research and Clinical Practice, pp. 149–167, Humana Press, 2010.

[79] X. Huang, F. Wang, W. Chen, Y. Chen, N. Wang, and K. von Maltzan, "Possible link between the cognitive dysfunction associated with diabetes mellitus and the neurotoxicity of methylglyoxal," *Brain Research*, vol. 1469, pp. 82–91, 2012.

[80] A. Szent-Gyorgyi, *Bioelectronics: A Study in cellular regulations, Defense, and cancer*, Academic Press, New York, NY, USA, 1968.

[81] H. Kon and A. Szent Gyorgyi, "Charge transfer between amine and carbonyl," *Proceedings of the National Academy of Sciences of the United States of America*, vol. 70, no. 11, pp. 3139–3140, 1973.

[82] M. P. Kalapos, A. Littauer, and H. De Groot, "Has reactive oxygen a role in methylglyoxal toxicity? A study on cultured rat hepatocytes," *Archives of Toxicology*, vol. 67, no. 5, pp. 369–372, 1993.

[83] P. H. Yu, S. Wright, E. H. Fan, Z.-R. Lun, and D. Gubisne-Harberle, "Physiological and pathological implications of semicarbazide-sensitive amine oxidase," *Biochimica et Biophysica Acta*, vol. 1647, no. 1-2, pp. 193–199, 2003.

[84] J. M. Johnson, H. B. Halsall, and W. R. Heineman, "Redox activation of galactose oxidase: thin-layer electrochemical study," *Biochemistry*, vol. 24, no. 7, pp. 1579–1585, 1985.

[85] P. J. Kersten and T. K. Kirk, "Involvement of a new enzyme, glyoxal oxidase, in extracellular H_2O_2 production by phanerochaete chrysosporium," *Journal of Bacteriology*, vol. 169, no. 5, pp. 2195–2201, 1987.

[86] B. Leuthner, C. Aichinger, E. Oehmen et al., "A H_2O_2-producing glyoxal oxidase is required for filamentous growth and pathogenicity in Ustilago maydis," *Molecular Genetics and Genomics*, vol. 272, no. 6, pp. 639–650, 2005.

[87] Y. Hiraku, J. Sugimoto, T. Yamaguchi, and S. Kawanishi, "Oxidative DNA damage induced by aminoacetone, an amino acid metabolite," *Archives of Biochemistry and Biophysics*, vol. 365, no. 1, pp. 62–70, 1999.

[88] F. Dutra, F. S. Knudsen, D. Curi, and E. J. H. Bechara, "Aerobic oxidation of aminoacetone, a threonine catabolite: iron catalysis and coupled iron release from ferritin," *Chemical Research in Toxicology*, vol. 14, no. 9, pp. 1323–1329, 2001.

[89] C. C. C. Vidigal and G. Cilento, "Evidence for the generation of excited methylglyoxal in the myoglobin catalyzed oxidation of acetoacetate," *Biochemical and Biophysical Research Communications*, vol. 62, no. 2, pp. 184–190, 1975.

[90] K. Takayama, M. Nakano, and K. Zinner, "Generation of electronic energy in the myoglobin catalyzed oxidation of acetoacetate to methylglyoxal," *Archives of Biochemistry and Biophysics*, vol. 176, no. 2, pp. 663–670, 1976.

[91] T. Yamaguchi and K. Nakagawa, "Mutagenicity of and formation of oxygen radicals by trioses and glyoxal derivatives," *Agricultural and Biological Chemistry*, vol. 47, no. 11, pp. 2461–2465, 1983.

[92] P. Thornalley, S. Wolff, J. Crabbe, and A. Stern, "The autoxidation of glyceraldehyde and other simple monosaccharides under physiological conditions catalysed by buffer ions," *Biochimica et Biophysica Acta*, vol. 797, no. 2, pp. 276–287, 1984.

[93] P. J. Thornalley, S. P. Wolff, M. J. Crabbe, and A. Stern, "The oxidation of oxyhaemoglobin by glyceraldehyde and other simple monosaccharides," *The Biochemical Journal*, vol. 217, no. 3, pp. 615–622, 1984.

[94] R. Atkinson, W. P. L. Carter, K. R. Darnall, M. Winer, and J. N. Pitts, "A smog chamber and modeling study of the gas phase NOx—air photooxidation of toluene and the cresols," *International Journal of Chemical Kinetics*, vol. 12, no. 11, pp. 779–836, 1980.

[95] H. Nukaya, Y. Inaoka, H. Ishida et al., "Modification of the amino group of guanosine by methylglyoxal and other α-ketoaldehydes in the presence of hydrogen peroxide," *Chemical and Pharmaceutical Bulletin*, vol. 41, no. 4, pp. 649–653, 1993.

[96] C. Angeloni, S. Turroni, L. Bianchi et al., "Novel targets of sulforaphane in primary cardiomyocytes identified by proteomic analysis," *PLoS ONE*, vol. 8, no. 12, Article ID e83283, 2013.

[97] T. Chang, R. Wang, and L. Wu, "Methylglyoxal-induced nitric oxide and peroxynitrite production in vascular smooth muscle cells," *Free Radical Biology and Medicine*, vol. 38, no. 2, pp. 286–293, 2005.

[98] C. Ho, P.-H. Lee, W.-J. Huang, Y.-C. Hsu, C.-L. Lin, and J.-Y. Wang, "Methylglyoxal-induced fibronectin gene expression through ras-mediated NADPH oxidase activation in renal mesangial cells," *Nephrology*, vol. 12, no. 4, pp. 348–356, 2007.

[99] R. A. Ward and K. R. McLeish, "Methylglyoxal: a stimulus to neutrophil oxygen radical production in chronic renal failure?" *Nephrology Dialysis Transplantation*, vol. 19, no. 7, pp. 1702–1707, 2004.

[100] J. Nicolay, J. Schneider, O. Niemoeller et al., "Stimulation of suicidal erythrocyte death by methylglyoxal," *Cellular Physiology and Biochemistry*, vol. 18, no. 4-5, pp. 223–232, 2006.

[101] Y. S. Park, Y. H. Koh, M. Takahashi et al., "Identification of the binding site of methylglyoxal on gluthathione peroxidase: methylglyoxal inhibits glutathione peroxidase activity via binding to glutathione binding sites Arg 184 and 185," *Free Radical Research*, vol. 37, no. 2, pp. 205–211, 2003.

[102] P. J. Thornalley, "Glutathione-dependent detoxification of α-oxoaldehydes by the glyoxalase system: Involvement in disease mechanisms and antiproliferative activity of glyoxalase I inhibitors," *Chemico-Biological Interactions*, vol. 111-112, pp. 137–151, 1998.

[103] J. H. Kang, "Modification and inactivation of human Cu,Zn-superoxide dismutase by methylglyoxal," *Molecules and Cells*, vol. 15, no. 2, pp. 194–199, 2003.

[104] N. Rabbani and P. J. Thornalley, "Dicarbonyls linked to damage in the powerhouse: glycation of mitochondrial proteins and oxidative stress," *Biochemical Society Transactions*, vol. 36, part5, pp. 1045–1050, 2008.

[105] M. G. Rosca, T. G. Mustata, M. T. Kinter et al., "Glycation of mitochondrial proteins from diabetic rat kidney is associated with excess superoxide formation," *The American Journal of Physiology: Renal Physiology*, vol. 289, no. 2, pp. F420–F430, 2005.

[106] J. Du, H. Suzuki, F. Nagase et al., "Superoxide-mediated early oxidation and activation of ASK1 are important for initiating methylglyoxal-induced apoptosis process," *Free Radical Biology and Medicine*, vol. 31, no. 4, pp. 469–478, 2001.

[107] G. Basta, G. Lazzerini, M. Massaro et al., "Advanced glycation end products activate endothelium through signal-transduction receptor RAGE a mechanism for amplification of inflammatory responses," *Circulation*, vol. 105, no. 7, pp. 816–822, 2002.

[108] J. Chen, S. V. Brodsky, D. M. Goligorsky et al., "Glycated collagen I induces premature senescence-like phenotypic changes in endothelial cells," *Circulation Research*, vol. 90, no. 12, pp. 1290–1298, 2002.

[109] S. Kikuchi, K. Shinpo, M. Takeuchi et al., "Glycation—a sweet tempter for neuronal death," *Brain Research Reviews*, vol. 41, no. 2-3, pp. 306–323, 2003.

[110] M.-P. Wautier, O. Chappey, S. Corda, D. M. Stern, A. M. Schmidt, and J.-L. Wautier, "Activation of NADPH oxidase by AGE links oxidant stress to altered gene expression via RAGE," *The American Journal of Physiology: Endocrinology and Metabolism*, vol. 280, no. 5, pp. E685–E694, 2001.

[111] M. E. Westwood and P. J. Thornalley, "Induction of synthesis and secretion of interleukin 1β in the human monocytic THP-1 cells by human serum albumins modified with methylglyoxal and advanced glycation endproducts," *Immunology Letters*, vol. 50, no. 1-2, pp. 17–21, 1996.

[112] P. J. Thornalley, "Cell activation by glycated proteins. AGE receptors, receptor recognition factors and functional classification of AGEs," *Cellular and Molecular Biology*, vol. 44, no. 7, pp. 1013–1023, 1998.

[113] A. Bierhaus, S. Chevion, M. Chevion et al., "Advanced glycation end product-induced activation of NF-κB is suppressed by α-lipoic acid in cultured endothelial cells," *Diabetes*, vol. 46, no. 9, pp. 1481–1490, 1997.

[114] M. P. Vitek, K. Bhattacharya, J. M. Glendening et al., "Advanced glycation end products contribute to amyloidosis in Alzheimer disease," *Proceedings of the National Academy of Sciences of the United States of America*, vol. 91, no. 11, pp. 4766–4770, 1994.

[115] T. Kimura, J. Takamatsu, N. Araki et al., "Are advanced glycation end-products associated with amyloidosis in Alzheimer's disease?" *NeuroReport*, vol. 6, no. 6, pp. 866–868, 1995.

[116] S.-Y. Ko, Y.-P. Lin, Y.-S. Lin, and S.-S. Chang, "Advanced glycation end products enhance amyloid precursor protein expression by inducing reactive oxygen species," *Free Radical Biology and Medicine*, vol. 49, no. 3, pp. 474–480, 2010.

[117] X. H. Li, L. L. Du, X. S. Cheng et al., "Glycation exacerbates the neuronal toxicity of beta-amyloid," *Cell Death and Disease*, vol. 4, article e673, 2013.

[118] H. M. Schipper, "Apolipoprotein E: implications for AD neurobiology, epidemiology and risk assessment," *Neurobiology of Aging*, vol. 32, no. 5, pp. 778–790, 2011.

[119] G. Bu, "Apolipoprotein e and its receptors in Alzheimer's disease: pathways, pathogenesis and therapy," *Nature Reviews Neuroscience*, vol. 10, no. 5, pp. 333–344, 2009.

[120] Y. Namba, M. Tomonaga, H. Kawasaki, E. Otomo, and K. Ikeda, "Apolipoprotein E immunoreactivity in cerebral amyloid deposits and neurofibrillary tangles in Alzheimer's disease and kuru plaque amyloid in Creutzfeldt-Jakob disease," *Brain Research*, vol. 541, no. 1, pp. 163–166, 1991.

[121] E. Kok, S. Haikonen, T. Luoto et al., "Apolipoprotein E-dependent accumulation of alzheimer disease-related lesions begins in middle age," *Annals of Neurology*, vol. 65, no. 6, pp. 650–657, 2009.

[122] T. Polvikoski, R. Sulkava, M. Haltia et al., "Apolipoprotein E, dementia, and cortical deposition of β-amyloid protein," *The New England Journal of Medicine*, vol. 333, no. 19, pp. 1242–1247, 1995.

[123] Y. M. Li and D. W. Dickson, "Enhanced binding of advanced glycation endproducts (AGE) by the ApoE4 isoform links the mechanism of plaque deposition in Alzheimer's disease," *Neuroscience Letters*, vol. 226, no. 3, pp. 155–158, 1997.

[124] G. Münch, B. Westcott, T. Menini, and A. Gugliucci, "Advanced glycation endproducts and their pathogenic roles in neurological disorders," *Amino Acids*, vol. 42, no. 4, pp. 1221–1236, 2012.

[125] J. J. Li, M. Surini, S. Catsicas, E. Kawashima, and C. Bouras, "Age-dependent accumulation of advanced glycosylation end products in human neurons," *Neurobiology of Aging*, vol. 16, no. 1, pp. 69–76, 1995.

[126] A. Wong, H.-J. Lüth, W. Deuther-Conrad et al., "Advanced glycation endproducts co-localize with inducible nitric oxide synthase in Alzheimer's disease," *Brain Research*, vol. 920, no. 1-2, pp. 32–40, 2001.

[127] V. Prakash Reddy, M. E. Obrenovich, C. S. Atwood, G. Perry, and M. A. Smith, "Involvement of Maillard reactions in Alzheimer disease," *Neurotoxicity Research*, vol. 4, no. 3, pp. 191–209, 2002.

[128] M. A. Smith, S. Taneda, P. L. Richey et al., "Advanced Maillard reaction end products are associated with Alzheimer disease pathology," *Proceedings of the National Academy of Sciences of the United States of America*, vol. 91, no. 12, pp. 5710–5714, 1994.

[129] V. V. Shuvaev, I. Laffont, J.-M. Serot, J. Fujii, N. Taniguchi, and G. Siest, "Increased protein glycation in cerebrospinal fluid of Alzheimer's disease," *Neurobiology of Aging*, vol. 22, no. 3, pp. 397–402, 2001.

[130] K. J. Bär, S. Franke, B. Wenda et al., "Pentosidine and Nε-(carboxymethyl)-lysine in Alzheimer's disease and vascular dementia," *Neurobiology of Aging*, vol. 24, no. 2, pp. 333–338, 2003.

[131] L. Mucke, "Neuroscience: Alzheimer's disease," *Nature*, vol. 461, no. 7266, pp. 895–897, 2009.

[132] M. S. Beeri, E. Moshier, J. Schmeidler et al., "Serum concentration of an inflammatory glycotoxin, methylglyoxal, is associated with increased cognitive decline in elderly individuals," *Mechanisms of Ageing and Development*, vol. 132, no. 11-12, pp. 583–587, 2011.

[133] M. A. Lovell, C. Xie, and W. R. Markesbery, "Acrolein is increased in Alzheimer's disease brain and is toxic to primary hippocampal cultures," *Neurobiology of Aging*, vol. 22, no. 2, pp. 187–194, 2001.

[134] J. K. Andersen, "Oxidative stress in neurodegeneration: cause or consequence?" *Nature Medicine*, vol. 5, pp. S18–S25, 2004.

[135] A. Nunomura, G. Perry, G. Aliev et al., "Oxidative damage is the earliest event in Alzheimer disease," *Journal of Neuropathology and Experimental Neurology*, vol. 60, no. 8, pp. 759–767, 2001.

[136] R. H. Swerdlow, "Brain aging, Alzheimer's disease, and mitochondria," *Biochimica et Biophysica Acta*, vol. 1812, no. 12, pp. 1630–1639, 2011.

[137] P. F. Good, P. Werner, A. Hsu, C. W. Olanow, and D. P. Perl, "Evidence for neuronal oxidative damage in Alzheimer's disease," *The American Journal of Pathology*, vol. 149, no. 1, pp. 21–28, 1996.

[138] S. G. de Arriba, G. Stuchbury, J. Yarin, J. Burnell, C. Loske, and G. Münch, "Methylglyoxal impairs glucose metabolism and leads to energy depletion in neuronal cells-protection by carbonyl scavengers," *Neurobiology of Aging*, vol. 28, no. 7, pp. 1044–1050, 2007.

[139] S.-M. Huang, H.-C. Chuang, C.-H. Wu, and G.-C. Yen, "Cytoprotective effects of phenolic acids on methylglyoxal-induced apoptosis in Neuro-2A cells," *Molecular Nutrition and Food Research*, vol. 52, no. 8, pp. 940–949, 2008.

[140] Y.-J. Chen, X.-B. Huang, Z.-X. Li, L.-L. Yin, W.-Q. Chen, and L. Li, "Tenuigenin protects cultured hippocampal neurons

against methylglyoxal-induced neurotoxicity," *European Journal of Pharmacology*, vol. 645, no. 1–3, pp. 1–8, 2010.

[141] Q. Q. Yin, C. F. Dong, S. Q. Dong et al., "AGEs induce cell death via oxidative and endoplasmic reticulum stresses in both human SH-SY5Y neuroblastoma cells and rat cortical neurons," *Cellular and Molecular Neurobiology*, vol. 32, no. 8, pp. 1299–1309, 2012.

[142] F. Liu, Z. Liang, and C. X. Gong, "Hyperphosphorylation of tau and protein phosphatases in Alzheimer disease," *Panminerva Medica*, vol. 48, no. 2, pp. 97–108, 2006.

[143] K. Iqbal, F. Liu, C.-X. Gong, A. C. del Alonso, and I. Grundke-Iqbal, "Mechanisms of tau-induced neurodegeneration," *Acta Neuropathologica*, vol. 118, no. 1, pp. 53–69, 2009.

[144] E. Planel, T. Miyasaka, T. Launey et al., "Alterations in glucose metabolism induce hypothermia leading to tau hyperphosphorylation through differential inhibition of kinase and phosphatase activities: implications for Alzheimer's disease," *Journal of Neuroscience*, vol. 24, no. 10, pp. 2401–2411, 2004.

[145] M. Hu, J. F. Waring, M. Gopalakrishnan, and J. Li, "Role of GSK-3β activation and α7 nAChRs in Aβ 1-42-induced tau phosphorylation in PC12 cells," *Journal of Neurochemistry*, vol. 106, no. 3, pp. 1371–1377, 2008.

[146] C. X. Gong, "Dephosphorylation of Alzheimer's disease abnormally phosphorylated tau by protein phosphatase-2A," *Neuroscience*, vol. 61, no. 4, pp. 765–772, 1994.

[147] J.-Z. Wang, C.-X. Gong, T. Zaidi, I. Grundke-Iqbal, and K. Iqbal, "Dephosphorylation of Alzheimer paired helical filaments by protein phosphatase-2A and -2B," *The Journal of Biological Chemistry*, vol. 270, no. 9, pp. 4854–4860, 1995.

[148] X. H. Li, J. Z. Xie, X. Jiang et al., "Methylglyoxal induces tau hyperphosphorylation via promoting AGEs formation," *NeuroMolecular Medicine*, vol. 14, no. 4, pp. 338–348, 2012.

[149] M. A. Smith, M. Rudnicka-Nawrot, P. L. Richey et al., "Carbonyl-related posttranslational modification of neurofilament protein in the neurofibrillary pathology of Alzheimer's disease," *Journal of Neurochemistry*, vol. 64, no. 6, pp. 2660–2666, 1995.

[150] P. Cras, M. A. Smith, P. L. Richey, S. L. Siedlak, P. Mulvihill, and G. Perry, "Extracellular neurofibrillary tangles reflect neuronal loss and provide further evidence of extensive protein cross linking in Alzheimer disease," *Acta Neuropathologica*, vol. 89, no. 4, pp. 291–295, 1995.

[151] B. Kuhla, C. Haase, K. Flach, H. J. Luth, T. Arendt, and G. Munch, "Effect of pseudophosphorylation and cross-linking by lipid peroxidation and advanced glycation end product precursors on tau aggregation and filament formation," *J Biol Chem*, vol. 282, no. 10, pp. 6984–6991, 2007.

[152] M. T. Lin and M. F. Beal, "Mitochondrial dysfunction and oxidative stress in neurodegenerative diseases," *Nature*, vol. 443, no. 7113, pp. 787–795, 2006.

[153] D. Praticò, "Oxidative stress hypothesis in Alzheimer's disease: a reappraisal," *Trends in Pharmacological Sciences*, vol. 29, no. 12, pp. 609–615, 2008.

[154] X. Zhu, H.-G. Lee, A. K. Raina, G. Perry, and M. A. Smith, "The role of mitogen-activated protein kinase pathways in Alzheimer's disease," *NeuroSignals*, vol. 11, no. 5, pp. 270–281, 2002.

[155] A. Chiarini, I. Dal Pra, M. Marconi, B. Chakravarthy, J. F. Whitfield, and U. Armato, "Calcium-sensing receptor (CaSR) in human brain's pathophysiology: Roles in late-onset Alzheimer's disease (LOAD)," *Current Pharmaceutical Biotechnology*, vol. 10, no. 3, pp. 317–326, 2009.

[156] Y. Hashimoto, O. Tsuji, T. Niikura et al., "Involvement of c-Jun N-terminal kinase in amyloid precursor protein-mediated neuronal cell death," *Journal of Neurochemistry*, vol. 84, no. 4, pp. 864–877, 2003.

[157] C. A. Marques, U. Keil, A. Bonert et al., "Neurotoxic mechanisms caused by the alzheimer's disease-linked Swedish amyloid precursor protein. Mutation oxidative stress, caspases, and the JNK pathway," *The Journal of Biological Chemistry*, vol. 278, no. 30, pp. 28294–28302, 2003.

[158] B. Puig, T. Gómez-Isla, E. Ribé et al., "Expression of stress-activated kinases c-Jun N-terminal kinase (SAPK/JNK-P) and p38 kinase (p38-P), and tau hyperphosphorylation in neurites surrounding βA plaques in APP Tg2576 mice," *Neuropathology and Applied Neurobiology*, vol. 30, no. 5, pp. 491–502, 2004.

[159] E. Tamagno, M. Parola, P. Bardini et al., "β-site APP cleaving enzyme up-regulation induced by 4-hydroxynonenal is mediated by stress-activated protein kinases pathways," *Journal of Neurochemistry*, vol. 92, no. 3, pp. 628–636, 2005.

[160] C. Shen, Y. Chen, H. Liu et al., "Hydrogen peroxide promotes Aβ production through JNK-dependent activation of γ-secretase," *The Journal of Biological Chemistry*, vol. 283, no. 25, pp. 17721–17730, 2008.

[161] A. Colombo, A. Bastone, C. Ploia et al., "JNK regulates APP cleavage and degradation in a model of Alzheimer's disease," *Neurobiology of Disease*, vol. 33, no. 3, pp. 518–525, 2009.

[162] Z. Muresan and V. Muresan, "The amyloid-β precursor protein is phosphorylated via distinct pathways during differentiation, mitosis, stress, and degeneration," *Molecular Biology of the Cell*, vol. 18, no. 10, pp. 3835–3844, 2007.

[163] X. Fan, R. Subramaniam, M. F. Weiss, and V. M. Monnier, "Methylglyoxal-bovine serum albumin stimulates tumor necrosis factor alpha secretion in RAW 264.7 cells through activation of mitogen-activating protein kinase, nuclear factor κB and intracellular reactive oxygen species formation," *Archives of Biochemistry and Biophysics*, vol. 409, no. 2, pp. 274–286, 2003.

[164] A. Pal, I. Bhattacharya, K. Bhattacharya, C. Mandal, and M. Ray, "Methylglyoxal induced activation of murine peritoneal macrophages and surface markers of T lymphocytes in Sarcoma-180 bearing mice: Involvement of MAP kinase, NF-$\kappa\beta$ signal transduction pathway," *Molecular Immunology*, vol. 46, no. 10, pp. 2039–2044, 2009.

[165] S.-M. Huang, C.-L. Hsu, H.-C. Chuang, P.-H. Shih, C.-H. Wu, and G.-C. Yen, "Inhibitory effect of vanillic acid on methylglyoxal-mediated glycation in apoptotic Neuro-2A cells," *NeuroToxicology*, vol. 29, no. 6, pp. 1016–1022, 2008.

[166] L. Heimfarth, S. O. Loureiro, P. Pierozan et al., "Methylglyoxal-induced cytotoxicity in neonatal rat brain: a role for oxidative stress and MAP kinases," *Metabolic Brain Disease*, vol. 28, no. 3, pp. 429–438, 2013.

[167] P. Matafome, C. Sena, and R. Seica, "Methylglyoxal, obesity, and diabetes," *Endocrine*, vol. 43, no. 3, pp. 472–484, 2013.

Hindawi Publishing Corporation
BioMed Research International
Volume 2014, Article ID 546453, 11 pages
http://dx.doi.org/10.1155/2014/546453

Research Article

PPAR-γ Impairment Alters Peroxisome Functionality in Primary Astrocyte Cell Cultures

Lorenzo Di Cesare Mannelli, Matteo Zanardelli, Laura Micheli, and Carla Ghelardini

Dipartimento di Neuroscienze, Psicologia, Area del Farmaco e Salute del Bambino—(Neurofarba)—Sezione di Farmacologia e Tossicologia, Università di Firenze, Viale Pieraccini 6, 50139 Florence, Italy

Correspondence should be addressed to Lorenzo Di Cesare Mannelli; lorenzo.mannelli@unifi.it

Received 15 November 2013; Revised 4 January 2014; Accepted 7 January 2014; Published 4 March 2014

Academic Editor: Cristina Angeloni

Peroxisomes provide glial cells with protective functions against the harmful effects of H_2O_2 on neurons and peroxisome impairment results in nervous lesions. Agonists of the γ-subtype of the Peroxisome-Proliferator-Activated-Receptors (PPAR) have been proposed as neuroprotective agents in neurodegenerative disorders. Nevertheless, the role of PPAR-γ alterations in pathophysiological mechanisms and the relevance of peroxisome functions in the PPAR-γ effects are not yet clear. In a primary cell culture of rat astrocytes, the irreversible PPAR-γ antagonist GW9662 concentration-dependently decreased the activity of catalase, the most important antioxidant defense enzyme in peroxisomes. Catalase functionality recovered in a few days and the PPAR-γ agonist rosiglitazone promoted reversal of enzymatic damage. The reversible antagonist G3335 reduced both the activity and expression of catalase in a rosiglitazone-prevented manner. G3335 reduced also the glutathione reductase expression, indicating that enzyme involved in glutathione regeneration was compromised. Neither the PPAR-α target gene Acyl-Coenzyme-A-oxidase-1 nor the mitochondrial detoxifying enzyme NADH:ubiquinone-oxidoreductase (NDFUS3) was altered by PPAR-γ inhibition. In conclusion, PPAR-γ inhibition induced impairment of catalase in astrocytes. A general decrease of the antioxidant defenses of the cell suggests that a PPAR-γ hypofunction could participate in neurodegenerative mechanisms through peroxisomal damage. This series of experiments could be a useful model for studying compounds able to restore peroxisome functionality.

1. Introduction

Hydrogen peroxide (H_2O_2) is ascribed to Reactive Oxygen Species (ROS), although it has no unpaired electrons. It can be formed by the dismutation reaction of $O_2^{\bullet-}$ via the hydroperoxyl radical. Although H_2O_2 is not harmful, its conversion, through the Fenton reaction catalyzed by metal ions, generates the hydroxyl radical ($^{\bullet}OH$), probably the most highly reactive and toxic form of oxygen [1–3]. Catalase is a heme-containing peroxisomal enzyme that breaks down hydrogen peroxide to water and oxygen and is a main antioxidant defense [4, 5]. De Duve and Baudhuin [6] first described a respiratory pathway in peroxisomes in which electrons removed from various metabolites reduce O_2 to H_2O_2, which is further reduced to H_2O. The high peroxisomal consumption of O_2, the demonstration of the production of H_2O_2, $O_2^{\bullet-}$, $^{\bullet}OH$, and recently of $^{\bullet}NO$ [6–9], and the discovery of several ROS metabolizing enzymes in peroxisomes has supported the notion that these ubiquitous organelles play a key role in both the production and scavenging of ROS in the cell [1].

Together with oxygen metabolism, peroxisomes fulfill multiple tasks [10]. The functional relevance of these organelles is dramatically highlighted in the nervous system by peroxisomal disorders. Genetic diseases classified as peroxisome biogenesis disorders and single peroxisomal enzyme deficiencies imply severe demyelination, axonal degeneration, and neuroinflammation that result in a variety of neurological abnormalities [11–15]. On the other hand, peroxisomes have recently been involved in cell aging [16] and in the development and progression of specific degenerative diseases [14, 17–22].

Since a common feature of several neurodegenerative diseases is inflammation [23], several studies have pointed

to the potential use of agonists of the Peroxisome Proliferator Activated Receptor-γ (PPAR-γ). Increasing evidence demonstrates the neuroprotective effects of PPAR-γ agonists in a variety of preclinical models of neurological disorders such as Alzheimer's disease [24–26], Parkinson's disease [27], amyotrophic lateral sclerosis [28], Huntington's disease [29], and ischemic damage [30]. Nevertheless, evidence of PPAR-γ impairment in the physiopathology of neurodegenerative diseases is lacking, as well as the effects induced by its hypofunctionality in the nervous system. The theoretical basis of a PPAR-γ therapeutic approach in neurodegenerative disorders is generally founded on the anti-inflammatory effect. A clear relationship with peroxisome impairments is not well established. Although PPARs can transactivate genes pivotal for the functionality of these organelles [31, 32], the role of peroxisomes in PPAR-γ agonist efficacy, or in PPAR-γ hypofunction, remains unclear.

By focusing on astrocytes, glial cells strongly implicated in several degenerative diseases [33–35], we aimed to characterize the relevance of peroxisome functionality in PPAR-γ-dependent cell signaling. We have evaluated the damage evoked by PPAR-γ antagonists in a primary cell culture by analyzing characteristic peroxisome enzymes.

2. Material and Methods

2.1. Astrocyte Cultures. Primary cultures of astrocytes were obtained according to the method described by McCarthy and De Vellis [36]. Briefly, the cerebral cortex of newborn (P1–P3) Sprague-Dawley rats (Harlan, Udine, Italy) was dissociated in Hanks' balanced salt solution containing 0.5% trypsin/EDTA and 1% DNase (Sigma-Aldrich, Milan, Italy) for 30 min at 37°C. The suspension was mechanically homogenized and filtered. Cells were plated in high-glucose DMEM with 10% FBS. Confluent primary glial cultures were used to isolate astrocytes, removing microglia and oligodendrocytes by shaking. The purity of astrocyte cultures was determined immunocytochemically by staining for GFAP (Dako, Glostrup, Denmark). Cells were fixed in 4% paraformaldehyde, then incubated with the antibody (1 : 200), and visualized using Alexa Fluor-conjugated secondary antibody (Life Technologies, Monza, Italy). Nuclei were stained with 4,6-diamidino-2-phenylindole dihydrochloride. 90% of cells in astrocyte cultures were GFAP-positive. Experiments were performed 21 days after cell isolation. Formal approval to conduct the experiments described was obtained from the Animal Subjects Review Board of the University of Florence. The ethics policy of the University of Florence complies with the Guide for the Care and Use of Laboratory Animals of the US National Institutes of Health (NIH Publication number 85-23, revised 1996; University of Florence Assurance number A5278-01).

2.2. Catalase Activity. On day 21 of culture, astrocytes were plated in 12-well cell culture ($2 \cdot 10^5$/well; Corning, Tewksbury MA, USA) and experiments were performed after 48 h. Cells were treated with GW9662 (1–100 mM), G3335 (1–100 mM), and rosiglitazone (100 mM) for 2 or 5 days. All compounds were purchased from Sigma-Aldrich (Milan, Italy). After incubation, cells were washed once with PBS and scraped with PBS on ice. Cells were then collected, subjected to a freeze-thaw cycle, and centrifuged at 11,000 ×g for 10 min at 4°C. Catalase activity was measured in the supernatant by Amplex Red Catalase Assay Kit (Invitrogen, Monza, Italy) following the manufacturer's instructions. Protein concentration was quantified by bicinchoninic acid assay (Sigma-Aldrich, Milan, Italy). Catalase activity for each sample was normalized to protein concentration. Control conditions in the absence of treatment were set as 100%. Basal catalase activity was not different on days 0 (48 h after plating), 2, 4, 7, or 10 of culturing.

2.3. Hydrogen Peroxide Levels. On day 21 of culture, astrocytes were plated in 6-wells cell culture ($5 \cdot 10^5$/well; Corning, Tewksbury MA, USA) and experiments were performed 48 h after. After treatments with G3335 and rosiglitazone (2 and 5 days), cells were washed once with PBS and scraped with PBS on ice. Cells were then collected, subjected to a freeze-thaw cycle, and centrifuged at 11,000 ×g for 10 min at 4°C. Supernatants were treated with sorbitol to convert peroxide to a peroxyl radical, which oxidizes Fe^{+2} into Fe^{+3}. Then the reaction between Fe^{+3} and an equal molar amount of xylenol orange in the presence of acid was allowed to create a purple product. The absorbance was read at 595 nm (OxiSelect Hydrogen Peroxide Assay Kit, Cell Biolabs, San Diego, CA, USA).

2.4. Western Blotting Analysis. On day 21 of culture, astrocytes were plated in 6-wells cell culture ($5 \cdot 10^5$/well; Corning, Tewksbury MA, USA) and experiments were performed 48 h after. Treatments with G3335 and rosiglitazone lasted 2 and 5 days. After incubation, cells were washed once with PBS and scraped on ice with lysis buffer containing 50 mM Tris-HCl pH 8.0, 150 mM NaCl, 1 mM EDTA, 0.5% Triton X-100, Complete Protease Inhibitor (Roche, Milan, Italy). Cells were then collected, subjected to a freeze-thaw cycle, and centrifuged at 11,000 ×g for 10 min at 4°C; the supernatant was conserved. Astrocyte protein extract was quantified by bicinchoninic acid assay and 40 μg of each sample was resolved with 10% SDS-PAGE before electrophoretic transfer onto nitrocellulose membranes (Biorad, Milan, Italy). Membranes were blocked with 5% nonfat dry milk in PBS containing 0.1% Tween 20 (PBST) and then probed overnight at 4°C with primary antibody specific versus catalase (1 : 1000; 60 kDa; Novus Biological, Littleton, CO, USA), acyl-CoA oxidase 1 (ACOX1) (1 : 1000; 75 kDa; Santa Cruz Biotechnology, Santa Cruz, CA, USA), peroxisomal membrane protein of 70 kDa (PMP70) (1 : 1000; Abcam, Cambridge, MA, USA), glutathione reductase (1 : 1000; 65 kDa; Santa Cruz Biotechnology, Santa Cruz, CA, USA), NDUFS3, core subunit of Complex 1 NADH:ubiquinone oxidoreductase (1 : 1000; 30 kDa; Abcam, Cambridge, MA, USA), GAPDH (1 : 1000; 38 kDa; Cell Signaling, Boston, MA, USA), and β-Actin (1 : 1000; 42 kDa; Cell Signaling, Boston, MA, USA). Membranes were then incubated for 1 hour in PBST containing the appropriate horseradish peroxidase-conjugated secondary antibody

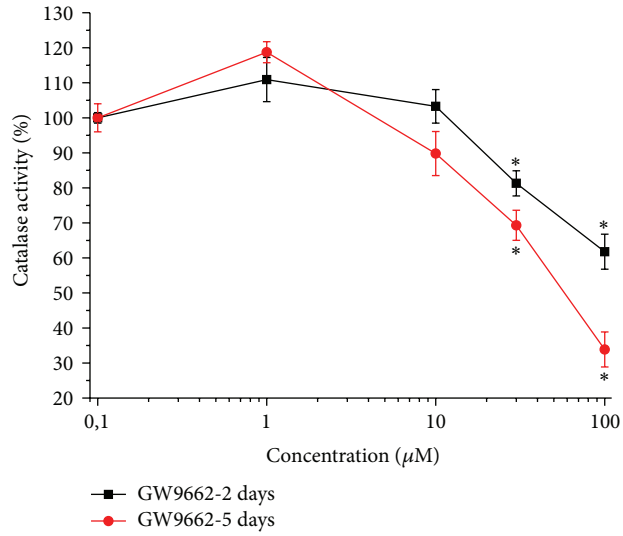

Figure 1: Catalase activity: effect of increasing concentrations of GW9662. Astrocytes ($2 \cdot 10^5$cells/well) were treated with the irreversible PPARγ antagonist GW9662 (1–100 μM) for 2 or 5 days. Values are expressed as the mean ± S.E.M. percent of control of three experiments. Control catalase activity was arbitrarily set as 100%. $^*P < 0.05$ in comparison to control conditions in the absence of treatment.

(1 : 5000; Cell Signalling, Boston, MA, USA). ECL (Enhanced chemiluminescence Pierce, Rockford, IL, USA) was used to visualize the peroxidase-coated bands. Densitometric analysis was performed using the "ImageJ" analysis software (ImageJ, NIH, Bethesda, Maryland, USA) and results were normalized to GAPDH or β-Actin immunoreactivity as internal control. Values are reported as percentages in comparison to control which was arbitrarily fixed at 100%.

2.5. Statistical Analysis. Results are expressed as mean ± S.E.M. and analysis of variance (ANOVA) was performed. A Bonferroni significant difference procedure was used as post hoc comparison. All assessments were made by researchers blinded to cell treatments. P values of less than 0.05 were considered significant. Data were analyzed using the Origin 8.1 software (OriginLab, Northampton, MA, USA).

3. Results

The activity of the peroxisomal enzyme catalase was evaluated in astrocyte cell culture using a fluorometric assay.

The irreversible PPAR-γ antagonist GW9662 reduced catalase activity in a dose-dependent manner over time. As shown in Figure 1, a 2-day incubation with 30 μM GW9662 decreased catalase activity to 81.4 ± 3.6% (control arbitrarily set at 100%), an effect comparable to that evoked by 100 μM H_2O_2 after 2 h incubation (data not shown). The enzymatic activity decreased to 69.8 ± 2.8% after a 5-day incubation in the presence of 30 μM GW9662 and to 32.7 ± 1.3% in the presence of 100 μM GW9662 (Figure 1).

The activity impairment induced by 100 μM GW9662 for 2 days (activity decreased to 61.0 ± 0.9%) was not prevented by the PPAR-γ agonist rosiglitazone (100 μM) (Figure 2(a)). Allowing a further 2-day incubation in the absence of GW9662 (day 4), catalase activity was fully restored (97.4 ± 6.7%) and in the presence of rosiglitazone was stimulated up to 136.1 ± 5.4%. On day 7, which was 5 days after GW9662 washout, activity was about 140% both in the absence and presence of rosiglitazone.

The strong catalase activity decrease induced by a 5 day-incubation with 100 μM GW9662 (Figure 2(b)) was restored by a 2-day washout (day 7). The stimulatory effect of rosiglitazone was significant on day 10 (151.4 ± 6.0%; Figure 2(b)).

As shown in Figure 3, the reversible PPAR-γ antagonist G3335 (30 μM) induced catalase impairment (after a 2-day incubation 77.3 ± 4.1%; after 5 days 62.2 ± 5.3%) comparable to that evoked by GW9662 but this effect seems to be maximal since a higher concentration (100 μM) did not increase the damage (Figure 4). G3335-dependent catalase damage was prevented in the presence of 100 μM rosiglitazone both at 2 and 5 days (Figures 4(a) and 4(b)). Rosiglitazone was also able to improve catalase activity over 100% after a 2-day incubation (Figure 4(a)). The expression level of catalase was unaltered by 30 μM G3335 after a 2-day incubation. On the contrary, a 30% decrease induced by 5 days' incubation of G3335 was fully prevented by 100 μM rosiglitazone (Figure 5). Catalase impairment was associated with a time-dependent increase of hydrogen peroxide levels (about 50 and 100% after 2- and 5-day incubation, resp., Figure 6). In the presence of rosiglitazone H_2O_2 levels were normalized.

G3335 did not alter PMP70 expression levels at both times evaluated (2 and 5 days, Figure 7(a)). G3335 did not alter ACOX1 expression levels at both times evaluated (2 and 5 days, Figure 7(b)). Expressions of the antioxidant enzyme glutathione reductase and Complex 1 NADH dehydrogenase were also measured to evaluate the protective response of astrocytes to the presence of G3335. The NDUFS3 subunit of the mitochondrial enzyme Complex 1 expression was not modified by G3335 (Figure 7(c)).

Glutathione reductase expression was progressively reduced by 30 μM G3335 over time. After 5 days' incubation, protein levels decreased by about 40% (Figure 8), whereas 100 μM rosiglitazone prevented this effect (Figure 8).

4. Discussion

PPARs are members of the nuclear receptor superfamily, actively involved in immunoregulation through their ability to regulate membrane lipid composition, cell proliferation, sensitivity to apoptosis, energy homeostasis, and various inflammatory transcription factors, mainly through their transrepression capabilities [23]. Although all three subtypes of PPARs (α, β/δ, and γ [37]) have been implicated in brain damage, PPAR-γ is the most extensively studied [23, 38–40]. PPAR-γ agonists may ameliorate AD-related pathology and improved learning and memory in animal models and memory and cognition in AD patients [24–26]. Activation of

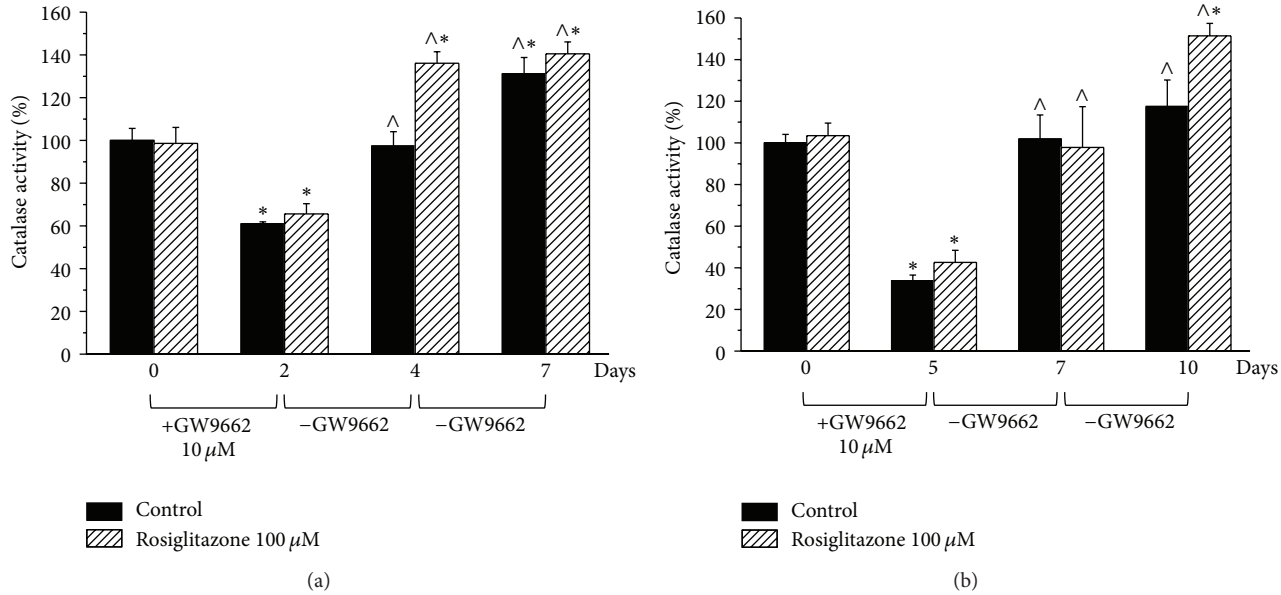

FIGURE 2: Restoration of catalase activity over time after treatment with GW9662. Astrocytes ($2 \cdot 10^5$ cells/well) were treated with the irreversible PPARγ antagonist GW9662 (100 μM) for (a) 2 days in the absence or presence of the PPARγ agonist rosiglitazone (10 μM). Cultures were continued for a further 2 or 5 days in the absence of GW9662 and in the absence or presence of rosiglitazone. Catalase activity was measured on days 0, 2, 4, and 7. (b) Cells were treated with GW9662 (100 μM) for 5 days in the absence or presence of the PPARγ agonist rosiglitazone (100 μM). Cultures were allowed for further 2 or 5 days in the absence of GW9662 and in the absence or presence of Rosiglitazone. Catalase activity was measured on days 0, 5, 7, and 10. Values are expressed as the mean ± S.E.M. percent of control of three experiments. Control catalase activity (day 0) was arbitrarily set as 100%. $^*P < 0.05$ in comparison to control conditions in the absence of treatment on day 0; $^\wedge P < 0.05$ in comparison to control on days 2 (a) or 5 (b).

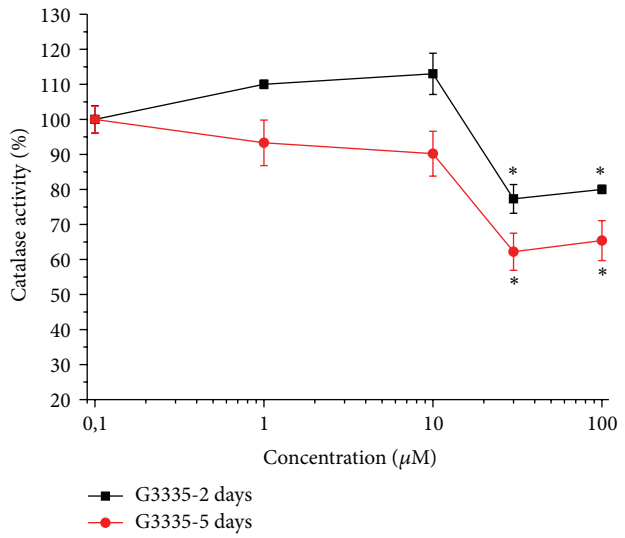

FIGURE 3: Catalase activity: effect of increasing concentrations of G3335. Astrocytes ($2 \cdot 10^5$cells/well) were treated with the reversible PPARγ antagonist G3335 (1–100 μM) for 2 or 5 days. Values are expressed as the mean ± S.E.M. percent of control of three experiments. Control catalase activity was arbitrarily set as 100%. $^*P < 0.05$ in comparison to control conditions in the absence of treatment.

PPAR-γ by pioglitazone induces behavioral recovery associated with preservation of nigrostriatal dopaminergic markers and reduction of CD68-positive cells in Parkinsonian monkeys [27]. PPAR-γ agonists have beneficial effects in an experimental model of Huntington's disease by interfering with the NF-κB signaling pathway [29]. Heneka et al. [30] showed that rosiglitazone delays neuronal damage by interfering with glial activations and increases anti-inflammatory cytokines in response to ischemic damage. On the other hand, there is scanty knowledge about the pathophysiological effects induced by PPAR-γ dysfunctions. In the present results a relationship between PPAR-γ inhibition in astrocytes and peroxisomal function impairment is shown. The irreversible PPAR-γ antagonist GW9662 concentration-dependently decreases catalase activity up to 30%. As expected, GW9662-dependent impairment is not prevented by the PPAR-γ agonist rosiglitazone. On the contrary, catalase functionality recovers in a few days in cell culture in the absence of GW9662, suggesting the plasticity of peroxisome in adverse conditions. Rosiglitazone stimulates the physiological restoration of the enzymatic damage leading to the hypothesis that PPAR-γ agonists may positively intervene in rescue signaling. The reversible antagonist G3335 reduces progressively catalase activity to 60% reaching a plateau for concentrations higher than 30 μM. Two days of incubation are needed for enzyme hypofunctionality, and decreased expression follows 3 days later. Both activity and expression reduction of catalase are prevented by rosiglitazone.

Catalase is the most important antioxidant defense enzyme in mammalian peroxisomes. In rodent liver peroxisomes, rough estimates indicate that each molecule of H_2O_2-producing oxidase possesses at least one molecule

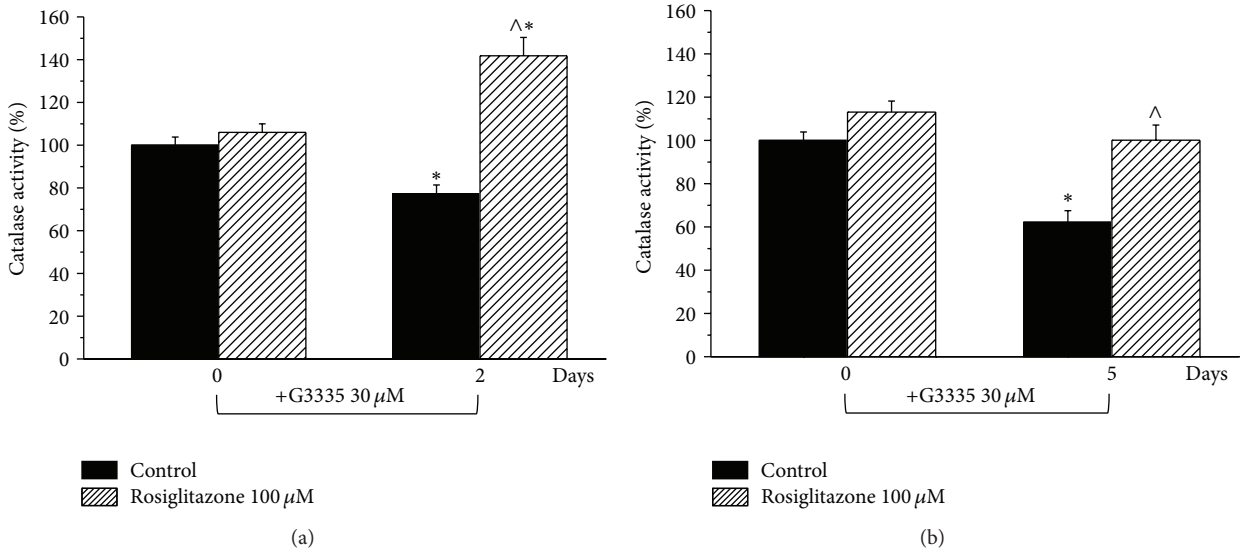

FIGURE 4: Catalase activity: effect of rosiglitazone on G3335-induced enzymatic impairment. Astrocytes ($2 \cdot 10^5$ cells/well) were treated with the reversible PPARγ antagonist G3335 (30 μM) for (a) 2 days or (b) 5 days, in the absence or presence of the PPARγ agonist rosiglitazone (100 μM). Catalase activity was measured on days 0, 2, and 5. Values are expressed as the mean ± S.E.M. percent of control of three experiments. Control catalase activity (day 0) was arbitrarily set as 100%. $^*P < 0.05$ in comparison to control conditions in the absence of treatment on day 0; $^\wedge P < 0.05$ in comparison to control on days 2 (a) or 5 (b).

of catalase as a functional counterpart [41]. Considering that mammalian peroxisomes are densely populated by enzymes that form ROS (most of them are FAD- or FMN-dependent oxidases generating H_2O_2; [42]) it is not surprising that peroxisomes are well equipped with antioxidant defense systems composed mainly of enzymes involved in the decomposition of H_2O_2 [43]. Catalase impairment has been observed in neurodegenerative conditions [44] as well as in complex neurodevelopmental disorders such as autism spectrum, whose neurobiology is proposed to be associated with oxidative stress [45]. On the other hand, oxidative stress may result from an increase in ROS generation as well as from an impairment of catabolic phenomena. Alterations in consumer enzymes may vary the net rate between production and consumption and induce a release of ROS from the organelles to the cell [46]. H_2O_2, unlike $O_2^{\bullet -}$, is able to cross membranes and is free to leave the organelle and to induce cell damage [43]. On the contrary, catalase stimulation is protective against nervous injuries [47]. In the present results, a progressive increase of H_2O_2 parallels with catalase hypofunction.

Conversely, G3335-induced PPAR-γ block does not alter the expression of another major peroxisome protein, PMP70, a membrane protein possessing multiple peroxisome-targeting signals [48]. PMP70 is a half-type ABC-transporter [49] involved in the transport of long and branched chain acyl-CoA [50]. These data suggest lack of a relationship between PPAR-γ and PMP70 in astrocytes.

β-oxidation of a number of carboxylates that cannot be handled by mitochondria is one of the most important metabolic reactions occurring in peroxisomes [51, 52] and this process also contributes to the formation of H_2O_2 [53, 54]. ACOX1 catalyzes the first and rate-limiting step of straight-chain fatty acid β-oxidation [55, 56]. ACOX1 is considered to be a PPAR-α target gene predictive of peroxisome proliferation [57, 58] but, given that PPAR subtypes recognize and activate gene expression through a common DNA binding site [59], ACOX1 could be regulated also by PPAR-γ. In the present results, G3335 does not modify the full length ACOX1 protein expression levels in astrocytes suggesting a specific regulation of PPAR-γ target genes.

To fulfill their functions, peroxisomes physically and functionally interact with other cell organelles, including mitochondria, the endoplasmic reticulum, and lipid droplets [1, 60]. It is well established that peroxisomes and mitochondria are metabolically linked in mammals [61]. Disturbance in peroxisomal metabolism triggers signaling/communication events that ultimately result in increased mitochondrial stress [62, 63]. To evaluate the effect of PPAR-γ inhibition on a characteristic enzyme of the detoxificant machinery of mitochondria we evaluated the expression levels of NDUFS3, a core subunit of Complex 1, the first and largest of the four multiprotein complexes that constitute the mitochondrial respiratory chain involved in oxidative phosphorylation [64]. In particular, NDUFS3 primarily initiates the *in vivo* assembly of Complex 1 in the mitochondrial matrix [65]. Our results show that G3335 does not alter NDUFS3 expression in astrocytes, suggesting that these conditions are specific to peroxisomal damage. However, peroxisome impairment is enough to decrease glutathione reductase expression levels in a rosiglitazone-prevented manner. Glutathione reductase generates reduced glutathione, the main protector of the cell [66] and low levels of this enzyme may have implications for oxidative stress. Glutathione reductase has been described to be reduced in neurodegenerative diseases like PD [67], AD [44], adrenoleukodystrophy [66],

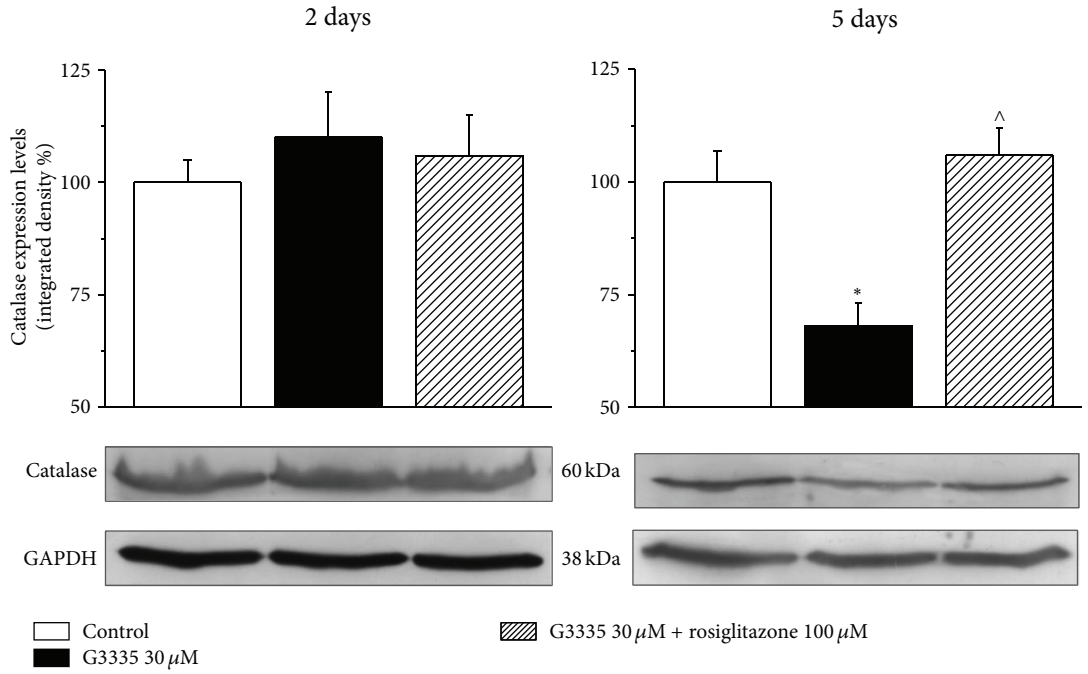

Figure 5: Catalase expression: effect of G3335. Astrocytes ($5 \cdot 10^5$ cells/well) were treated with the reversible PPARγ antagonist G3335 (30 μM) for 2 days or 5 days, in the absence or presence of the PPARγ agonist rosiglitazone (100 μM). Values are expressed as the mean ± S.E.M. percent of control of three experiments. Control condition was arbitrarily set as 100%. $^*P < 0.05$ in comparison to control conditions in the absence of treatment; $^\wedge P < 0.05$ in comparison to G3335 treatment on day 5.

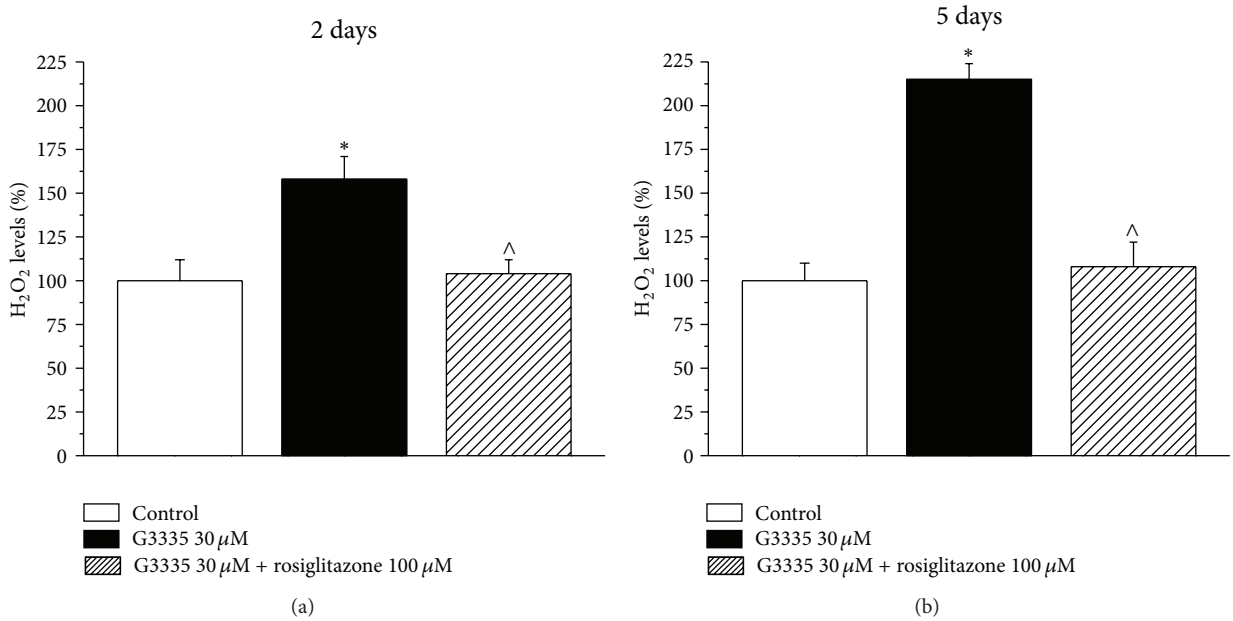

Figure 6: Hydrogen peroxide levels: effect of G3335. Astrocytes ($5 \cdot 10^5$ cells/well) were treated with the reversible PPARγ antagonist G3335 (30 μM) for 2 days or 5 days, in the absence or presence of the PPARγ agonist rosiglitazone (100 μM). Values are expressed as the mean ± S.E.M. percent of control of three experiments. Control condition was arbitrarily set as 100%. $^*P < 0.05$ in comparison to control conditions in the absence of treatment; $^\wedge P < 0.05$ in comparison to G3335 treatment on days 2 or 5.

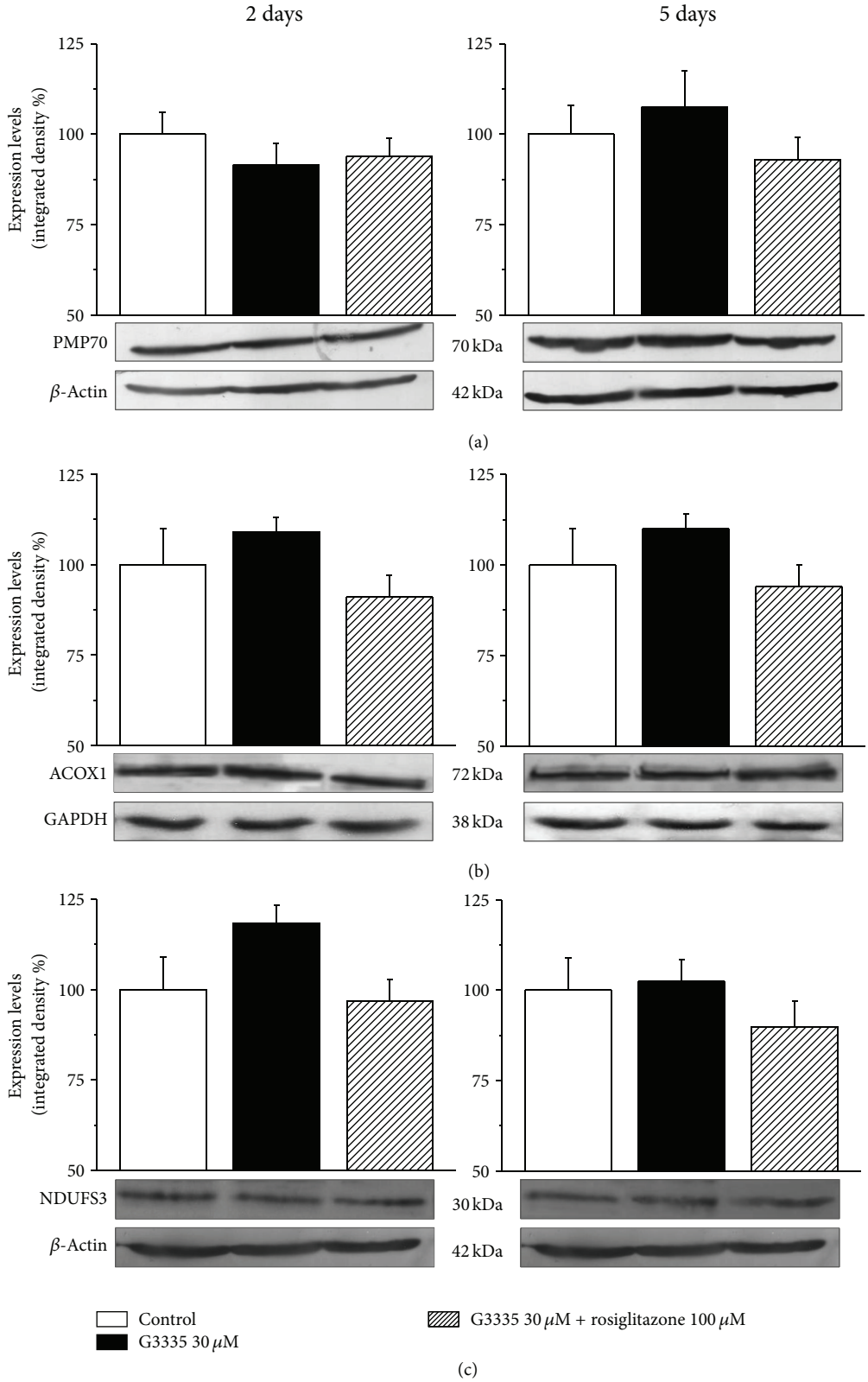

Figure 7: (a) PMP70, (b) ACOX1, and (c) NDUFS3 expression: effect of G3335. Astrocytes ($5 \cdot 10^5$ cells/well) were treated with the reversible PPARγ antagonist G3335 (30 μM) for 2 days or 5 days, in the absence or presence of the PPARγ agonist rosiglitazone (100 μM). Values are expressed as the mean ± S.E.M. percent of control of three experiments. Control condition was arbitrarily set as 100%.

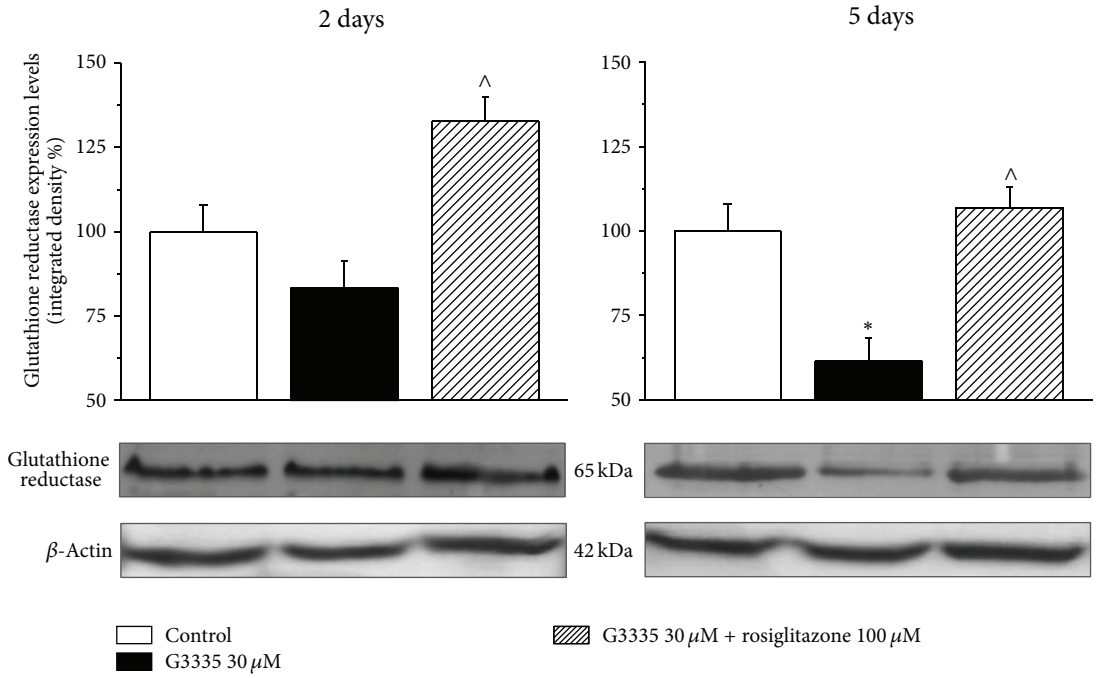

Figure 8: Glutathione reductase expression: effect of G3335. Astrocytes ($5 \cdot 10^5$cells/well) were treated with the reversible PPARγ antagonist G3335 (30 μM) for 2 days or 5 days, in the absence or presence of the PPARγ agonist rosiglitazone (100 μM). Values are expressed as the mean ± S.E.M. percent of control of three experiments. Control condition was arbitrarily set as 100%. $^*P < 0.05$ in comparison to control condition in the absence of treatment; $^\wedge P < 0.05$ in comparison to G3335 treatment on days 2 or 5.

and amyotrophic lateral sclerosis [68]. Astrocytes exert neuroprotective effects by providing neurons with substrates for antioxidants such as glutathione [69]. Astrocytes contain high levels of antioxidant molecules such as vitamins E and C and the antioxidant enzymes Mn- and Cu, Zn-superoxide dismutases (Mn- and Cu, Zn-SOD), catalase, and glutathione peroxidase, which play a major neuroprotective role against the deleterious effects of ROS [70, 71]. Although astrocytes are generally less susceptible to oxidative injury than neurons, there is strong evidence that oxidative stress also alters astrocyte functions [40, 72]. In particular, glial cells are extremely vulnerable to H_2O_2 and astrocytic apoptosis is observed in brain injuries caused by trauma and ischemia [73, 74] and in models of neuropathies [75]. Protection of astrocytes from oxidative attack appears essential to maintain cerebral antioxidant competence and to prevent neuronal damage as well as to facilitate neuronal recovery [76]. It has been shown that peroxisomes provide glial cells with neuroprotective and anti-inflammatory functions [77] and loss or impairment of peroxisomal function results in characteristic patterns of central nervous system lesions [11, 12]. This is best illustrated by pathomorphological examinations of the brain of patients (and mice) in which one or more peroxisomal functions are lost [12, 77–81].

5. Conclusion

In this report we highlight that the PPAR-γ block in astrocytes is strictly related to reduced catalase functionality and expression with a general decrease in antioxidant defenses of the cell. The relevance of the damage induced by PPAR-γ impairment suggests that hypofunctionality of this receptor in glial cells could be present in neurodegenerative diseases and participate in pathological mechanisms through peroxisomal damage. The present series of experiments could offer a useful model for the study of PPAR-γ agonists or, in general, compounds able to restore peroxisome functionality.

Conflict of Interests

The authors declare that there is no conflict of interests regarding the publication of this paper.

Acknowledgment

This work was supported by the Italian Ministry of Instruction, University and Research.

References

[1] M. Schrader and H. D. Fahimi, "Peroxisomes and oxidative stress," *Biochimica et Biophysica Acta*, vol. 1763, no. 12, pp. 1755–1766, 2006.

[2] L. Moldovan and N. I. Moldovan, "Oxygen free radicals and redox biology of organelles," *Histochemistry and Cell Biology*, vol. 122, no. 4, pp. 395–412, 2004.

[3] P. Ježek and L. Hlavatá, "Mitochondria in homeostasis of reactive oxygen species in cell, tissues, and organism," *International*

Journal of Biochemistry and Cell Biology, vol. 37, no. 12, pp. 2478–2503, 2005.

[4] C. D. Putnam, A. S. Arvai, Y. Bourne, and J. A. Tainer, "Active and inhibited human catalase structures: ligand and NADPH binding and catalytic mechanism," *Journal of Molecular Biology*, vol. 296, no. 1, pp. 295–309, 2000.

[5] S. K. Powers and M. J. Jackson, "Exercise-induced oxidative stress: cellular mechanisms and impact on muscle force production," *Physiological Reviews*, vol. 88, no. 4, pp. 1243–1276, 2008.

[6] C. De Duve and P. Baudhuin, "Peroxisomes (microbodies and related particles)," *Physiological Reviews*, vol. 46, no. 2, pp. 323–357, 1966.

[7] B. M. Elliott, N. J. F. Dodd, and C. R. Elcombe, "Increased hydroxyl radical production in liver peroxisomal fractions from rats treated with peroxisome proliferators," *Carcinogenesis*, vol. 7, no. 5, pp. 795–799, 1986.

[8] R. M. Zwacka, A. Reuter, E. Pfaff et al., "The glomerulosclerosis gene Mpv17 encodes a peroxisomal protein producing reactive oxygen species," *The EMBO Journal*, vol. 13, no. 21, pp. 5129–5134, 1994.

[9] D. B. Stolz, R. Zamora, Y. Vodovotz et al., "Peroxisomal localization of inducible nitric oxide synthase in hepatocytes," *Hepatology*, vol. 36, no. 1, pp. 81–93, 2002.

[10] R. J. A. Wanders and H. R. Waterham, "Biochemistry of mammalian peroxisomes revisited," *Annual Review of Biochemistry*, vol. 75, pp. 295–332, 2006.

[11] J. M. Powers and H. W. Moser, "Peroxisomal disorders: genotype, phenotype, major neuropathologic lesions, and pathogenesis," *Brain Pathology*, vol. 8, no. 1, pp. 101–120, 1998.

[12] M. Baes and P. Aubourg, "Peroxisomes, myelination, and axonal integrity in the CNS," *Neuroscientist*, vol. 15, no. 4, pp. 367–379, 2009.

[13] A. Bottelbergs, S. Verheijden, P. P. Van Veldhoven, W. Just, R. Devos, and M. Baes, "Peroxisome deficiency but not the defect in ether lipid synthesis causes activation of the innate immune system and axonal loss in the central nervous system," *Journal of Neuroinflammation*, p. 61, 2012.

[14] D. Trompier, A. Vejux, A. Zarrouk et al., "Brain peroxisomes," *Biochimie*, 2013.

[15] A. D'amico and E. Bertini, "Metabolic neuropathies and myopathies," *Handbook of Clinical Neurology*, vol. 113, pp. 1437–1455, 2013.

[16] C. R. Giordano and S. R. Terlecky, "Peroxisomes, cell senescence, and rates of aging," *Biochimica et Biophysica Acta*, vol. 1822, pp. 1358–1362, 2012.

[17] A. Cimini, S. Moreno, M. D'Amelio et al., "Early biochemical and morphological modifications in the brain of a transgenic mouse model of Alzheimer's disease: a role for peroxisomes," *Journal of Alzheimer's Disease*, vol. 18, no. 4, pp. 935–952, 2009.

[18] P. L. Wood, R. Mankidy, S. Ritchie et al., "Circulating plasmalogen levels and Alzheimer disease assessment scale-cognitive scores in Alzheimer patients," *Journal of Psychiatry and Neuroscience*, vol. 35, no. 1, pp. 59–62, 2010.

[19] M. Igarashi, K. Ma, F. Gao, H.-W. Kim, S. I. Rapoport, and J. S. Rao, "Disturbed choline plasmalogen and phospholipid fatty acid concentrations in Alzheimer's disease prefrontal cortex," *Journal of Alzheimer's Disease*, vol. 24, no. 3, pp. 507–517, 2011.

[20] J. Kou, G. G. Kovacs, R. Höftberger et al., "Peroxisomal alterations in Alzheimer's disease," *Acta Neuropathologica*, vol. 122, no. 3, pp. 271–283, 2011.

[21] M. Fransen, M. Nordgren, B. Wang, and O. Apanasets, "Role of peroxisomes in ROS/RNS-metabolism: implications for human disease," *Biochimica et Biophysica Acta*, vol. 1822, pp. 1363–1373, 2012.

[22] R. Shi, Y. Zhang, Y. Shi, S. Shi, and L. Jiang, "Inhibition of peroxisomal beta-oxidation by thioridazine increases the amount of VLCFAs and Abeta generation in the rat brain," *Neuroscience Letters*, vol. 528, pp. 6–10, 2012.

[23] R. L. Hunter and G. Bing, "Agonism of peroxisome proliferator receptor-gamma may have therapeutic potential for neuroinflammation and Parkinson's disease," *Current Neuropharmacology*, vol. 5, no. 1, pp. 35–46, 2007.

[24] G. Landreth, Q. Jiang, S. Mandrekar, and M. Heneka, "PPARγ agonists as therapeutics for the treatment of Alzheimer's disease," *Neurotherapeutics*, vol. 5, no. 3, pp. 481–489, 2008.

[25] Y.-J. Lee, S. B. Han, S.-Y. Nam, K.-W. Oh, and J. T. Hong, "Inflammation and Alzheimer's disease," *Archives of Pharmacal Research*, vol. 33, no. 10, pp. 1539–1556, 2010.

[26] M. V. Lourenco and J. H. Ledo, "Targeting Alzheimer's pathology through PPARγ signaling: modulation of microglial function," *The Journal of Neuroscience*, vol. 33, pp. 5083–5084, 2013.

[27] C. R. Swanson, V. Joers, V. Bondarenko et al., "The PPAR-γ agonist pioglitazone modulates inflammation and induces neuroprotection in parkinsonian monkeys," *Journal of Neuroinflammation*, vol. 8, article 91, 2011.

[28] V. Benedusi, F. Martorana, L. Brambilla, A. Maggi, and D. Rossi, "The peroxisome proliferator-activated receptor γ (PPARγ) controls natural protective mechanisms against lipid peroxidation in amyotrophic lateral sclerosis," *The Journal of Biological Chemistry*, vol. 287, no. 43, pp. 35899–35911, 2012.

[29] M. Napolitano, L. Costa, R. Palermo, A. Giovenco, A. Vacca, and A. Gulino, "Protective effect of pioglitazone, a PPARγ ligand, in a 3 nitropropionic acid model of Huntington's disease," *Brain Research Bulletin*, vol. 85, no. 3-4, pp. 231–237, 2011.

[30] M. T. Heneka, G. E. Landreth, and M. Hüll, "Drug Insight: effects mediated by peroxisome proliferator-activated receptor-γ in CNS disorders," *Nature Clinical Practice Neurology*, vol. 3, no. 9, pp. 496–504, 2007.

[31] I. Issemann and S. Green, "Activation of a member of the steroid hormone receptor superfamily by peroxisome proliferators," *Nature*, vol. 347, no. 6294, pp. 645–650, 1990.

[32] G. D. Girnun, F. E. Domann, S. A. Moore, and M. E. C. Robbins, "Identification of a functional peroxisome proliferator-activated receptor response element in the rat catalase promoter," *Molecular Endocrinology*, vol. 16, no. 12, pp. 2793–2801, 2002.

[33] C. Li, R. Zhao, K. Gao et al., "Astrocytes: implications for neuroinflammatory pathogenesis of Alzheimer's disease," *Current Alzheimer Research*, vol. 8, no. 1, pp. 67–80, 2011.

[34] M. Kipp, P. van der Valk, and S. Amor, "Pathology of multiple sclerosis," *CNS & Neurological Disorders—Drug Targets*, vol. 11, pp. 506–517, 2012.

[35] L. Brambilla, F. Martorana, and D. Rossi, "Astrocyte signaling and neurodegeneration: new insights into CNS disorders," *Prion*, vol. 7, pp. 28–36, 2013.

[36] K. D. McCarthy and J. De Vellis, "Preparation of separate astroglial and oligodendroglial cell cultures from rat cerebral tissue," *Journal of Cell Biology*, vol. 85, no. 3, pp. 890–902, 1980.

[37] M. Ahmadian, J. M. Suh, N. Hah et al., "PPARγ signaling and metabolism: the good, the bad and the future," *Nature Medicine*, vol. 19, pp. 557–566, 2013.

[38] C. Jiang, A. T. Ting, and B. Seed, "PPAR-γ agonists inhibit production of monocyte inflammatory cytokines," *Nature*, vol. 391, no. 6662, pp. 82–86, 1998.

[39] M. Ricote, A. C. Li, T. M. Willson, C. J. Kelly, and C. K. Glass, "The peroxisome proliferator-activated receptor-γ is a negative regulator of macrophage activation," *Nature*, vol. 391, no. 6662, pp. 79–82, 1998.

[40] Y.-C. Chen, J.-S. Wu, H.-D. Tsai et al., "Peroxisome proliferator-activated receptor gamma (PPAR-γ) and neurodegenerative disorders," *Molecular Neurobiology*, vol. 46, pp. 114–124, 2012.

[41] V. D. Antonenkov, R. T. Sormunen, and J. K. Hiltunen, "The behavior of peroxisomes in vitro: mammalian peroxisomes are osmotically sensitive particles," *American Journal of Physiology*, vol. 287, no. 6, pp. C1623–C1635, 2004.

[42] P. A. Loughran, D. B. Stolz, Y. Vodovotz, S. C. Watkins, R. L. Simmons, and T. R. Billiar, "Monomeric inducible nitric oxide synthase localizes to peroxisomes in hepatocytes," *Proceedings of the National Academy of Sciences of the United States of America*, vol. 102, no. 39, pp. 13837–13842, 2005.

[43] G. C. Brown and V. Borutaite, "There is no evidence that mitochondria are the main source of reactive oxygen species in mammalian cells," *Mitochondrion*, vol. 12, no. 1, pp. 1–4, 2012.

[44] C. Venkateshappa, G. Harish, A. Mahadevan, M. M. Srinivas Bharath, and S. K. Shankar, "Elevated oxidative stress and decreased antioxidant function in the human hippocampus and frontal cortex with increasing age: implications for neurodegeneration in Alzheimer's disease," *Neurochemical Research*, vol. 37, pp. 1601–1614, 2012.

[45] A. Ghanizadeh, S. Akhondzadeh, M. Hormozi, A. Makarem, M. Abotorabi-Zarchi, and A. Firoozabadi, "Glutathione-related factors and oxidative stress in autism, a review," *Current Medicinal Chemistry*, vol. 19, pp. 4000–4005, 2012.

[46] S. Mueller, A. Weber, R. Fritz et al., "Sensitive and real-time determination of H_2O_2 release from intact peroxisomes," *Biochemical Journal*, vol. 363, no. 3, pp. 483–491, 2002.

[47] S. Cardaci, G. Filomeni, G. Rotilio, and M. R. Ciriolo, "p38MAPK/p53 signalling axis mediates neuronal apoptosis in response to tetrahydrobiopterin-induced oxidative stress and glucose uptake inhibition: implication for neurodegeneration," *Biochemical Journal*, vol. 430, no. 3, pp. 439–451, 2010.

[48] S. Iwashita, M. Tsuchida, M. Tsukuda et al., "Multiple organelle-targeting signals in the N-terminal portion of peroxisomal membrane protein PMP70," *Journal of Biochemistry*, vol. 147, no. 4, pp. 581–590, 2010.

[49] M. Kikuchi, N. Hatano, S. Yokota, N. Shimozawa, T. Imanaka, and H. Taniguchi, "Proteomic analysis of rat liver peroxisome. Presence of peroxisome-specific isozyme of Lon protease," *Journal of Biological Chemistry*, vol. 279, no. 1, pp. 421–428, 2004.

[50] M. Morita and T. Imanaka, "Peroxisomal ABC transporters: structure, function and role in disease," *Biochimica et Biophysica Acta*, vol. 1822, pp. 1387–1396, 2012.

[51] J. Vamecq, M. Cherkaoui-Malki, P. Andreoletti, and N. Latruffe, "The human peroxisome in health and disease: the story of an oddity becoming a vital organelle," *Biochimie*, vol. 98C, pp. 4–15, 2013.

[52] G. P. Mannaerts and P. P. Van Veldhoven, "Metabolic pathways in mammalian peroxisomes," *Biochimie*, vol. 75, no. 3-4, pp. 147–158, 1993.

[53] Y. Poirier, V. D. Antonenkov, T. Glumoff, and J. K. Hiltunen, "Peroxisomal β-oxidation-A metabolic pathway with multiple functions," *Biochimica et Biophysica Acta*, vol. 1763, no. 12, pp. 1413–1426, 2006.

[54] L. A. Del Río, "Peroxisomes as a cellular source of reactive nitrogen species signal molecules," *Archives of Biochemistry and Biophysics*, vol. 506, no. 1, pp. 1–11, 2011.

[55] B. T. Poll-The, F. Roels, H. Ogier et al., "A new peroxisomal disorder with enlarged peroxisomes and a specific deficiency of acyl-CoA oxidase (pseudo-neonatal adrenoleukodystrophy)," *American Journal of Human Genetics*, vol. 42, no. 3, pp. 422–434, 1988.

[56] Z. Jia, Z. Pei, Y. Li, L. Wei, K. D. Smith, and P. A. Watkins, "X-linked adrenoleukodystrophy: role of very long-chain acyl-CoA synthetases," *Molecular Genetics and Metabolism*, vol. 83, no. 1-2, pp. 117–127, 2004.

[57] J. E. Klaunig, M. A. Babich, K. P. Baetcke et al., "PPARα agonist-induced rodent tumors: modes of action and human relevance," *Critical Reviews in Toxicology*, vol. 33, no. 6, pp. 655–780, 2003.

[58] J. K. Reddy, S. K. Goel, and M. R. Nemali, "Transcriptional regulation of peroxisomal fatty acyl-CoA oxidase and enoyl-CoA hydratase/3-hydroxyacyl-CoA dehydrogenase in rat liver by peroxisome proliferators," *Proceedings of the National Academy of Sciences of the United States of America*, vol. 83, no. 6, pp. 1747–1751, 1986.

[59] J. C. Corton, S. P. Anderson, and A. Stauber, "Central role of peroxisome proliferator-activated receptors in the actions of peroxisome proliferators," *Annual Review of Pharmacology and Toxicology*, vol. 40, pp. 491–518, 2000.

[60] B. Wang, P. P. Van Veldhoven, C. Brees et al., "Mitochondria are targets for peroxisome-derived oxidative stress in cultured mammalian cells," *Free Radical Biology and Medicine*, vol. 65, pp. 882–894, 2013.

[61] R. J. A. Wanders, "Peroxisomes, lipid metabolism, and peroxisomal disorders," *Molecular Genetics and Metabolism*, vol. 83, no. 1-2, pp. 16–27, 2004.

[62] O. Ivashchenko, P. P. Van Veldhoven, C. Brees, Y.-S. Ho, S. R. Terlecky, and M. Fransen, "Intraperoxisomal redox balance in mammalian cells: oxidative stress and interorganellar cross-talk," *Molecular Biology of the Cell*, vol. 22, no. 9, pp. 1440–1451, 2011.

[63] P. A. Walton and M. Pizzitelli, "Effects of peroxisomal catalase inhibition non mitochondrial function," *Frontiers in Physiology*, vol. 3, p. 108, 2012.

[64] M. Mimaki, X. Wang, M. McKenzie, D. R. Thorburn, and M. T. Ryan, "Understanding mitochondrial complex I assembly in health and disease," *Biochimica et Biophysica Acta*, vol. 11, pp. 851–862, 2012.

[65] R. O. Vogel, C. E. J. Dieteren, L. P. W. J. Van Den Heuvel et al., "Identification of mitochondrial complex I assembly intermediates by tracing tagged NDUFS3 demonstrates the entry point of mitochondrial subunits," *Journal of Biological Chemistry*, vol. 282, no. 10, pp. 7582–7590, 2007.

[66] L. Morató, J. Galino, M. Ruiz et al., "Pioglitazone halts axonal degeneration in a mouse model of X-linked adrenoleukodystrophy," *Brain*, vol. 136, pp. 2432–2443, 2013.

[67] M. M. Khan, A. Ahmad, T. Ishrat et al., "Resveratrol attenuates 6-hydroxydopamine-induced oxidative damage and dopamine depletion in rat model of Parkinson's disease," *Brain Research*, vol. 1328, pp. 139–151, 2010.

[68] E. Cova, P. Bongioanni, C. Cereda et al., "Time course of oxidant markers and antioxidant defenses in subgroups of amyotrophic lateral sclerosis patients," *Neurochemistry International*, vol. 56, no. 5, pp. 687–693, 2010.

[69] O. Elekes, K. Venema, F. Postema, R. Dringen, B. Hamprecht, and J. Korf, "Evidence that stress activates glial lactate formation

in vivo assessed with rat hippocampus lactography," *Neuroscience Letters*, vol. 208, no. 1, pp. 69–72, 1996.

[70] J. Lotharius, J. Falsig, J. Van Beek et al., "Progressive degeneration of human mesencephalic neuron-derived cells triggered by dopamine-dependent oxidative stress is dependent on the mixed-lineage kinase pathway," *Journal of Neuroscience*, vol. 25, no. 27, pp. 6329–6342, 2005.

[71] R. Resende, P. I. Moreira, T. Proença et al., "Brain oxidative stress in a triple-transgenic mouse model of Alzheimer disease," *Free Radical Biology and Medicine*, vol. 44, no. 12, pp. 2051–2057, 2008.

[72] J.-H. Choi, D.-H. Kim, I.-J. Yun, J.-H. Chang, B.-G. Chun, and S.-H. Choi, "Zaprinast inhibits hydrogen peroxide-induced lysosomal destabilization and cell death in astrocytes," *European Journal of Pharmacology*, vol. 571, no. 2-3, pp. 106–115, 2007.

[73] K. Takuma, A. Baba, and T. Matsuda, "Astrocyte apoptosis: implications for neuroprotection," *Progress in Neurobiology*, vol. 72, no. 2, pp. 111–127, 2004.

[74] R. G. Giffard and R. A. Swanson, "Ischemia-induced programmed cell death in astrocytes," *Glia*, vol. 50, no. 4, pp. 299–306, 2005.

[75] L. Di Cesare Mannelli, M. Zanardelli, P. Failli, and C. Ghelardini, "Oxaliplatin-induced oxidative stress in nervous system-derived cellular models: could it correlate with in vivo neuropathy?" *Free Radical Biology and Medicine*, vol. 61, pp. 143–150, 2013.

[76] Y. Hamdi, O. Masmoudi-Kouki, H. Kaddour et al., "Protective effect of the octadecaneuropeptide on hydrogen peroxide-induced oxidative stress and cell death in cultured rat astrocytes," *Journal of Neurochemistry*, vol. 118, no. 3, pp. 416–428, 2011.

[77] C. M. Kassmann, C. Lappe-Siefke, M. Baes et al., "Axonal loss and neuroinflammation caused by peroxisome-deficient oligodendrocytes," *Nature Genetics*, vol. 39, no. 8, pp. 969–976, 2007.

[78] S. Ferdinandusse, A. W. M. Zomer, J. C. Komen et al., "Ataxia with loss of Purkinje cells in a mouse model for Refsum disease," *Proceedings of the National Academy of Sciences of the United States of America*, vol. 105, no. 46, pp. 17712–17717, 2008.

[79] A. Pujol, C. Hindelang, N. Callizot, U. Bartsch, M. Schachner, and J. L. Mandel, "Late onset neurological phenotype of the X-ALD gene inactivation in mice: a mouse model for adrenomyeloneuropathy," *Human Molecular Genetics*, vol. 11, no. 5, pp. 499–505, 2002.

[80] M. Baes, P. Gressens, E. Baumgart et al., "A mouse model for Zellweger syndrome," *Nature Genetics*, vol. 17, no. 1, pp. 49–57, 1997.

[81] L. Hulshagen, O. Krysko, A. Bottelbergs et al., "Absence of functional peroxisomes from mouse CNS causes dysmyelination and axon degeneration," *Journal of Neuroscience*, vol. 28, no. 15, pp. 4015–4027, 2008.

Hindawi Publishing Corporation
BioMed Research International
Volume 2014, Article ID 456937, 11 pages
http://dx.doi.org/10.1155/2014/456937

Research Article

Nuclear Nox4-Derived Reactive Oxygen Species in Myelodysplastic Syndromes

Marianna Guida,[1] Tullia Maraldi,[1] Francesca Beretti,[1] Matilde Y. Follo,[2] Lucia Manzoli,[2] and Anto De Pol[1]

[1] *Department of Surgical, Medical, Dental and Morphological Sciences with interest in Transplant, Oncology and Regenerative Medicine, University of Modena and Reggio Emilia, Via Del Pozzo 71, 41124 Modena, Italy*
[2] *Department of Human Anatomic Sciences, University of Bologna, Via Irnerio 48, 40100 Bologna, Italy*

Correspondence should be addressed to Tullia Maraldi; tullia.maraldi@unimore.it

Received 15 November 2013; Accepted 21 January 2014; Published 26 February 2014

Academic Editor: Cristina Angeloni

A role for intracellular ROS production has been recently implicated in the pathogenesis and progression of a wide variety of neoplasias. ROS sources, such as NAD(P)H oxidase (Nox) complexes, are frequently activated in AML (acute myeloid leukemia) blasts and strongly contribute to their proliferation, survival, and drug resistance. Myelodysplastic syndromes (MDS) comprise a heterogeneous group of disorders characterized by ineffective hematopoiesis, with an increased propensity to develop AML. The molecular basis for MDS progression is unknown, but a key element in MDS disease progression is the genomic instability. NADPH oxidases are now recognized to have specific subcellular localizations, this targeting to specific compartments for localized ROS production. Local Nox-dependent ROS production in the nucleus may contribute to the regulation of redox-dependent cell growth, differentiation, senescence, DNA damage, and apoptosis. We observed that Nox1, 2, and 4 isoforms and p22phox and Rac1 subunits are expressed in MDS/AML cell lines and MDS samples, also in the nuclear fractions. Interestingly, Nox4 interacts with ERK and Akt1 within nuclear speckle domain, suggesting that Nox4 could be involved in regulating gene expression and splicing factor activity. These data contribute to the elucidation of the molecular mechanisms used by nuclear ROS to drive MDS evolution to AML.

1. Introduction

The progression of a premalignant condition to a lethal malignancy is thought to involve an accumulation of mutations in genes that regulate cellular proliferation, survival, and differentiation [1, 2]. The myelodysplastic syndromes (MDSs) can be considered as a representative premalignant hematopoietic disorder that can transform to acute myeloid leukemia (AML) [3].

(Da Watson) MDS comprises a group of anemic disorders of uncertain etiology characterized by abnormal cell morphology in the bone marrow (BM) and peripheral blood cytopenias [4]. According to the International Prognostic Scoring System, the patients with MDS can be divided into 4 prognostic categories: low, intermediate I, intermediate II, and high risk [5]. In about one-third of the patients with MDS, the disease transforms into AML, within months to a few years. These patients usually have a high risk disease, including Int II or high-risk MDS [6]. The causative agent(s) for these secondary events is poorly understood. The excess ROS are known to be a genotoxic stress that can induce DNA damage and mutation following ineffective repair of DNA damage [7–10]. Increased levels of ROS have been detected in both AML and chronic myeloid leukemia [11, 12]. With regard to MDS and oxidative stress, several studies have reported that increased levels of ROS or oxidative DNA damage could be detected in hematopoietic cells from MDS patients [13–15].

It has been demonstrated that RAS mutations in myelodysplastic syndromes/myeloproliferative diseases result in ROS production [16]. Moreover, another player of inositide

signaling; that is, phosphatidylinositol 3 kinase (PI3K) has been suggested to be involved, via its substrate Akt, in the survival of MDS blasts [17].

NAD(P)H oxidase complexes, as ROS sources, are frequently activated in AML blasts and strongly contribute to proliferation, survival, and drug resistance of these cells [18–20]. In leukemia cells, ROS generated by Nox4, at least in part, transmit survival signals through the Akt-PI3K pathway while their depletion leads to apoptosis [21]. Furthermore, NADPH oxidases are now recognized to have specific subcellular localizations, thus being required for localized ROS production [22]. Various ROS-generating and ROS-degrading systems seem to play an important role in different compartments of the cell. The nucleus itself contains a number of proteins with oxidizable thiols that are essential for transcription, chromatin stability, nuclear protein import and export, and DNA replication and repair [23].

Kuroda et al. demonstrated that the endogenous Nox4 preferentially localizes to the nucleus in human endothelial cells [24]. Thus, local Nox4-dependent ROS production in the nucleus may contribute to regulation of redox-dependent transcription factor and gene expression involved in cell growth, differentiation, senescence, and apoptosis. In fact, many transcription factors, including AP-1, NF-κB, Nrf2, p53, glucocorticoid receptor, and nuclear kinases, such as PKC (Protein kinase C), Akt, ERK2, and PKA (Protein kinase A), are redox sensitive [22, 25].

In spite of these striking observations, most ROS nuclear substrates have so far remained elusive, as well as nuclear Nox4-derived ROS functions. Therefore, the first aim of this study is to determine if Nox4 isoform is present in the nucleus of MDS cells and the specific localization area of Nox4 complex. We therefore used the human cell line MOLM-13, established from AML secondary to myelodysplastic syndrome and the AML cell line THP1 and/or human blasts obtained from patients with MDS. The broad object of this research is to elucidate the role of nuclear Nox-derived ROS in myelodysplastic syndromes. Therefore, Nox4 expression has been down-regulated and ROS decrease in the nucleus has been checked in order to confirm the nuclear localization and activity of NADPH oxidase.

Then, we searched for binding partners in the nucleus, in particular signaling key molecules. To reveal the interactome proteins that reside in nuclear Nox complex in human MDS/AML cell line, coimmunoprecipitation assay has been performed in order to check Nox interactions with nuclear signaling players. Identification of substrates or binding partners of nuclear NAD(P)H oxidases will pave the way to finding new pharmacological treatments.

The data resulting from the present study could contribute to shedding the light on the molecular mechanisms used by this key intracellular pathway to drive MDS evolution to AML and, in general, in hematological dysfunctions.

2. Materials and Methods

2.1. Patient Characteristics. Peripheral blood samples (PBMCs) came from 10 MDS patients and 3 healthy normal volunteers who had given informed consent according to the Declaration of Helsinki. The samples came from the Department of Hematology and Medical Oncology (L. e A. Seràgnoli) of the Policlinico S. Orsola, Bologna, Italy. In all of the subjects participating in this study, MDS diagnosis was defined according to WHO classification [26]. For *in vitro* experiments, PBMCs were isolated by Ficoll-Paque (Amersham Biosciences, Sunnyvale, CA, USA) density-gradient centrifugation, according to the manufacturer's protocol.

2.2. Cell Culture. The MDS cell line MOLM13 and the AML cell line THP1 were purchased from DSMZ (German Resource Centre for Biological Material). MOLM-13 cells express FLT3-ITD and have been derived from the peripheral blood of a patient with post-MDS AML [27, 28]. MOLM-13 carries internal tandem duplication of FLT3. THP1 is an acute monocytic leukemia cell line.

Cell lines were cultured with 5% CO_2 at 37°C in RPMI (Mediatech, Inc., Herndon, VA) with 10% fetal calf serum (FCS) and supplemented with 2 mM L-glutamine, 100 U/mL penicillin, and 100 μg/mL streptomycin (all from EuroClone Spa, Italy).

2.3. Nox4 Silencing. Retroviral supernatants were produced according to HuSH shRNA Plasmid Panels (29-mer) Application Guide; AM12 cells were transfected with an empty vector (pRS Vector, TR20003), a scrambled vector (HuSH 29-mer non effective pRS vector, TR30012), and four NOX4 gene specific shRNA expression pRS vectors (TI311637, TI311638, TI311639, and TI311640) for 48 h. Retroviral supernatants were then centrifuged at 2000 ×g for 5 minutes and used for target cells (THP1) infection. Where indicated, cells were infected with NOX4 shRNA retroviral vectors, empty vector, or scrambled vector. Forty-eight hours after infection, cells were exposed to 2 μg/mL puromycin (Sigma Aldrich) for 24 hours, and subjected to evaluation of Nox4 expression by Western blotting and confocal analysis and detection of intracellular ROS levels.

2.4. Preparation of Cell Extracts. Cell extracts were obtained as described by Maraldi et al. [29]. Briefly, cells were extracted by addition of AT lysis buffer (20 mM Tris-Cl, pH 7.0; 1% Nonidet P-40; 150 mM NaCl; 10% glycerol; 10 mM EDTA; 20 mM NaF; 5 mM sodium pyrophosphate; and 1 mM Na3VO4) and freshly added Sigma Aldrich Protease Inhibitor Cocktail at 4°C for 30 min. Lysates were sonicated, cleared by centrifugation, and immediately boiled in SDS sample buffer or used for immunoprecipitation experiments, as described below.

2.5. Nuclei Purification. Cell nuclei were purified as reported by Cenni et al. [30]. Briefly, 400 μL of nuclear isolation buffer (10 mM Tris-HCl, pH 7.8, 1% Nonidet P-40, 10 mM β-mercaptoethanol, 0.5 mM phenylmethylsulfonyl fluoride, 1 μg/mL aprotinin and leupeptin, and 5 mM NaF) was added to 5×10^6 cells for 8 min on ice. MilliQ water (400 μL) was then added to swell cells for 3 min. Cells were sheared by

passages through a 22-gauge needle. Nuclei were recovered by centrifugation at 400 ×g at 4°C for 6 min and washed once in 400 μL of washing buffer (10 mM Tris-HCl, pH 7.4, and 2 mM $MgCl_2$, plus inhibitors as described earlier in the text). Supernatants (containing the cytosolic fractions) were further centrifuged for 30 min at 4000 ×g. Isolated nuclear and cytoplasmic extracts were finally lysed in AT lysis buffer, sonicated, and cleared by centrifugation.

2.6. Immunoprecipitation and Electrophoresis. Immunoprecipitation was performed as reported by Bertacchini et al. [31]. For preclearing procedure nuclear lysates were incubated with 2 μg anti-M2 for 1 hour (Sigma Aldrich) and then with beads for additionally 30 min, which were then removed and discarded prior to the immunoprecipitation. Precleared lysates, whose protein concentration was determined by the Bradford method, were incubated 4 hours with 3 μg of anti-Nox4 (Novus Biologicals, CO, USA). Then samples were treated with 30 μL of 50% (v/v) of protein A/G agarose slurry (GE Healthcare Biosciences, Uppsala, Sweden) at 4°C with gentle rocking for 1 h. Pellets were washed twice with 20 mM Tris-Cl, pH 7.0; 1% Nonidet P-40; 150 mM NaCl; 10% glycerol; 10 mM EDTA; 20 mM NaF; 5 mM sodium pyrophosphate, once with 10 mM Tris-Cl, pH 7.4, boiled in SDS sample buffer, and centrifuged. Supernatants were loaded onto SDS-polyacrylamide gel, blotted on Immobilon-P membranes (Millipore, Waltham, MA, USA), and processed by Western blot with the indicated antibodies.

2.7. Western Blot. The protocols of the Western blot were performed as described by Hanson et al. [32]. Briefly, protein extracts, quantified by a Bradford Protein Assay (Bio-Rad Laboratories, CA, USA), underwent SDS-polyacrylamide gel electrophoresis and were transferred to Immobilon-P membranes. The following antibodies were used: rabbit anti-ERK1/2, goat anti-Matrin3, goat anti-βactin, anti-p22phox (Santa Cruz Biotechnology, Santa Cruz, CA, USA) diluted 1 : 500, rabbit anti-Akt1, rabbit anti-Rac1, and rabbit anti-ERK1/2 (Cell Signalling Technology, Beverly, MA, USA), mouse anti-tubulin, rabbit anti-Nox1, and mouse anti-sc-35 (Sigma Aldrich St. Louis, MO, USA), rabbit anti-Nox4 (Novus Biologicals, CO, USA), rabbit anti-Nox2, and mouse anti-pH2A(Ser139) (Millipore, Billerica, MA, USA) diluted 1 : 1000; peroxidase-labelled anti-rabbit, mouse and goat secondary antibodies diluted 1 : 3000 (Pierce Antibodies, Thermo Scientific; Rockford, IL, USA). Ab dilution was performed in TBS-T pH 7.6 containing 3% BSA. The membranes were visualized using Supersignal substrate chemiluminescence detection kit (Pierce, Rockford, IL, USA). Anti-βactin antibody was used as control of protein loading. Quantization of the signal was obtained by chemiluminescence detection on a Kodak Image Station 440CF and analysis with the Kodak 1D Image software.

2.8. Confocal Microscopy. Cells were fixed for 20 min in 4% ice-cold paraformaldehyde and then permeabilized with 0.1% Triton X-100 in ice-cold phosphate-buffered saline (PBS) for 5 min. Permeabilized samples were then blocked with 3% of bovine serum albumin (BSA) in PBS for 30 min at room temperature and incubated with primary antibodies (Abs): rabbit anti-Nox4 (Santa Cruz, CA, USA) (diluted 1 : 50), mouse anti-sc-35 (Sigma Aldrich St. Louis, MO, USA) and mouse anti pH2A (Ser139) (Millipore, Billerica, MA, USA) (diluted 1 : 100), in PBS containing 3% BSA for 1 h at RT. Secondary antibody was diluted 1 : 200 in PBS containing 3% BSA (goat anti-mouse Alexa 647 and goat anti-rabbit Alexa 488). After washing in PBS, samples were stained with 1 μg/mL DAPI in H_2O for 1 min and then mounted with antifading medium (0.21 M DABCO and 90% glycerol in 0.02 M Tris, pH 8.0). Negative controls consisted of samples not incubated with the primary antibody, but only with the secondary antibody.

Confocal imaging was performed on a Nikon A1 confocal laser scanning microscope as previously described [33].

Spectral analysis was carried out to exclude overlapping between two signals or the influence of autofluorescence background on the fluorochrome signals, as previously shown [34]. The confocal serial sections were processed with Image J software to obtain three-dimensional projections, as previously described [35]. The image rendering was performed by Adobe Photoshop software.

2.9. Nuclear ROS Imaging. Nuclear ROS were detected with nuclear-localized fluorescent probe for H_2O_2, Nuclear Peroxy Emerald 1 (NucPE1) [36–39]. For all experiments, 5 μM solutions of NucPE1 (from 5 mM stocks in DMSO) were made in PBS/glucose. The cells were then kept in an incubator (37°C, 5% CO_2) for a total of 30 min in the dark. Fluorescence was measured on a multiwell plate reader (Appliskan, Thermo Scientific) using 488 nm filter for excitation and 535 nm filter for emission.

Confocal fluorescence imaging studies were performed with a Nikon A1 confocal laser scanning microscope. Excitation of NucPE1-loaded cells at 488 nm was carried out with an Ar laser and emission was collected at 535 nm. All images in an experiment were collected simultaneously using identical microscope settings. Image analysis was performed in Image J.

2.10. Statistical Analysis. *In vitro* experiments were performed in triplicate. For quantitative comparisons, values were reported as mean ± SD based on triplicate analysis for each sample. To test the significance of observed differences between the study groups, unpaired Student's t-test was applied. A P value <0.05 was considered to be statistically significant.

3. Results

3.1. Patient Characteristics. Peripheral blood (PB) MCs from 10 patients affected by MDS (5 treated with azacitidine, 2 with hydroxyurea, 1 with erythropoietin and 2 with best supportive care only) were examined. Median age was 70 years (range 65 to 82 years). MDS was diagnosed following World Health Organization (WHO) classification [26]. Patient demographics and disease characteristics are summarized in Table 1.

Table 1: Clinical, hematologic, and cytogenetic characteristics of MDS patients.

WHO diagnosis	Karyotype	Treatment	Clinical outcome
RARS	Normal		Stable disease
RCMD	del (7q)		Disease progression, death
RCMD	del (20q)	EPO	AML
RAEB1	Normal	5-aza	RAEB2
RAEB1	del (5q)	Idrossiurea (HU)	Stable disease
RAEB1	del (7q)	Idrossiurea (HU)	Stable disease
RAEB2	Tris (8)	5-aza	AML, death
RAEB2	Tris (8)	5-aza	AML, death
RAEB2	Normal	5-aza	AML, death
AML	Normal	5-aza	AML, death

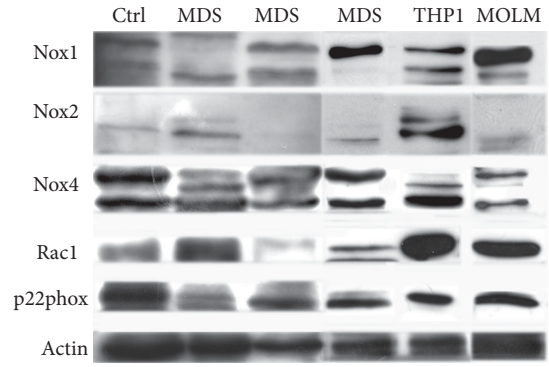

Figure 1: Expression of NADPH oxidases and their subunits. Representative images of Western blot analysis of total lysates of PBMC healthy donor (ctrl), MDS, MOLM-13, and THP1 samples revealed with antibodies against NADPH oxidase isoforms 1, 2, and 4, Rac1, and p22phox subunits. βactin was used as loading internal control.

Karyotype analysis shows that different abnormalities are present in the study group as well as different disease gravity levels, as shown by WHO classification.

3.2. NADPH Oxidases Expression in MDS Samples and MDS/AML Cell Lines. At first, we tested the expression level of NADPH oxidase isoforms and their subunits by Western blot (WB) analysis of total lysates of all the MDS collected samples and of human MDS/AML cell lines (THP1 and MOLM-13).

By using different kinds of affinity-purified antibodies raised against distinct immunogens from human Nox1, Nox2, Nox4, p22phox, and Rac1, we demonstrated that all these proteins are present in MDS samples and human MDS/AML cell lines. Figure 1 shows the expression pattern of three representative MDS samples compared to MOLM-13 and THP1 cell lines and PBMC healthy donor. Nox1 and Nox4 isoforms seem to be highly expressed in all samples.

Interestingly, Nox4 is both expressed into the nucleus and in the cytoplasm. In fact, confocal analysis (Figure 2(a)) demonstrated that in different MDS samples (images representative of RAEB1, RAEB2, and RARS are shown) a punctate staining of Nox4 is detectable inside the nuclei. Nox1 and Nox2 signals show a cytoplasmic localization (not shown). The same pattern has been observed also in MDS/AML cell lines (Figure 2(b)).

In order to demonstrate the specificity of the immunofluorescence signal, we performed Western blot analysis of nuclear and cytoplasm subfractions (Figure 3). Also with this approach we can see a high presence of Nox4 in nuclear portions; moreover, the Nox4 subunit p22phox is present in both the subfractions.

Rac, an important downstream effector of RAS, is an activator of Nox2 and Nox4 and, in leukemic cells, Rac-1 and Akt activate Nox2 and Nox4 [20, 40]. RAS/Nox have been also demonstrated to be modulators of cell growth and proliferation via activating the mitogen-activated protein kinase ERK1/2 signaling pathway [41]. Beside Nox4 and its regulators p22phox and Rac-1, here we show that Akt1 and ERK1/2 are also present in nuclear protein portions of both MOLM-13 and THP1 cell lines (Figure 3).

3.3. Modulation of Nox-Derived Nuclear ROS Production. In order to investigate the NADPH oxidase activity inside the nuclei, we used a nuclear selective probe for H_2O_2, Nuclear peroxy Emerald 1 (Figure 4). Confocal microscopy confirms that there is a ROS production inside the nuclei (Figure 4(a)).

Even if the use of Nox4 synthetic inhibitor, diphenyleneiodonium (DPI), is not directed to the nuclear part of Nox4, as demonstrated by the fluorogenic probe assay, the Nox4 activity inhibition reduces the nuclear ROS production (Figures 4(a) and 4(b)).

A more selective approach, as Nox4 silencing, confirms the Nox4 role in nuclear ROS production. The highest downregulation of Nox4 was obtained with shRNA TI311638 and TI311640, as demonstrated by Western blot (Figure 4(d)). Immunofluorescence assay (Figure 4(c)) shows that the decrease in Nox4 expression occurs both in cytoplasmic and nuclear compartments. Overall, THP1 cells, treated with all shRNA sequences, show a significant decrease in nuclear ROS level.

3.4. Nuclear Nox4 Role. The production of ROS directly inside the nuclei can be linked to DNA damage. In fact, increasing evidence suggests that genetic changes in myeloid malignancies lead to increased production of endogenous sources of DNA damage, such as reactive oxygen species.

It has been shown recently that the phosphorylation level of H2AX is crucial to determining whether cells will survive after DNA damage [42].

Looking at nuclear H2A foci, as expected, we found that, compared to healthy donor, MDS samples exhibit a huge status of H2A phosphorylation (Figure 5), suggesting that nNox4-generated ROS can induce nuclear DNA damage.

Then, we investigated the nuclear Nox4 binding network (Figure 6). Based on the punctate Nox4 signal previously observed (Figure 2), we tested whether this distribution

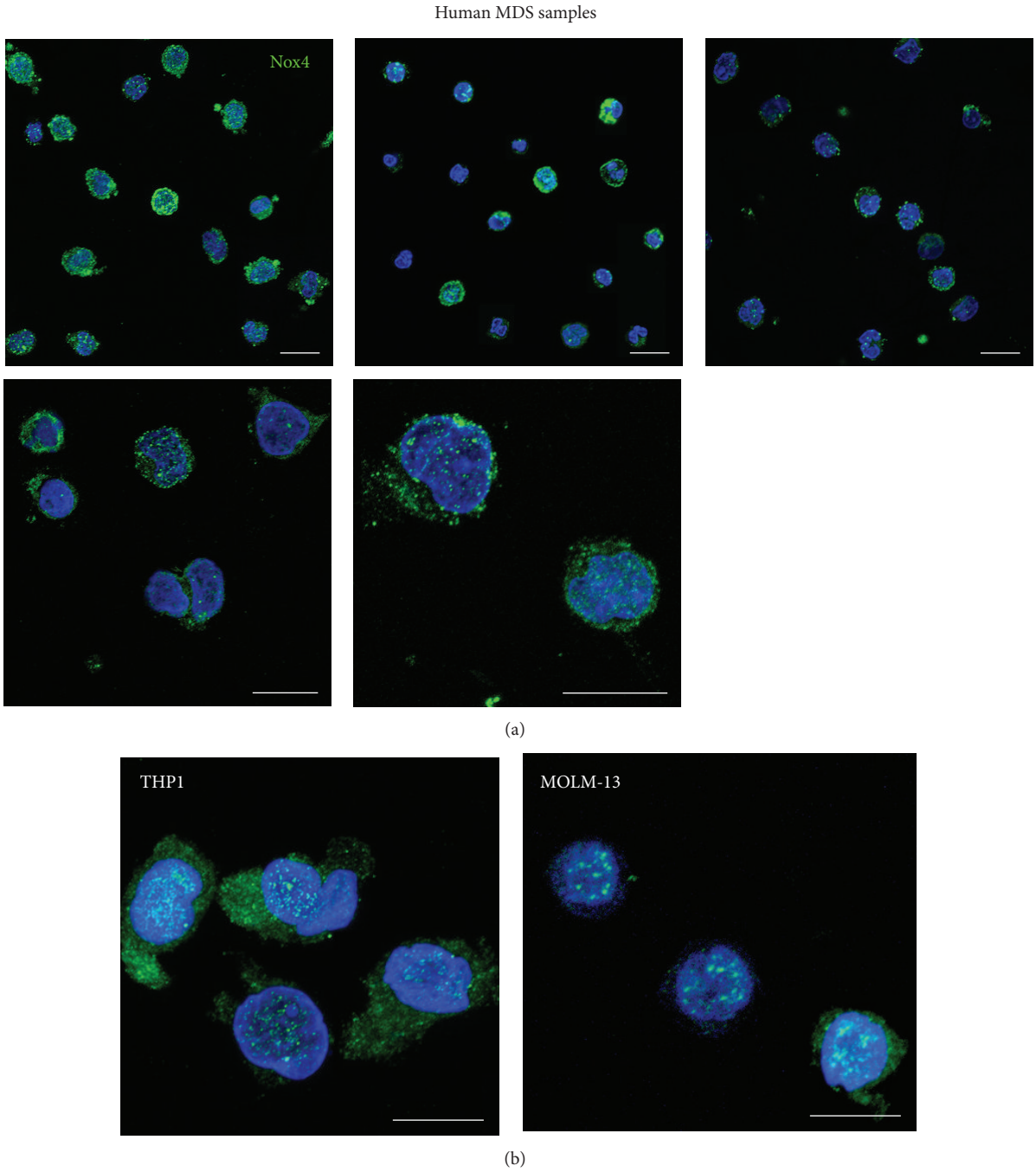

Figure 2: Immunofluorescence analysis of Nox4 expression. (a) Representative images at different magnifications showing superimposing between DAPI (blue) and Nox4 (green) signals in three human MDS samples (from left to right RAEB1, RAEB2, and RARS first row and RAEB1 and RAEB2 in the second row). (b) Representative images showing superimposing between DAPI (blue) and Nox4 (green) signals in MOLM-13 and THP1 samples. Scale bar: 10 μm.

follows the localization of speckles nuclear domains by using an antibody directed against sc-35. Sc-35 is involved in pre-mRNA splicing and is found in the bodies in the nucleus referred to as speckles, sc-35 domains, or splicing factor compartments (SFCs). Figure 6(a) shows that the nuclear signal of Nox4 (green) often colocalizes with the one of sc-35 (red), generating an orange staining. The arrow indicates, as example, the colocalization in MDS sample.

The interaction of Nox4 with sc-35 was confirmed also by coimmunoprecipitation experiment (Figure 6(b)). Nuclear extracts (NL) of THP1 were used for coimmunoprecipitation analysis with anti-Nox4 (IPNox4), since this cell line express the highest level of nuclear Nox4. Preclearing fraction, obtained as described in method section, is shown as control for nonspecific interactions with protein A/G: the only one band is the one of IgG used in the preclearing step. This

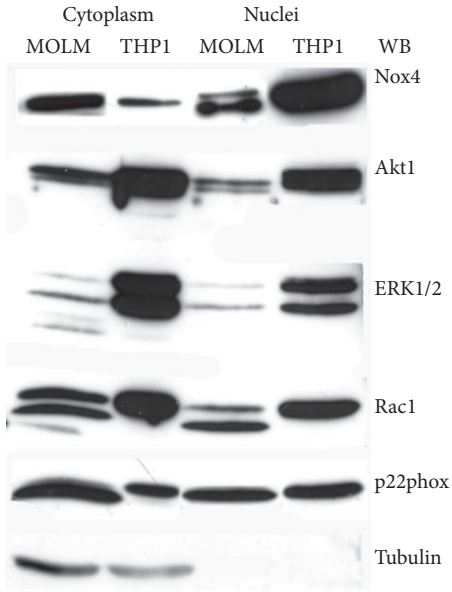

Figure 3: Western blot analysis of cytosol (cyto) and nuclear fractions (nuclei) of MOLM-13 and THP1 samples revealed with anti-Nox4, anti-Akt1, anti-ERK1/2, anti-Rac1, and anti-p22phox. Tubulin absence was used as index of nuclear extract's purification. Presented data are representative of three independent experiments.

experiment also confirms the interaction between Nox4 and the subunit p22phox. Furthermore, Nox4 seems to be linked with nuclear matrix protein, Matrin3, and with ERK1/2 and Akt1, suggesting a direct role in nuclear MAPK and Akt signaling regulation.

4. Discussion

Myelodysplastic syndromes refer to a heterogeneous group of closely related hematological disorders that are characterized by an ineffective production of blood cells (dysplasia) and a hypercellular or hypocellular marrow with impaired morphology and maturation (dysmyelopoiesis) [5]. Although the genetic basis of MDS is not completely understood, a significant percentage of MDS cases are characterized by chromosomal aberrations [43, 44] and the transformation of MDS to AML is often accompanied by additional mutations [45]. Approximately, 30% myelodysplastic syndrome (MDS) cases progress to acute myelogenous leukemia.

It is now well established that the progression of normal cells to neoplastic transformation results from the accumulation of mutations in genes that control cellular proliferation, survival, and differentiation [1].

It has been proposed that AML requires a minimum of two complementary mutations, one leading to enhanced proliferation and the second leading to impaired differentiation [46].

A significant percentage of MDS cases is characterized by chromosomal deletions of 5q or 7q [3] and has previously been reported to be high in a proportion of myeloid malignancies [47, 48]. The next most frequent genetic alteration in MDS is activating mutations of the RAS homologues occurring in 20% of MDS patients reviewed in [49, 50]. Tumor progression is accompanied by an increase in ROS, which leads to an increased DNA damage. It is well established that activation of oncogenes can lead to ROS production [51], and ROS is an established source of endogenous double-strand breaks [52]. Thus, acquisition of oncogenic changes can initiate a cycle of genomic instability that has the potential to create further mutations, which in turn may facilitate leukemic disease progression. Several lines of evidence now indicate that activation of RAS-mitogen-activated protein (MAP) kinase pathways can generate increased ROS. In fact, one candidate pathway for ROS production in MDS may be signaling through RAC1 [53]. Another candidate pathway for ROS production is signaling through extracellular signal-regulated kinase 1/2 (ERK1/2).

It has been previously demonstrated that ERK phosphorylation occurred downstream from the Nox4 pathway, but through the RAS activation in endoplasmic reticulum [54]. The presence and the activity in the nucleus of both PI3K/Akt [55] and NAD(P)H oxidase isoform 4 have been described [24]. Indeed, the altered expression of Nox4 could be involved in a dysregulation of cell cycle and has also an important meaning in high risk MDS patients. ROS can inactivate nuclear-localized phosphatases and thereby enhance kinase activation. Moreover, excessive production of ROS also could lead to oxidative DNA damage.

In this point of view, the subcellular localization of Nox4 is likely to be especially important, given its constitutive activity, unlike isoforms, such as Nox1 or Nox2, that require agonist activation.

We observed in human MDS samples, showing DNA damage sign and obtained from different disease grade patients, that Nox4 isoform is, interestingly, localized into the nucleus. Inhibition of Nox4 activity, obtained with DPI or Nox4 silencing, induces a decline of nuclear ROS production, confirming the activity of Nox4 within the nuclei.

Confocal and coimmunoprecipitation analysis demonstrate Nox4 presences in speckle domains suggesting that Nox4 could be involved in regulating DNA-mRNA processing machinery by ROS production in specific nuclear area. Also Matrin 3 has been demonstrated to bind DNA at sites termed scaffold/matrix attachment regions to regulate gene expression through interactions with chromatin remodeling [56]. Here, we show that Nox4 coimmunoprecipitates also with Matrin 3. Thus, Matrin 3 could be a docking site where nuclear ROS signaling may exert its function on transcription/pre-mRNA modulation in specific nuclear domains.

Moreover, immunoprecipitation analysis demonstrated that Nox4 interacts with Akt and ERK signaling, suggesting a role in nuclear signaling dysregulation leading to MDS progression. The identification of these binding partners of nuclear Nox4 may pave the way to finding new pharmacological treatments.

Taken together, we suggest that nNox4 regulation may have important pathophysiologic effects in MDS through

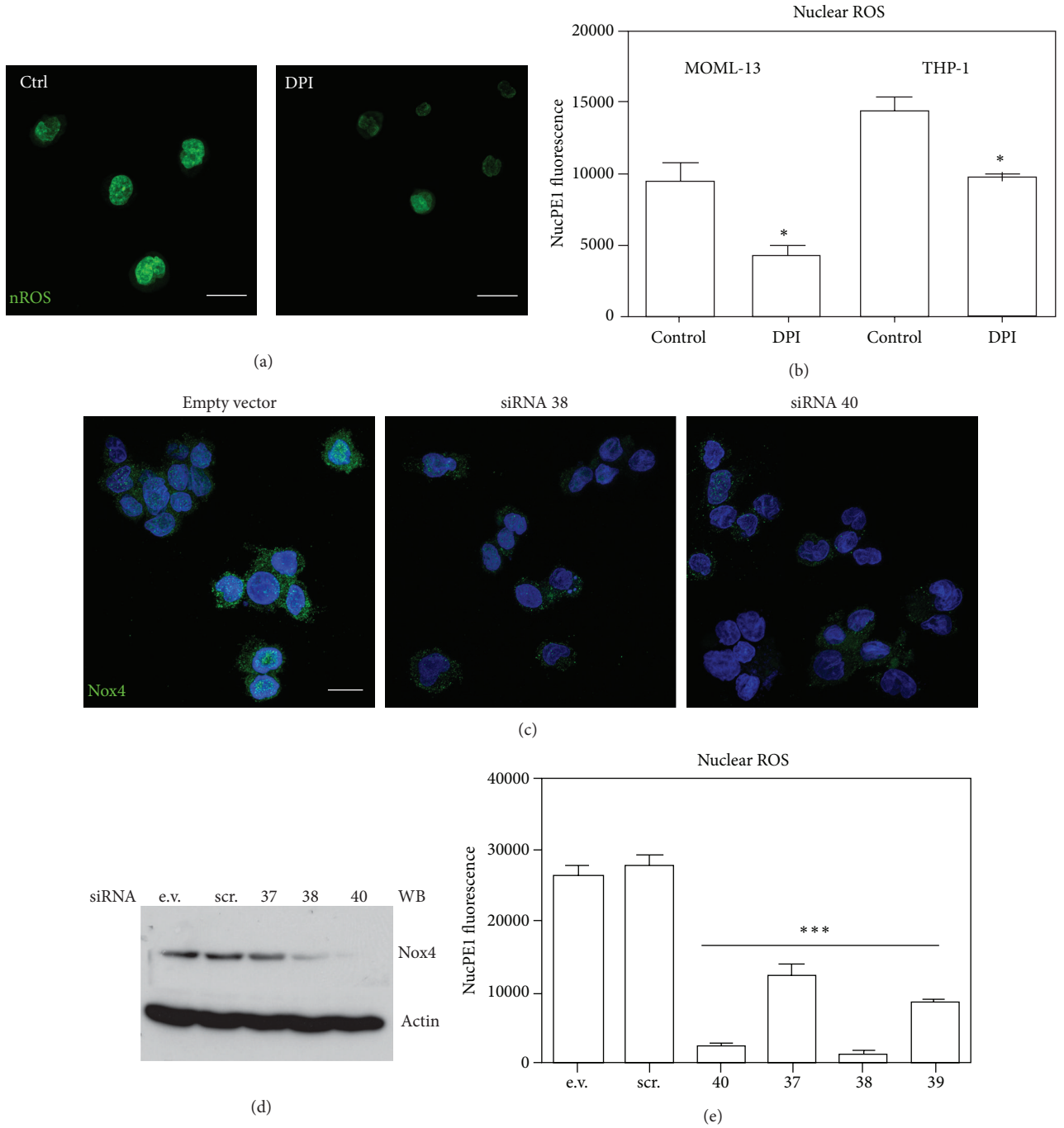

Figure 4: Effect of Nox4 inhibition on nuclear ROS production. (a) Representative images showing staining with nuclear ROS probe (nuclear peroxy Emerald 1) of THP1 in the presence or absence of 2 μM DPI for 18 hours. Scale bar: 10 μm. (b) Graph representing fluorescence intensity of nuclear ROS probe (Nuclear peroxy Emerald 1) of MOLM-13 and THP1 in the presence or absence of 2 μM DPI for 18 hours. (c) Representative images showing: superimposing between DAPI (blue) and Nox4 SC (green) signals of THP1 treated with empty vector (EV) or Nox4-directed siRNA (38 and 40) as reported in Section 2. Scale bar: 10 μm. (d) Representative images of Western blot analysis of Nox4 silencing in THP1 cells. βactin was used as loading internal control. (e) Graph representing fluorescence intensity of nuclear ROS probe (Nuclear peroxy Emerald 1) of THP1 treated with empty vector (EV), scrambled siRNA (SCR), or Nox4-directed siRNA (37, 38, 39, and 40). Presented data are representative of three independent experiments. $^{*}P < 0.05$ and $^{***}P < 0.001$ versus Control.

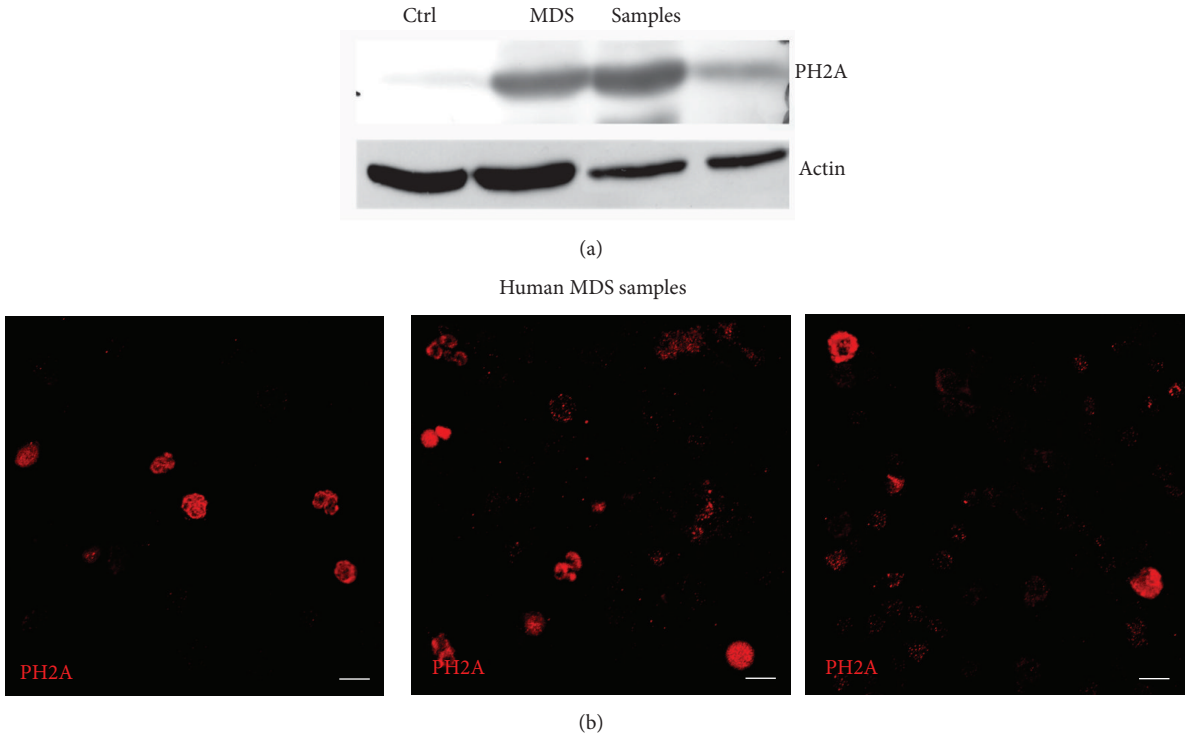

Figure 5: DNA damage in MDS samples. (a) Representative images showing staining with anti-PH2A (red), as marker of DNA damage, in three human MDS samples. Scale bar: 10 μm. (b) Western blot analysis of total lysates of MDS samples revealed with anti-PH2A. βactin was used as loading internal control.

modulation of nuclear signaling and DNA damage. For example, Nox4 can be a critical mediator in oncogenic RAS-induced DNA-damage response.

In addition to antioxidant therapy, targeted therapy for STAT, RAS, and PI3K pathways, such as RAC1 [16], may be amenable to inhibition of nuclear ROS sources and genomic instability using small molecule inhibitors.

These therapeutic options are likely to represent important treatments in MDS/AML. Nevertheless, efficacy of ROS reduction on the reversal of genomic instability and disease progression may rely on elucidation of the major routes for ROS overproduction in cancer with multiple genetic alterations.

Abbreviations

AML: acute myeloid leukemia
BM: bone marrow
BSA: bovine serum albumin
DABCO: 1,4-diazabicyclo(2.2.2)octane
DAPI: 4′,6-diamidino-2-phenylindole
DPI: diphenyleneiodonium
EDTA: ethylenediaminetetraacetic acid
PBMCs: peripheral blood samples
PBS: phosphate buffered saline
MDSs: myelodysplastic syndromes
Nox: NADPH oxidase
nNox4: nuclear NOX4
RA: refractory anemia
PI3K: phosphatidylinositol 3 kinase
RARS: RA with ringed sideroblasts
RAEB: RA with excess of blasts
RCMD: refractory cytopenia with multilineage dysplasia
ROS: reactive oxygen species
TBS: Tris-buffered saline
Tx: Triton-X-100.

Conflict of Interests

The authors declare that there is no conflict of interests regarding the publication of this paper.

Authors' Contribution

Marianna Guida and Tullia Maraldi equally contributed to this work.

Acknowledgments

The authors thank Dr. Christopher J. Chang and Dr. Bryan C. Dickinson, Department of Chemistry, University of California, Berkeley, CA, USA, for gently providing Nuclear

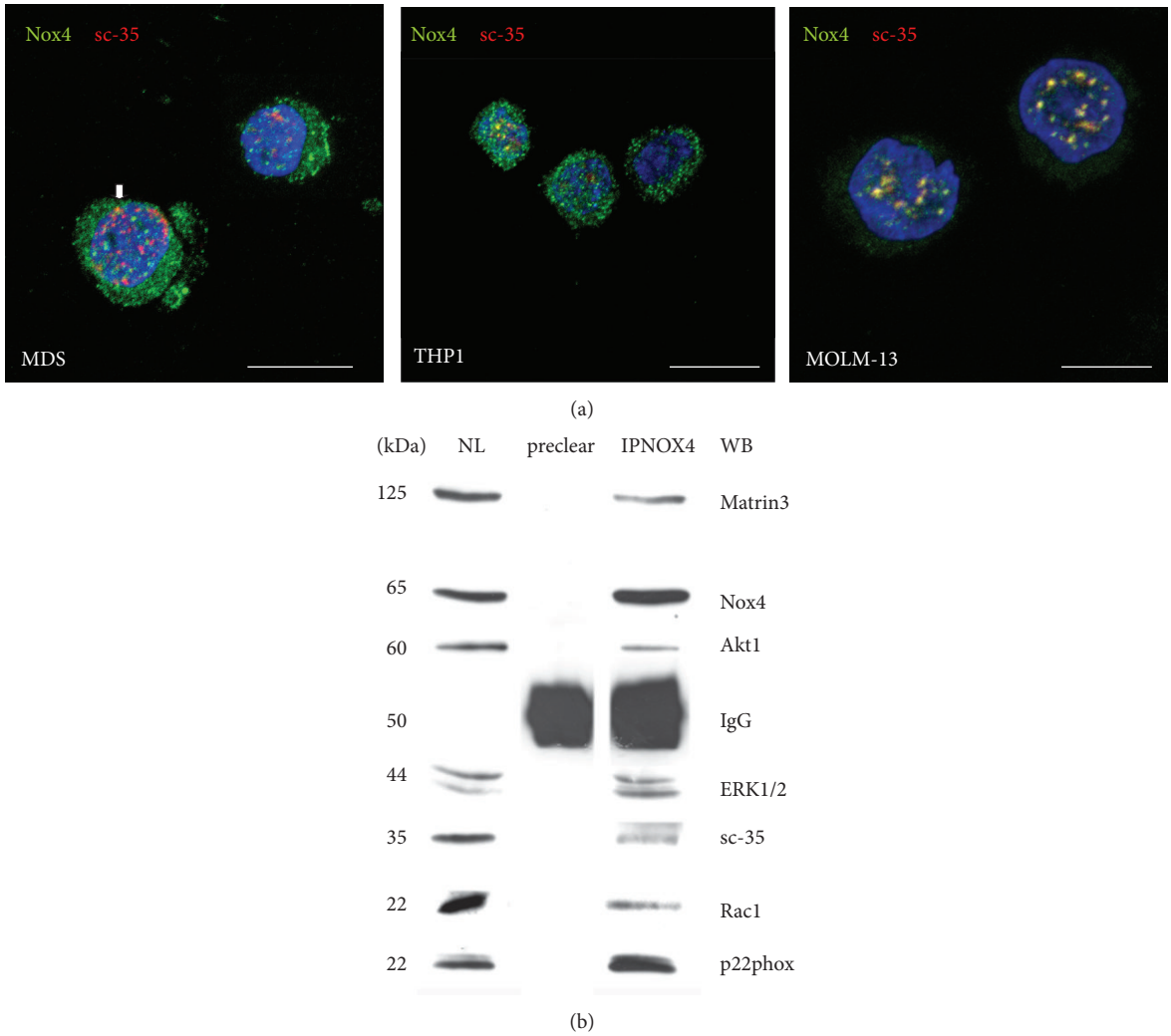

Figure 6: Nox4 nuclear interaction. (a) Representative images showing superimposing between DAPI (blue), Nox4 (green), and sc-35 (red) signals in MDS, MOLM-13, and THP1 cells. Scale bar: 10 μm. (b) Representative images of Western blot analysis of nuclear lysate (NL), preclearing (preclear) sample obtained, as described in methods section, before immunoprecipitation experiment with Nox4 antibody (IPNOX4): these samples were then revealed with anti-Matrin3, anti-Nox4, anti-Akt1, anti-ERK1/2, anti-sc-35, anti-Rac1, and anti-p22phox. All presented data are representative of three independent experiments.

peroxy Emerald 1. This work was supported by grants from MIUR PRIN 2009 Prot: 200938XJLA_002. The authors thank Professor Lucio I. Cocco for the project design.

References

[1] F. V. Rassool, T. J. Gaymes, N. Omidvar et al., "Reactive oxygen species, DNA damage, and error-prone repair: a model for genomic instability with progression in myeloid leukemia?" *Cancer Research*, vol. 67, no. 18, pp. 8762–8771, 2007.

[2] W. Guo, Z. Keckesova, J. L. Donaher et al., "Slug and Sox9 cooperatively determine the mammary stem cell state," *Cell*, vol. 148, no. 5, pp. 1015–1028, 2012.

[3] A. Mijović and G. J. Mufti, "The myelodysplastic syndromes: towards a functional classification," *Blood Reviews*, vol. 12, no. 2, pp. 73–83, 1998.

[4] A. S. Watson, M. Mortensen, and A. K. Simon, "Autophagy in the pathogenesis of myelodysplastic syndrome and acute myeloid leukemia," *Cell Cycle*, vol. 10, no. 11, pp. 1719–1725, 2011.

[5] S. D. Nimer, "Myelodysplastic syndromes," *Blood*, vol. 111, no. 10, pp. 4841–4851, 2008.

[6] P. Greenberg, C. Cox, M. M. LeBeau et al., "International scoring system for evaluating prognosis in myelodysplastic syndromes," *Blood*, vol. 89, no. 6, pp. 2079–2088, 1997.

[7] O. A. Sedelnikova, C. E. Redon, J. S. Dickey, A. J. Nakamura, A. G. Georgakilas, and W. M. Bonner, "Role of oxidatively induced DNA lesions in human pathogenesis," *Mutation Research*, vol. 704, no. 1–3, pp. 152–159, 2010.

[8] G. Slupphaug, B. Kavli, and H. E. Krokan, "The interacting pathways for prevention and repair of oxidative DNA damage," *Mutation Research*, vol. 531, no. 1-2, pp. 231–251, 2003.

[9] F. Steinboeck, M. Hubmann, A. Bogusch, P. Dorninger, T. Lengheimer, and E. Heidenreich, "The relevance of oxidative stress and cytotoxic DNA lesions for spontaneous mutagenesis

in non-replicating yeast cells," *Mutation Research*, vol. 688, no. 1-2, pp. 47–52, 2010.

[10] M. Themeli, L. Petrikkos, M. Waterhouse et al., "Alloreactive microenvironment after human hematopoietic cell transplantation induces genomic alterations in epithelium through an ROS-mediated mechanism: in vivo and in vitro study and implications to secondary neoplasia," *Leukemia*, vol. 24, no. 3, pp. 536–543, 2010.

[11] A. Sallmyr, J. Fan, K. Datta et al., "Internal tandem duplication of FLT3 (FLT3/ITD) induces increased ROS production, DNA damage, and misrepair: implications for poor prognosis in AML," *Blood*, vol. 111, no. 6, pp. 3173–3182, 2008.

[12] M. J. Farquhar and D. T. Bowen, "Oxidative stress and the myelodysplastic syndromes," *International Journal of Hematology*, vol. 77, no. 4, pp. 342–350, 2003.

[13] H. Ghoti, J. Amer, A. Winder, E. Rachmilewitz, and E. Fibach, "Oxidative stress in red blood cells, platelets and polymorphonuclear leukocytes from patients with myelodysplastic syndrome," *European Journal of Haematology*, vol. 79, no. 6, pp. 463–467, 2007.

[14] B. Novotna, Y. Bagryantseva, M. Siskova, and R. Neuwirtova, "Oxidative DNA damage in bone marrow cells of patients with low-risk myelodysplastic syndrome," *Leukemia Research*, vol. 33, no. 2, pp. 340–343, 2009.

[15] C. M. Peddie, C. R. Wolf, L. I. Mclellan, A. R. Collins, and D. T. Bowen, "Oxidative DNA damage in $CD34^+$ myelodysplastic cells is associated with intracellular redox changes and elevated plasma tumour necrosis factor-α concentration," *British Journal of Haematology*, vol. 99, no. 3, pp. 625–631, 1997.

[16] A. Sallmyr, J. Fan, and F. V. Rassool, "Genomic instability in myeloid malignancies: increased reactive oxygen species (ROS), DNA double strand breaks (DSBs) and error-prone repair," *Cancer Letters*, vol. 270, no. 1, pp. 1–9, 2008.

[17] Q. Xu, S.-E. Simpson, T. J. Scialla, A. Bagg, and M. Carroll, "Survival of acute myeloid leukemia cells requires PI3 kinase activation," *Blood*, vol. 102, no. 3, pp. 972–980, 2003.

[18] C. Prata, T. Maraldi, D. Fiorentini, L. Zambonin, G. Hakim, and L. Landi, "Nox-generated ROS modulate glucose uptake in a leukaemic cell line," *Free Radical Research*, vol. 42, no. 5, pp. 405–414, 2008.

[19] T. Maraldi, C. Prata, F. Vieceli Dalla Sega et al., "NAD(P)H oxidase isoform Nox2 plays a prosurvival role in human leukaemia cells," *Free Radical Research*, vol. 43, no. 11, pp. 1111–1121, 2009.

[20] T. Maraldi, C. Prata, C. Caliceti et al., "VEGF-induced ROS generation from NAD(P)H oxidases protects human leukemic cells from apoptosis," *International Journal of Oncology*, vol. 36, no. 6, pp. 1581–1589, 2010.

[21] T. Finkel, "Intracellular redox regulation by the family of small GTPases," *Antioxidants and Redox Signaling*, vol. 8, no. 9-10, pp. 1857–1863, 2006.

[22] M. Ushio-Fukai, "Compartmentalization of redox signaling through NaDPH oxidase-derived rOS," *Antioxidants and Redox Signaling*, vol. 11, no. 6, pp. 1289–1299, 2009.

[23] T. Kietzmann, "Intracellular redox compartments: mechanisms and significances," *Antioxidants and Redox Signaling*, vol. 13, no. 4, pp. 395–398, 2010.

[24] J. Kuroda, K. Nakagawa, T. Yamasaki et al., "The superoxide-producing NAD(P)H oxidase Nox4 in the nucleus of human vascular endothelial cells," *Genes to Cells*, vol. 10, no. 12, pp. 1139–1151, 2005.

[25] M. Lukosz, S. Jakob, N. Büchner, T.-C. Zschauer, J. Altschmied, and J. Haendeler, "Nuclear redox signaling," *Antioxidants and Redox Signaling*, vol. 12, no. 6, pp. 713–742, 2010.

[26] J. W. Vardiman, N. L. Harris, and R. D. Brunning, "The World Health Organization (WHO) classification of the myeloid neoplasms," *Blood*, vol. 100, no. 7, pp. 2292–2302, 2002.

[27] Y. Matsuo, R. A. F. MacLeod, C. C. Uphoff et al., "Two acute monocytic leukemia (AML-M5a) cell lines (MOLM-13 and MOLM-14) with interclonal phenotypic heterogeneity showing MLL-AF9 fusion resulting from an occult chromosome insertion, ins(11;9)(q23;p22p23)," *Leukemia*, vol. 11, no. 9, pp. 1469–1477, 1997.

[28] C. Fabre, G. Carvalho, E. Tasdemir et al., "NF-κB inhibition sensitizes to starvation-induced cell death in high-risk myelodysplastic syndrome and acute myeloid leukemia," *Oncogene*, vol. 26, no. 28, pp. 4071–4083, 2007.

[29] T. Maraldi, J. Bertacchini, M. Benincasa et al., "Reverse-phase protein microarrays (RPPA) as a diagnostic and therapeutic guide in multidrug resistant leukemia," *International Journal of Oncology*, vol. 38, no. 2, pp. 427–435, 2011.

[30] V. Cenni, A. Bavelloni, F. Beretti et al., "Ankrd2/ARPP is a novel Akt2 specific substrate and regulates myogenic differentiation upon cellular exposure to H_2O_2," *Molecular Biology of the Cell*, vol. 22, no. 16, pp. 2946–2956, 2011.

[31] J. Bertacchini, F. Beretti, V. Cenni et al., "The protein kinase Akt/PKB regulates both prelamin A degradation and Lmna gene expression," *The FASEB Journal*, vol. 27, no. 6, pp. 2145–2155, 2013.

[32] C. J. Hanson, M. D. Bootman, C. W. Distelhorst, T. Maraldi, and H. L. Roderick, "The cellular concentration of Bcl-2 determines its pro- or anti-apoptotic effect," *Cell Calcium*, vol. 44, no. 3, pp. 243–258, 2008.

[33] E. Resca, M. Zavatti, L. Bertoni et al., "Enrichment in c-Kit+ enhances mesodermal and neural differentiation of human chorionic placental cells," *Placenta*, vol. 34, no. 7, pp. 526–535, 2013.

[34] A. Pisciotta, M. Riccio, G. Carnevale et al., "Human serum promotes osteogenic differentiation of human dental pulp stem cells in vitro and in vivo," *PLoS ONE*, vol. 7, no. 11, Article ID e50542, 2012.

[35] M. Riccio, E. Resca, T. Maraldi et al., "Human dental pulp stem cells produce mineralized matrix in 2D and 3D cultures," *European Journal of Histochemistry*, vol. 54, no. 4, article e46, 2010.

[36] B. C. Dickinson, Y. Tang, Z. Chang, and C. J. Chang, "A nuclear-localized fluorescent hydrogen peroxide probe for monitoring sirtuin-mediated oxidative stress responses in vivo," *Chemistry and Biology*, vol. 18, no. 8, pp. 943–948, 2011.

[37] A. R. Lippert, G. C. Van De Bittner, and C. J. Chang, "Boronate oxidation as a bioorthogonal reaction approach for studying the chemistry of hydrogen peroxide in living systems," *Accounts of Chemical Research*, vol. 44, no. 9, pp. 793–804, 2011.

[38] V. S. Lin, B. C. Dickinson, and C. J. Chang, "Boronate-based fluorescent probes: imaging hydrogen peroxide in living systems," *Methods in Enzymology*, vol. 526, pp. 19–43, 2013.

[39] B. C. Dickinson and C. J. Chang, "Chemistry and biology of reactive oxygen species in signaling or stress responses," *Nature Chemical Biology*, vol. 7, no. 8, pp. 504–511, 2011.

[40] J. L. Kissil, M. J. Walmsley, L. Hanlon et al., "Requirement for Rac1 in a K-ras-induced lung cancer in the mouse," *Cancer Research*, vol. 67, no. 17, pp. 8089–8094, 2007.

[41] P. Ranjan, V. Anathy, P. M. Burch, K. Weirather, J. D. Lambeth, and N. H. Heintz, "Redox-dependent expression of cyclin D1 and cell proliferation by Nox1 in mouse lung epithelial cells," *Antioxidants and Redox Signaling*, vol. 8, no. 9-10, pp. 1447–1460, 2006.

[42] P. J. Cook, B. G. Ju, F. Telese, X. Wang, C. K. Glass, and M. G. Rosenfeld, "Tyrosine dephosphorylation of H2AX modulates apoptosis and survival decisions," *Nature*, vol. 458, no. 7238, pp. 591–596, 2009.

[43] M. L. Heaney and D. W. Golde, "Myelodysplasia," *The New England Journal of Medicine*, vol. 340, no. 21, pp. 1649–1660, 1999.

[44] S. J. Corey, M. D. Minden, D. L. Barber, H. Kantarjian, J. C. Y. Wang, and A. D. Schimmer, "Myelodysplastic syndromes: the complexity of stem-cell diseases," *Nature Reviews Cancer*, vol. 7, no. 2, pp. 118–129, 2007.

[45] M. J. Walter, D. Shen, L. Ding et al., "Clonal Architecture of Secondary Acute Myeloid Leukemia," *The New England Journal of Medicine*, vol. 366, no. 12, pp. 1090–1098, 2012.

[46] D. G. Gilliland and M. S. Tallman, "Focus on acute leukemias," *Cancer Cell*, vol. 1, no. 5, pp. 417–420, 2002.

[47] N. Mori, R. Morosetti, E. Hoflehner, M. Lübbert, H. Mizoguchi, and H. P. Koeffler, "Allelic loss in the progression of myelodysplastic syndrome," *Cancer Research*, vol. 60, no. 11, pp. 3039–3042, 2000.

[48] N. Mori, R. Morosetti, H. Mizoguchi, and H. P. Koeffler, "Progression of myelodysplastic syndrome: allelic loss on chromosomal arm 1p," *British Journal of Haematology*, vol. 122, no. 2, pp. 226–230, 2003.

[49] R. A. Padua, B.-A. Guinn, A. I. Al-Sabah et al., "RAS, FMS and p53 mutations and poor clinical outcome in myelodysplasias: a 10-year follow-up," *Leukemia*, vol. 12, no. 6, pp. 887–892, 1998.

[50] P. Fenaux, "Chromosome and molecular abnormalities in myelodysplastic syndromes," *International Journal of Hematology*, vol. 73, no. 4, pp. 429–437, 2001.

[51] X. Deng, F. Gao, and W. S. May Jr., "Bcl2 retards G1/S cell cycle transition by regulating intracellular ROS," *Blood*, vol. 102, no. 9, pp. 3179–3185, 2003.

[52] K. D. Mills, D. O. Ferguson, and F. W. Alt, "The role of DNA breaks in genomic instability and tumorigenesis," *Immunological Reviews*, vol. 194, pp. 77–95, 2003.

[53] M. Kochetkova, P. O. Iversen, A. F. Lopez, and M. F. Shannon, "Deoxyribonucleic acid triplex formation inhibits granulocyte macrophage colony-stimulating factor gene expression and suppresses growth in juvenile myelomonocytic leukemic cells," *Journal of Clinical Investigation*, vol. 99, no. 12, pp. 3000–3008, 1997.

[54] R. Serù, P. Mondola, S. Damiano et al., "HaRas activates the NADPH oxidase complex in human neuroblastoma cells via extracellular signal-regulated kinase 1/2 pathway," *Journal of Neurochemistry*, vol. 91, no. 3, pp. 613–622, 2004.

[55] A. M. Martelli, L. Cocco, S. Capitani, S. Miscia, S. Papa, and F. A. Manzoli, "Nuclear phosphatidylinositol 3,4,5-trisphosphate, phosphatidylinositol 3-kinase, Akt, and PTen: emerging key regulators of anti-apoptotic signaling and carcinogenesis," *European Journal of Histochemistry*, vol. 51, pp. 125–131, 2007.

[56] M. J. Zeitz, K. S. Malyavantham, B. Seifert, and R. Berezney, "Matrin 3: chromosomal distribution and protein interactions," *Journal of Cellular Biochemistry*, vol. 108, no. 1, pp. 125–133, 2009.

Hindawi Publishing Corporation
BioMed Research International
Volume 2014, Article ID 131737, 14 pages
http://dx.doi.org/10.1155/2014/131737

Review Article

Redox Signaling as a Therapeutic Target to Inhibit Myofibroblast Activation in Degenerative Fibrotic Disease

Natalie Sampson,[1] Peter Berger,[2] and Christoph Zenzmaier[3]

[1] *Division of Experimental Urology, Department of Urology, Innsbruck Medical University, Anichstrasse 35, A-6020 Innsbruck, Austria*
[2] *Institute for Biomedical Aging Research, University of Innsbruck, 6020 Innsbruck, Austria*
[3] *Department of Internal Medicine III, Innsbruck Medical University, Anichstrasse 35, A-6020 Innsbruck, Austria*

Correspondence should be addressed to Natalie Sampson; natalie.sampson@i-med.ac.at and
Christoph Zenzmaier; christoph.zenzmaier@i-med.ac.at

Received 5 October 2013; Accepted 6 January 2014; Published 20 February 2014

Academic Editor: David Vauzour

Degenerative fibrotic diseases encompass numerous systemic and organ-specific disorders. Despite their associated significant morbidity and mortality, there is currently no effective antifibrotic treatment. Fibrosis is characterized by the development and persistence of myofibroblasts, whose unregulated deposition of extracellular matrix components disrupts signaling cascades and normal tissue architecture leading to organ failure and death. The profibrotic cytokine transforming growth factor beta (TGFβ) is considered the foremost inducer of fibrosis, driving myofibroblast differentiation in diverse tissues. This review summarizes recent *in vitro* and *in vivo* data demonstrating that TGFβ-induced myofibroblast differentiation is driven by a prooxidant shift in redox homeostasis. Elevated NADPH oxidase 4 (NOX4)-derived hydrogen peroxide (H_2O_2) supported by concomitant decreases in nitric oxide (NO) signaling and reactive oxygen species scavengers are central factors in the molecular pathogenesis of fibrosis in numerous tissues and organs. Moreover, complex interplay between NOX4-derived H_2O_2 and NO signaling regulates myofibroblast differentiation. Restoring redox homeostasis via antioxidants or NOX4 inactivation as well as by enhancing NO signaling via activation of soluble guanylyl cyclases or inhibition of phosphodiesterases can inhibit and reverse myofibroblast differentiation. Thus, dysregulated redox signaling represents a potential therapeutic target for the treatment of wide variety of different degenerative fibrotic disorders.

1. Introduction: Fibrosis and Degenerative Fibrotic Diseases

The wound healing response in which damaged/dead cells are replaced following acute injury (such as infection, autoimmune reaction, or mechanical injury) is essential to maintain tissue architecture and function [1–4]. However, if the healing process continues unchecked, for example, due to repeated/chronic injury, fibrosis ensues as characterized by substantial deposition and remodeling of the extracellular matrix (ECM) and permanent scar tissue formation, which destroys correct tissue architecture and may ultimately lead to organ failure and death [1–4].

There are numerous degenerative fibrotic diseases, including multisystemic disorders such as systemic sclerosis, chronic graft versus host disease, and nephrogenic systemic fibrosis as well as organ-specific diseases, for example, cardiac fibrosis, idiopathic pulmonary fibrosis (IPF), intestinal fibrosis, liver cirrhosis, progressive kidney disease, macular degeneration, and benign prostatic hyperplasia (BPH) [1–3, 5–12]. In addition, a multitude of disorders with prominent tissue remodeling also have a significant fibrotic component, including asthma, atherosclerosis, and the reactive stromal response to solid tumors, such as breast, liver, and prostate cancer [13–16]. Thus, it is perhaps not surprising that approximately 45% of the mortality in Western nations is attributed to fibrotic diseases, a figure that is certainly even higher in less developed countries [12].

Despite the considerable morbidity and mortality caused by fibrosis, there are currently no effective treatments for

many of these diseases and no approved antifibrotic therapies. In part, this is due to our current lack of knowledge regarding (i) the precise etiology of the initiating injury/infection and (ii) the mechanisms that drive fibrosis progression. Thus, a better understanding of the molecular pathways underlying fibrosis and the initiating signals/causes is urgently required for the development of effective therapeutic strategies. This review focuses on accumulating evidence that redox signaling plays a fundamental and integral role in the molecular pathogenesis of fibrosis in many different tissues and organs and as such represents a potential therapeutic target for the treatment of wide variety of different fibrotic disorders.

2. The Myofibroblast: Biology, Origin, and Role in Fibrosis

Fibrotic diseases are clearly distinct in their etiology and clinical manifestation. Nonetheless, fibrogenesis in most organs and tissues progresses in a remarkably similar manner, characterized in particular by the development and persistence of large numbers of myofibroblasts [3, 7, 9, 12]. During the normal wound healing response, myofibroblasts accumulate to promote wound closure by virtue of their contractile and ECM- and growth factor-secreting properties, with the latter serving to attract epithelial cells, a process termed "reepithelialization". Normal tissue function and architecture are restored upon completion of reepithelialization via poorly understood mechanisms that result in massive apoptosis of myofibroblasts and vascular cells, which are subsequently cleared from the wound site [7, 17, 18]. Tissue and organ fibrosis are thought to arise from failure of myofibroblast apoptosis during wound healing [3, 19]. Again, however, the mechanisms underlying this apparent "apoptosis-resistant" myofibroblast phenotype remain ill-defined [20]. The resulting persistent myofibroblast activation leads to excessive ECM deposition, altered growth factor signaling and consequently cellular proliferation, progressive remodeling and destruction of normal tissue architecture, organ dysfunction, and failure [3, 19, 21]. Thus, the myofibroblast is widely considered the main effector cell of fibrosis and thereby a major therapeutic target.

Myofibroblasts are a specialized cell type that combines the ECM-producing characteristics of fibroblasts with the cytoskeletal and contractile properties of smooth muscle cells (SMCs) as reviewed recently [2]. Myofibroblasts are defined by (i) their *de novo* expression of alpha-smooth muscle cell actin (α-SMA, encoded by the gene *ACTA2*) in stress fibers and (ii) contractile force. The cellular origin of myofibroblasts remains somewhat controversial but may differ depending on the organ and/or the initiating stimulus (reviewed [2, 22]). Myofibroblasts have been described to originate from differentiation of vascular SMCs, bone marrow-derived fibrocytes, hepatic stellate cells, resident epithelial cells via epithelial-to-mesenchymal transition, and endothelial cells via endothelial-to-mesenchymal transition [3, 23]. However, although these cell types undergo differentiation into myofibroblasts *in vitro*, the extent of their contribution to the myofibroblast pool *in vivo* is the subject of considerable debate. Rather, it is widely accepted that myofibroblasts predominantly originate from the differentiation of local tissue fibroblasts [23].

Fibroblast-to-myofibroblast differentiation occurs via a two-step process. Following injury or during chronic inflammation, changes in mechanical tension of the ECM are transmitted to the fibroblast cytoskeleton via RhoA/ROCK signaling [24]. Consequently, fibroblasts adopt an "activated" phenotype (termed "protomyofibroblast") and deposit new ECM components [25]. Soluble factors and cytokines, in particular the splice variant ED-A of cellular fibronectin and profibrotic cytokine TGFβ, which are produced initially by platelets and infiltrating leukocytes at the wound site, are major inducers of fibroblast-to-myofibroblast differentiation [25]. However, protomyofibroblasts and myofibroblasts themselves also secrete and activate TGFβ thus generating an autocrine feed-forward loop driving continued myofibroblast differentiation [26, 27] (Figure 1). It may be noted, however, that, although inflammation frequently occurs prior to fibrosis, fibrogenesis can also occur independently of inflammatory mechanisms indicating that inflammation is not always the driving initiator [28].

Although several TGFβ-independent mechanisms of fibrosis have been described, such as interleukins 4 and 13 and platelet-derived growth factor (reviewed [34, 35]), TGFβ1 is widely considered the foremost inducer of fibrosis and drives myofibroblast differentiation in cells of diverse histological origin, including breast, skin, prostate, kidney, heart, lung, and liver [36–42]. Consistently, elevated TGFβ1 levels and signaling are observed in many fibrotic disorders [19, 43–50]. TGFβ1 exerts its effects via downstream activation of canonical Smad2/3 signaling or via noncanonical Smad-independent activation of mitogen-activated protein kinase (MAPK) and PI3 kinase/Akt pathways [2, 26, 51]. Collectively, signaling via these pathways leads to ECM deposition and secretion of paracrine- and autocrine-acting growth factors [26, 52]. Notably, the ECM can directly bind to and release growth factors; for example, heparan sulfate can bind to and release fibroblast growth factor 2 [53]. On the one hand, such interactions sequester growth factors thereby protecting them from degradation but can also enhance their bioactivity due to increased half-life [54]. Moreover, indirect interactions are required for signal transduction of some growth factors; for example, integrin binding is necessary for induction of angiogenesis by vascular endothelial cell growth factor [55]. Thus, remodeling and enhanced deposition of ECM in fibrosis contributes to disease pathogenesis not only by disrupting normal tissue architecture but also by modulating cellular signaling cascades (Figure 1).

TGFβ undoubtedly plays a pivotal role in pathogenic fibrogenesis. Therapeutic approaches designed to interfere with downstream TGFβ signaling processes that culminate in myofibroblast activation may represent an alternative viable strategy for the treatment of fibrotic disease. In this respect, a convincing body of data implicates dysregulated redox signaling by NADPH oxidase 4 (NOX4) and nitric oxide (NO) in the pathophysiology of fibrosis.

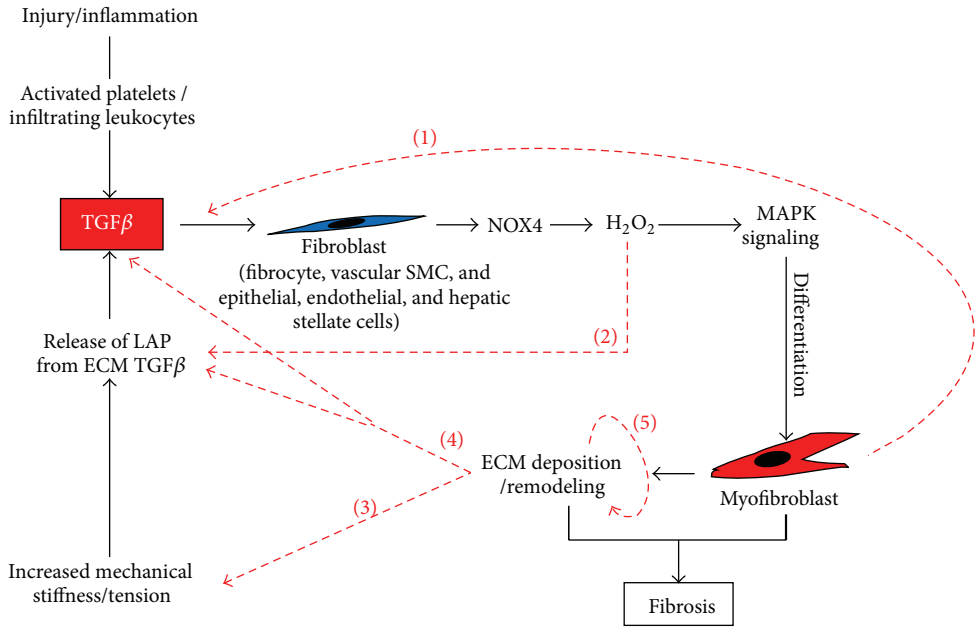

Figure 1: Feed-forward loop of TGFβ activation and myofibroblast differentiation in fibrosis. Upon injury activated platelets, infiltrating inflammatory and vascular cells secrete TGFβ, which acts on local fibroblasts and other precursor cells (e.g., hepatic stellate cells, fibrocytes) inducing their production of NOX4-derived H_2O_2. Consequently, downstream MAPK signaling cascades are activated resulting in differentiation into myofibroblasts, whose production of ECM components facilitates wound closure. Prolonged injury or inflammation leads to persistent myofibroblast activation via a feed-forward loop driven by several different factors. For example, myofibroblasts themselves secrete and produce large amounts of active TGFβ and thereby generate an autocrine feed-forward loop that is characteristic of persisting myofibroblast activity (1) [27]. Activation of latent TGFβ in ECM deposits via dissociation of latency associated peptide (LAP) is promoted by various mechanisms, including direct oxidative modification (2) [29–31]. Thus, NOX4-derived H_2O_2 may drive myofibroblast differentiation not only by oxidative modulation of MAPK signaling cascades that culminate in downstream transcriptional programs of differentiation [26], but also via its ability to freely diffuse across biological membranes and oxidatively modulate components in the extracellular space. Myofibroblasts also secrete high levels of ECM components. The resulting increase in mechanical tension and tissue stiffness can activate ECM-bound latent TGFβ due to mechanical pulling of LAP by specific integrins at the myofibroblast cell surface (3) [32]. Thereby, TGFβ is released and activated from the latent complex, which in turn drives further myofibroblast contraction and differentiation as well as ECM deposition [25]. In addition to this physical mechanism of TGFβ activation by the remodeled ECM, components of the remodeled ECM can modulate TGFβ signaling in a biochemical manner (4), for example, latent TGFβ binding proteins, fibrillins, fibulins, fibronectin, and proteoglycans (reviewed [33]). Moreover, a number of targets downstream of TGFβ signaling provide feedback modulation of the ECM either directly or indirectly, for example, thrombospondin-1 (TSP-1), collagens/ECM components themselves, and ECM remodeling components such as matrix metalloproteinases (5) (MMP2, -9), plasminogen activator inhibitor (PAI-1), and tissue inhibitors of metalloproteinases (TIMPs) [26]. Thus, the stiffened/remodeled ECM together with autocrine production of TGFβ and NOX4-derived H_2O_2 actively perpetuate TGFβ signaling and myofibroblast differentiation leading to fibrosis.

3. Signaling by NOX4-Derived Reactive Oxygen Species in the Regulation of Myofibroblast Differentiation

High levels of free radicals can result in nonspecific oxidative damage to cell structures and biomolecules. However, when produced in a regulated manner, reactive oxygen species (ROS), NO, and reactive nitrogen species play a critical role as biological second messengers in a variety of cellular processes, including myofibroblast differentiation [56]. NADPH oxidase (NOX) enzymes are unique in that ROS production is their primary and sole function [57]. This is in contrast to ROS-producing enzyme systems such as xanthine oxidase or uncoupled endothelial NO synthase, whose production of ROS occurs secondary to their primary function.

The seven members of the NOX family catalyze the transfer of electrons across biological membranes from NADPH to oxygen thereby generating superoxide ($O_2^{\bullet -}$) [58]. However, the major detected product and primary effector ROS of the constitutively active NOX4 is hydrogen peroxide (H_2O_2), although this most likely is a result of rapid superoxide dismutation [59–61]. It is thought that a highly conserved histidine residue within the E-loop of NOX4 promotes rapid dismutation of superoxide before it leaves the enzyme [61], although this aspect of NOX4 biology requires further clarification. Irrespectively, the greater stability but lower reactivity of H_2O_2 compared to superoxide is consistent with a signaling function of NOX4-derived ROS [26, 62, 63]. NOX-derived ROS exert their signaling functions by modulating biological activity of target proteins such as transcription

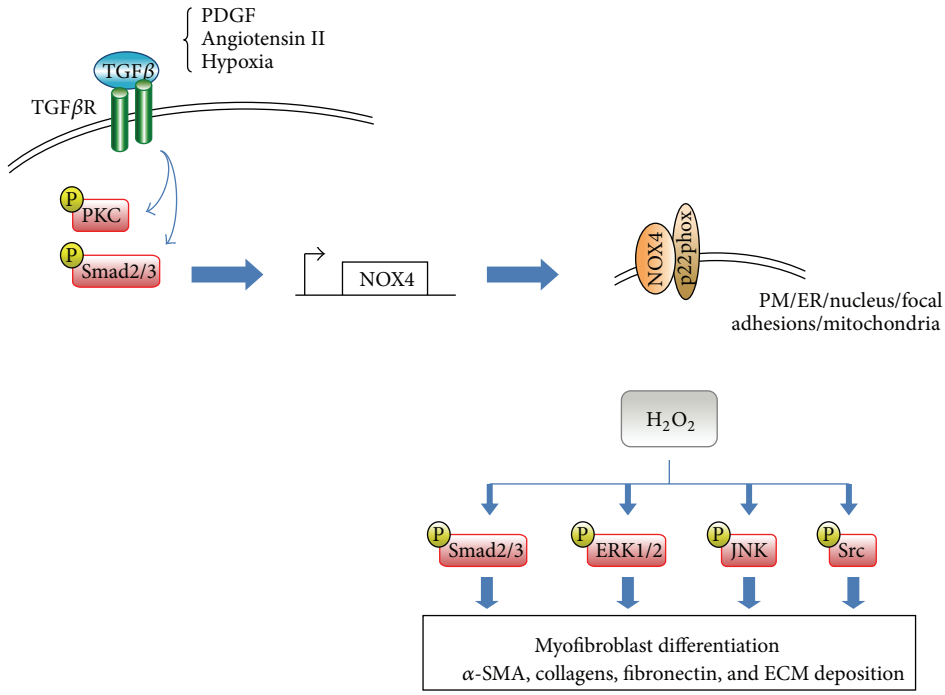

Figure 2: Signaling pathways that activate NOX4 and downstream targets of NOX4-derived ROS in myofibroblasts. NOX4 activity is predominantly regulated at the transcriptional level [59, 65]. TGFβ is one of the main inducers of *NOX4* during myofibroblast activation. Additionally, hypoxia, angiotensin II, and platelet-derived growth factor (PDGF) have also been shown to activate *NOX4* expression leading to myofibroblast activation; however, this most likely occurs as a result of their indirect activation of TGFβ signaling [75–77]. Upon binding of TGFβ ligand, heteromeric complexes of TGFβ receptor type I and type II recruit and activate the canonical signal transducers Smad2/3 as well as less well understood noncanonical signal transducers, such as mitogen-activated protein kinases (MAPKs) and protein kinase C (PKC). TGFβ signal transducers subsequently activate the transcription of target genes that include *NOX4*. TGFβ-mediated induction of NOX4 expression has largely shown to be Smad2/3-dependent [39, 40]; however, PKC has also been implicated in TGFβ-dependent upregulation of NOX4 [78]. The subcellular localization of NOX4 appears to be cell-, tissue-, and perhaps even context-specific with its reported localization to the plasma membrane (PM), endoplasmic reticulum (ER), nucleus, focal adhesions, and mitochondria [62]. NOX4 requires the cofactor $p22^{phox}$ for production of ROS, of which predominantly H_2O_2 is detected [59–61]. NOX4-derived H_2O_2 activates signaling intermediates such as Smad2/3, ERK1/2, JNK and Src [26, 39, 40, 77, 79–81], which subsequently induce the transcription of downstream target genes, such as α-smooth muscle cell actin (α-SMA), collagens, and fibronectin leading to ECM deposition and myofibroblast differentiation/activation.

factors, MAPKs, protein tyrosine phosphatases (PTPs), and protein tyrosine kinases via reversible oxidation of thiol groups of low pKa cysteine residues [63, 64].

Unlike other NOX isoforms, NOX4 is constitutively active with primary regulation occurring at the transcriptional level [59, 65]. NOX4 expression is activated in vascular SMCs and fibroblasts by several cytokines implicated in the pathogenesis of fibrosis, including TGFβ, angiotensin II, and platelet-derived growth factor [5] and elevated NOX4 levels are observed in tissues bearing hallmarks of fibrosis (Figure 2). For example, *NOX4* mRNA levels specifically correlated with the myofibroblast phenotype in benign prostatic tissue [26]. Similarly, NOX4 expression was higher in pulmonary fibroblasts from patients with IPF compared with controls and correlated with myofibroblast marker expression [66]. In addition, NOX4 was found to be expressed in fibroblastic foci in the lung of IPF patients and two mouse models of pulmonary fibrosis [67]. Recently, high levels of NOX4, which colocalized with α-SMA, were observed in liver biopsy samples from patients with autoimmune hepatitis [42]. These observations together with findings from functional studies indicate that elevated NOX4-derived ROS play a critical role in the pathophysiology of numerous fibrotic disorders (Figures 1–3) [26, 40, 67–71]. For example, we demonstrated that NOX4-derived ROS drive myofibroblast differentiation of prostatic fibroblasts in response to TGFβ1 [26]. Similar findings were observed for cardiac, pulmonary, renal, and adventitial fibroblasts and hepatic stellate cells [39, 40, 42, 66, 67, 72]. In vascular endothelial cells, NOX4 also mediates TGFβ1-induced cytoskeletal remodeling and maintains the differentiated phenotype of vascular SMCs [73, 74].

Several *in vivo* studies have provided more definitive evidence that NOX4-derived ROS play a direct role in the pathogenesis of fibrosis. For example, inhibition of NOX4 via genetic deletion, antisense oligonucleotides, siRNA, or NOX inhibitors attenuated disease progression in rodent models of pulmonary, renal, and liver fibrosis [42, 67, 82–84].

NOX4 induction appears to contribute to fibrogenesis not via oxidative stress-induced damage [26, 62, 63], but rather by chronic dysregulation of downstream signaling pathways (Figure 2). The precise oxidative target(s) of NOX4-derived ROS that culminate in myofibroblast differentiation

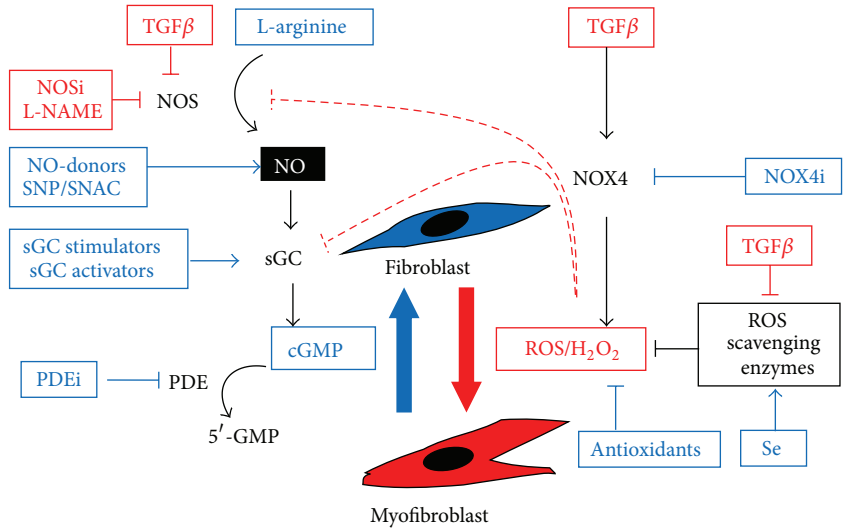

Figure 3: Potential therapeutic targeting of myofibroblast differentiation. Myofibroblast differentiation plays a central role in the etiology of fibrosis. TGFβ, which is widely considered the foremost inducer of fibrosis, induces NOX4 resulting in a persistent prooxidant shift in intracellular redox homeostasis mediated via ROS (in particular H_2O_2), which modulates downstream phosphorylation signaling cascades and transcriptional events culminating in fibroblast-to-myofibroblast differentiation. The concomitant downregulation of selenium (Se)-dependent ROS scavenging enzymes by TGFβ further potentiates NOX4-derived ROS signaling. In parallel, TGFβ and H_2O_2 attenuate NO signaling, which is associated with the fibroblast phenotype, via attenuation of NOS and sGC activities. Likewise, NOS inhibitors (NOSi/L-NAME) attenuate NO signaling and aggravate fibrosis. Fibroblast-to-myofibroblast differentiation and subsequent tissue fibrosis are reversible processes. Thus, targeting persistent NOX4-derived ROS levels in the diseased tissue by NOX4 inhibitors (NOX4i) or by ROS scavenging with Se or antioxidants results in inhibition of myofibroblast differentiation and, moreover, in dedifferentiation/inactivation of myofibroblasts to a quiescent fibroblast-like phenotype. Similarly, enhancement of NO signaling by administration of the NOS substrate L-arginine, NO-donors (SNP/SNAC), sGC stimulators/activators, or PDE inhibitors (PDEi) maintains the fibroblast phenotype or induces dedifferentiation/inactivation of preexisting myofibroblasts.

in response to TGFβ remain(s) largely unknown. However, TGFβ1-induced NOX4-derived ROS have been shown to directly oxidatively inactivate MKP1, a dual specificity MAPK phosphatase that targets JNK and p38 [79]. Consistently, JNK phosphorylation by NOX4-derived ROS was essential for TGFβ1-induced myofibroblast differentiation of prostatic fibroblasts and cardiomyocyte differentiation of pluripotent embryonal carcinoma cells [26, 80]. Other targets activated by NOX4-derived ROS in fibrogenic signaling cascades include ERK1/2 and Src [39, 81]. Thus, it appears that the NOX4-dependent fibrotic response can be mediated via multiple oxidative targets (Figure 2). Interestingly, activation and release of TGFβ from its latency association peptide (LAP) are also induced by oxidative modification of LAP with free radicals capable of stimulating TGFβ expression and secretion in many cell types [29, 85] (Figure 1).

Although NOX4 induction by TGFβ1 does not typically result in oxidative stress-induced damage in fibroblasts [26, 62, 63], primary alveolar epithelial cells exposed to TGFβ1 undergo apoptosis in a NOX4-dependent manner [86], an event that can also be indirectly mediated via paracrine release of H_2O_2 by activated myofibroblasts [87]. Thus, NOX4 may promote fibrosis not only by driving cytokine-induced fibroblast-to-myofibroblast differentiation but also by impairing epithelial regenerative capacity during wound healing.

In summary, whilst acute induction of NOX4 may be beneficial in inducing the myofibroblast phenotype during wound healing, the persistence of myofibroblasts together with autocrine TGFβ signaling may result in chronic NOX4 activation and ROS production resulting in a self-perpetuating cycle of myofibroblast differentiation and accumulation, fibrosis, and organ dysfunction (Figure 1). Thus, targeting elevated NOX4-derived ROS either directly via NOX4 inhibition or indirectly by increasing the activity of ROS scavenging enzymes represents a promising therapeutic strategy for the treatment of diverse fibrotic pathologies (Figure 3).

There are numerous ROS-scavenging systems that maintain cellular redox homeostasis; however, of particular interest are the selenium (Se)-dependent enzymes. We observed downregulation of the Se transporter SEPP1 and Se-containing ROS scavengers glutathione peroxidase 3 (GPX3) and thioredoxin reductase 1 (TXNRD1) during TGFβ1-mediated prostatic myofibroblast differentiation [26]. Moreover, SEPP1 was specifically lost in tumor-associated stroma of prostate cancer patients, indicating reduced activity of ROS scavenging enzymes in the diseases tissue [26]. Se is an essential trace element that is incorporated as selenocysteine into the active sites of GPX3 and TXNRD1 enzymes and required for proper protein folding/function [88]. Consistent with the role of SEPP1 in delivering Se to peripheral tissues for selenoprotein biosynthesis [89, 90], exogenous Se restored expression of GPX3 and TXNRD1 as well as TXNRD1 enzyme activity, depleted TGFβ1-induced ROS downstream of NOX4

induction, and inhibited myofibroblast differentiation of prostatic fibroblasts [26]. Similarly, exogenous Se also inhibited TGFβ-mediated myofibroblast transdifferentiation of hepatic stellate cells [91]. Furthermore, we observed that exogenous Se restores morphological and molecular characteristics typical of the fibroblast phenotype to *in vitro* differentiated prostatic myofibroblasts even in the continued presence of the TGFβ differentiation-inducing stimulus [4]. Similarly, studies employing myofibroblasts from IPF patients and a three-dimensional coculture model of porcine skin fibrosis also demonstrated the potential utility of ROS scavenging in promoting myofibroblast dedifferentiation [92, 93]. Consistently, pharmacological inhibition of NOX4 after induction of liver fibrosis in mice was shown to reduce ROS levels and significantly attenuate fibrosis [42].

Collectively, a large body of *in vitro* and *in vivo* data indicates that myofibroblast differentiation in fibrotic disorders and tumor-reactive stroma is driven by a prooxidant shift in intracellular redox signaling caused by elevated ROS and/or reduced antioxidative potential. NOX4 appears to be the major source of elevated ROS and central mediator of TGFβ-induced myofibroblast differentiation in diverse tissues. Thus, restoring cellular redox homeostasis by (i) targeting NOX4, (ii) Se supplementation, and/or (iii) application of antioxidants may represent a promising therapeutic strategy for fibrotic disease (Figure 3). Moreover, rather than simply inhibiting myofibroblast differentiation to prevent disease progression, clearing the myofibroblast pool in fibrotic disorders by inducing their dedifferentiation to the nonactivated fibroblast/progenitor phenotype may be a feasible therapeutic strategy that potentially represents a curative treatment.

4. Nitric Oxide Signaling in the Regulation of Myofibroblast Differentiation

The free radical NO is an important signaling molecule in a variety of biological processes that is biosynthesized *in vivo* from L-arginine by nitric oxide synthases (NOS), involving the oxidation of NADPH and the reduction of molecular oxygen. NO signaling is mediated via activation of soluble guanylyl cyclase (sGC). The second messenger cyclic guanosine monophosphate (cGMP) that is subsequently generated by sGC regulates the activity of cGMP-dependent protein kinases such as protein kinase G (PKG), cyclic nucleotide phosphodiesterases (PDEs), and cation channels and may have other unknown effects [94].

In terms of fibroblast-to-myofibroblast differentiation, NO signaling appears to be a central pathway associated with the fibroblast phenotype (Figure 3). Treatment of dermal fibroblasts with TGFβ1 significantly reduced NOS activity and NO levels, whereas the NOS inhibitor N_ω-nitro-L-arginine methyl ester (L-NAME) synergistically potentiated TGFβ1-induced collagen production [95]. Consistently, NOS inhibition or knockout attenuated fibrosis in several animal models [96–99]. We previously demonstrated that the soluble NO donor sodium nitroprusside (SNP) dose-dependently inhibited TGFβ1-induced myofibroblast differentiation of human prostatic fibroblasts *in vitro* [100]. These findings are in line with suppression of TGFβ1-induced collagen production by SNP in dermal fibroblasts *in vitro* and attenuation of fibrosis in rodent model systems using the NOS substate L-arginine or the NO donor *S*-Nitroso-*N*-acetylcysteine (SNAC), respectively [95, 98, 101]. Moreover, parallel NO donation and cyclooxygenase inhibition prevented bleomycin-induced lung fibrosis in mice [102].

Since NO activates sGC, increasing sGC activity via NO-independent heme-dependent sGC stimulators represents an alternative approach to enhance NO signaling (Figure 3). Similarly to observations with NO donors, the sGC stimulator BAY 41-2272 inhibited *in vitro* myofibroblast differentiation of cardiac fibroblasts and dermal fibroblasts from healthy subjects and patients with systemic sclerosis [103, 104]. *In vivo* BAY 41-2272 limited disease progression in models of renal, cardiac, and dermal fibrosis [103–106] and similar inhibitory effects were documented for the sGC stimulator riociguat (BAY 63-2521) in rat models [107, 108]. In contrast to sGC stimulators that require the presence of a reduced heme moiety in the prosthetic group of the enzyme, sGC activators can bind to and activate oxidized or heme-deficient sGC [109]. Under conditions of oxidative stress, the heme moiety can be oxidized and lost, rendering sGC no longer responsive to NO. Thus, these heme-independent activators may be beneficial in the treatment of a variety of diseases associated with oxidative stress [109]. Of note, the sGC activator BAY 60-2770 inhibited myofibroblast differentiation in prostatic and dermal fibroblasts (our unpublished observations) and attenuated liver fibrosis in rat models [110], whilst the sGC activator cinaciguat (BAY 58-2667) prevented disease progression in a rat model of chronic renal failure [111].

The fact that treatment with the cell-permeable cGMP analog 8-bromo-cGMP is able to mimic the inhibitory effects of enhanced NO/sGC signaling on myofibroblast differentiation clearly indicates that inhibition is mediated downstream via cGMP [95, 112]. Thus, inhibitors of certain phosphodiesterase isoforms (PDE) represent an additional approach to enhance NO/cGMP signaling. PDEs comprise a superfamily of phosphohydrolases that degrade cellular cGMP and cAMP. PDE type 5 (PDE5), which specifically hydrolyzes cGMP, is the major therapeutic target in erectile dysfunction, and is additionally approved for the treatment of pulmonary arterial hypertension and BPH [113–115]. Increased PDE5 expression was observed in anti-Thy1-induced mesangial proliferative glomerulonephritis in rats and PDE5 inhibition showed beneficial antiproliferative and antifibrotic effects *in vivo*, indicating an active role of PDE5 in fibrogenesis [116]. We previously demonstrated that pharmacological inhibition or shRNA-mediated silencing of PDE5 significantly attenuated TGFβ1-induced myofibroblast differentiation of prostatic fibroblasts *in vitro* [100]. Likewise, PDE5 inhibition prevented myofibroblast differentiation in fibroblasts form Peyronie's disease plaques *in vitro* and counteracted fibrosis in TGFβ1-induced Peyronie's disease-like plaques in rats [117, 118]. Moreover, in lung fibroblasts PDE5 inhibition in combination with the sGC activator cinaciguat attenuated myofibroblast differentiation [41].

Similarly to exogenous Se, we recently reported that PDE5 inhibition in *in vitro* differentiated prostatic myofibroblasts restored morphological and molecular characteristics typical

of the fibroblast phenotype, indicating that enhancement of NO signaling not only prevents but also might reverse fibrosis [119]. Consistently, the NO donor SNAC induced dedifferentiation of activated hepatic stellate cells *in vitro* [120] and *in vivo* sGC stimulation by BAY 41-8543 decreased tubulointerstitial fibrosis after relief of unilateral ureteral obstruction in rats [121]. Similarly, BAY 41-2272 reduced established fibrosis in modified mouse models of dermal fibrosis [34] and PDE5 inhibition reduced myofibroblast numbers and total size of preformed TGFβ1-induced Peyronie's disease-like plaques in rats [117]. Of note, various PDE5 inhibitors selectively increased the apoptotic index in TGFβ1-induced Peyronie's disease-like plaques in rats [117, 118], indicating clearance of myofibroblasts by apoptosis upon enhancement of NO signaling.

Collectively, findings from *in vitro* and *in vivo* model systems indicate that the fibroblast phenotype is maintained by NO signaling and that myofibroblast differentiation is associated with an attenuation/inhibition of the NO/sGC/cGMP signaling cascade, while stimulation of NO signaling is capable of even reverting myofibroblast differentiation. Thus, enhancement of NO signaling by NO donors, stimulators, and activators of sGC or inhibition of cGMP degradation via PDE inhibitors might be of therapeutic benefit for patients suffering from degenerative fibrotic disease (Figure 3).

5. Crosstalk between NOX4/H_2O_2 and NO Signaling Networks in the Regulation of Myofibroblast Differentiation

The fact that elevated NO signaling attenuates and reverses myofibroblast differentiation while NOX4-derived ROS play a key role in driving differentiation in response to TGFβ indicates that the fibroblast/myofibroblast phenotype is regulated via crosstalk between both signaling pathways. The main ROS effector of NOX4 is H_2O_2 [59–61]; however, by virtue of its catalytic structure [122] its primary product like other NOX isoforms is superoxide (see chapter 3) [59–61]. Even assuming that NOX4-derived superoxide undergoes rapid dismutation, residual superoxide could potentially cross-react with NO signaling; for example, superoxide can react with NO generating peroxynitrite ($ONOO^-$), thereby depleting NO levels [123]. In addition, superoxide can oxidize the critical nitric oxide synthase (NOS) cofactor tetrahydrobiopterin (BH_4) leading to NOS uncoupling and superoxide generation rather than NO production [124]. Indeed, in some models, NOX4 has been implicated in the generation of peroxynitrite and subsequent NOS uncoupling [125–128]. However, since NOX4 is primarily associated with constitutive H_2O_2 production [60, 61], which unlike superoxide does not appear to react directly with NO, any opposing regulation of TGFβ-induced myofibroblast differentiation by NO and NOX4-derived ROS signaling presumably predominantly occurs via distinct mechanisms (summarized Figure 3).

There are several mechanisms by which NOX4-derived H_2O_2 may affect NO signaling. H_2O_2 impaired NO production in porcine aortic endothelial cells possibly via direct oxidative inactivation of eNOS cofactors [129]. Moreover, H_2O_2 decreased sGC expression and consequently NO-dependent cGMP generation in pulmonary arterial SMCs from lambs with persistent pulmonary hypertension of the newborn and in rat aortic SMCs or freshly isolated vessels [130, 131]. H_2O_2 or PTP inhibitors promoted tyrosine phosphorylation of the beta 1 subunit of sGC, presumably via Src-like kinases. Since c-Src-dependent phosphorylation of sGC has been shown to attenuate sGC activity and cGMP formation [132, 133], these data suggest that elevated NOX4-derived H_2O_2 during myofibroblast differentiation may inactivate PTPs and/or activate Src kinase, leading to sGC phosphorylation and consequently reduced cGMP formation.

Additionally, NOX4-derived H_2O_2 and NO signaling may interact via common cofactors. Both NOS and NOX require NADPH as an electron donor for enzyme activity. Since NOX4 induction is an early event during TGFβ1-mediated differentiation [26, 40], NADPH consumption/depletion due to elevated NOX4 activity may attenuate NOS activity and consequently NO signaling. Furthermore, opposing interaction may occur via mutually exclusive modification of NOX/NO target proteins. For example, NO activates sarco/endoplasmic reticulum Ca2+ ATPase (SERCA) via *S*-glutathiolation on cysteine 674, while induction of NOX4 via TGFβ1, exposure to H_2O_2, or high glucose resulted in SERCA oxidation of the same thiol group that inhibited NO-mediated *S*-glutathiolation [134–136].

Taken together these findings clearly indicates that H_2O_2 and NO appear to interact in a functionally opposing manner during myofibroblast differentiation via multiple mechanisms, whereby TGFβ1-mediated induction of NOX4-derived H_2O_2 leads to downregulation of NO signaling and thereby promotes fibroblast-to-myofibroblast differentiation. Consistently, TGFβ1 significantly decreased NO production in dermal fibroblasts [95]. Thus, stimulating sGC generation and/or inhibiting cGMP degradation potentially counteract ROS-mediated inactivation of NO signaling to consequently prevent and reverse myofibroblast differentiation. Of note, enhancing cGMP levels inhibited and reversed differentiation without impairing NOX4 mRNA induction by TGFβ1 (our unpublished observations) [119], indicating that NO signaling acts downstream of NOX4-derived H_2O_2 production. Since treatment with 8-bromo-cGMP is sufficient to inhibit myofibroblast differentiation [95], the H_2O_2-counteracting effects of elevated NO signaling appear to be mediated via downstream cGMP-dependent mechanisms and not via the NO radical *per se*.

6. Clinical Implications

In order to develop broadly effective antifibrotic therapies, it will be necessary to identify common features of different fibrotic disorders that affect distinct tissues and/or are initiated by different stimuli (e.g., chronic scarring of the liver due to hepatitis versus the tumor-associated reactive stromal response to prostate cancer). However, in some cases it may be necessary/advantageous to identify tissue-specific signaling mechanisms/inducers whose specific targeting is less likely to be associated with adverse side effects on healthy tissues. The observation that fibroblasts and myofibroblasts

are interconvertible phenotypes, with phenotypic switching apparently regulated via crosstalk between NOX4/H_2O_2 and NO signaling, has significant clinical implications. Targeting redox signaling, for example, via inhibitors of NOX4 or PDE5, antioxidants such as Se or enhancers of NO signaling, represents a promising therapeutic strategy to modulate the fibroblast/myofibroblast ratio in pathological conditions such as degenerative fibrotic diseases (Figure 3).

TGFβ unequivocally plays a central role in fibrogenesis in diverse tissues and organs. However, given its essential role in a wide range of fundamental cellular functions, there are concerns that systemic approaches directly targeting TGFβ for the treatment of fibrotic conditions will potentially exert undesirable toxic effects [51, 137]. Indeed, this was the case in the CAT-192 clinical trial [138]. Nonetheless, several clinical trials on fibrosis employing anti-TGFβ agents have been completed and several others are underway. Unfortunately, to date, these trials have largely yielded disappointing results despite promising *in vitro* observations (reviewed recently [139, 140]).

Induction of NOX4-derived H_2O_2 and reduced NO signaling are apparently central downstream components of TGFβ-mediated myofibroblast differentiation in diverse tissues and organs. Thus, therapeutic targeting of redox homeostasis in degenerative fibrotic diseases might also be expected to elicit broad and undesirable effects. However, it should be noted that, unlike TGFβ that drives myofibroblast differentiation and fibrosis via Smad-dependent and -independent pathways [51, 141], NOX4 does not modulate noncanonical signaling by TGFβ1 in prostatic fibroblasts [26, 40, 65]. Moreover, Nox4 knockout animals display no obvious basal phenotype and a dual NOX1/NOX4 inhibitor was well tolerated in animal models and in phase I clinical trials [42, 57]. Furthermore, PDE(5) inhibitors are clinically employed for a variety of conditions and have a history of safe use with minimal side effects in humans [113–115].

Despite intense research efforts, there currently remains no NOX4-specific inhibitor and several attempts to generate peptides that disrupt NOX4 function have been unsuccessful with the authors concluding that, unlike other NOX isoforms, NOX4 exists in a tightly assembled and active conformation, which cannot be disrupted by conventional means [142, 143]. Nonetheless, several studies have successfully employed a dual NOX1/NOX4 inhibitor GKT137831, which showed promising results in mouse models of liver fibrosis and hypoxia-induced pulmonary hypertension [42, 57, 84, 144] and is currently entering a phase II clinical trial for diabetic nephropathy. Recently, attenuation of NOX4-dependent ROS signaling and fibrosis by sodium hydrosulfide and nifedipine (an L-type dihydropyridine calcium channel blocker) was reported in rodent models of cardiac fibrosis [145, 146]. However, it remains to be determined whether these compounds inhibit NOX4 in a specific and isoform-selective manner or exert their effects via nonspecific and nonselective mechanisms.

Given that the signaling potential of NOX4-derived ROS is regulated by antioxidant systems, enhancing the activity of ROS scavenging enzymes may represent an alternative potential therapeutic strategy (Figure 3). Animal and human clinical data clearly demonstrate that Se deficiency or supplementation increases or reduces tumor incidence, respectively [147–152]. In addition, however, serum Se levels have been reported to be lower in patients with several different fibrotic disorders, including systemic sclerosis, primary Raynaud's phenomenon, and oral submucous fibrosis [153, 154]. Unfortunately, there are few studies investigating the potential therapeutic benefit of Se supplementation in degenerative fibrotic disease. Although proof-of-principle is provided by reports that exogenous Se was shown to decrease hepatic fibrosis in mice [155], Se deficiency promoted thyroid fibrosis in a TGFβ-dependent manner in rats [156]. However, there may be a potential increased risk of diabetes with Se supplementation [157]; thus further studies are required to better understand the biological effects of Se to allow its use in the prevention and treatment of degenerative fibrotic disease.

Inhibitors of PDE5 are clinically approved for the treatment of erectile dysfunction, pulmonary arterial hypertension, and BPH [113–115] and apparently have significant efficacy in Raynaud's phenomenon secondary to systemic sclerosis [158, 159]. The sGC stimulator riociguat significantly improved primary and secondary endpoints in recently presented phase III clinical trials in patients with pulmonary arterial hypertension and chronic thromboembolic pulmonary hypertension [160, 161]. Although the clinical development of the heme-independent sGC activators cinaciguat and ataciguat stopped in clinical phase II trials, the perspective to specifically activate oxidated, heme-free sGC generated by the influence of oxidative stress, seems very promising of offering novel therapies for various disorders associated with oxidative stress and several second-generation sGC activators have been developed recently [162, 163].

Due to the presence of multiple NOX, PDE, and GC isoforms, modulation of NOX4, PDE5, and/or sGC activities may permit continued physiological H_2O_2 and NO signaling. In addition, the fact that these enzymes belong to multimembered families may be clinically exploited to selectively target tissue or disease-specific isoforms. For example, selective targeting of PDE1A, that appears to play a critical role in cardiac fibrosis, led to regression of cardiac remodeling in rodents [164].

7. Conclusions

Fibrogenesis is widely considered the result of a dysregulated wound healing response. In particular, failure of the wave of myofibroblast apoptosis during wound healing combined with an autocrine feed-forward loop of TGFβ production leads to the development and persistence of large numbers of myofibroblasts, a hallmark of fibrotic disorders (Figure 1). TGFβ plays a key role in initiating myofibroblast differentiation from diverse precursors, most importantly fibroblasts, in a variety of organs and tissues. A large body of *in vitro* and *in vivo* data indicates that TGFβ-induced myofibroblast differentiation is driven via induction of NOX4-derived ROS (Figure 2) and supported by the concomitant downregulation of Se-dependent ROS scavenging enzymes. The resulting prooxidant shift in redox homeostasis modulates

redox-sensitive signaling cascades leading to myofibroblast differentiation (Figure 2). Interestingly, myofibroblast differentiation appears to be subject to opposing regulation via complex interplay between NOX4-derived H_2O_2 and NO signaling. Whilst TGFβ and NOX4-derived H_2O_2 attenuate NO signaling by impairing NOS and sGC activities and thus relieve inhibition of myofibroblast differentiation by NO, enhancement of NO signaling prevents TGFβ-induced myofibroblast differentiation (Figure 3). Moreover, targeting NOX4 or enhancing NO signaling induces the dedifferentiation/reversal of preexisting myofibroblasts to a quiescent fibroblast phenotype and ameliorates fibrosis *in vivo* indicating that fibroblasts and myofibroblasts are interconvertible phenotypes. Thus, pharmacological interference of these redox signaling processes to restore the physiological fibroblast:myofibroblast ratio offers a promising strategy for the treatment of fibrosis and degenerative fibrotic diseases. Therapeutic intervention could be potentially achieved at multiple levels, for example, by (i) targeting NOX4 directly using specific inhibitors, (ii) indirectly inhibiting NOX4 using antioxidants or Se to scavenge ROS/H_2O_2, (iii) enhancing NO signaling via NO-donors, stimulators/activators of sGC, and/or (iv) preventing cGMP degradation using PDE inhibitors. It is hoped that the recent findings summarized herein can be applied and translated into effective therapeutic strategies for the treatment of debilitating fibrotic disorders.

Abbreviations

α-SMA:	Alpha smooth muscle cell actin
BPH:	Benign prostatic hyperplasia
cAMP:	Cyclic adenosine monophosphate
cGMP:	Cyclic guanosine monophosphate
ECM:	Extracellular matrix
IPF:	Idiopathic pulmonary fibrosis
LAP:	Latency associated peptide
L-NAME:	N_ω-Nitro-L-arginine methyl ester
MAPK:	Mitogen-associated protein kinase
NO:	Nitric oxide
NOS:	Nitric oxide synthase
NOX:	NADPH oxidase
PDE:	Phosphodiesterase
PKG:	Protein kinase G
PTP:	Protein tyrosine phosphatase
ROS:	Reactive oxygen species
Se:	Selenium
sGC:	Soluble guanylyl cyclase
SMC:	Smooth muscle cell
SNAC:	*S*-Nitroso-*N*-acetylcysteine
SNP:	Sodium nitroprusside
TGFβ:	Transforming growth factor beta.

Conflict of Interests

The authors declare that there is no conflict of interests regarding the publication of this paper.

Acknowledgments

N. Sampson is supported by an Elise Richter PostDoctoral Fellowship from the Austrian Science Fund (FWF; V216-B13). P. Berger is supported by the Austrian Science Fund (FWF; NRN S9307-B05).

References

[1] G. Gabbiani, "The myofibroblast in wound healing and fibrocontractive diseases," *Journal of Pathology*, vol. 200, no. 4, pp. 500–503, 2003.

[2] B. Hinz, S. H. Phan, V. J. Thannickal et al., "Recent developments in myofibroblast biology: paradigms for connective tissue remodeling," *The American Journal of Pathology*, vol. 180, no. 4, pp. 1340–1355, 2012.

[3] K. Kis, X. Liu, and J. S. Hagood, "Myofibroblast differentiation and survival in fibrotic disease," *Expert Reviews in Molecular Medicine*, vol. 13, article e27, 2011.

[4] N. Sampson, P. Berger, and C. Zenzmaier, "Therapeutic Targeting of Redox Signaling in Myofibroblast Differentiation and Age-Related Fibrotic Disease," *Oxidative Medicine and Cellular Longevity*, vol. 2012, Article ID 458276, 15 pages, 2012.

[5] J. L. Barnes and Y. Gorin, "Myofibroblast differentiation during fibrosis: role of NAD(P)H oxidases," *Kidney International*, vol. 79, no. 9, pp. 944–956, 2011.

[6] S. Bhattacharyya, J. Wei, W. G. Tourtellotte et al., "Fibrosis in systemic sclerosis: common and unique pathobiology," *Fibrogenesis Tissue Repair*, vol. 5, supplement 1, article S18, 2012.

[7] B. Hinz, S. H. Phan, V. J. Thannickal, A. Galli, M.-L. Bochaton-Piallat, and G. Gabbiani, "The myofibroblast: one function, multiple origins," *The American Journal of Pathology*, vol. 170, no. 6, pp. 1807–1816, 2007.

[8] P. Kong, P. Christia, and N. G. Frangogiannis, "The pathogenesis of cardiac fibrosis," *Cellular and Molecular Life Sciences*, vol. 71, no. 4, pp. 549–574, 2014.

[9] J. Rosenbloom, S. V. Castro, and S. A. Jimenez, "Narrative review: fibrotic diseases: cellular and molecular mechanisms and novel therapies," *Annals of Internal Medicine*, vol. 152, no. 3, pp. 159–166, 2010.

[10] S. Speca, I. Giusti, F. Rieder et al., "Cellular and molecular mechanisms of intestinal fibrosis," *World Journal of Gastroenterology*, vol. 18, no. 28, pp. 3635–3661, 2012.

[11] V. J. Thannickal, "Mechanisms of pulmonary fibrosis: role of activated myofibroblasts and NADPH oxidase," *Fibrogenesis Tissue Repair*, vol. 5, supplement 1, article S23, 2012.

[12] T. A. Wynn, "Cellular and molecular mechanisms of fibrosis," *Journal of Pathology*, vol. 214, no. 2, pp. 199–210, 2008.

[13] N. Hirota and J. G. Martin, "Mechanisms of airway remodeling," *Chest*, vol. 144, no. 3, pp. 1026–1032, 2013.

[14] T. H. Lan, X. Q. Huang, and H. M. Tan, "Vascular fibrosis in atherosclerosis," *Cardiovascular Pathology*, vol. 22, no. 5, pp. 401–407, 2013.

[15] T. Marsh, K. Pietras, and S. S. McAllister, "Fibroblasts as architects of cancer pathogenesis," *Biochimica et Biophysica Acta*, vol. 1832, no. 7, pp. 1070–1078, 2012.

[16] M. Otranto, V. Sarrazy, F. Bonte et al., "The role of the myofibroblast in tumor stroma remodeling," *Cell Adhesion & Migration*, vol. 6, no. 3, pp. 203–219, 2012.

[17] A. Desmouliere, M. Redard, I. Darby, and G. Gabbiani, "Apoptosis mediates the decrease in cellularity during the transition

between granulation tissue and scar," *The American Journal of Pathology*, vol. 146, no. 1, pp. 56–66, 1995.

[18] A. Desmoulière, C. Chaponnier, and G. Gabbiani, "Tissue repair, contraction, and the myofibroblast," *Wound Repair and Regeneration*, vol. 13, no. 1, pp. 7–12, 2005.

[19] S. Chabaud, M.-P. Corriveau, T. Grodzicky et al., "Decreased secretion of MMP by non-lesional late-stage scleroderma fibroblasts after selection via activation of the apoptotic fas-pathway," *Journal of Cellular Physiology*, vol. 226, no. 7, pp. 1907–1914, 2011.

[20] V. J. Thannickal and J. C. Horowitz, "Evolving concepts of apoptosis in idiopathic pulmonary fibrosis," *Proceedings of the American Thoracic Society*, vol. 3, no. 4, pp. 350–356, 2006.

[21] C. Shimbori, J. Gauldie, and M. Kolb, "Extracellular matrix microenvironment contributes actively to pulmonary fibrosis," *Current Opinion in Pulmonary Medicine*, vol. 19, no. 5, pp. 446–452, 2013.

[22] R. Kramann, D. P. DiRocco, and B. D. Humphreys, "Understanding the origin, activation and regulation of matrix-producing myofibroblasts for treatment of fibrotic disease," *The Journal of Pathology*, vol. 231, no. 3, pp. 273–289, 2013.

[23] S. Ueha, F. H. Shand, and K. Matsushima, "Cellular and molecular mechanisms of chronic inflammation-associated organ fibrosis," *Frontiers in Immunology*, vol. 3, article 71, 2012.

[24] M. Amano, M. Nakayama, and K. Kaibuchi, "Rho-kinase/ROCK: a key regulator of the cytoskeleton and cell polarity," *Cytoskeleton*, vol. 67, no. 9, pp. 545–554, 2010.

[25] J. J. Tomasek, G. Gabbiani, B. Hinz, C. Chaponnier, and R. A. Brown, "Myofibroblasts and mechano: regulation of connective tissue remodelling," *Nature Reviews Molecular Cell Biology*, vol. 3, no. 5, pp. 349–363, 2002.

[26] N. Sampson, R. Koziel, C. Zenzmaier et al., "ROS signaling by NOX4 drives fibroblast-to-myofibroblast differentiation in the diseased prostatic stroma," *Molecular Endocrinology*, vol. 25, no. 3, pp. 503–515, 2011.

[27] Y. Kojima, A. Acar, E. N. Eaton et al., "Autocrine TGF-β and stromal cell-derived factor-1 (SDF-1) signaling drives the evolution of tumor-promoting mammary stromal myofibroblasts," *Proceedings of the National Academy of Sciences of the United States of America*, vol. 107, no. 46, pp. 20009–20014, 2010.

[28] T. A. Wynn, "Fibrotic disease and the TH1/TH2 paradigm," *Nature Reviews Immunology*, vol. 4, no. 8, pp. 583–594, 2004.

[29] M. F. Jobling, J. D. Mott, M. T. Finnegan et al., "Isoform-specific activation of latent transforming growth factor β (LTGF-β) by reactive oxygen species," *Radiation Research*, vol. 166, no. 6, pp. 839–848, 2006.

[30] D. A. Pociask, P. J. Sime, and A. R. Brody, "Asbestos-derived reactive oxygen species activate TGF-β1," *Laboratory Investigation*, vol. 84, no. 8, pp. 1013–1023, 2004.

[31] M. H. Barcellos-Hoff and T. A. Dix, "Redox-mediated activation of latent transforming growth factor-β1," *Molecular Endocrinology*, vol. 10, no. 9, pp. 1077–1083, 1996.

[32] F. Grinnell and W. M. Petroll, "Cell motility and mechanics in three-dimensional collagen matrices," *Annual Review of Cell and Developmental Biology*, vol. 26, pp. 335–361, 2010.

[33] M. Horiguchi, M. Ota, and D. B. Rifkin, "Matrix control of transforming growth factor-beta function," *Journal of Biochemistry*, vol. 152, no. 4, pp. 321–329, 2012.

[34] C. Beyer and J. H. Distler, "Tyrosine kinase signaling in fibrotic disorders: translation of basic research to human disease," *Biochimica et Biophysica Acta*, vol. 1832, no. 7, pp. 897–904, 2013.

[35] L. A. Borthwick, T. A. Wynn, and A. J. Fisher, "Cytokine mediated tissue fibrosis," *Biochimica et Biophysica Acta*, vol. 1832, no. 7, pp. 1049–1060, 2013.

[36] L. Ronnov-Jessen and O. W. Petersen, "Induction of α-smooth muscle actin by transforming growth factor-β1 in quiescent human breast gland fibroblasts," *Laboratory Investigation*, vol. 68, no. 6, pp. 696–707, 1993.

[37] A. Desmouliere, A. Geinoz, F. Gabbiani, and G. Gabbiani, "Transforming growth factor-β1 induces α-smooth muscle actin expression in granulation tissue myofibroblasts and in quiescent and growing cultured fibroblasts," *Journal of Cell Biology*, vol. 122, no. 1, pp. 103–111, 1993.

[38] D. M. Peehl and R. G. Sellers, "Induction of smooth muscle cell phenotype in cultured human prostatic stromal cells," *Experimental Cell Research*, vol. 232, no. 2, pp. 208–215, 1997.

[39] C. D. Bondi, N. Manickam, D. Y. Lee et al., "NAD(P)H oxidase mediates TGF-β1-induced activation of kidney myofibroblasts," *Journal of the American Society of Nephrology*, vol. 21, no. 1, pp. 93–102, 2010.

[40] I. Cucoranu, R. Clempus, A. Dikalova et al., "NAD(P)H oxidase 4 mediates transforming growth factor-β1-induced differentiation of cardiac fibroblasts into myofibroblasts," *Circulation Research*, vol. 97, no. 9, pp. 900–907, 2005.

[41] T. R. Dunkern, D. Feurstein, G. A. Rossi, F. Sabatini, and A. Hatzelmann, "Inhibition of TGF-β induced lung fibroblast to myofibroblast conversion by phosphodiesterase inhibiting drugs and activators of soluble guanylyl cyclase," *European Journal of Pharmacology*, vol. 572, no. 1, pp. 12–22, 2007.

[42] J. X. Jiang, X. Chen, N. Serizawa et al., "Liver fibrosis and hepatocyte apoptosis are attenuated by GKT137831, a novel NOX4/NOX1 inhibitor in vivo," *Free Radical Biology and Medicine*, vol. 53, no. 2, pp. 289–296, 2012.

[43] J. T. Cronkhite, C. Xing, G. Raghu et al., "Telomere shortening in familial and sporadic pulmonary fibrosis," *American Journal of Respiratory and Critical Care Medicine*, vol. 178, no. 7, pp. 729–737, 2008.

[44] A. L. Degryse, X. C. Xu, J. L. Newman et al., "Telomerase deficiency does not alter bleomycin-induced fibrosis in mice," *Experimental Lung Research*, vol. 38, no. 3, pp. 124–134, 2012.

[45] C. K. Garcia, "Idiopathic pulmonary fibrosis: update on genetic discoveries," *Proceedings of the American Thoracic Society*, vol. 8, no. 2, pp. 158–162, 2011.

[46] J. C. Horowitz, D. S. Rogers, V. Sharma et al., "Combinatorial activation of FAK and AKT by transforming growth factor-β1 confers an anoikis-resistant phenotype to myofibroblasts," *Cellular Signalling*, vol. 19, no. 4, pp. 761–771, 2007.

[47] B. Hu, D. C. Tack, T. Liu, Z. Wu, M. R. Ullenbruch, and S. H. Phan, "Role of Smad3 in the regulation of rat telomerase reverse transcriptase by TGFβ," *Oncogene*, vol. 25, no. 7, pp. 1030–1041, 2006.

[48] H. Ikushima and K. Miyazono, "TGFB 2 signalling: a complex web in cancer progression," *Nature Reviews Cancer*, vol. 10, no. 6, pp. 415–424, 2010.

[49] P. Kulasekaran, C. A. Scavone, D. S. Rogers, D. A. Arenberg, V. J. Thannickal, and J. C. Horowitz, "Endothelin-1 and transforming growth factor-β1 independently induce fibroblast resistance to apoptosis via AKT activation," *American Journal of Respiratory Cell and Molecular Biology*, vol. 41, no. 4, pp. 484–493, 2009.

[50] H. Li, D. Xu, J. Li, M. C. Berndt, and J.-P. Liu, "Transforming growth factor β suppresses human telomerase reverse transcriptase (hTERT) by Smad3 interactions with c-Myc and

the hTERT gene," *Journal of Biological Chemistry*, vol. 281, no. 35, pp. 25588–25600, 2006.

[51] A. Biernacka, M. Dobaczewski, and N. G. Frangogiannis, "TGF-β signaling in fibrosis," *Growth Factors*, vol. 29, no. 5, pp. 196–202, 2011.

[52] G. Untergasser, R. Gander, C. Lilg, G. Lepperdinger, E. Plas, and P. Berger, "Profiling molecular targets of TGF-β1 in prostate fibroblast-to-myofibroblast transdifferentiation," *Mechanisms of Ageing and Development*, vol. 126, no. 1, pp. 59–69, 2005.

[53] J. Folkman, M. Klagsbrun, J. Sasse, M. Wadzinski, D. Ingber, and I. Vlodavsky, "A heparin-binding angiogenic protein-basic fibroblast growth factor-is stored within basement membrane," *The American Journal of Pathology*, vol. 130, no. 2, pp. 393–400, 1988.

[54] G. S. Schultz and A. Wysocki, "Interactions between extracellular matrix and growth factors in wound healing," *Wound Repair and Regeneration*, vol. 17, no. 2, pp. 153–162, 2009.

[55] D. R. Senger, K. P. Claffey, J. E. Benes, C. A. Perruzzi, A. P. Sergiou, and M. Detmar, "Angiogenesis promoted by vascular endothelial growth factor: regulation through $\alpha1\beta1$ and $\alpha2\beta1$ integrins," *Proceedings of the National Academy of Sciences of the United States of America*, vol. 94, no. 25, pp. 13612–13617, 1997.

[56] H. J. Forman, J. M. Fukuto, T. Miller, H. Zhang, A. Rinna, and S. Levy, "The chemistry of cell signaling by reactive oxygen and nitrogen species and 4-hydroxynonenal," *Archives of Biochemistry and Biophysics*, vol. 477, no. 2, pp. 183–195, 2008.

[57] S. Altenhofer, P. W. Kleikers, K. A. Radermacher et al., "The NOX toolbox: validating the role of NADPH oxidases in physiology and disease," *Cellular and Molecular Life Sciences*, vol. 69, no. 14, pp. 2327–2343, 2012.

[58] F. Jiang, Y. Zhang, and G. J. Dusting, "NADPH oxidase-mediated redox signaling: roles in cellular stress response, stress tolerance, and tissue repair," *Pharmacological Reviews*, vol. 63, no. 1, pp. 218–242, 2011.

[59] K. D. Martyn, L. M. Frederick, K. Von Loehneysen, M. C. Dinauer, and U. G. Knaus, "Functional analysis of Nox4 reveals unique characteristics compared to other NADPH oxidases," *Cellular Signalling*, vol. 18, no. 1, pp. 69–82, 2006.

[60] S. I. Dikalov, A. E. Dikalova, A. T. Bikineyeva, H. H. H. W. Schmidt, D. G. Harrison, and K. K. Griendling, "Distinct roles of Nox1 and Nox4 in basal and angiotensin II-stimulated superoxide and hydrogen peroxide production," *Free Radical Biology and Medicine*, vol. 45, no. 9, pp. 1340–1351, 2008.

[61] I. Takac, K. Schröder, L. Zhang et al., "The E-loop is involved in hydrogen peroxide formation by the NADPH oxidase Nox4," *Journal of Biological Chemistry*, vol. 286, no. 15, pp. 13304–13313, 2011.

[62] K. Bedard and K.-H. Krause, "The NOX family of ROS-generating NADPH oxidases: physiology and pathophysiology," *Physiological Reviews*, vol. 87, no. 1, pp. 245–313, 2007.

[63] D. Trachootham, W. Lu, M. A. Ogasawara, N. R.-D. Valle, and P. Huang, "Redox regulation of cell survival," *Antioxidants and Redox Signaling*, vol. 10, no. 8, pp. 1343–1374, 2008.

[64] D. P. Jones, "Radical-free biology of oxidative stress," *The American Journal of Physiology—Cell Physiology*, vol. 295, no. 4, pp. C849–C868, 2008.

[65] L. Serrander, L. Cartier, K. Bedard et al., "NOX4 activity is determined by mRNA levels and reveals a unique pattern of ROS generation," *Biochemical Journal*, vol. 406, no. 1, pp. 105–114, 2007.

[66] N. Amara, D. Goven, F. Prost, R. Muloway, B. Crestani, and J. Boczkowski, "NOX4/NADPH oxidase expression is increased in pulmonary fibroblasts from patients with idiopathic pulmonary fibrosis and mediates TGFβ1-induced fibroblast differentiation into myofibroblasts," *Thorax*, vol. 65, no. 8, pp. 733–738, 2010.

[67] L. Hecker, R. Vittal, T. Jones et al., "NADPH oxidase-4 mediates myofibroblast activation and fibrogenic responses to lung injury," *Nature Medicine*, vol. 15, no. 9, pp. 1077–1081, 2009.

[68] K. A. Graham, M. Kulawiec, K. M. Owens et al., "NADPH oxidase 4 is an oncoprotein localized to mitochondria," *Cancer Biology and Therapy*, vol. 10, no. 3, pp. 223–231, 2010.

[69] J. Kuroda, T. Ago, S. Matsushima, P. Zhai, M. D. Schneider, and J. Sadoshima, "NADPH oxidase 4 (Nox4) is a major source of oxidative stress in the failing heart," *Proceedings of the National Academy of Sciences of the United States of America*, vol. 107, no. 35, pp. 15565–15570, 2010.

[70] B. Zhang, Z. Liu, and X. Hu, "Inhibiting cancer metastasis via targeting NAPDH oxidase 4," *Biochemical Pharmacology*, vol. 86, no. 2, pp. 253–266, 2013.

[71] U. Weyemi, C. E. Redon, P. R. Parekh et al., "NADPH Oxidases NOXs and DUOXs as putative targets for cancer therapy," *Anti-Cancer Agents in Medicinal Chemistry*, vol. 13, no. 3, pp. 502–514, 2013.

[72] S. J. Guo, L. Y. Wu, W. L. Shen et al., "Gene profile for differentiation of vascular adventitial myofibroblasts," *Sheng Li Xue Bao*, vol. 58, no. 4, pp. 337–344, 2006.

[73] R. E. Clempus, D. Sorescu, A. E. Dikalova et al., "Nox4 is required for maintenance of the differentiated vascular smooth muscle cell phenotype," *Arteriosclerosis, Thrombosis, and Vascular Biology*, vol. 27, no. 1, pp. 42–48, 2007.

[74] T. Hu, S. P. RamachandraRao, S. Siva et al., "Reactive oxygen species production via NADPH oxidase mediates TGF-β-induced cytoskeletal alterations in endothelial cells," *The American Journal of Physiology—Renal Physiology*, vol. 289, no. 4, pp. F816–F825, 2005.

[75] Y. M. Moon, H. J. Kang, J. S. Cho et al., "Nox4 mediates hypoxia-stimulated myofibroblast differentiation in nasal polyp-derived fibroblasts," *International Archives of Allergy and Immunology*, vol. 159, no. 4, pp. 399–409, 2012.

[76] B. D. Uhal, J. K. Kim, X. Li, and M. Molina-Molina, "Angiotensin-TGF-β1 crosstalk in human idiopathic pulmonary fibrosis: autocrine mechanisms in myofibroblasts and macrophages," *Current Pharmaceutical Design*, vol. 13, no. 12, pp. 1247–1256, 2007.

[77] B. Crestani, V. Besnard, and J. Boczkowski, "Signalling pathways from NADPH oxidase-4 to idiopathic pulmonary fibrosis," *International Journal of Biochemistry and Cell Biology*, vol. 43, no. 8, pp. 1086–1089, 2011.

[78] X. F. Wei, Q. G. Zhou, F. F. Hou, B. Y. Liu, and M. Liang, "Advanced oxidation protein products induce mesangial cell perturbation through PKC-dependent activation of NADPH oxidase," *The American Journal of Physiology—Renal Physiology*, vol. 296, no. 2, pp. F427–F437, 2009.

[79] R.-M. Liu, J. Choi, J.-H. Wu et al., "Oxidative modification of nuclear mitogen-activated protein kinase phosphatase 1 is involved in transforming growth factor β1-induced expression of plasminogen activator inhibitor 1 in fibroblasts," *Journal of Biological Chemistry*, vol. 285, no. 21, pp. 16239–16247, 2010.

[80] T. V. Murray, I. Smyrnias, A. M. Shah et al., "NADPH oxidase 4 regulates cardiomyocyte differentiation via redox activation

of c-Jun protein and the cis-regulation of GATA-4 gene transcription," *Journal of Biological Chemistry*, vol. 288, no. 22, pp. 15745–15759, 2013.

[81] K. Block, A. Eid, K. K. Griendling, D.-Y. Lee, Y. Wittrant, and Y. Gorin, "Nox4 NAD(P)H oxidase mediates Src-dependent tyrosine phosphorylation of PDK-1 in response to angiotensin II: role in mesangial cell hypertrophy and fibronectin expression," *Journal of Biological Chemistry*, vol. 283, no. 35, pp. 24061–24076, 2008.

[82] Y. Gorin, K. Block, J. Hernandez et al., "Nox4 NAD(P)H oxidase mediates hypertrophy and fibronectin expression in the diabetic kidney," *Journal of Biological Chemistry*, vol. 280, no. 47, pp. 39616–39626, 2005.

[83] E. R. Jarman, V. S. Khambata, C. Cope et al., "An inhibitor of NADPH oxidase-4 attenuates established pulmonary fibrosis in a rodent disease model," *The American Journal of Respiratory Cell and Molecular Biology*, vol. 50, no. 1, pp. 158–169, 2014.

[84] T. Aoyama, Y. H. Paik, S. Watanabe et al., "Nicotinamide adenine dinucleotide phosphate oxidase in experimental liver fibrosis: GKT137831 as a novel potential therapeutic agent," *Hepatology*, vol. 56, no. 6, pp. 2316–2327, 2012.

[85] W. Zhao, T. Zhao, Y. Chen, R. A. Ahokas, and Y. Sun, "Oxidative stress mediates cardiac fibrosis by enhancing transforming growth factor-beta1 in hypertensive rats," *Molecular and Cellular Biochemistry*, vol. 317, no. 1-2, pp. 43–50, 2008.

[86] S. Carnesecchi, C. Deffert, Y. Donati et al., "A key role for NOX4 in epithelial cell death during development of lung fibrosis," *Antioxidants and Redox Signaling*, vol. 15, no. 3, pp. 607–619, 2011.

[87] M. Waghray, Z. Cui, J. C. Horowitz et al., "Hydrogen peroxide is a diffusible paracrine signal for the induction of epithelial cell death by activated myofibroblasts," *FASEB Journal*, vol. 19, no. 7, pp. 854–856, 2005.

[88] F. P. Bellinger, A. V. Raman, M. A. Reeves, and M. J. Berry, "Regulation and function of selenoproteins in human disease," *Biochemical Journal*, vol. 422, no. 1, pp. 11–22, 2009.

[89] M. S. Crane, A. F. Howie, J. R. Arthur, F. Nicol, L. K. Crosley, and G. J. Beckett, "Modulation of thioredoxin reductase-2 expression in EAhy926 cells: implications for endothelial selenoprotein hierarchy," *Biochimica et Biophysica Acta*, vol. 1790, no. 10, pp. 1191–1197, 2009.

[90] S. C. Low, E. Grundner-Culemann, J. W. Harney, and M. J. Berry, "SECIS-SBP2 interactions dictate selenocysteine incorporation efficiency and selenoprotein hierarchy," *EMBO Journal*, vol. 19, no. 24, pp. 6882–6890, 2000.

[91] E. Mezey, X. Liu, and J. J. Potter, "The combination of selenium and vitamin e inhibits type i collagen formation in cultured hepatic stellate cells," *Biological Trace Element Research*, vol. 140, no. 1, pp. 82–94, 2011.

[92] M. Bocchino, S. Agnese, E. Fagone et al., "Reactive oxygen species are required for maintenance and differentiation of primary lung fibroblasts in idiopathic pulmonary fibrosis," *PLoS ONE*, vol. 5, no. 11, Article ID e14003, 2010.

[93] M.-C. Vozenin-Brotons, V. Sivan, N. Gault et al., "Antifibrotic action of Cu/Zn SOD is mediated by TGF-β1 repression and phenotypic reversion of myofibroblasts," *Free Radical Biology and Medicine*, vol. 30, no. 1, pp. 30–42, 2001.

[94] F. Murad, "Nitric oxide and cyclic GMP in cell signaling and drug development," *The New England Journal of Medicine*, vol. 355, no. 19, pp. 2003–2011, 2006.

[95] A. J. Chu and J. K. Prasad, "Up-regulation by human recombinant transforming growth factor β-1 of collagen production in cultured dermal fibroblasts is mediated by the inhibition of nitric oxide signaling," *Journal of the American College of Surgeons*, vol. 188, no. 3, pp. 271–280, 1999.

[96] M. G. Ferrini, S. Rivera, J. Moon, D. Vernet, J. Rajfer, and N. F. Gonzalez-Cadavid, "The genetic inactivation of inducible nitric oxide synthase (iNOS) intensifies fibrosis and oxidative stress in the penile corpora cavernosa in type 1 diabetes," *Journal of Sexual Medicine*, vol. 7, no. 9, pp. 3033–3044, 2010.

[97] A. Kazakov, R. Hall, P. Jagoda et al., "Inhibition of endothelial nitric oxide synthase induces and enhances myocardial fibrosis," *Cardiovascular Research*, vol. 100, no. 2, pp. 211–221, 2013.

[98] D. Sun, Y. Wang, C. Liu et al., "Effects of nitric oxide on renal interstitial fibrosis in rats with unilateral ureteral obstruction," *Life Sciences*, vol. 90, no. 23-24, pp. 900–909, 2012.

[99] D. Vernet, M. G. Ferrini, E. G. Valente et al., "Effect of nitric oxide on the differentiation of fibroblasts into myofibroblasts in the Peyronie's fibrotic plaque and in its rat model," *Nitric Oxide*, vol. 7, no. 4, pp. 262–276, 2002.

[100] C. Zenzmaier, N. Sampson, D. Pernkopf, E. Plas, G. Untergasser, and P. Berger, "Attenuated proliferation and transdifferentiation of prostatic stromal cells indicate suitability of phosphodiesterase type 5 inhibitors for prevention and treatment of benign prostatic hyperplasia," *Endocrinology*, vol. 151, no. 8, pp. 3975–3984, 2010.

[101] R. Vercelino, I. Crespo, G. F. P. De Souza et al., "S-nitroso-N-acetylcysteine attenuates liver fibrosis in cirrhotic rats," *Journal of Molecular Medicine*, vol. 88, no. 4, pp. 401–411, 2010.

[102] A. Pini, S. Viappiani, M. Bolla, E. Masini, and D. Bani, "Prevention of bleomycin-induced lung fibrosis in mice by a novel approach of parallel inhibition of cyclooxygenase and nitric-oxide donation using NCX 466, a prototype cyclooxygenase inhibitor and nitric-oxide donor," *Journal of Pharmacology and Experimental Therapeutics*, vol. 341, no. 2, pp. 493–499, 2012.

[103] C. Beyer, N. Reich, S. C. Schindler et al., "Stimulation of soluble guanylate cyclase reduces experimental dermal fibrosis," *Annals of the Rheumatic Diseases*, vol. 71, no. 6, pp. 1019–1026, 2012.

[104] H. Masuyama, T. Tsuruda, Y. Sekita et al., "Pressure-independent effects of pharmacological stimulation of soluble guanylate cyclase on fibrosis in pressure-overloaded rat heart," *Hypertension Research*, vol. 32, no. 7, pp. 597–603, 2009.

[105] Y. Wang, S. Krämer, T. Loof et al., "Stimulation of soluble guanylate cyclase slows progression in anti-thy1-induced chronic glomerulosclerosis," *Kidney International*, vol. 68, no. 1, pp. 47–61, 2005.

[106] Y. Wang, S. Krämer, T. Loof et al., "Enhancing cGMP in experimental progressive renal fibrosis: soluble guanylate cyclase stimulation vs. phosphodiesterase inhibition," *The American Journal of Physiology—Renal Physiology*, vol. 290, no. 1, pp. F167–F176, 2006.

[107] S. Geschka, A. Kretschmer, Y. Sharkovska et al., "Soluble guanylate cyclase stimulation prevents fibrotic tissue remodeling and improves survival in salt-sensitive dahl rats," *PLoS ONE*, vol. 6, no. 7, Article ID e21853, 2011.

[108] Y. Sharkovska, P. Kalk, B. Lawrenz et al., "Nitric oxide-independent stimulation of soluble guanylate cyclase reduces organ damage in experimental low-renin and high-renin models," *Journal of Hypertension*, vol. 28, no. 8, pp. 1666–1675, 2010.

[109] H. H. Schmidt, P. M. Schmidt, and J. P. Stasch, "NO- and haem-independent soluble guanylate cyclase activators," in *cGMP: Generators, Effectors and Therapeutic Implications*, vol. 191 of *Handbook of Experimental Pharmacology*, pp. 309–339, 2009.

[110] A. Knorr, C. Hirth-Dietrich, C. Alonso-Alija et al., "Nitric oxide-independent activation of soluble guanylate cyclase by BAY 60-2770 in experimental liver fibrosis," *Arzneimittel-Forschung/Drug Research*, vol. 58, no. 2, pp. 71–80, 2008.

[111] P. Kalk, M. Godes, K. Relle et al., "NO-independent activation of soluble guanylate cyclase prevents disease progression in rats with 5/6 nephrectomy," *British Journal of Pharmacology*, vol. 148, no. 6, pp. 853–859, 2006.

[112] P. Li, D. Wang, J. Lucas et al., "Atrial natriuretic peptide inhibits transforming growth factor β-induced Smad signaling and myofibroblast transformation in mouse cardiac fibroblasts," *Circulation Research*, vol. 102, no. 2, pp. 185–192, 2008.

[113] J. Houtchens, D. Martin, and J. R. Klinger, "Diagnosis and management of pulmonary arterial hypertension," *Pulmonary Medicine*, vol. 2011, Article ID 845864, 13 pages, 2011.

[114] M. Oelke, F. Giuliano, V. Mirone, L. Xu, D. Cox, and L. Viktrup, "Monotherapy with tadalafil or tamsulosin similarly improved lower urinary tract symptoms suggestive of benign prostatic hyperplasia in an international, randomised, parallel, placebo-controlled clinical trial," *European Urology*, vol. 61, no. 5, pp. 917–925, 2012.

[115] R. C. Rosen and J. B. Kostis, "Overview of phosphodiesterase 5 inhibition in erectile dysfunction," *The American Journal of Cardiology*, vol. 92, no. 9, supplement 1, pp. 9–18, 2003.

[116] B. Hohenstein, C. Daniel, S. Wittmann, and C. Hugo, "PDE-5 inhibition impedes TSP-1 expression, TGF-β activation and matrix accumulation in experimental glomerulonephritis," *Nephrology Dialysis Transplantation*, vol. 23, no. 11, pp. 3427–3436, 2008.

[117] M. G. Ferrini, I. Kovanecz, G. Nolazco, J. Rajfer, and N. F. Gonzalez-Cadavid, "Effects of long-term vardenafil treatment on the development of fibrotic plaques in a rat model of Peyronie's disease," *BJU International*, vol. 97, no. 3, pp. 625–633, 2006.

[118] E. G. A. Valente, D. Vernet, M. G. Ferrini, A. Qian, J. Rajfer, and N. F. Gonzalez-Cadavid, "L-Arginine and phosphodiesterase (PDE) inhibitors counteract fibrosis in the Peyronie's fibrotic plaque and related fibroblast cultures," *Nitric Oxide*, vol. 9, no. 4, pp. 229–244, 2003.

[119] C. Zenzmaier, J. Kern, N. Sampson et al., "Phosphodiesterase type 5 inhibition reverts prostate fibroblast-to-myofibroblast trans-differentiation," *Endocrinology*, vol. 153, no. 11, pp. 5546–5555, 2013.

[120] J. T. Stefano, B. Cogliati, F. Santos et al., "S-Nitroso-N-acetyl-cysteine induces de-differentiation of activated hepatic stellate cells and promotes antifibrotic effects in vitro," *Nitric Oxide*, vol. 25, no. 3, pp. 360–365, 2011.

[121] Y. Wang-Rosenke, A. Mika, D. Khadzhynov, T. Loof, H.-H. Neumayer, and H. Peters, "Stimulation of soluble guanylate cyclase improves renal recovery after relief of unilateral ureteral obstruction," *Journal of Urology*, vol. 186, no. 3, pp. 1142–1149, 2011.

[122] K. Block and Y. Gorin, "Aiding and abetting roles of NOX oxidases in cellular transformation," *Nature Reviews Cancer*, vol. 12, no. 9, pp. 627–637, 2012.

[123] G. M. Rubanyi and P. M. Vanhoutte, "Superoxide anions and hyperoxia inactivate endothelium-derived relaxing factor," *The American Journal of Physiology*, vol. 250, no. 5, pp. H822–H827, 1986.

[124] N. D. Roe and J. Ren, "Nitric oxide synthase uncoupling: a therapeutic target in cardiovascular diseases," *Vascular Pharmacology*, vol. 57, no. 5-6, pp. 168–172, 2012.

[125] N. S. R. De Mochel, S. Seronello, S. H. Wang et al., "Hepatocyte NAD(P)H oxidases as an endogenous source of reactive oxygen species during hepatitis C virus infection," *Hepatology*, vol. 52, no. 1, pp. 47–59, 2010.

[126] N. Ito, U. T. Ruegg, A. Kudo et al., "Activation of calcium signaling through Trpv1 by nNOS and peroxynitrite as a key trigger of skeletal muscle hypertrophy," *Nature Medicine*, vol. 19, no. 1, pp. 101–106, 2013.

[127] A. A. Eid, D. Y. Lee, L. J. Roman et al., "Sestrin 2 and AMPK connect hyperglycemia to Nox4-dependent endothelial nitric oxide synthase uncoupling and matrix protein expression," *Molecular and Cellular Biology*, vol. 33, no. 17, pp. 3439–3460, 2013.

[128] D. Y. Lee, F. Wauquier, A. A. Eid et al., "Nox4 NADPH oxidase mediates peroxynitrite-dependent uncoupling of endothelial nitric-oxide synthase and fibronectin expression in response to angiotensin II: role of mitochondrial reactive oxygen species," *Journal of Biological Chemistry*, vol. 288, no. 40, pp. 28668–28686, 2013.

[129] E. A. Jaimes, C. Sweeney, and L. Raij, "Effects of the reactive oxygen species hydrogen peroxide and hypochlorite on endothelial nitric oxide production," *Hypertension*, vol. 38, no. 4, pp. 877–883, 2001.

[130] C. Gerassimou, A. Kotanidou, Z. Zhou, D. D. C. Simoes, C. Roussos, and A. Papapetropoulos, "Regulation of the expression of soluble guanylyl cyclase by reactive oxygen species," *British Journal of Pharmacology*, vol. 150, no. 8, pp. 1084–1091, 2007.

[131] S. Wedgwood, R. H. Steinhorn, M. Bunderson et al., "Increased hydrogen peroxide downregulates soluble guanylate cyclase in the lungs of lambs with persistent pulmonary hypertension of the newborn," *The American Journal of Physiology—Lung Cellular and Molecular Physiology*, vol. 289, no. 4, pp. L660–L666, 2005.

[132] S. Meurer, S. Pioch, S. Gross, and W. Müller-Esterl, "Reactive oxygen species induce tyrosine phosphorylation of and Src kinase recruitment to NO-sensitive guanylyl cyclase," *Journal of Biological Chemistry*, vol. 280, no. 39, pp. 33149–33156, 2005.

[133] K. S. Murthy, "Inhibitory phosphorylation of soluble guanylyl cyclase by muscarinic m2 receptors via G$\beta\gamma$-dependent activation of c-Src kinase," *Journal of Pharmacology and Experimental Therapeutics*, vol. 325, no. 1, pp. 183–189, 2008.

[134] T. Adachi, R. Matsui, R. M. Weisbrod, S. Najibi, and R. A. Cohen, "Reduced sarco/endoplasmic reticulum Ca^{2+} uptake activity can account for the reduced response to NO, but not sodium nitroprusside, in hypercholesterolemic rabbit aorta," *Circulation*, vol. 104, no. 9, pp. 1040–1045, 2001.

[135] X. Tong, X. Hou, D. Jourd'Heuil, R. M. Weisbrod, and R. A. Cohen, "Upregulation of Nox4 by TGFβ1 oxidizes SERCA and inhibits NO in arterial smooth muscle of the prediabetic zucker rat," *Circulation Research*, vol. 107, no. 8, pp. 975–983, 2010.

[136] J. Ying, X. Tong, D. R. Pimentel et al., "Cysteine-674 of the sarco/endoplasmic reticulum calcium ATPase is required for the inhibition of cell migration by nitric oxide," *Arteriosclerosis, Thrombosis, and Vascular Biology*, vol. 27, no. 4, pp. 783–790, 2007.

[137] A. Leask, "Potential therapeutic targets for cardiac fibrosis: TGFβ, angiotensin, endothelin, CCN2, and PDGF, partners in fibroblast activation," *Circulation Research*, vol. 106, no. 11, pp. 1675–1680, 2010.

[138] C. P. Denton, P. A. Merkel, D. E. Furst et al., "Recombinant human anti-transforming growth factor β1 antibody therapy

in systemic sclerosis: a multicenter, randomized, placebo-controlled phase I/II trial of CAT-192," *Arthritis and Rheumatism*, vol. 56, no. 1, pp. 323–333, 2007.

[139] J. Rosenbloom, F. A. Mendoza, and S. A. Jimenez, "Strategies for anti-fibrotic therapies," *Biochimica et Biophysica Acta*, vol. 1832, no. 7, pp. 1088–1103, 2013.

[140] L. A. Van Meeteren and P. Ten Dijke, "Regulation of endothelial cell plasticity by TGF-β," *Cell and Tissue Research*, vol. 347, no. 1, pp. 177–186, 2012.

[141] Y. E. Zhang, "Non-Smad pathways in TGF-β signaling," *Cell Research*, vol. 19, no. 1, pp. 128–139, 2009.

[142] G. Csanyi and P. J. Pagano, "Strategies aimed at Nox4 oxidase inhibition employing peptides from Nox4 B-loop and C-terminus and $p22^{phox}$ N-terminus: an elusive target," *International Journal of Hypertension*, vol. 2013, Article ID 842827, 9 pages, 2013.

[143] I. Dahan and E. Pick, "Strategies for identifying synthetic peptides to act as inhibitors of NADPH oxidases, or 'All that you did and did not want to know about Nox inhibitory peptides'," *Cellular and Molecular Life Sciences*, vol. 69, no. 14, pp. 2283–2305, 2012.

[144] D. E. Green, T. C. Murphy, B. Y. Kang et al., "The Nox4 inhibitor GKT137831 attenuates hypoxia-induced pulmonary vascular cell proliferation," *American Journal of Respiratory Cell and Molecular Biology*, vol. 47, no. 5, pp. 718–726, 2012.

[145] Y. Jia, J. Xu, Y. Yu et al., "Nifedipine inhibits angiotensin II-induced cardiac fibrosis via downregulating Nox4-derived ROS generation and suppressing ERK1/2, JNK signaling pathways," *Pharmazie*, vol. 68, no. 6, pp. 435–441, 2013.

[146] L. L. Pan, X. H. Liu, Y. Q. Shen et al., "Inhibition of NADPH oxidase 4-related signaling by sodium hydrosulfide attenuates myocardial fibrotic response," *International Journal of Cardiology*, vol. 168, no. 4, pp. 3770–3778, 2013.

[147] V. Diwadkar-Navsariwala, G. S. Prins, S. M. Swanson et al., "Selenoprotein deficiency accelerates prostate carcinogenesis in a transgenic model," *Proceedings of the National Academy of Sciences of the United States of America*, vol. 103, no. 21, pp. 8179–8184, 2006.

[148] B. C. Pence, E. Delver, and D. M. Dunn, "Effects of dietary selenium on UVB-induced skin carcinogenesis and epidermal antioxidant status," *Journal of Investigative Dermatology*, vol. 102, no. 5, pp. 759–761, 1994.

[149] M. Selenius, A.-K. Rundlöf, E. Olm, A. P. Fernandes, and M. Björnstedt, "Selenium and the selenoprotein thioredoxin reductase in the prevention, treatment and diagnostics of cancer," *Antioxidants and Redox Signaling*, vol. 12, no. 7, pp. 867–880, 2010.

[150] A. J. Duffield-Lillico, B. L. Dalkin, M. E. Reid et al., "Selenium supplementation, baseline plasma selenium status and incidence of prostate cancer: an analysis of the complete treatment period of the Nutritional Prevention of Cancer Trial," *BJU International*, vol. 91, no. 7, pp. 608–612, 2003.

[151] R. Hurst, L. Hooper, T. Norat et al., "Selenium and prostate cancer: systematic review and meta-analysis," *The American Journal of Clinical Nutrition*, vol. 96, no. 1, pp. 111–122, 2012.

[152] M. S. Geybels, B. A. Verhage, F. J. van Schooten et al., "Advanced prostate cancer risk in relation to toenail selenium levels," *Journal of the National Cancer Institute*, vol. 105, no. 18, pp. 1394–1401, 2013.

[153] A. L. Herrick, F. Rieley, D. Schofield, S. Hollis, J. M. Braganza, and M. I. V. Jayson, "Micronutrient antioxidant status in patients with primary Raynaud's phenomenon and systemic sclerosis," *Journal of Rheumatology*, vol. 21, no. 8, pp. 1477–1483, 1994.

[154] S. Khanna, A. C. Udas, G. K. Kumar et al., "Trace elements (copper, zinc, selenium and molybdenum) as markers in oral sub mucous fibrosis and oral squamous cell carcinoma," *Journal of Trace Elements in Medicine and Biology*, vol. 27, no. 4, pp. 307–311, 2013.

[155] M. Ding, J. J. Potter, X. Liu, M. S. Torbenson, and E. Mezey, "Selenium supplementation decreases hepatic fibrosis in mice after chronic carbon tetrachloride administration," *Biological Trace Element Research*, vol. 133, no. 1, pp. 83–97, 2010.

[156] B. Contempre, O. Le Moine, J. E. Dumont, J.-F. Denef, and M. C. Many, "Selenium deficiency and thyroid fibrosis. A key role for macrophages and transforming growth factor β (TGF-β)," *Molecular and Cellular Endocrinology*, vol. 124, no. 1-2, pp. 7–15, 1996.

[157] M. P. Rayman and S. Stranges, "Epidemiology of selenium and type 2 diabetes: can we make sense of it?" *Free Radical Biology and Medicine*, vol. 65, pp. 1557–1564, 2013.

[158] A. J. Impens, K. Phillips, and E. Schiopu, "PDE-5 inhibitors in scleroderma raynaud phenomenon and digital ulcers: current status of clinical trials," *International Journal of Rheumatology*, vol. 2011, Article ID 392542, 2011.

[159] M. Roustit, S. Blaise, Y. Allanore et al., "Phosphodiesterase-5 inhibitors for the treatment of secondary Raynaud's phenomenon: systematic review and meta-analysis of randomised trials," *Annals of the Rheumatic Diseases*, vol. 72, no. 10, pp. 1696–1699, 2013.

[160] H. A. Ghofrani, A. M. D'Armini, F. Grimminger et al., "Riociguat for the treatment of chronic thromboembolic pulmonary hypertension," *The New England Journal of Medicine*, vol. 369, no. 4, pp. 319–329, 2013.

[161] H. A. Ghofrani, N. Galie, F. Grimminger et al., "Riociguat for the treatment of pulmonary arterial hypertension," *The New England Journal of Medicine*, vol. 369, no. 4, pp. 330–340, 2013.

[162] M. Follmann, N. Griebenow, M. G. Hahn et al., "The chemistry and biology of soluble guanylate cyclase stimulators and activators," *Angewandte Chemie International Edition*, vol. 52, no. 36, pp. 9442–9462, 2013.

[163] M. Gheorghiade, S. J. Greene, G. Filippatos et al., "Cinaciguat, a soluble guanylate cyclase activator: results from the randomized, controlled, phase IIb COMPOSE programme in acute heart failure syndromes," *European Journal of Heart Failure*, vol. 14, no. 9, pp. 1056–1066, 2012.

[164] C. L. Miller, Y. Cai, M. Oikawa et al., "Cyclic nucleotide phosphodiesterase 1A: a key regulator of cardiac fibroblast activation and extracellular matrix remodeling in the heart," *Basic Research in Cardiology*, vol. 106, no. 6, pp. 1023–1039, 2011.

Hindawi Publishing Corporation
BioMed Research International
Volume 2014, Article ID 318714, 8 pages
http://dx.doi.org/10.1155/2014/318714

Review Article

ROS, Notch, and Wnt Signaling Pathways: Crosstalk between Three Major Regulators of Cardiovascular Biology

C. Caliceti,[1] P. Nigro,[2] P. Rizzo,[1] and R. Ferrari[1]

[1] *Department of Cardiology and Laboratory for Technologies of Advanced Therapies (LTTA Center), University Hospital of Ferrara and Maria Cecilia Hospital, GVM Care & Research, E.S. Health Science Foundation, Cotignola, Italy*
[2] *Centro Cardiologico Monzino (IRCCS), Laboratorio di Biologia Vascolare e Medicina Rigenerativa, Milan, Italy*

Correspondence should be addressed to C. Caliceti; cristiana.caliceti@gmail.com

Received 17 November 2013; Accepted 28 December 2013; Published 4 February 2014

Academic Editor: Tullia Maraldi

Reactive oxygen species (ROS), traditionally viewed as toxic by-products that cause damage to biomolecules, now are clearly recognized as key modulators in a variety of biological processes and pathological states. The development and regulation of the cardiovascular system require orchestrated activities; Notch and Wnt/β-catenin signaling pathways are implicated in many aspects of them, including cardiomyocytes and smooth muscle cells survival, angiogenesis, progenitor cells recruitment and differentiation, arteriovenous specification, vascular cell migration, and cardiac remodelling. Several novel findings regarding the role of ROS in Notch and Wnt/β-catenin modulation prompted us to review their emerging function in the cardiovascular system during embryogenesis and postnatally.

1. Introduction

Cardiovascular disease is the number one cause of death worldwide [1]. It has become clear that increases in reactive oxygen species ($O_2^{-\bullet}$, H_2O_2, and $^{\bullet}OH$) represent a common pathogenic mechanism for cardiovascular diseases including atherosclerosis, hypertension, and congestive heart failure [2].

In the last decade the scientific community clarified the importance of low levels of ROS as key signaling molecules in physiological functions such as the regulation of cell signaling, proliferation, and differentiation [3]. Different authors provided scientific evidences regarding a sequential and direct link between Notch and Wnt signaling pathways in tuning endothelial cells (ECs) and cardiomyocytes functions and vascular morphogenesis [4].

The purpose of this review is to describe how ROS regulate Notch and Wnt pathways. Understanding the molecular mechanism regulated by ROS could lead to the development of new therapeutic approaches for cardiovascular diseases.

2. Role of ROS in Cardiovascular System

Vascular ROS formation can be stimulated by mechanical stress, environmental factors, platelet-derived growth factor (PDGF), angiotensin II (AngII), and low-density lipoproteins [4–7]. Because many risk factors for coronary artery disease such as hyperlipidemia, hypertension, diabetes, and smoking increase production of ROS, it has been suggested that changes in vessel redox state are a common pathway in the pathogenesis of atherosclerosis [8–10].

A particularly important mechanism for ROS-mediated cardiovascular disease appears to be via stimulation of pro-inflammatory events [11]. These, in turn, cause endothelial cell (ECs) dysfunction that predisposes to atherosclerosis by augmenting thrombosis, inflammation, VSMC growth, and lipid accumulation. The strongest data that link AngII, oxidative stress, and ECs dysfunction are animal studies in which rats were made hypertensive to ~200 mm Hg by infusion of either AngII or norepinephrine. ECs dysfunction was observed only with AngII and correlated with increased superoxide production by arteries [12]. Similar results were obtained from the TREND and HOPE clinical studies which demonstrated that inhibiting AngII restores ECs function and decreases cardiovascular events [13, 14]. More recently, Harrison's lab has shown that AngII stimulates T cell inflammatory responses in a redox-dependent (NAD(P)H oxidases) manner that contributes to hypertension [15].

It has been previously reported that, in response to ROS, VSMC may secrete proteins that participate in autocrine/paracrine growth [16].

ROS are produced at low levels prevalently as byproducts of the mitochondrial electron transport chain and through NAD(P)H oxidase family. They play a physiologically important role in the regulation of various biological responses such as cell migration, proliferation, gene expression, and angiogenesis [17, 18].

NAD(P)H oxidase (Nox) enzymes are membrane-associated enzymatic complexes and structural homologues of phagocytic Nox (gp91phox/Nox2) and consist of both single (Nox1–Nox5) and dual (Duox1 and Duox2) oxidases [19]. ROS are generated by an electron transport through the membrane forming $O_2^{-\bullet}$ that can further disproportionate forming hydrogen peroxide (H_2O_2) or, in presence of nitric oxide ($^{\bullet}NO$), creating peroxynitrite (ONOO–).

Nox2 and Nox4 are critical ROS-generating complexes in ECs; they are activated by various stimulants and agonists, for instance, VEGF. Nox1 isoform is more abundant in epithelium, even if it was detected also in ECs and VSMCs [20].

VEGF stimulates ROS production from Nox2 that in turn promotes VEGFR2 autophosphorylation through oxidation/inhibition of phosphatase enzymes. The result is an enhancement in cell proliferation, migration, and angiogenesis [21, 22].

Khatri et al. [23] have shown that vascular Nox2-derived ROS promotes VEGF expression and neovascularization in transgenic mice overexpressing p22phox, a binding partner of Nox. Nox4 is more abundantly expressed compared to Nox2 in ECs. Recently, Datla et al. [24] reported that Nox4 small-interference RNA (siRNA) inhibits VEGF-induced ECs migration and proliferation. Interestingly, Vallet et al. [25] showed that Nox4 expression is upregulated during ischemia-induced angiogenesis of mice. Gene knockout and overexpression studies on Nox4 suggest that Nox4-derived ROS have vascular protective function [26].

Urao and Ushio-Fukai [27] demonstrated that hindlimb ischemia increases Nox2-dependent ROS production in isolated bone marrow-derived mononuclear cells (BM-MNCs) and that postischemic neovascularization and mobilization of BM cells (BMCs) are impaired in Nox2 knockout mice concluding that Nox2-derived ROS regulate progenitor cell expansion and reparative mobilization in response to ischemia.

Furthermore, Nox1-dependent redox signaling pathway modulates the phosphatase PTP-PEST/PTPN12, an important regulator of endothelial cell migration and adhesion [28]. In particular, Nox1-derived ROS were found to promote intestinal mucosa wound repair by inactivating PTEN and PTP-PEST, with consequent activation of focal adhesion kinase (FAK) and paxillin [29].

3. Notch Signaling in the Cardiovascular System

Notch pathway is a highly conserved signaling system that controls cell fate decisions [30]. It is a short range communication system between two adjacent cells based on a ligand-activated receptor. In mammals there are four highly homologous receptors (Notch 1, 2, 3, and 4) and five ligands (Delta-like ligands 1, 3, and 4 and Jagged 1 and 2). Both receptors and ligands are membrane-spanning proteins. Ligand binding induces a conformational change that allows the first proteolytic cut by "A Disintegrin And Metalloprotease," ADAM (the principal involved are 10 and 17) [31] which removes the extracellular portion of Notch and creates a membrane-tethered intermediate that is a substrate for γ-secretase, a cleaving protease complex. γ-secretase in turn generates the active form of Notch (Notch intracellular fragment, NIC) which translocates to the nucleus where it binds the transcriptional factor CSL (CBF1, Suppressor of Hairless, Lag-1) also known as recombinant signal binding protein 1 for Jκ (RBP-Jκ). Such NIC binding displaces repressor molecules and promotes the recruitment of coactivator molecules. This in turn activates the transcription of specific Notch target genes such as Hes (hairy/enhancer of split), Hey (Hes-related proteins), Nrarp (Notch-regulated andrin repeat protein), cMyc, cyclin D1, and many other genes that control ECs proliferation, differentiation, and apoptosis as well as stem cells maintenance and angiogenesis [32].

Notch receptors 1, 2 as well as Jagged1, Delta-like ligand 1 and 4 (Dll1 and Dll4), are preferentially expressed in ECs and have a key role in developmental and postnatal angiogenesis. During early embryogenesis, Notch induces differentiation of angioblasts to ECs, whereas at later stages it controls specification of ECs into arterial and venous identity [33]. Mice embryos with single Notch1 or double mutations of Notch1 and Notch4 display severe defects in vascular development. In ECs, VEGF-A induces the formation of filopodia, conferring the so-called tip cells phenotype. Tip cells promote a line of angiogenesis while inhibiting branching by adjacent cells (called static or stalk cells) which need to remain angiogenically quiescent. VEGF-A promotes the expression of Dll4 and Notch activation in human ECs, resulting in downregulation of VEGFR2 in tip cells. Thus, this interplay between Notch and VEGF-A regulates angiogenesis with selective sprouting through the activation of the tip cells and suppression of branching through activation of stalk cells. Given its specificity in the regulation of angiogenesis, the endothelial Dll4-mediated Notch signaling has been used as target for intervention in induction of new arteries or inhibition of tumor angiogenesis [34]. VEGFR3, the main receptor for VEGF-C, is also strongly modulated by Notch. Notch inhibition in mouse retina caused an increase in protein levels of VEGFR3 while VEGFR2 levels were unaffected showing that VEGFR2 and VEGFR3 are regulated in a differential manner by Notch [35]. These data have added a new player, VEGFR3, to the model used so far to describe the molecular crosstalk between VEGF and Notch pathways in angiogenesis.

In the context of sprouting angiogenesis, Notch signaling regulates not only the frequency of sprouts but also their ability to anastomose. Retinas of mice heterozygous for a myeloid-specific Notch1 mutation were characterized by long sprouts unable to anastomose and by lack of macrophages at the edge of vascular branch points [36].

Several studies have recognized the central role of Notch-mediated signaling also in cardiac development [37]. In

cardiomyocytes, the expression of Notch is not constant over time; it is high in embryonic and proliferating immature cells but disappears when the cells lose the ability to proliferate [38]. Nemir et al. observed that Notch signaling activation inhibits cardiac progenitor cells (CPCs) differentiation into cardiomyocytes [39]. The prolonged activation of Notch in adult cardiomyocytes may have different consequences. Campa et al. observed that in adult cardiomyocytes Notch activation is associated with the block of cell cycle progression and apoptosis, suggesting that a prolonged and uncontrolled activation of Notch can be fatal for these cells [40].

4. Wnt/β-Catenin Signaling in Cardiovascular System

Notch signaling modulates endothelial homeostasis by crosstalking with other signaling pathways such as receptor tyrosine kinases (i.e., VEGFR2) [41–43] and estrogen receptor [41, 44]. Crosstalk between Notch and Wnt has also been described [41, 45–47]. The Wnt signaling pathway, also called Wnt/β-catenin signaling, plays a key role in vascular biology [45, 48]. Mice deficient for Wnt2 displayed vascular abnormalities including defective placental vasculature [49]. Knock-out mice for the Wnt receptor gene, Frizzled5, died in utero due to defects in yolk sac angiogenesis [50]. Defects of the β-catenin gene in ECs caused aberrant vascular patterning and increased vascular fragility [51].

The canonical Wnt signaling pathway is driven by β-catenin, a scaffold protein, linking the cytoplasmic tail of classical cadherins in the endothelium (vascular endothelial (VE) cadherin and N-cadherin) via α-catenin to the actin cytoskeleton. Without Wnt stimulation, cytoplasmic β-catenin levels are kept low by a degradation complex, consisting of Axin, Adenomatous polyposis coli (APC), Casein kinase1a (CK1a), and Glycogen synthase kinase 3-β (GSK3-β). Binding of Wnt to its receptors Frizzled and lipoprotein receptor-related protein (LRP) leads to inhibition of the degradation complex function, enabling β-catenin signaling. Wnt allows β-catenin to accumulate and translocate to the nucleus where it binds to several transcription factors, for example, T-cell factor (TCF) and LEF-1 [52, 53].

Dishevelled (Dvl) is an essential adaptor protein for Wnt signaling that interacts with several molecules, including Axin, inactivating the β-catenin degradation complex [49–52]. Dvl has a dual role: it is an activator of downstream Wnt signaling and an inhibitor of Notch activity. Thus Dv1 is a key regulator of cell-fate decisions in which Wnt and Notch have opposing effects [54].

The noncanonical Wnt pathway can be categorized largely into two classes, the Wnt/Ca^{2+} and Wnt/planar cell polarity (PCP) pathways. The Wnt/Ca^{2+} pathway, mediated by G-protein signaling, stimulates the release of intracellular Ca^{2+} and activation of Ca^{2+}-sensitive kinases, such as the protein kinase C and Ca^{2+}-calmodulin kinase II. PKC is a family of Ca^{2+}-dependent and Ca^{2+}-independent isoforms that have different distributions in various blood vessels, and individual members can have different roles in a plethora of biological and pathological events [54–56]. The PCP pathway, also referred to as the Wnt/Jun-N-terminal kinase (JNK) pathway, was originally identified as a pathway affecting cytoskeletal reorganization [57]. This pathway activates small GTPases, including RhoA, Rac, Cdc42, and JNK.

5. Crosstalk of Notch and Wnt/β-Catenin Signaling Pathways

Notch and Wnt signaling pathways can have opposing effects on cell-fate decisions with each pathway promoting an alternate outcome. For example, in both the skin and mammary gland, Wnt signaling promotes the maintenance of the stem cell fate whereas Notch signaling promotes lineage commitment and differentiation [54, 58–60]. In this case, the inhibition of Notch signaling would help to maintain the stem cell population. The Notch and Wnt pathways also have opposing effects at later steps within a cell lineage. For example, Notch and Wnt signaling influence terminal differentiation within the intestinal epithelium, with Notch activity biasing cells towards the absorptive fate and Wnt signaling favouring secretory cell differentiation [61–64]. Wnt pathway activation promotes neuronal differentiation and inhibits Notch signaling of primary human glioblastoma multiforme- (GBM-) derived cells [65].

Disregulation of Wnt-Notch signaling crosstalk alters early vascular development. Corada et al. [66] found that endothelial-specific early and sustained stabilization of Wnt/β-catenin induces activation of the Notch pathway by increasing the transcription of Dll4. This, in turn, prevents a correct endothelial cell differentiation, altering vascular remodeling and arteriovenous specification. Sustained Wnt/β-catenin signaling increases Dll4 in tumor vessels and induces Notch signaling that mediates a reduced angiogenic response and normalizes tumor vasculature [67]. Overexpression of Wnt/β-catenin signaling leads to alterations of vascular morphology by inhibiting angiogenesis, through stimulation of Dll4/Notch signaling. These effects of β-catenin were detectable only during embryonic vasculogenesis and angiogenesis but were lost at late stage of development or postnatally [68].

Yamamizu et al. [69] investigated signal transduction events downstream of the cAMP pathway in embryonic stem cells (ESCs) differentiation and demonstrated that simultaneous activation of Notch and β-catenin signaling can constructively reproduce the induction processes of arterial ECs from vascular progenitors expressing VEGFR2 through the formation of an arterial-specific protein complex. In particular these authors reported that RBP-Jk, NICD, and β-catenin formed a protein complex that promoted the transcription of genes specifically expressed in arterial but not venous districts in ESCs both *in vitro* and *in vivo*. Moreover, dual induction of NICD and β-catenin enhanced promoter activity of Notch target genes *in vitro* (Dll4, Hes1, and EphrinB2) and arterial gene expression during *in vivo* angiogenesis in adult mice.

The finding that a baseline level of Wnt and Notch activity can be detected during vascular development [70–74] and angiogenesis [67] suggests a mechanism in which the level of Wnt and Notch signaling is tightly balanced, that is, through

inhibition of Notch/CSL by Dvl [54], and crucial for proper vascular development.

Wnt signaling has been identified as a downstream target of Notch1 that regulates expression of cardiac transcription factors during mouse cardiogenesis and is essential for cardiac development facilitating transcription of target genes involved in cell fate regulation [75, 76]. Kwon et al. [77] recently demonstrated that Notch1 antagonizes Wnt/β-catenin signaling by reducing levels of active β-catenin in CPCs.

Crosstalk between Notch and Wnt pathways may be partially mediated by specific regulation of GSK3-β, a multifunctional kinase that regulates many cellular processes including proliferation, differentiation, and apoptosis [78]. GSK3-β is constitutively active in resting cells and is negatively regulated in response to external stimuli by phosphorylation on serine *via* activation of several kinases, including Akt and protein kinase C (PKC) [78]. Endoplasmic reticulum (ER) stress signaling through activation of GSK3β is involved in a mechanism of accelerated atherosclerosis in hyperglycemic, hyperhomocysteinemic, and high-fat-fed apolipoprotein E-deficient (apoE$^{(-/-)}$) mouse models; McAlpine et al. showed that atherosclerosis can be attenuated by promoting GSK3β phosphorylation [79]. In diabetes mellitus, increased basal GSK3β activity contributes to accelerated EPC cellular senescence, effect reversed by small molecule antagonism of GSK3β which enhances cell-based therapy following vascular injury [80].

GSK3-β directly binds to Notch and inhibits transcriptional activation of different Notch target genes [81–83]. Activated GSK3-β reduced NICD degradation by the proteasome, while low GSK3-β activity and high Notch signaling correlate with the highly proliferative, undifferentiated nature of EPCs [82]. Phosphorylation of Notch2 by GSK3-β is reversed in the presence of Wnt1, resulting in the upregulation of Hes1 [81].

Integrin signaling is linked to Wnt signaling. Rallis et al. showed that, *in vitro*, Integrin-Linked Kinase (ILK) could phosphorylate GSK3-β and, in turn, activate Wnt signaling. ILK can also activate Notch signaling. Therefore, the phosphorylation of GSK3-β *via* ILK directs Wnt and, thereby, Notch signaling activation [84].

On the other hand a recent report [85] showed that GSK3-β positively regulates the activity of Notch1 and 3 in VSMCs. Ectopic expression of GSK3-β in VSMCs increased NICD levels, promoted CBF-1/RBP-Jκ transactivation, and enhanced Notch target genes expression. Coincidentally, inhibition of GSK3-β activity using a pharmacological inhibitor or reduction in GSK3-β levels by siRNA knockdown resulted in attenuation of Notch activity.

6. Could ROS Modulate Notch and Wnt/β-Catenin Signaling Pathways?

Studies conducted in the last several years have provided clear evidences that both Notch and Wnt/β-catenin pathways are regulated at least in part by Nox-derived ROS [86, 87].

Stretch-induced mechanotransduction in VSMCs is known to be regulated by redox signaling initiated by stretch-induced activation of Nox and consequently increased ROS level [88, 89]. In response to stretch, ROS, in particular H_2O_2, contribute to the activation of arteriolar myogenic response, contraction, and reorientation, through p38 MAPK signaling activation in VSMCs [90–92]. Zhu et al. [93] showed that cyclic, uniaxial stretch of human VSMCs increased Nox derived-ROS formation and Notch3 activation. Catalase, an antioxidant enzyme that degrades H_2O_2, prevented the stretch-induced translocation of Notch3 to the nucleus, increased Hes1 expression, and decreased Notch3 extracellular domain.

In bone marrow-derived mesenchymal stem cells Boopathy et al. [94] observed upregulation of Notch1 and cardiogenic gene expression involving Wnt11 after a myocardial infarction, which induced increased level of H_2O_2. These results are in line with other authors: an increase in Wnt11 expression after oxidative stress injury induced cardiomyogenic differentiation of ESCs and mouse bone marrow mononuclear cells [95].

H_2O_2 decreases the amount of nuclear β-catenin and TCF/LEF-dependent transcription in human embryonic kidney cells. Overexpression of Dvl1 abrogated H_2O_2-induced downregulation of β-catenin suggesting that H_2O_2 negatively modulates Wnt signaling pathway through downregulation of β-catenin [96]. A recent study by Funato et al. [87, 97] identified a thioredoxin-related protein, nucleoredoxin (NRX) as a redox sensitive negative regulator of the canonical Wnt signaling through its interaction with Dvl. NRX usually interacts with Dvl but ROS cause dissociation of NRX from Dvl and enable Dvl to activate the downstream Wnt signaling pathway. Furthermore Kajla et al. [98] demonstrated that Wnt treatment of mouse intestinal cells induced ROS production through Nox1 via activation of the Rac1 guanine nucleotide exchange factor Vav2. Nox1-generated ROS oxidize and inactivate NRX, thereby releasing the NRX-dependent suppression of Wnt/β-catenin signaling through dissociation of NRX from Dvl. Nox1 siRNA inhibits cell response to Wnt, including stabilization of β-catenin, expression of cyclin D1, and c-Myc via the TCF transcription factor.

Msx2, a profibrotic, proosteogenic transcription factor upregulates the expression of multiple Wnt ligands during angiogenesis [99] and enhances aortic canonical Wnt signaling [100]. Msx2-Wnt signaling pathways are induced by tumor necrosis factor α (TNFα) in arterial myofibroblast via tumor necrosis factor receptor 1 (TNFR1). *In vitro* and *in vivo* gene expression studies established that Nox/mitochondria-derived ROS inhibition reduces Msx2 induction by TNFα. Wnt7b as well as β-catenin levels were also reduced, suggesting that ROS metabolism contributes to TNFα induction of Msx2 and Wnt signaling in myofibroblasts via TNFR1 [101].

APC mutation causes Wnt signaling activation and is commonly found in colorectal cancer [102]. Myant et al. [103] showed that activation of Rac1, a component of Nox protein complex, is required for Wnt-driven intestinal stem cell transformation through ROS production and NF-κB activation. Accordingly, increased ROS might contribute to tumorigenesis by activating specific signaling pathways in different cell types [104], one of which is Wnt signaling.

The cardioprotective effect of ischemic preconditioning (IPC) is abolished by overexpression of secreted frizzled protein 1 (sFRP1), an antagonist of the Wnt/Frizzled pathway, and this effect is related to the ability of sFRP1 to decrease the phosphorylation/inhibition of GSK3-β [105]. Cardioprotection involves a link between the mTOR prosurvival pathway and the Wnt pathway *via* ROS that promote activation of Akt and inhibition of GSK3-β. The disruption of the Wnt pathway modulates this loop and induces GSK3-β activation [106].

Coant et al. [86] reported that direct or indirect redox modulation of the PI3K/Akt and Wnt signaling pathways by Nox1 results in phosphorylation/inhibition of GSK3-β and β-catenin translocation into the nucleus as well as Notch1 activation. They show that loss of Nox1 results in increased PTEN activity that in turn inhibits Akt signaling pathway, as well as Wnt/β-catenin and Notch1 signaling. As previously discussed, GSK3-β is an important mediator of Notch-Wnt crosstalk; therefore, it could be a key player by which ROS regulate both pathways.

Taken together these results suggest that redox-dependent regulation of Notch and Wnt/β-catenin signaling could provide further insight into their involvement in vascular biology.

7. Conclusion and Future Perspectives

ROS have long been deemed as noxious molecules in cardiovascular diseases, including systemic and pulmonary hypertension, atherosclerosis, cardiac hypertrophy, and heart failure. With years of efforts, ROS are becoming increasingly recognized as important modulator for a variety of biological functions and pathophysiological states. Recent evidences suggest an even more significant role of ROS: Notch and Wnt/β-catenin signaling modulation. A clear distinction between Notch and Wnt responses is vital for appropriate and robust cell-fate decisions, and ROS modulation of these signaling pathways would provide clues for clinical strategies and drug discovery targeting cardiovascular diseases and cancer.

Above we have discussed how ROS modulation of Notch and Wnt signaling regulates vascular development in different aspects, including stem cells differentiation, angiogenesis, VEGF signaling, endothelial as well as cardiac progenitor cells recruitment, and vascular cell migration. Nonetheless, more details regarding the ROS signaling and pathophysiological functions remain to be elucidated. A deeper insight into the mechanism of how ROS affect normal vascular development, especially CPCs, VSMCs, and ECs differentiation from stem cells, could contribute to a brighter future for regenerative medicine in cardiovascular therapies. Factors that selectively control ROS modulation of Notch and Wnt/β-catenin signaling pathways could have therapeutic effects repressing angiogenesis in tumours or favouring it in ischemic tissues.

Abbreviations

ROS: Reactive oxygen species
Nox: NAD(P)H oxidase
VEGF: Vascular endothelial growth factor
TNFα: Tumor necrosis factor α
GSK3-β: Glycogen synthase kinase 3-β
Dll: Delta-like ligand
Hes: Hairy/enhancer of split
Hey: Hes-related proteins
Dvl: Dishevelled
NRX: Nucleoredoxin
HUVECs: Human umbilical vein endothelial cells
EPCs: Endothelial progenitor cells
CPCs: Cardiac progenitor cells
ESCs: Embryonic stem cells
VSMCs: Vascular smooth muscle cells.

Conflict of Interests

The authors declare no competing financial interests.

Acknowledgments

The authors are grateful to Dr. Laura Landi for her suggestions and comments, which have contributed to the revision of the paper. This work was supported by a grant from Fondazione Annamaria Sechi per il Cuore (FASC), Italy. The funders had no role in study design, data collection and analysis, decision to publish, or preparation of the paper.

References

[1] T. Gaziano, K. S. Reddy, F. Paccaud, S. Horton, and V. Chaturvedi, *Cardiovascular Disease. NBK11767*, 2006.

[2] K. Sugamura and J. F. Keaney Jr., "Reactive oxygen species in cardiovascular disease," *Free Radical Biology and Medicine*, vol. 51, pp. 978–992, 2011.

[3] J. Oshikawa, S.-J. Kim, E. Furuta et al., "Novel role of p66shc in ROS-dependent VEGF signaling and angiogenesis in endothelial cells," *American Journal of Physiology—Heart and Circulatory Physiology*, vol. 302, no. 3, pp. H724–H732, 2012.

[4] C. E. Oon and A. L. Harris, "New pathways and mechanisms regulating and responding to Delta-like ligand 4-Notch signalling in tumour angiogenesis," *Biochemical Society Transactions*, vol. 39, no. 6, pp. 1612–1618, 2011.

[5] K. K. Griendling, C. A. Minieri, J. D. Ollerenshaw, and R. W. Alexander, "Angiotensin II stimulates NADH and NADPH oxidase activity in cultured vascular smooth muscle cells," *Circulation Research*, vol. 74, no. 6, pp. 1141–1148, 1994.

[6] M. Sundaresan, Z.-X. Yu, V. J. Ferrans, K. Irani, and T. Finkel, "Requirement for generation of H2O2 for platelet-derived growth factor signal transduction," *Science*, vol. 270, no. 5234, pp. 296–299, 1995.

[7] B. S. Wung, J. J. Cheng, H. J. Hsieh, Y. J. Shyy, and D. L. Wang, "Cyclic strain-induced monocyte chemotactic protein-1 gene expression in endothelial cells involves reactive oxygen species activation of activator protein 1," *Circulation Research*, vol. 81, no. 1, pp. 1–7, 1997.

[8] S. Rajagopalan, S. Kurz, T. Münzel et al., "Angiotensin II-mediated hypertension in the rat increases vascular superoxide production via membrane NADH/NADPH oxidase activation: contribution to alterations of vasomotor tone," *Journal of Clinical Investigation*, vol. 97, no. 8, pp. 1916–1923, 1996.

[9] K. K. Griendling and G. A. FitzGerald, "Oxidative stress and cardiovascular Injury: part II: animal and human studies," *Circulation*, vol. 108, no. 17, pp. 2034–2040, 2003.

[10] B. Halliwell, "Current status review: free radicals, reactive oxygen species and human disease: a critical evaluation with special reference to atherosclerosis," *British Journal of Experimental Pathology*, vol. 70, no. 6, pp. 737–757, 1989.

[11] K. K. Griendling and G. A. FitzGerald, "Oxidative stress and cardiovascular injury: part II: animal and human studies," *Circulation*, vol. 108, no. 17, pp. 2034–2040, 2003.

[12] J. B. Laursen, S. Rajagopalan, Z. Galis, M. Tarpey, B. A. Freeman, and D. G. Harrison, "Role of superoxide in angiotensin II-induced but not catecholamine- induced hypertension," *Circulation*, vol. 95, no. 3, pp. 588–593, 1997.

[13] G. B. Mancini, G. C. Henry, C. Macaya et al., "Angiotensin-converting enzyme inhibition with quinapril improves endothelial vasomotor dysfunction in patients with coronary artery disease. The TREND (Trial on Reversing ENdothelial Dysfunction) Study," *Circulation*, vol. 94, pp. 258–265, 1996.

[14] S. Yusuf, P. Sleight, J. Pogue, J. Bosch, R. Davies, and G. Dagenais, "Effects of an angiotensin-converting-enzyme inhibitor, ramipril, on cardiovascular events in high-risk patients. The heart outcomes prevention evaluation study investigators," *The New England Journal of Medicine*, vol. 342, pp. 145–153, 2000.

[15] T. J. Guzik, N. E. Hoch, K. A. Brown et al., "Role of the T cell in the genesis of angiotensin II-induced hypertension and vascular dysfunction," *Journal of Experimental Medicine*, vol. 204, no. 10, pp. 2449–2460, 2007.

[16] K. Satoh, P. Nigro, A. Zeidan et al., "Cyclophilin a promotes cardiac hypertrophy in apolipoprotein e-deficient mice," *Arteriosclerosis, Thrombosis, and Vascular Biology*, vol. 31, no. 5, pp. 1116–1123, 2011.

[17] K. K. Griendling, D. Sorescu, and M. Ushio-Fukai, "NAD(P)H oxidase: role in cardiovascular biology and disease," *Circulation Research*, vol. 86, no. 5, pp. 494–501, 2000.

[18] S. G. Rhee, Y. S. Bae, S. R. Lee, and J. Kwon, "Hydrogen peroxide: a key messenger that modulates protein phosphorylation through cysteine oxidation," *Science's STKE*, vol. 2000, no. 53, p. pe1, 2000.

[19] J. D. Lambeth, "NOX enzymes and the biology of reactive oxygen," *Nature Reviews Immunology*, vol. 4, pp. 181–189, 2004.

[20] L. Ahmarani, L. Avedanian, J. Al-Khoury, C. Perreault, D. Jacques, and G. Bkaily, "Whole-cell and nuclear NADPH oxidases levels and distribution in human endocardial endothelial, vascular smooth muscle, and vascular endothelial cells," *Canadian Journal of Physiology and Pharmacology*, vol. 91, pp. 71–79, 2013.

[21] M. Ushio-Fukai, Y. Tang, T. Fukai et al., "Novel role of gp91phox-containing NAD(P)H oxidase in vascular endothelial growth factor-induced signaling and angiogenesis," *Circulation Research*, vol. 91, no. 12, pp. 1160–1167, 2002.

[22] M. Ushio-Fukai, "Redox signaling in angiogenesis: role of NADPH oxidase," *Cardiovascular Research*, vol. 71, pp. 226–235, 2006.

[23] J. J. Khatri, C. Johnson, R. Magid et al., "Vascular oxidant stress enhances progression and sngiogenesis of experimental atheroma," *Circulation*, vol. 109, no. 4, pp. 520–525, 2004.

[24] S. R. Datla, H. Peshavariya, G. J. Dusting, K. Mahadev, B. J. Goldstein, and F. Jiang, "Important role of Nox4 type NADPH oxidase in angiogenic responses in human microvascular endothelial cells in vitro," *Arteriosclerosis, Thrombosis, and Vascular Biology*, vol. 27, no. 11, pp. 2319–2324, 2007.

[25] P. Vallet, Y. Charnay, K. Steger et al., "Neuronal expression of the NADPH oxidase NOX4, and its regulation in mouse experimental brain ischemia," *Neuroscience*, vol. 132, no. 2, pp. 233–238, 2005.

[26] M. Zhang, A. C. Brewer, K. Schröder et al., "NADPH oxidase-4 mediates protection against chronic load-induced stress in mouse hearts by enhancing angiogenesis," *Proceedings of the National Academy of Sciences of the United States of America*, vol. 107, no. 42, pp. 18121–18126, 2010.

[27] N. Urao and M. Ushio-Fukai, "Redox regulation of stem/progenitor cells and bone marrow niche," *Free Radical Biology & Medicine*, vol. 54, pp. 26–39, 2013.

[28] C. M. Souza, D. Davidson, I. Rhee, J. P. Gratton, E. C. Davis, and A. Veillette, "The phosphatase PTP-PEST/PTPN12 regulates endothelial cell migration and adhesion, but not permeability, and controls vascular development and embryonic viability," *The Journal of Biological Chemistry*, vol. 287, pp. 43180–43190, 2012.

[29] G. Leoni, A. Alam, P. A. Neumann et al., "Annexin A1, formyl peptide receptor, and NOX1 orchestrate epithelial repair," *The Journal of Clinical Investigation*, vol. 123, pp. 443–454, 2013.

[30] S. Artavanis-Tsakonas, M. D. Rand, and R. J. Lake, "Notch signaling: cell fate control and signal integration in development," *Science*, vol. 284, no. 5415, pp. 770–776, 1999.

[31] L. M. Christian, "The ADAM family: insights into Notch proteolysis," *Fly*, vol. 6, pp. 30–34, 2012.

[32] L. Miele, "Notch signaling," *Clinical Cancer Research*, vol. 12, pp. 1074–1079, 2006.

[33] Z. A. Al Haj and P. Madeddu, "Notch signalling in ischaemia-induced angiogenesis," *Biochemical Society Transactions*, vol. 37, pp. 1221–1227, 2009.

[34] P. Rizzo, L. Miele, and R. Ferrari, "The Notch pathway: a crossroad between the life and death of the endothelium," *European Heart Journal*, vol. 34, pp. 2504–2509, 2013.

[35] R. Benedito, S. F. Rocha, M. Woeste et al., "Notch-dependent VEGFR3 upregulation allows angiogenesis without VEGF-VEGFR2 signalling," *Nature*, vol. 484, no. 7392, pp. 110–114, 2012.

[36] H. H. Outtz, I. W. Tattersall, N. M. Kofler, N. Steinbach, and J. Kitajewski, "Notch1 controls macrophage recruitment and Notch signaling is activated at sites of endothelial cell anastomosis during retinal angiogenesis in mice," *Blood*, vol. 118, no. 12, pp. 3436–3439, 2011.

[37] J. L. de la Pompa and J. A. Epstein, "Coordinating tissue interactions: notch signaling in cardiac development and disease," *Developmental Cell*, vol. 22, pp. 244–254, 2012.

[38] C. Collesi, L. Zentilin, G. Sinagra, and M. Giacca, "Notch1 signaling stimulates proliferation of immature cardiomyocytes," *Journal of Cell Biology*, vol. 183, no. 1, pp. 117–128, 2008.

[39] M. Nemir, A. Croquelois, T. Pedrazzini, and F. Radtke, "Induction of cardiogenesis in embryonic stem cells via downregulation of Notch1 signaling," *Circulation Research*, vol. 98, no. 12, pp. 1471–1478, 2006.

[40] V. M. Campa, R. Gutiérrez-Lanza, F. Cerignoli et al., "Notch activates cell cycle reentry and progression in quiescent cardiomyocytes," *Journal of Cell Biology*, vol. 183, no. 1, pp. 129–141, 2008.

[41] Y. Funahashi, C. J. Shawber, M. Vorontchikhina, A. Sharma, H. H. Outtz, and J. Kitajewski, "Notch regulates the angiogenic response via induction of VEGFR-1," *Journal of Angiogenesis Research*, vol. 2, no. 1, article 3, 2010.

[42] M. Koyanagi, P. Bushoven, M. Iwasaki, C. Urbich, A. M. Zeiher, and S. Dimmeler, "Notch signaling contributes to the expression of cardiac markers in human circulating progenitor cells," *Circulation Research*, vol. 101, no. 11, pp. 1139–1145, 2007.

[43] J.-L. Li, R. C. A. Sainson, C. E. Oon et al., "DLL4-Notch signaling mediates tumor resistance to anti-VEGF therapy in vivo," *Cancer Research*, vol. 71, no. 18, pp. 6073–6083, 2011.

[44] C. Caliceti, G. Aquila, M. Pannella et al., "17beta-estradiol enhances signalling mediated by VEGF-A-delta-like ligand 4-notch1 axis in human endothelial cells," *PLoS One*, vol. 8, Article ID e71440, 2013.

[45] G. M. Collu, A. Hidalgo-Sastre, A. Acar et al., "Dishevelled limits Notch signalling through inhibition of CSL," *Development*, vol. 139, pp. 4405–4415, 2012.

[46] P. Hayward, K. Brennan, P. Sanders et al., "Notch modulates Wnt signalling by associating with Armadillo/β-catenin and regulating its transcriptional activity," *Development*, vol. 132, no. 8, pp. 1819–1830, 2005.

[47] M. Shin, H. Nagai, and G. Sheng, "Notch mediates Wnt and BMP signals in the early separation of smooth muscle progenitors and blood/endothelial common progenitors," *Development*, vol. 136, no. 4, pp. 595–603, 2009.

[48] A. M. Goodwin and P. A. D'Amore, "Wnt signaling in the vasculature," *Angiogenesis*, vol. 5, no. 1-2, pp. 1–9, 2002.

[49] S. J. Monkley, S. J. Delaney, D. J. Pennisi, J. H. Christiansen, and B. J. Wainwright, "Targeted disruption of the Wnt2 gene results in placentation defects," *Development*, vol. 122, no. 11, pp. 3343–3353, 1996.

[50] T.-O. Ishikawa, Y. Tamai, A. M. Zorn et al., "Mouse Wnt receptor gene Fzd5 is essential for yolk sac and placental angiogenesis," *Development*, vol. 128, no. 1, pp. 25–33, 2001.

[51] A. Cattelino, S. Liebner, R. Gallini et al., "The conditional inactivation of the β-catenin gene in endothelial cells causes a defective vascular pattern and increased vascular fragility," *Journal of Cell Biology*, vol. 162, no. 6, pp. 1111–1122, 2003.

[52] M. Bienz and H. Clevers, "Linking colorectal cancer to Wnt signaling," *Cell*, vol. 103, no. 2, pp. 311–320, 2000.

[53] B. M. Gumbiner, "Carcinogenesis: a balance between β-catenin and APC," *Current Biology*, vol. 7, no. 7, pp. R443–R446, 1997.

[54] G. M. Collu, A. Hidalgo-Sastre, A. Acar et al., "Dishevelled limits Notch signalling through inhibition of CSL," *Development*, vol. 139, pp. 4405–4415, 2012.

[55] M. Kuhl, L. C. Sheldahl, M. Park, J. R. Miller, and R. T. Moon, "The Wnt/Ca2+ pathway: a new vertebrate Wnt signaling pathway takes shape," *Trends in Genetics*, vol. 16, no. 7, pp. 279–283, 2000.

[56] M. Kühl, L. C. Sheldahl, C. C. Malbon, and R. T. Moon, "Ca2+/calmodulin-dependent protein kinase II is stimulated by Wnt and Frizzled homologs and promotes ventral cell fates in Xenopus," *Journal of Biological Chemistry*, vol. 275, no. 17, pp. 12701–12711, 2000.

[57] M. Simons and M. Mlodzik, "Planar cell polarity signaling: from fly development to human disease," *Annual Review of Genetics*, vol. 42, pp. 517–540, 2008.

[58] T. Bouras, B. Pal, F. Vaillant et al., "Notch signaling regulates mammary stem cell function and luminal cell-fate commitment," *Cell Stem Cell*, vol. 3, no. 4, pp. 429–441, 2008.

[59] S. Lowell, P. Jones, I. le Roux, J. Dunne, and F. M. Watt, "Stimulation of human epidermal differentiation by Delta-Notch signalling at the boundaries of stem-cell clusters," *Current Biology*, vol. 10, no. 9, pp. 491–500, 2000.

[60] Y. A. Zeng and R. Nusse, "Wnt proteins are self-renewal factors for mammary stem cells and promote their long-term expansion in culture," *Cell Stem Cell*, vol. 6, no. 6, pp. 568–577, 2010.

[61] S. Fre, M. Huyghe, P. Mourikis, S. Robine, D. Louvard, and S. Artavanis-Tsakonas, "Notch signals control the fate of immature progenitor cells in the intestine," *Nature*, vol. 435, no. 7044, pp. 964–968, 2005.

[62] B. Z. Stanger, R. Datar, L. C. Murtaugh, and D. A. Melton, "Direct regulation of intestinal fate by Notch," *Proceedings of the National Academy of Sciences of the United States of America*, vol. 102, no. 35, pp. 12443–12448, 2005.

[63] J. H. van Es, M. E. van Gijn, O. Riccio et al., "Notch/γ-secretase inhibition turns proliferative cells in intestinal crypts and adenomas into goblet cells," *Nature*, vol. 435, no. 7044, pp. 959–963, 2005.

[64] J. H. van Es, P. Jay, A. Gregorieff et al., "Wnt signalling induces maturation of Paneth cells in intestinal crypts," *Nature Cell Biology*, vol. 7, no. 4, pp. 381–386, 2005.

[65] E. Rampazzo, L. Persano, F. Pistollato et al., "Wnt activation promotes neuronal differentiation of glioblastoma," *Cell Death & Disease*, vol. 4, p. e500, 2013.

[66] M. Corada, D. Nyqvist, F. Orsenigo et al., "The Wnt/beta-catenin pathway modulates vascular remodeling and specification by upregulating Dll4/Notch signaling," *Developmental Cell*, vol. 18, no. 6, pp. 938–949, 2010.

[67] M. Reis, C. J. Czupalla, N. Ziegler et al., "Endothelial Wnt/beta-catenin signaling inhibits glioma angiogenesis and normalizes tumor blood vessels by inducing PDGF-B expression," *The Journal of Experimental Medicine*, vol. 209, pp. 1611–1627, 2012.

[68] H. Clevers, "Wnt/beta-catenin signaling in development and disease," *Cell*, vol. 127, pp. 469–480, 2006.

[69] K. Yamamizu, T. Matsunaga, H. Uosaki et al., "Convergence of Notch and β-catenin signaling induces arterial fate in vascular progenitors," *Journal of Cell Biology*, vol. 189, no. 2, pp. 325–338, 2010.

[70] R. Daneman, D. Agalliu, L. Zhou, F. Kuhnert, C. J. Kuo, and B. A. Barres, "Wnt/β-catenin signaling is required for CNS, but not non-CNS, angiogenesis," *Proceedings of the National Academy of Sciences of the United States of America*, vol. 106, pp. 641–646, 2009.

[71] S. Liebner, M. Corada, T. Bangsow et al., "Wnt/β-catenin signaling controls development of the blood—brain barrier," *Journal of Cell Biology*, vol. 183, no. 3, pp. 409–417, 2008.

[72] S. Maretto, M. Cordenonsi, S. Dupont et al., "Mapping Wnt/β-catenin signaling during mouse development and in colorectal tumors," *Proceedings of the National Academy of Sciences of the United States of America*, vol. 100, no. 6, pp. 3299–3304, 2003.

[73] L.-K. Phng and H. Gerhardt, "Angiogenesis: a team effort coordinated by notch," *Developmental Cell*, vol. 16, no. 2, pp. 196–208, 2009.

[74] J. M. Stenman, J. Rajagopal, T. J. Carroll, M. Ishibashi, J. McMahon, and A. P. McMahon, "Canonical Wnt signaling regulates organ-specific assembly and differentiation of CNS vasculature," *Science*, vol. 322, no. 5905, pp. 1247–1250, 2008.

[75] E. D. Cohen, M. F. Miller, Z. Wang, R. T. Moon, and E. E. Morrisey, "Wnt5a and Wnt11 are essential for second heart field progenitor development," *Development*, vol. 139, pp. 1931–1940, 2012.

[76] A. Klaus, M. Muller, H. Schulz, Y. Saga, J. F. Martin, and W. Birchmeier, "Wnt/beta-catenin and Bmp signals control

distinct sets of transcription factors in cardiac progenitor cells," *Proceedings of the National Academy of Sciences of the United States of America*, vol. 109, pp. 10921–10926, 2012.

[77] S. M. Kwon, C. Alev, and T. Asahara, "The role of notch signaling in endothelial progenitor cell biology," *Trends in Cardiovascular Medicine*, vol. 19, pp. 170–173, 2009.

[78] T. Force and J. R. Woodgett, "Unique and overlapping functions of GSK-3 isoforms in cell differentiation and proliferation and cardiovascular development," *Journal of Biological Chemistry*, vol. 284, no. 15, pp. 9643–9647, 2009.

[79] C. S. McAlpine, A. J. Bowes, M. I. Khan, Y. Shi, and G. H. Werstuck, "Endoplasmic reticulum stress and glycogen synthase kinase-3beta activation in apolipoprotein E-deficient mouse models of accelerated atherosclerosis," *Arteriosclerosis, Thrombosis, and Vascular Biology*, vol. 32, pp. 82–91, 2012.

[80] B. Hibbert, J. R. Lavoie, X. Ma et al., "Glycogen synthase kinase-3beta inhibition augments diabetic endothelial progenitor cell Abundance and functionality via cathepsin B: a novel therapeutic opportunity for arterial repair," *Diabetes*, 2013.

[81] L. Espinosa, J. Inglés-Esteve, C. Aguilera, and A. Bigas, "Phosphorylation by glycogen synthase kinase-3β down-regulates Notch activity, a link for Notch and Wnt pathways," *Journal of Biological Chemistry*, vol. 278, no. 34, pp. 32227–32235, 2003.

[82] D. Foltz, M. C. Santiago, B. E. Berechid, and J. S. Nye, "Glycogen synthase kinase-3β modulates notch signaling and stability," *Current Biology*, vol. 12, no. 12, pp. 1006–1011, 2002.

[83] Y. H. Jin, H. Kim, M. Oh, H. Ki, and K. Kim, "Regulation of Notch1/NICD and Hes1 expressions by GSK-3α/β," *Molecules and Cells*, vol. 27, no. 1, pp. 15–19, 2009.

[84] C. Rallis, S. M. Pinchin, and D. Ish-Horowicz, "Cell-autonomous integrin control of Wnt and Notch signalling during somitogenesis," *Development*, vol. 137, no. 21, pp. 3591–3601, 2010.

[85] S. Guha, J. P. Cullen, D. Morrow et al., "Glycogen synthase kinase 3 beta positively regulates Notch signaling in vascular smooth muscle cells: role in cell proliferation and survival," *Basic Research in Cardiology*, vol. 106, no. 5, pp. 773–785, 2011.

[86] N. Coant, S. B. Mkaddem, E. Pedruzzi et al., "NADPH oxidase 1 modulates WNT and NOTCH1 signaling to control the fate of proliferative progenitor cells in the colon," *Molecular and Cellular Biology*, vol. 30, no. 11, pp. 2636–2650, 2010.

[87] Y. Funato and H. Miki, "Redox regulation of Wnt signalling via nucleoredoxin," *Free Radical Research*, vol. 44, no. 4, pp. 379–388, 2010.

[88] E. Mata-Greenwood, A. Grobe, S. Kumar, Y. Noskina, and S. M. Black, "Cyclic stretch increases VEGF expression in pulmonary arterial smooth muscle cells via TGF-β1 and reactive oxygen species: a requirement for NAD(P)H oxidase," *American Journal of Physiology—Lung Cellular and Molecular Physiology*, vol. 289, no. 2, pp. L288–L298, 2005.

[89] T. Ohmine, Y. Miwa, F. Takahashi-Yanaga, S. Morimoto, Y. Maehara, and T. Sasaguri, "The involvement of aldosterone in cyclic stretch-mediated activation of NADPH oxidase in vascular smooth muscle cells," *Hypertension Research*, vol. 32, no. 8, pp. 690–699, 2009.

[90] Q. Chen, W. Li, Z. Quan, and B. E. Sumpio, "Modulation of vascular smooth muscle cell alignment by cyclic strain is dependent on reactive oxygen species and P38 mitogen-activated protein kinase," *Journal of Vascular Surgery*, vol. 37, no. 3, pp. 660–668, 2003.

[91] P. T. Nowicki, S. Flavahan, H. Hassanain et al., "Redox signaling of the arteriolar myogenic response," *Circulation Research*, vol. 89, no. 2, pp. 114–116, 2001.

[92] B. Su, S. Mitra, H. Gregg et al., "Redox regulation of vascular smooth muscle cell differentiation," *Circulation Research*, vol. 89, no. 1, pp. 39–46, 2001.

[93] J.-H. Zhu, C.-L. Chen, S. Flavahan, J. Harr, B. Su, and N. A. Flavahan, "Cyclic stretch stimulates vascular smooth muscle cell alignment by redoxdependent activation of Notch3," *American Journal of Physiology—Heart and Circulatory Physiology*, vol. 300, no. 5, pp. H1770–H1780, 2011.

[94] A. V. Boopathy, K. D. Pendergrass, P. L. Che, Y. S. Yoon, and M. E. Davis, "Oxidative stress-induced Notch1 signaling promotes cardiogenic gene expression in mesenchymal stem cells," *Stem Cell Research & Therapy*, vol. 4, p. 43, 2013.

[95] M. P. Flaherty, A. Abdel-Latif, Q. Li et al., "Noncanonical Wnt11 signaling is sufficient to induce cardiomyogenic differentiation in unfractionated bone marrow mononuclear cells," *Circulation*, vol. 117, no. 17, pp. 2241–2252, 2008.

[96] S. Y. Shin, C. G. Kim, E. H. Jho et al., "Hydrogen peroxide negatively modulates Wnt signaling through downregulation of beta-catenin," *Cancer Letters*, vol. 212, pp. 225–231, 2004.

[97] Y. Funato, T. Terabayashi, R. Sakamoto et al., "Nucleoredoxin sustains Wnt/β-catenin signaling by retaining a pool of inactive dishevelled protein," *Current Biology*, vol. 20, no. 21, pp. 1945–1952, 2010.

[98] S. Kajla, A. S. Mondol, A. Nagasawa et al., "A crucial role for Nox 1 in redox-dependent regulation of Wnt-beta-catenin signaling," *The FASEB Journal*, vol. 26, pp. 2049–2059, 2012.

[99] A. M. Goodwin and P. A. D'Amore, "Wnt signaling in the vasculature," *Angiogenesis*, vol. 5, no. 1-2, pp. 1–9, 2002.

[100] B. Mao, W. Wu, G. Davidson et al., "Kremen proteins are Dickkopf receptors that regulate Wnt/β-catenin signalling," *Nature*, vol. 417, no. 6889, pp. 664–667, 2002.

[101] C. F. Lai, J. S. Shao, A. Behrmann, K. Krchma, S. L. Cheng, and D. A. Towler, "TNFR1-activated reactive oxidative species signals up-regulate osteogenic Msx2 programs in aortic myofibroblasts," *Endocrinology*, vol. 153, pp. 3897–3910, 2012.

[102] E. R. Fearon, "Molecular genetics of colorectal cancer," *Annual Review of Pathology*, vol. 6, pp. 479–507, 2011.

[103] K. B. Myant, P. Cammareri, E. J. McGhee et al., "ROS production and NF-kappaB activation triggered by RAC1 facilitate WNT-driven intestinal stem cell proliferation and colorectal cancer initiation," *Cell Stem Cell*, vol. 12, pp. 761–773, 2013.

[104] T. Maraldi, C. Prata, D. Fiorentini, L. Zambonin, L. Landi, and G. Hakim, "Induction of apoptosis in a human leukemic cell line via reactive oxygen species modulation by antioxidants," *Free Radical Biology and Medicine*, vol. 46, no. 2, pp. 244–252, 2009.

[105] L. Barandon, P. Dufourcq, P. Costet et al., "Involvement of FrzA/sFRP-1 and the Wnt/Frizzled pathway in ischemic preconditioning," *Circulation Research*, vol. 96, no. 12, pp. 1299–1306, 2005.

[106] F. Vigneron, P. Dos Santos, S. Lemoine et al., "GSK-3β at the crossroads in the signalling of heart preconditioning: implication of mTOR and Wnt pathways," *Cardiovascular Research*, vol. 90, no. 1, pp. 49–56, 2011.

Hindawi Publishing Corporation
BioMed Research International
Volume 2014, Article ID 569563, 8 pages
http://dx.doi.org/10.1155/2014/569563

Research Article

Oxidative Stress and Bone Resorption Interplay as a Possible Trigger for Postmenopausal Osteoporosis

Carlo Cervellati,[1] Gloria Bonaccorsi,[2] Eleonora Cremonini,[1] Arianna Romani,[1] Enrica Fila,[2] Maria Cristina Castaldini,[2] Stefania Ferrazzini,[2] Melchiorre Giganti,[2,3] and Leo Massari[2,4]

[1] *Department of Biomedical and Specialist Surgical Sciences, Section of Medical Biochemistry, Molecular Biology and Genetics, University of Ferrara, Via Borsari 46, 44121 Ferrara, Italy*
[2] *Department of Morphology, Surgery and Experimental Medicine, Menopause and Osteoporosis Centre, University of Ferrara, Via Boschetto 29, 44124 Ferrara, Italy*
[3] *Department of Morphology, Surgery and Experimental Medicine, Laboratory of Nuclear Medicine, University of Ferrara, Via Aldo Moro 8, Cona, 44124 Ferrara, Italy*
[4] *Department of Morphology, Surgery and Experimental Medicine, Section of Orthopaedic Clinic, University of Ferrara, Via Aldo Moro 8, Cona, 44124 Ferrara, Italy*

Correspondence should be addressed to Carlo Cervellati; crvcrl@unife.it

Received 15 November 2013; Accepted 18 December 2013; Published 12 January 2014

Academic Editor: Tullia Maraldi

The underlying mechanism in postmenopausal osteoporosis (PO) is an imbalance between bone resorption and formation. This study was conducted to investigate whether oxidative stress (OxS) might have a role in this derangement of bone homeostasis. In a sample of 167 postmenopausal women, we found that increased serum levels of a lipid peroxidation marker, hydroperoxides, were negatively and independently associated with decreased *bone mineral density* (BMD) in total body ($r = -0.192$, $P < 0.05$), lumbar spine ($r = -0.282$, $P < 0.01$), and total hip ($r = -0.282$, $P < 0.05$), as well as with increased bone resorption rate ($r = 0.233$, $P < 0.05$), as assessed by the serum concentration of C-terminal telopeptide of type I collagen (CTX-1). On the contrary, the OxS marker failed to be correlated with the serum levels of bone-specific alkaline phosphatase (BAP), that is, elective marker of bone formation. Importantly, multiple regression analysis revealed that hydroperoxides is a determinant factor for the statistical association between lumbar spine BMD and CTX-1 levels. Taken together, our data suggest that OxS might mediate, by enhancing bone resorption, the uncoupling of bone turnover that underlies PO development.

1. Introduction

Bone is a dynamic organ that undergoes continuous remodeling by the coordinated, and balanced, resorption and formation activities of, respectively, osteoclasts and osteoblasts [1]. The estrogen decline occurring in women after menopause frequently leads to a derangement of this homeostasis, with an increase of bone turnover rate and a state where resorption exceeds formation [2, 3]. These metabolic changes underlie the onset of postmenopausal osteoporosis (PO), a progressive disease characterized by low bone mass density (BMD), that predispose patients to an increased skeleton fragility and risk of fracture [2, 3]. Consistently, the *in vivo* determination of bone turnover is currently regarded as a helpful tool for the prediction of osteoporotic fractures and, mainly, for the monitoring of therapeutic efficacy [4]. Indeed, there are bone turnover markers that, reflecting the whole-body rates of either bone resorption or formation, provide reliable information regarding the health state of this tissue [4, 5].

In spite of the remarkable progresses achieved in the understanding of how estrogen deficiency induces PO, the underlying pathogenic mechanisms have been found to be complex and multifaceted [2]. One of the most intriguing hypothesis at this regard considers the ability of these sexual hormones to protect bone against oxidative stress (OxS) by acting as antioxidant [6]. *In vitro* and animal experiments, indeed, showed that estrogen withdrawal alters the generation of reactive oxygen species (ROS) and the antioxidant

defense capacity of the cell [7], leading to an accumulation of these oxidant species, which, in turn, are able to stimulate osteoclast formation and resorption activity [8, 9].

This challenging body of evidence prompted us to investigate whether, also *in vivo*, OxS might be an influencing factor for the bone turnover impairment underlying PO development. To address this issue we evaluated a panel of distinct indicators of systemic OxS, along with marker of bone formation (bone-specific alkaline phosphatase, BAP) and resorption (C-terminal telopeptide of type I collagen, CTX-1) in a large population sample, including healthy, osteopenic and osteoporotic, postmenopausal women.

2. Materials and Methods

2.1. Subjects. The subjects examined in the present study were recruited among women undergoing bone densitometry evaluation at the Menopause and Osteoporosis Centre (MOC) of University of Ferrara (Ferrara, Italy). This study was carried out in accordance with the Declaration of Helsinki (World Medical Association, http://www.wma.net/) and the guidelines for Good Clinical Practice (European Medicines Agency, http://www.ema.europa.eu/) and it was approved by the Human research ethics committee of the University. Inclusion criteria were women in postmenopausal status, which was defined as cessation of menses for at least 1 year in accordance with the recent ReSTAGE's modification of the Stages of Reproductive Aging Workshop (STRAW) staging criteria [10]. Postmenopausal status was also checked by the assessment of follicle-stimulating hormone (FSH) and 17-β estradiol (E2) blood levels. According to a priori defined exclusion criteria, we excluded from the study those women who, while the study was being carried out, were using supplements containing the most common antioxidants such as vitamins E, C, and A, beta-carotene, and selenium or following vegetarian or vegan diet; drinking more than 20 g/day of alcohol; either affected by chronic diseases such as diabetes, malabsorption, and *cardiovascular disease* (CVD) or not diagnosed with a chronic disease, but taking medications (antiobesity medications, thyroid hormones, diuretics, antihypertensives, and anticholesterol drugs); undergoing hormone replacement therapy.

One hundred sixty-seven subjects were found to be eligible and were enrolled in the study after signing an informed consent. Each of these women underwent the measurement of body weight, standing height, and waist circumference by trained personnel. Fresh blood (7 mL) was drawn into Vacutainer tubes without anticoagulant by venipuncture after an overnight fast. After 30 minutes of incubation at room temperature, blood samples were centrifuged (4.650 g for 20 min), and the obtained sera were stored at −80°C until analysis.

2.2. Biochemical Assays. All the following assays were performed on serum samples using Tecan Sunrise-96 well microplate spectrophotometer (Tecan group Ltd., UK).

The levels of hydroperoxides were evaluated by colorimetric assay based on the reaction between these lipid peroxidation by-products and the chromogenic compound, that is, N,N-diethyl-para-phenylendiamine (from Sigma-Aldrich, St. Louis, MO, USA) [11–13]. Briefly, for each subject, 5 μL of serum or standard (H_2O_2) was added to a solution containing 190 μL of acetate buffer (pH 4.8) and 5 μL of chromogen (0.0028 M). The solution was incubated at 37°C and then read for optical density after 1 and 4 minutes. The concentration of hydroperoxides was obtained by the average ΔA_{505}/min and expressed as Carratelli Units (CU), where 1 CU corresponds to 0.023 mM of H_2O_2 [11, 12].

The concentration of advanced oxidation protein products (AOPP) was quantified as previously reported [14], with minor modifications. The AOPP assay includes a sample preparation procedure to precipitate triglicerides (3.000 g for 10 minutes in the presence of 25 mM/L $MgCl_2$ and 0.5 mM/L phosphotungstic acid) which strongly interfere with the determination of the marker [14]. Subsequently, 30 μL of supernatant serum (or the standard chloramine-T) was diluted 1 : 5 in phosphate-buffered saline. This solution was added into each well and mixed with 10 μL of 1.16 M potassium iodide and 20 μL of glacial acetic acid to each well. AOPP were measured at 340 nm and expressed as μmol/L of chloramine-T (Sigma-Aldrich) equivalents [14].

The measurement of paraoxonase-1 (PON-1) basal activity was performed as described elsewhere [15]. After addition of 10 μL of 3.3 mmol/L paraoxon (Sigma-Aldrich) to the assay mixture containing 5 μL of serum and 2 mmol/L $CaCl_2$ (in 100 mmol/L Tris/buffer, pH 8), to reach a final volume of 200 μL, the formation of p-nitrophenol was monitored at 412 nm for 3 min. PON-1 basal activity was expressed as U/mL, where one unit is equivalent to 1 nmol of paraoxon hydrolysed/minute/mL.

Total concentration of thiols was determined by the colorimetric 5,5′-Dithiobis(2-nitrobenzoic acid)- (DTNB-) based assay described by Hu [16]. Serum (20 μL), or standard (cysteine), was mixed with 160 μL of 0.2 M Na_2HPO_4 and 2 mM EDTA at pH 8.0 into each well. The absorbance was determined at 405 nm, and 20 μL of 10 mM DTNB (Sigma-Aldrich) in methanol was added to the sample. The absorbance obtained before the addition of DTNB was subtracted from that obtained after incubation with the chromogen. The concentration of thiol groups was expressed as μmoles/L.

The total concentration of nonenzymatic antioxidants (such as uric acid, ascorbic acid, and α-tocopherol) was determined by Ferric Reduction Antioxidant Power (FRAP) assay [17] with slight modifications [18]. FRAP method measures the ability of water- and fat-soluble antioxidants to reduce ferric-tripyridyltriazine (Fe^{3+}-TPTZ) to the ferrous form (Fe^{2+}) which absorbs at 593 nm. Briefly, acetate buffer (pH 3.6), TPTZ (10 mM), and $FeCl_3$ (20 mM) were mixed in the ratio 10 : 1 : 1 to give the working solution. Serum (10 μL), or standard ($FeSO_4$), was added to 190 μL of this solution. The reaction mixture was then incubated at room temperature for 6 minutes and the absorbance value was recorded at 595 nm. The results of this assay were expressed as FRAP units, where 1 FRAP unit corresponds to 100 μmoles/L of Fe^{3+} reduced to Fe^{2+} in 6 minutes.

Levels of ceruloplasmin (expressed as μg/mL) were measured by quantitative competitive sandwich ELISA (AssayPro, St Charles, USA) according to the manufacturer's guidelines.

The measurement of BAP and CTX-1 concentration were performed using OCTEIA Ostase BAP immunoenzymometric assay and ß Cross-Laps Siero (CTx I), respectively, (both kits were from Immunodiagnostic Systems Ltd., Boldon, Tyne and Wear, UK) according to the manufacturer's guidelines.

Concentrations of E2 and FSH were determined by conventional chemiluminescent microparticle immunoassay using the commercial kits Architect Estradiol and Architect FSH from Abbot Laboratories (Abbott Park, IL, USA), respectively, according to the manufacturer's guidelines.

2.3. Bone Densitometry Assessment. Areal bone density was assessed at lumbar spine, hip, and total body by Discovery dual energy X-ray absorptiometry scanner (Hologic Inc, Bedford, MA). Postmenopausal osteoporosis was diagnosed when BMD T-score (the number of standard deviations below the average for a young adult at peak bone density) was lower than 2.5 standard deviations from BMD peak at either femoral neck or lumbar spine, according to WHO guidelines [19]. In accordance with these criteria, women with T-score at either skeleton area between −2.5 and −1.0 were classified as osteopenic and those with a value higher than −1.0 as normal.

2.4. Statistical Analysis. Data were analyzed using SPSS 18.0 for Windows (IBM, Chicago, IL, USA). Continuous variables were first analyzed for the normal distribution by the Kolmogorov-Smirnov and the Shapiro-Wilkinson test. Because the distribution of lumbar spine and neck BMD, CTX-1, hydroperoxides, AOPP, and thiols were highly skewed, we used their *base-10 logarithm* values as the outcome variables. One-way analysis of variance (ANOVA) and of covariance (ANCOVA) for unequal variances (implemented with Bonferroni *post hoc* test to compare two groups at a time) were used to evaluate the difference between sample groups before and after adjustment for confounding factors, respectively. Preliminary multiple regression analyses were performed to evaluate the possibility of collinearity problem among variables to include as covariates in multivariate analysis. Values of variance inflation factor (VIF) above 2.5 were regarded as indicative of multicollinearity. After this analysis, body mass index (BMI) was not included in the covariates set, because of its collinearity with waist circumference and of its weaker correlation with the variables of interest. Finally, univariate (by Pearson's correlation test) and multivariate (by partial correlation or multiple regression) analyses were performed to check the associations between continuous variables. A two-tailed probability value <0.05 was considered statistically significant.

3. Results

The characteristics of the 167 postmenopausal women enrolled in the present study are shown in Table 1. Women with PO were significantly ($P < 0.01$) older compared to those included in the other two study groups. Osteopenic and osteoporotic women presented lower mean values of years since menopause, BMI, and waist circumference compared to the healthy ($P < 0.05$ for all). On the contrary, frequency of smokers and serum levels of E2 and FSH did not significantly vary across the groups. By definition, total, neck, and lumbar spine BMD, as well as the correspondent T-score values, were significantly ($P < 0.01$) higher in healthy with respect to osteopenic and osteoporotic women. Finally, the levels of CTX-1 and BAP were not different among the groups.

As shown in Table 2, there were no significant differences in serum levels of OxS markers among the groups. However, osteopenia and osteoporosis appeared to be associated with a worse oxidative balance. Indeed, compared to healthy women, those affected by these two conditions presented higher levels of the lipid oxidative damage marker, hydroperoxides, and lower levels of total antioxidant power and ceruloplasmin.

The possible association of OxS markers with levels of BMD and bone markers was initially checked by univariate analysis. Among the serum indicators of OxS considered in our study, only hydroperoxides showed significant associations with the parameters we used to evaluate bone health. In specific, this marker was found to be significantly associated with BMD at lumbar spine ($P < 0.01$), total body BMD ($P < 0.05$), and CTX-1 ($P < 0.05$) (Figures 1(a), 1(b), and 1(c), and Table 3). Moreover, these correlations remained significant after adjusting for potential confounding factors such as age, years since menopause, smoking, and waist circumference. Actually, as shown in Table 3, the strengths of the multivariate correlations between the OxS marker and the biochemical and densitometric bone parameters appeared to be stronger than the respective univariate. This effect was more evident for the correlation between hydroperoxides and total hip BMD that resulted to be significant ($P < 0.05$) only in the multivariate analysis.

Since higher levels of CTX-1 and hydroperoxides were found to be predictors of lower lumbar spine BMD, multiple regression analyses were run to unveil whether these associations were independent to each other. To this aim, three separate multiple regression models were performed, where each one included age, years since menopause, smoking, and waist circumference plus the following: hydroperoxides (model 1), CTX-1 (model 2), and hydroperoxides and CTX-1 (model 3). As displayed in Table 4, *the correlation between hydroperoxides and lumbar spine BMD* was significant ($P < 0.01$) regardless of the presence of CTX-1 among the covariates. On the contrary, the association between CTX-1 and lumbar spine BMD did not persist when the OxS marker was included in the multivariate model.

4. Discussion

The widely accepted concept of OxS as a condition that is mutually correlated with aging [20, 21] *has* represented the rationale of several studies on the link between accumulation

Table 1: Principal characteristics of healthy, osteopenic, and osteoporotic postmenopausal women.

	Healthy (n = 38)	Osteopenia (n = 73)	Osteoporosis (n = 56)
Age, years	53.7 ± 4.6	55.6 ± 4.5	58.4 ± 4.3[a,b]
Years since menopause, years	7.4 ± 0.8	7.0 ± 0.8[a]	6.9 ± 0.7[a]
BMI, kg/m^2	26.4 ± 4.1	24.4 ± 2.9[a]	24.2 ± 3.2[a]
Waist circumference, cm	89.3 ± 9.6	84.0 ± 9.2[a]	83.1 ± 8.4[a]
Smoking, %	17.8	14.7	12.9
E2, pg/mL	21.1 ± 7.1	12.9 ± 1.8	13.8 ± 2.6
FSH, mIU/mL	72.1 ± 7.2	85.2± 4.2	79.2 ± 5.2
DXA parameters			
Lumbar spine BMD, g/cm^2	1.04 ± 0.09	0.88 ± 0.09[a]	0.75 ± 0.08[a,b]
Lumbar spine T-score	−0.09 ± 0.77	−1.46 ± 0.73[a]	−2.77 ± 0.70[a,b]
Femoral neck BMD, g/cm^2	0.81 ± 0.06	0.69 ± 0.06[a]	0.62 ± 0.08[a,b]
Femoral neck T-score	−0.28 ± 0.59	−1.39 ± 0.6 [a]	−2.06 ± 0.74[a,b]
Total hip BMD, g/cm^2	0.90 ± 0.06	0.81 ± 0.07[a]	0.62 ± 0.07[a,b]
Total hip T-score	−0.21 ± 0.51	−1.04 ± 0.66[a]	−1.72 ± 0.62[a,b]
Total body BMD, g/cm^2	1.09 ± 0.16	1.05 ± 0.07[a]	0.95 ± 0.07[a,b]
Total T-score	0.35 ± 0.99	−0.67 ± 0.68[a]	−1.60 ± 0.74[a,b]
Bone markers			
CTX-1, ng/mL	0.60 ± 0.21	0.66 ± 0.39	0.67 ± 0.40
BAP, μg/L	27.7 ± 2.7	25.7 ± 1.2	25.1 ± 1.7

Data presented are expressed as % within the group for categorical and mean ± standard deviations for continuous variables.
[a]$P < 0.05$ versus healthy; [b]$P < 0.05$ versus osteopenia.
Abbreviations: BMI: body mass index; E2: estradiol; FSH: follicle stimulating hormones; BMD: bone mass density; CTX-1: C-terminal telopeptide of type I collagen; BAP: bone-specific alkaline phosphatase.

Table 2: OxS markers mean levels in healthy, osteopenic, and osteoporotic postmenopausal women.

	Healthy (n = 38)	Osteopenia (n = 73)	Osteoporosis (n = 56)
Hydroperoxides (CU)	349.3 ± 12.3	352.7 ± 11.7	370.6 ± 10.8
AOPP (μmoles/L)	82.1 ± 8.8	76.6 ± 2.9	87.4 ± 7.6
Thiols (μmoles/L)	225.9 ± 13.9	215.2 ± 12.7	225.0 ± 17.3
Total antioxidant power (FRAP units)	734.1 ± 28.2	675.7 ± 15.7	697.2 ± 21.6
PON-1 (U/mL)	134.1 ± 9.2	138.2 ± 9.3	122.1 ± 12.2
Ceruloplasmin (mg/dL)	52.6 ± 6.7	49.2 ± 4.0	45.9 ± 5.1

Data presented are expressed as mean ± standard errors for continuous variables.
Abbreviations: AOPP: advanced oxidation protein products; CU: Carratelli Units; FRAP: Ferric reduction antioxidant capacity; PON-1: paroxonase-1.

of oxidative damage to biomolecules and the onset of PO [6, 22, 23]. Actually, although PO is a common disease of the elderly, *its main initiating factor is the menopause-related estrogen decline rather than the aging* [3]. It is widely accepted, indeed, that these sexual hormones can protect women against bone loss during the reproductive age [2, 3]. Several lines of evidence suggest that one of the mechanisms adopted by estrogens to accomplish this aim consists of contrasting the, supposed deleterious action of ROS against bone health [2, 6–8]. The data in support of the interplay between OxS and PO onset have been mostly obtained from *in vitro* and animal experiments, which, overall, suggest a potential role of reactive species in uncoupling bone turnover [7, 8, 23]. However, the definitive consensus on the involvement of OxS in the derangement of bone homeostasis is still lacking, due to the controversial results of the few *in vivo* human studies so far conducted.

The present cross-sectional population-based study shows that PO and osteopenia are not associated with an evident impairment of systemic oxidative balance. Indeed, the observed trend of oxidative damage (hydroperoxides and AOPP) and antioxidant defence (thiols, total antioxidant power, PON-1, and ceruloplasmin) markers to increase and decrease, respectively, in subjects affected by these two conditions was not statistically significant. On the other hand, high levels of one of the markers examined, hydroperoxides, were significantly, and independently of potential confounding factors, associated with low BMD in two districts of skeleton, total hip, and lumbar spine, that are highly susceptible to PO-related fractures. These outcomes were in line with the previous few studies involving a homogenous postmenopausal female population [23–25] as ours, but also more heterogeneous populations of men and women [26, 27] or only of men [28]. The aforementioned

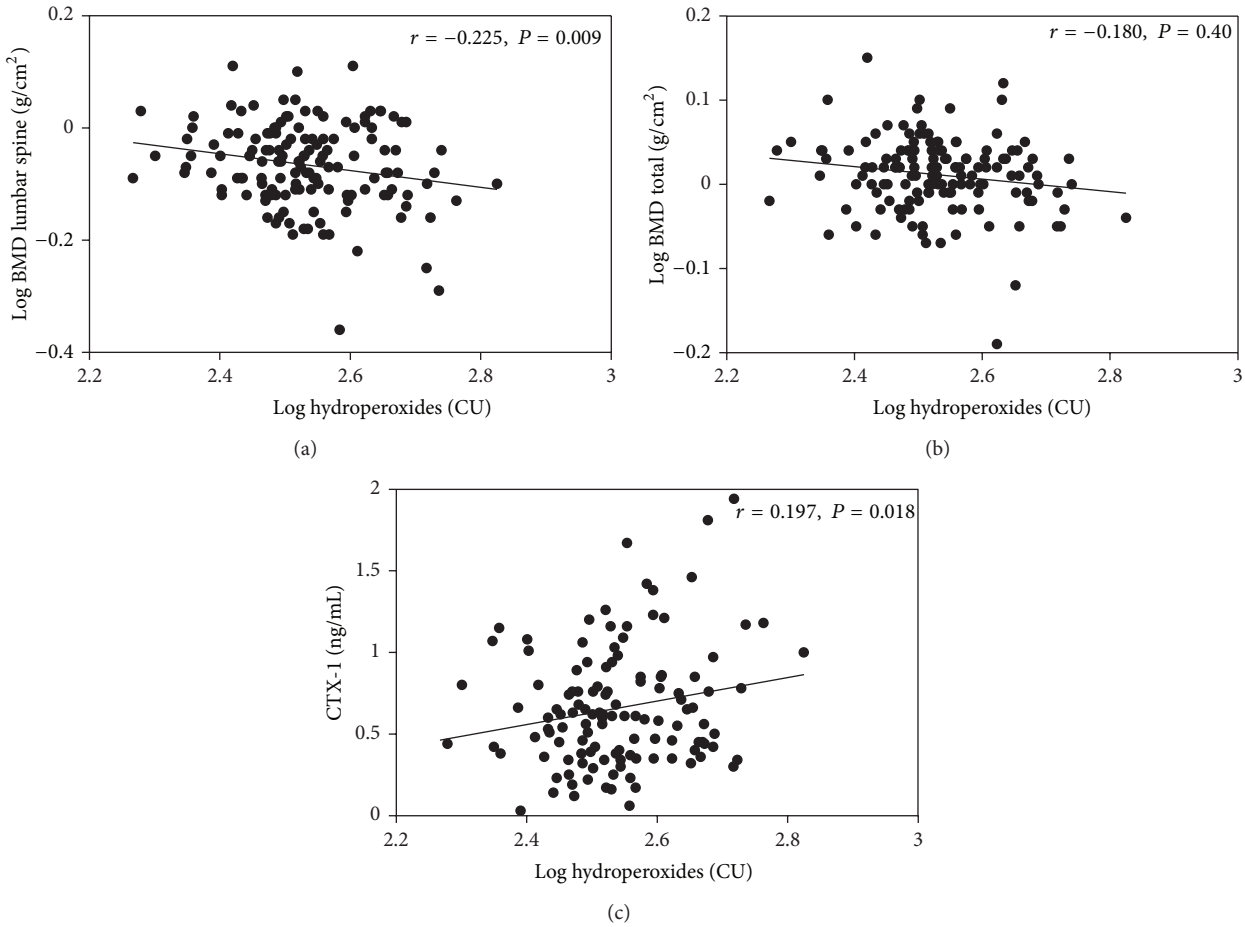

Figure 1: Scatterplots of the relationship between hydroperoxides and lumbar spine BMD (a), total body BMD (b), and CTX-1 (c) in the total sample ($n = 167$). Abbreviations: BMD: bone mass density; CTX-1: C-terminal telopeptide of type I collagen.

Table 3: Simple and partial correlation coefficients for the association of hydroperoxides with total, lumbar spine, and total hip BMD, as well as CTX-1 in the total sample ($n = 167$).

	Simple correlation (r)	Partial correlation (r)
Lumbar spine BMD	−0.225[b]	−0.282[b]
Total hip BMD	−0.120	−0.208[a]
Total body BMD	−0.180[a]	−0.192[a]
CTX-1	0.197[a]	0.233[a]

[a]$P < 0.05$, [b]$P < 0.01$.
Adjusting variables for partial correlation: age, years since menopause, smoking, and waist circumference.
Abbreviations: BMD: bone mass density; CTX-1: C-terminal telopeptide of type I collage.

negative correlation between hydroperoxides and BMD was not reflected in a significant increase of this marker in PO patients most probably because the diagnosis of this bone disease is conventionally based upon T-score, a parameter that is statistically derived from BMD, that, indeed, was not found to be associated with hydroperoxides. Moreover, detectable alterations in circulatory levels of OxS markers are mainly associated with diseases, where, differently from PO, there is an intense tissue damage with consequent release of prooxidant metal ions like iron and copper and mitochondrial impairment or in chronic metabolic disorders such as diabetes and vascular chronic inflammation [21, 29]. Thus, in line with previous studies [6, 25, 30], our results suggest that systemic OxS, *even if* it could not be by itself a distinctive condition of women with PO, *negatively affects bone health thereby increasing the risk to develop this bone degenerative disease*.

Among the findings of our study, the significant positive association between serum levels of hydroperoxides and CTX-1, that is, marker of bone resorption, was the one that mostly adds to the current literature. Indeed, to the best of our knowledge, only another population-based study found

Table 4: Multiple regression analysis of the association of hydroperoxides and CTX-1 with lumbar spine BMD.

Explanatory variables	B* (SE)	β#
	Model 1	
Hydroperoxides	0.262[b] (0.061)	−0.321
	Adjusted R^2 = 0.25	
	Model 2	
CTX-1	−0.044[a] (0.023)	−0.172
	Adjusted R^2 = 0.16	
	Model 3	
Hydroperoxides	−0.246[b] (0.066)	−0.301
CTX-1	−0.026 (0.023)	−0.100
	Adjusted R^2 = 0.25	

Model 1: age, years since menopause, smoking, waist circumference + hydroperoxides.
Model 2: age, years since menopause, smoking, waist circumference + CTX-1.
Model 3: age, years since menopause, smoking, waist circumference + hydroperoxides and CTX-1.
[a]$P < 0.05$; [b]$P < 0.01$.
*Unstandardized regression coefficient; #standardized regression coefficient.
Abbreviations: SE: standard error; CTX-1: C-terminal telopeptide of type I collagen.

this association among postmenopausal women, by using, however, different markers for OxS, that is, 8-hydroxy-2′-deoxyguanosine, and bone resorption, that is, cross-linked carboxyterminal telopeptide of type I collagen (ICTP). These methodological differences between the two works are not entirely negligible, mostly in relation to the latter marker. Indeed, as nicely described by Garnero et al. [31] and others [32, 33], ICTP and CTX-1 reflect different collagenolytic pathways, which in turn take place in distinct bone pathologies. When compared to the other markers, CTX-1 serum level was showed to *be* a more reliable indicator of the osteoclastic resorptive activity. Consistently, the assessment of CTX-1, but not of ICTP, is recommended for monitoring the effectiveness of antiresorptive therapy in patients affected by PO [31].

Further insight into the understanding of the "weight" of OxS in bone loss of postmenopausal women was provided by multivariate analysis. As shown in Table 4, the relationship between decrease in lumbar spine BMD and increase in CTX-1 serum levels was obvious after taking into account a set of strong potential predictors of bone loss (i.e., smoking, age, years since menopause, and waist circumference), but it disappeared after including also hydroperoxides in this set. This statistical outcome led us to speculate that the degradation of the main collagen component of bone organic matrix might be, at some extent, dependent on OxS. This hypothesis is vastly supported by previous *in vitro* studies showing that ROS stimulates osteoclast differentiation and bone resorption in mouse calvarial and bone marrow cultures [34, 35] and cocultures of mouse calvarial osteoblasts and spleen cells [36]. More recently, it has been shown that the increase of ROS, *mostly due to xanthine/xanthine oxidase activity* [37], stimulates the resorption process by triggering osteoclastogenic Nuclear Factor-kappa β (NF-$\kappa\beta$) ligand (RANKL)-RANK signaling between osteoblasts and osteoclast precursors [9, 37]. RANKL binding to RANK initiates osteoclast differentiation and activation and is critical for maintaining their survival and for promoting bone resorption [37]. Consistently, experiments on human bone marrow cells demonstrated that *hydrogen* peroxide is able to induce the expression of RANKL as well as macrophage colony stimulating factor (M-CSF), which activates the former by inducing the expression of RANK on myeloid cells.

Finally, it is fair to acknowledge that the cross-sectional nature of the present study limits our ability to establish any cause-effect relationship between OxS, CTX-1, and BMD. *However, our observations, although preliminary, may represent an important basis for a future longitudinal study aimed to evaluate the potential beneficial effects of nutritional antioxidants on bone health*.

5. Conclusion

In conclusion, our findings show an association between increased hydroperoxides serum levels and reduced bone density in postmenopausal women. Besides, this is the first population-based study showing a positive independent association between this lipid peroxidation marker and serum levels of CTX-1. These results would suggest that OxS might play a role in the development of PO *by* enhancing bone resorption rate. Additional studies are warranted to definitely establish a causal relationship between OxS and bone loss in postmenopause.

Conflict of Interests

The authors declare that there is no conflict of interests regarding the publication of this paper. The authors alone are responsible for the content and writing of the paper.

Acknowledgments

The authors thank Maria Grazia Bonora for her skilled organization of clinical protocol. They also want to thank Monica Squerzanti for her meaningful contribution in data collection and processing. The Study was supported by "Local Research Project" Grant from University of Ferrara, Italy.

References

[1] L. Masi and M. L. Brandi, "Physiopathological basis of bone turnover," *Quarterly Journal of Nuclear Medicine*, vol. 45, no. 1, pp. 2–6, 2001.

[2] M. N. Weitzmann and R. Pacifici, "Estrogen deficiency and bone loss: an inflammatory tale," *Journal of Clinical Investigation*, vol. 116, no. 5, pp. 1186–1194, 2006.

[3] R. Lindsay, "Estrogen deficiency," in *Osteoporosis: Etiology, Diagnosis, and Management*, B. L. Riggs and L. J. Melton,

Eds., pp. 133–160, Lippincott-Raven, Philadelphia, Pa, USA, 2nd edition, 1996.

[4] C. D. Arnaud, "Osteoporosis: using "bone markers" for diagnosis and monitoring," *Geriatrics*, vol. 51, no. 4, pp. 24–30, 1996.

[5] P. D. Delmas, "Clinical use of biochemical markers of bone remodeling in osteoporosis," *Bone*, vol. 13, supplement 1, pp. S17–S21, 1992.

[6] C. Cervellati, G. Bonaccorsi, E. Cremonini et al., "Bone mass density selectively correlates with serum markers of oxidative damage in post-menopausal women," *Clinical Chemistry and Laboratory Medicine*, vol. 51, no. 2, pp. 333–338, 2013.

[7] J. M. Lean, J. T. Davies, K. Fuller et al., "A crucial role for thiol antioxidants in estrogen-deficiency bone loss," *Journal of Clinical Investigation*, vol. 112, no. 6, pp. 915–923, 2003.

[8] J. Lean, B. Kirstein, Z. Urry, T. Chambers, and K. Fuller, "Thioredoxin-1 mediates osteoclast stimulation by reactive oxygen species," *Biochemical and Biophysical Research Communications*, vol. 321, no. 4, pp. 845–850, 2004.

[9] J. M. Hodge, F. M. Collier, N. J. Pavlos, M. A. Kirkland, and G. C. Nicholson, "M-csf potently augments rankl-induced resorption activation in mature human osteoclasts," *PLoS ONE*, vol. 6, no. 6, Article ID e21462, 2011.

[10] S. D. Harlow, S. Crawford, L. Dennerstein, H. G. Burger, E. S. Mitchell, and M.-F. Sowers, "Recommendations from a multistudy evaluation of proposed criteria for Staging Reproductive Aging," *Climacteric*, vol. 10, no. 2, pp. 112–119, 2007.

[11] C. Cervellati, F. S. Pansini, G. Bonaccorsi et al., "17β-estradiol levels and oxidative balance in a population of pre-, peri-, and post-menopausal women," *Gynecological Endocrinology*, vol. 27, no. 12, pp. 1028–1032, 2011.

[12] A. Alberti, L. Bolognini, D. Macciantelli, and M. Caratelli, "The radical cation of N,N-diethl-para-phenylendiamine: a possible indicator of oxidative stress in biological samples," *Research on Chemical Intermediates*, vol. 26, no. 3, pp. 253–267, 2000.

[13] C. Cervellati, E. Cremonini, C. Bosi C et al., "Systemic oxidative stress in older patients with mild cognitive impairment or late onset Alzheimer's disease," *Current Alzheimer Reseach*, vol. 10, no. 4, pp. 365–372, 2013.

[14] V. Witko-Sarsat, M. Friedlander, C. Capeillère-Blandin et al., "Advanced oxidation protein products as a novel marker of oxidative stress in uremia," *Kidney International*, vol. 49, no. 5, pp. 1304–1313, 1996.

[15] J. Bełtowski, G. Wójcicka, and A. Marciniak, "Species- and substrate-specific stimulation of human plasma paraoxonase 1 (PON1) activity by high chloride concentration," *Acta Biochimica Polonica*, vol. 49, no. 4, pp. 927–936, 2002.

[16] M. L. Hu, "Measurement of protein thiol groups and glutathione in plasma," *Methods in Enzymology*, vol. 233, pp. 380–385, 1994.

[17] I. F. Benzie and J. J. Strain, "Ferric reducing/antioxidant power assay: direct measure of total antioxidant activity of biological fluids and modified version for simultaneous measurement of total antioxidant power and ascorbic acid concentration," *Methods in Enzymology*, vol. 299, pp. 15–27, 1998.

[18] F. Pansini, C. Cervellati, A. Guariento et al., "Oxidative stress, body fat composition, and endocrine status in pre- and postmenopausal women," *Menopause*, vol. 15, no. 1, pp. 112–118, 2008.

[19] J. A. Kanis, "Osteoporosis III: diagnosis of osteoporosis and assessment of fracture risk," *The Lancet*, vol. 359, no. 9321, pp. 1929–1936, 2002.

[20] C. M. Bergamini, S. Gambetti, A. Dondi, and C. Cervellati, "Oxygen, reactive oxygen species and tissue damage," *Current Pharmaceutical Design*, vol. 10, no. 14, pp. 1611–1626, 2004.

[21] I. Dalle-Donne, R. Rossi, R. Colombo, D. Giustarini, and A. Milzani, "Biomarkers of oxidative damage in human disease," *Clinical Chemistry*, vol. 52, no. 4, pp. 601–623, 2006.

[22] G. Valacchi, C. Sticozzi, A. Pecorelli et al., "Cutaneous responses to environmental stressors," *Annals of the New York Academy of Science*, vol. 1271, pp. 75–81, 2012.

[23] S. Ozgocmen, H. Kaya, E. Fadillioglu, R. Aydogan, and Z. Yilmaz, "Role of antioxidant systems, lipid peroxidation, and nitric oxide in postmenopausal osteoporosis," *Molecular and Cellular Biochemistry*, vol. 295, no. 1-2, pp. 45–52, 2007.

[24] K. H. Baek, K. W. Oh, W. Y. Lee et al., "Association of oxidative stress with postmenopausal osteoporosis and the effects of hydrogen peroxide on osteoclast formation in human bone marrow cell cultures," *Calcified Tissue International*, vol. 87, no. 3, pp. 226–235, 2010.

[25] S. Ozgocmen, H. Kaya, E. Fadillioglu, R. Aydogan, and Z. Yilmaz, "Role of antioxidant systems, lipid peroxidation, and nitric oxide in postmenopausal osteoporosis," *Molecular and Cellular Biochemistry*, vol. 295, no. 1-2, pp. 45–52, 2007.

[26] D. Maggio, M. Barabani, M. Pierandrei et al., "Marked decrease in plasma antioxidants in aged osteoporotic women: results of a cross-sectional study," *Journal of Clinical Endocrinology and Metabolism*, vol. 88, no. 4, pp. 1523–1527, 2003.

[27] B. Östman, K. Michaëlsson, J. Helmersson et al., "Oxidative stress and bone mineral density in elderly men: antioxidant activity of alpha-tocopherol," *Free Radical Biology and Medicine*, vol. 47, no. 5, pp. 668–673, 2009.

[28] S. Basu, K. Michaëlsson, H. Olofsson, S. Johansson, and H. Melhus, "Association between oxidative stress and bone mineral density," *Biochemical and Biophysical Research Communications*, vol. 288, no. 1, pp. 275–279, 2001.

[29] R. A. Mangiafico, G. Malaponte, P. Pennisi et al., "Increased formation of 8-iso-prostaglandin F2α is associated with altered bone metabolism and lower bone mass in hypercholesterolaemic subjects," *Journal of Internal Medicine*, vol. 261, no. 6, pp. 587–596, 2007.

[30] B. Halliwell and J. M. C. Gutteridge, Eds., *Free Radicals in Biology and Medicine*, Oxford University Press, Oxford, UK, 4th edition, 2007.

[31] P. Garnero, M. Ferreras, M. A. Karsdal et al., "The type I collagen fragments ICTP and CTX reveal distinct enzymatic pathways of bone collagen degradation," *Journal of Bone and Mineral Research*, vol. 18, no. 5, pp. 859–867, 2003.

[32] M. A. Sánchez-Rodríguez, M. Ruiz-Ramos, E. Correa-Muñoz, and V. M. Mendoza-Núñez, "Oxidative stress as a risk factor for osteoporosis in elderly Mexicans as characterized by antioxidant enzymes," *BMC Musculoskeletal Disorders*, vol. 8, p. 124, 2007.

[33] P. D. Delmas, R. Eastell, P. Garnero, M. J. Seibel, and J. Stepan, "The use of biochemical markets of bone turnover in osteoporosis," *Osteoporosis International*, vol. 11, supplement 6, pp. S2–S17, 2000.

[34] P. Garnero, W. J. Shih, E. Gineyts, D. B. Karpf, and P. D. Delmas, "Comparison of new biochemical markers of bone turnover in late postmenopausal osteoporotic women in response to alendronate treatment," *Journal of Clinical Endocrinology and Metabolism*, vol. 79, no. 6, pp. 1693–1700, 1994.

[35] N. Suda, I. Morita, T. Kuroda, and S.-I. Murota, "Participation of oxidative stress in the process of osteoclast differentiation," *Biochimica et Biophysica Acta*, vol. 1157, no. 3, pp. 318–323, 1993.

[36] J. H. Fraser, M. H. Helfrich, H. M. Wallace, and S. H. Ralston, "Hydrogen peroxide, but not superoxide, stimulates bone resorption in mouse calvariae," *Bone*, vol. 19, no. 3, pp. 223–226, 1996.

[37] X. C. Bai, D. Lu, A. Liu et al., "Reactive oxygen species stimulates receptor activator of NF-κB ligand expression in osteoblast," *Journal of Biological Chemistry*, vol. 280, no. 17, pp. 17497–17506, 2005.

Hindawi Publishing Corporation
BioMed Research International
Volume 2014, Article ID 309507, 7 pages
http://dx.doi.org/10.1155/2014/309507

Research Article

Systemic Oxidative Stress and Conversion to Dementia of Elderly Patients with Mild Cognitive Impairment

Carlo Cervellati,[1] Arianna Romani,[1] Davide Seripa,[2] Eleonora Cremonini,[1] Cristina Bosi,[3] Stefania Magon,[3] Carlo M. Bergamini,[1] Giuseppe Valacchi,[4,5] Alberto Pilotto,[6] and Giovanni Zuliani[3]

[1] *Section of Medical Biochemistry, Molecular Biology and Genetics, Department of Biomedical and Specialist Surgical Sciences, University of Ferrara, Via Borsari 46, 44121 Ferrara, Italy*
[2] *Gerontology and Geriatric Research Laboratory, IRCCS Casa Sollievo Della Sofferenza, San Giovanni Rotondo, Viale Cappuccini 1, 71013 Foggia, Italy*
[3] *Section of Internal Medicine, Gerontology, and Clinical Nutrition, Department of Medical Science, University of Ferrara, Via Savonarola 9, 44100 Ferrara, Italy*
[4] *Department of Life Sciences and Biotechnology, University of Ferrara, Via Borsari 46, 44121 Ferrara, Italy*
[5] *Department of Food and Nutrition, Kyung Hee University, 1 Hoegi-dong, Dongdaemun-gu, Seoul 130-701, Republic of Korea*
[6] *Geriatrics Unit, Azienda ULSS 16 Padova, S. Antonio Hospital, Via Facciolati 71, 35127 Padova, Italy*

Correspondence should be addressed to Carlo Cervellati; crvcrl@unife.it

Received 13 November 2013; Accepted 13 December 2013; Published 12 January 2014

Academic Editor: Cristina Angeloni

Mild cognitive impairment (MCI) is regarded as a prodromal phase of late onset Alzheimer's disease (LOAD). It has been proposed that oxidative stress (OxS) might be implicated in the pathogenesis of LOAD. The aim of this study was to investigate whether a redox imbalance measured as serum level of hydroperoxides (i.e., by-products of lipid peroxidation) and/or serum antioxidant capacity might be predictive of the clinical progression of MCI to LOAD. The levels of these two markers were measured in 111 patients with MCI (follow-up: 2.0 ± 0.6 years), 105 patients with LOAD, and 118 nondemented healthy controls. Multivariate analysis adjusted for potential confounding factors, including age, gender, smoking, and comorbidities, showed a significant increase ($P < 0.05$) in baseline levels of OxS in MCI and LOAD as compared to cognitive healthy controls. No differences in either of OxS markers were found by comparing MCI patients who converted ($n = 29$) or not converted ($n = 82$) to LOAD. Overall, these results suggest that systemic OxS might be a precocious feature of MCI and LOAD. However, the role of OxS as an early prognostic marker of progression to LOAD needs further investigations.

1. Introduction

Mild cognitive impairment (MCI) is regarded as an intermediate state between normal aging and dementia [1]. This preclinical condition is characterized by short-term or long-term memory impairment which, at variance of dementia, is not associated with significant daily functional disability [2]. Importantly, almost one half of these individuals evolves to late onset Alzheimer's disease (LOAD), accounting for about 60% of the total cases of dementia in USA and Western countries [3].

In the last decades, the attention of the researchers has been intensely focused on the molecular mechanisms underlying the etiopathogenesis of LOAD in older individuals. These efforts have produced multiple proofs in support of a key role of oxidative stress (OxS) in the onset and development of LOAD [4, 5].

In physiological conditions, there is a balance between oxidant molecules, among which reactive oxygen species (ROS) are the most studied, and antioxidants species [6, 7]. OxS occurs when this balance shifts towards reactive species generation leading to cellular/tissue oxidative damage [8].

Growing *in vitro* and animal evidence [9–11] suggest that OxS might be the "armed hand" of the amyloid-β (Aβ) peptides aggregates, which are the main constituent of senile plaques in the brain of LOAD patients. Indeed, it has been shown that these peptides form oligomers that could exert neurotoxicity effects by enhancing ROS level in the brain [12]. More specifically, from these experiments it emerged that Aβ oligomers can directly generate H_2O_2 (through a cupper-dependent superoxide dismutase-like activity [13]), activate NADPH-oxidase in astrocytes, and induce ROS production in mitochondria, by modulating the activity of enzymes like Aβ-binding alcohol dehydrogenase and α-ketoglutarate dehydrogenase [12, 14].

Further proofs, although still controversial, of the association between LOAD and OxS have been gathered by human studies [15–17]. Most of these studies showed that, as compared with elderly controls, patients affected by MCI or LOAD display increased oxidative damage, in particular to lipids (peroxidation), along with decreased antioxidants levels in peripheral fluids [15, 17]. However, due to the cross-sectional design, most of these studies were unable to establish any cause-effect relationships between OxS and cognitive impairment or dementia.

To the best of our knowledge, the available literature lacks of longitudinal studies, based on large population sample, investigating the temporal relationship between OxS and dementia. To address this crucial issue, we conducted a prospective study with the aim of investigating whether baseline serum level of hydroperoxides (i.e., by-products of lipid peroxidation) and/or serum antioxidant capacity might be predictive in the clinical progression from MCI to LOAD.

2. Materials and Methods

2.1. Study Design. The present study was conducted according to the Declaration of Helsinki (World Medical Association, http://www.wma.net/), the guidelines for Good Clinical Practice (European Medicines Agency, http://www.ema.europa.eu/), and the guidelines Strengthening the Reporting of Observational Studies in Epidemiology guidelines (http://www.strobe-statement.org/), and it was approved by the local Ethic Committee for human experimentation.

Written informed consent for research was obtained from each patient or from relatives or a legal guardian.

Personal data and medical history were collected by a structured interview from patients and caregivers. All patients underwent a general and neurological examination. For neuropsychological assessment, all patients were given a battery of tests as previously described [18]. Routine analyses were performed to exclude causes of secondary cognitive impairment, including serum B_{12} vitamin, serum folate, liver function tests including ammonia, kidney function tests, thyroid function tests, blood cell count, and arterial oxygen saturation. Subjects affected by severe congestive heart failure, severe liver or kidney disease, severe chronic obstructive pulmonary disease, and cancer were excluded. There were no evidences of acute illnesses at the time of clinical observation and blood sampling; no subject was taking NSAIDS, antibiotics, or steroids at the time of recruitment.

Criteria used for the diagnosis of diabetes, arterial hypertension, and cardiovascular diseases (CVD) were reported elsewhere [18]. Smokers were defined as patients with present or previous significant history of smoking (>180 packs/years).

2.1.1. Diagnosis of MCI. From 1 January 2006 to 31 December 2012, one hundred eleven patients with diagnosis of MCI consecutive referring to the Day Hospital Services for Cognitive Decline (University of Ferrara, Italy) or to the Geriatric Unit of the IRCCS Casa Sollievo della Sofferenza (San Giovanni Rotondo, Italy) and followed for a mean period of 2 years (2.0 ± 0.6 years) were enrolled. Further 88 MCI patients were added to the MCI group (total number of MCI: 199) in the cross-sectional analysis.

MCI was defined as the presence of short/long-term memory impairment, with/without impairment in other single or multiple cognitive domains, in an individual who did not meet the standardized criteria for dementia [2]. We also required that the patient with MCI would be still independent in the activities of daily living (ADLs). Subjects with MCI due to known causes (e.g., severe depression, extensive white matter pathology, severe vitamin B_{12} deficiency) had been excluded. MCI patients were divided into 2 subgroups on the basis of clinical evolution at follow-up: (A) 82 patients whose cognitive performance remained stable or slightly improved (MCI/MCI); (B) 29 patients converted to LOAD during follow-up (MCI/LOAD). The diagnosis of LOAD during the follow-up was made according to the NINCDS-ADRDA criteria [19].

2.1.2. Diagnosis of LOAD. Trained geriatricians in 105 patients made diagnosis of LOAD according to the NINCDS-ADRDA criteria. Only patients with "probable" Alzheimer's disease were selected for the inclusion in the study in order to increase specificity. The Global Deterioration Scale ranged from stage 4 to stage 6.

2.1.3. Cognitive Healthy Controls. One hundred eighteen normal older individuals (controls) without any evidence of dementia and without any functional disability attributable to cognitive impairment were included in the study.

2.2. Assays of Biochemical Parameters. Venous blood was collected from subjects upon an overnight fast, between 8.30 and 9.30 A.M. Each blood sample was then stored for one hour at room temperature and centrifuged (3000 ×g for 10 minutes) to obtain serum which was then divided into aliquots and stored at –80° until analysis.

Hydroperoxides were assessed by colorimetric assay based on the reaction between these lipid peroxidation by-products and N,N-dimethyl-para-phenylenediamine [20, 21]. This method is based on the ability of transition metals to catalyze the formation of alkoxide and peroxide from hydroperoxides. These two radicals strongly interact with the chromogenic reagent, producing a radical cation that

absorbs at 505 nm. Briefly, for each subject, 20 μL of serum or standard (H_2O_2) were added to a solution containing 1960 μL of acetate buffer (pH 4.8) and 20 μL of chromogen (0.0028 M). The solution was incubated (37°C) and then read for optical density after 1 and 4 minutes. The concentration of hydroperoxides was obtained by the average ΔA_{505}/min and expressed as Carratelli Units (CU), where 1 CU corresponds to 0.023 mM of H_2O_2 [20, 21].

The total amount of nonenzymatic serum antioxidants (such as uric acid, ascorbic acid, and α-tocopherol) was spectrophotometrically determined by Ferric Reduction Antioxidant Power (FRAP) assay [22] with modifications described in our previous study [15]. FRAP method measures the ability of water and fat-soluble antioxidants to reduce ferric-tripyridyltriazine (Fe^{3+}-TPTZ) to the ferrous form (Fe^{2+}) which absorbs at 593 nm. Briefly, acetate buffer (pH 3.6), TPTZ (10 mM), and $FeCl_3$ (20 mM) were mixed in the ratio 10 : 1 : 1 to give the working solution. 30 μL of serum or standard ($FeSO_4$) were added to 970 μL of this solution. The reaction mixture was then incubated at room temperature for 6 minutes and the adsorbance value was recorded at 595 nm. The results of this assay were expressed as FRAP units, where 1 FRAP corresponds to 100 μmoles/L of Fe^{3+} reduced to Fe^{2+} in 6 minutes.

FRAP assay is strongly influenced by the amount of uric acid, of which role as physiological antioxidant is highly controversial [23]. To overcome this bias, urate concentration was separately assessed by direct enzymatic method (in which urate is oxidized by uricase coupled with peroxidase [23]) and then subtracted from FRAP values. The resulting parameter (expressed in FRAP units), that is, residual antioxidant power (RAP), affords a reliable index of antioxidant status in uric acid-rich fluids such as serum [22, 24].

2.3. Brain Computer Tomography Scan. All patients (LOAD and MCI) underwent a brain Computer Tomography (CT). The instrument used was a third-generation SIEMENS SOMATON HQ. The slice thickness was 10 mm. Radiograms were evaluated by trained radiologists who were not informed about the clinical characteristics of the patient. The CT scan information was used to support the clinical diagnosis and to diagnose possible brain pathologies associated with secondary cognitive impairment.

2.4. Statistical Analysis. Means were compared by ANOVA and ANCOVA (Fisher's least significant difference as *post hoc* test), while prevalences were compared by the χ^2 test. Since the distribution of RAP was skewed, the values were log-transformed in order to approximate a normal distribution before entering univariate and multivariate analysis. The covariates included in the ANCOVA analysis for OxS markers were the following: age (years), gender (M/F), CVD (yes/no), diabetes (yes/no), hypertension (yes/no), and smoking habit (current, never). A two-tailed probability value <0.05 was considered statistically significant. SPSS 17.00 for Windows (Chicago, IL, USA) was used for statistical analysis.

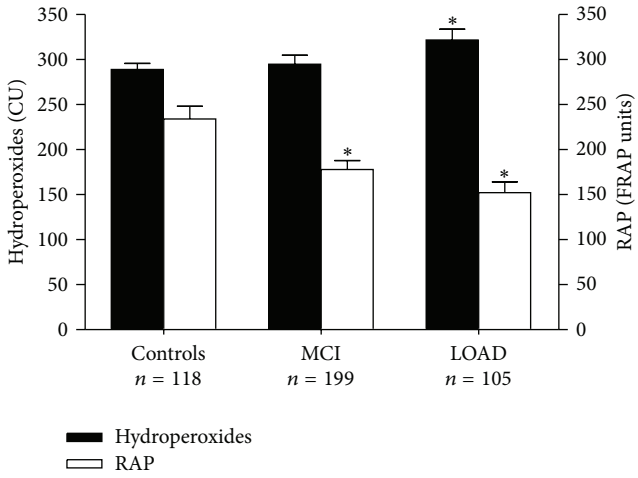

Figure 1: Mean levels of hydroperoxides and RAP in nondemented healthy controls, total MCI (MCI/MCI + MCI/LOAD + MCI no follow-up), and LOAD patients. CU = Carratelli Units; FRAP = Ferric reduction antioxidant capacity. In the ANCOVA model: age, gender, hypertension, cardiovascular diseases, diabetes, and smoking habit. $^*P < 0.01$ versus controls.

3. Results

The main characteristics of the four groups of subjects enrolled into the study are reported in Table 1. MCI/MCI, MCI/LOAD, and LOAD patients were older and had a lower formal education level compared to controls. Both MCI groups presented a lower percentage of women compared with the other two groups, while the frequency of smokers did not consistently vary among groups. As expected by selection criteria, the average Mini Mental State Examination (MMSE) score was pathological in LOAD, while it was within normal limits in both MCI groups and controls. As regards comorbidities, CVD and diabetes were more frequent in the MCI groups compared with controls and LOAD, while hypertension was more frequent in LOAD patients with respect to controls.

In Table 2 are described the mean levels of serum hydroperoxides and residual antioxidant power (RAP) in controls, MCI/MCI, MCI/LOAD, and LOAD patients. Compared to healthy individuals, serum hydroperoxides were higher while RAP was lower in LOAD, after taking into account the possible effect of age, gender, smoking, and comorbidities (ANCOVA *post hoc* $P < 0.01$). Serum hydroperoxides were higher in MCI/MCI subjects than in controls (ANCOVA *post hoc* $P < 0.05$), while no difference in either OxS markers emerged by comparing the two MCI subgroups. When the whole group of MCI (111 with follow-up plus 88 without follow-up) was considered, a significant increase in hydroperoxides (ANCOVA *post hoc* $P < 0.01$) together with a significant reduction of RAP (ANCOVA *post hoc* $P < 0.01$) was observed compared with controls (Figure 1).

Based on the median values of OxS markers from the whole sample (i.e., 305.0 CU for hydroperoxides, and

Table 1: Principal characteristics of nondemented healthy controls, MCI/MCI, MCI/LOAD, and LOAD patients.

	Controls (n = 118)	MCI/MCI (n = 82)	MCI/LOAD (n = 29)	LOAD (n = 105)
Age (years)	69.5 ± 9.1	75.9 ± 6.7[c]	78.6 ± 5.7[c]	78.1 ± 5.5[c]
Female gender (%)	72.0[a,b]	54.8	51.7	70.1[a,b]
Formal education (years)	9.1 ± 4.3	5.9 ± 3.4[c]	6.4 ± 4.1[c]	5.3 ± 3.5[c]
MMSE score (/30)	26.7 ± 2.7	25.8 ± 2.9[b,c]	24.1 ± 2.3[a,c]	20.4 ± 4.4[a,b,c]
GDS (/15)	6.2 ± 3.5	5.9 ± 2.6	5.4 ± 3.4	5.4 ± 3.3
Hypertension (%)	42.1	55.1	54	64.1[c]
Diabetes (%)	10.1[a,b]	20.1	24.2	13.7[a,b]
CVD (%)	9.5[a,b]	25.6	25.1	16.7[a,b]
Smoking (%)	8.5	5.1	4.7	8.1

Continuous variables are expressed as mean ± standard deviation. MCI/MCI: stable MCI patients; MCI/LOAD: MCI patients converted to LOAD. CVD: cardiovascular disease; MMSE: Mini Mental State Examination; GDS: Global Deterioration Scale.
[a]$P < 0.05$ versus MCI/MCI; [b]$P < 0.05$ versus MCI/LOAD; [c]$P < 0.05$ versus controls.

Table 2: Mean levels (mean ± standard error of the mean, SEM) of serum hydroperoxides and residual antioxidant power (RAP) in nondemented healthy controls, MCI/MCI, MCI/LOAD, and LOAD patients.

	Controls (n = 118)	MCI/MCI (n = 82)	MCI/LOAD (n = 29)	LOAD (n = 105)	ANCOVA (P)
Hydroperoxides (CU)	288.1 ± 11.9	295.8 ± 10.0[c]	281.2 ± 17.5	320.9 ± 12.9[c]	0.01
RAP (FRAP units)	234.5 ± 16.0	187.5 ± 16.2	205.1 ± 22.1	152.2 ± 15.5[c]	0.06

MCI/MCI: stable MCI patients; MCI/LOAD: MCI patients converted to LOAD. CU: Carratelli Units; FRAP: Ferric reduction antioxidant capacity. In the ANCOVA model: age, gender, hypertension, cardiovascular diseases, diabetes, and smoking habit.
[c]$P < 0.05$ or $P < 0.01$ versus controls.

208.8 FRAP units for RAP) three subgroups of individuals were identified: (1) favourable redox balance: low hydroperoxides and high RAP; (2) intermediate OxS: high hydroperoxides and high RAP or low hydroperoxides and low RAP; (3) full blown OxS: high hydroperoxides and low RAP. In Figure 2 are reported the within sample group (Controls, MCI/MCI, MCI/LOAD, and LOAD) percentages of subjects with different degree of OxS. In line with the ANCOVA results, controls and LOAD displayed opposite proportions as regards the two extreme states of oxidative balance. Notably, the relative percentages of favourable redox balance and full blown OxS in MCI/dementia were markedly different (about three times for both) from those of LOAD patients.

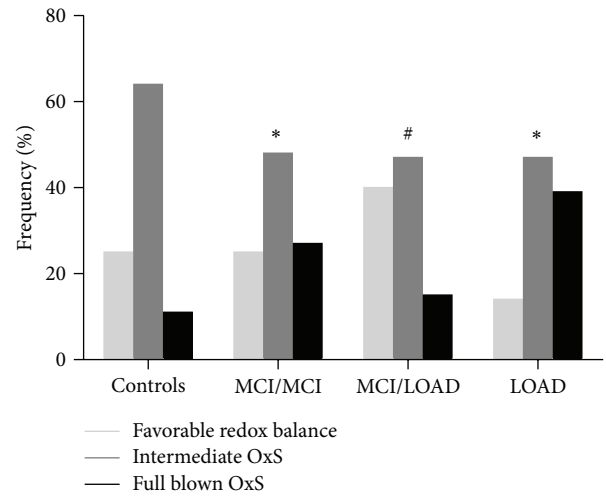

Figure 2: Within group percentages of subjects with Favorable Oxidative Balance, Intermediate OxS, or Full Blown OxS (for definitions see text). CU = Carratelli Units; FRAP = Ferric reduction antioxidant capacity. MCI/MCI: stable MCI patients. MCI/dementia: MCI patients converted to LOAD. *$P < 0.01$ versus Controls; #$P < 0.01$ versus LOAD.

4. Discussion

Most of the proofs supporting the involvement of OxS in LOAD development have been generated by experiments on cell cultures, animals and *postmortem* human brain tissues [9, 10, 25–27]. On the contrary, data from human studies are conflicting [15–17, 28, 29] and do not allow to draw a definitive picture about the role of OxS in the onset and progression of this neurodegenerative disorder.

In the present study, we evaluated the serum levels of hydroperoxides and RAP in a large sample of individuals including healthy controls, LOAD, and MCI patients that during 2-year follow-up remained either stable or converted to dementia. The main finding was that neither baseline level of the two peripheral markers was able to predict the progression from MCI to LOAD. In other words, the evaluation of systemic OxS by using these markers might not be a helpful tool in differencing MCI patients who are going to evolve to LOAD.

Overall, our data are consistent with those shown by one of the few other longitudinal studies employing a broad spectrum of nonenzymatic and enzymatic antioxidants, as well as lipid and protein oxidation markers [30]. In their prospective study conducted in a sample of 70 MCI subjects,

Baldeiras et al. did not find significant differences in any of the baseline indexes of oxidative damage and antioxidant defence measured between stable and progressing to dementia individuals [30]. In contrast, in another study conducted on a similar number of subjects, F2-isoprostanes measured in cerebrospinal fluid (CSF) were significantly higher in MCI patients who later converted to LOAD compared to stable patients [31]. The discrepancies between these data and ours might be mainly due to the differences regarding the markers (and biological fluids) that were employed for OxS detection as well as regarding the general characteristics (e.g., age and lifestyle habits) of the population samples.

However, some important indications arise from the analysis of our cross-sectional data, which appear to confirm the results of previous works conducted on smaller samples [13, 17]. Our data clearly suggest from one side that OxS might represent an early event in LOAD pathogenesis and also that the process of redox balance derangement might take place in its prodromal phase (Figure 1). Consistently, mitochondrial dysfunction [32] and iron homeostasis dysregulation [27], which are believed to be the major causes of cumulative oxidative damage observed in neurons of LOAD [14], are also present in subject with MCI. Moreover, *postmortem* studies on brain tissues identified similar level of ROS by-products in proteins, lipids, and DNA from hippocampus and prefrontal regions in MCI and LOAD patients [33]. In particular, the identification of carbonylated and nitrated proteins common for MCI and Alzheimer's disease by redox proteomic approach suggests that key oxidative pathways can be an early event and playing, therefore, a role in the initial progression of the neurodegenerative process [34]. Oxidative protein damage is not random, but highly selective, and affects enzymes involved in energy metabolism (enolase, lactate dehydrogenase, creatine kinase, etc.), protein turnover (ubiquitin carboxyl terminal hydroxylase L1, UCHL-1), and control of excitotoxicity (glutamine synthetase) [35, 36].

Notably, the biomolecules present in neurons of these patients are highly vulnerable to oxidative challenge, because the low expression of endogen antioxidants (e.g., glutathione and coenzyme Q10) [34, 35]. This phenomenon is mostly due to a process (most probably caused by Aβ deposition) that leads to low expression of nuclear factor, E2-related factor 2 (Nrf2), that is responsible for activating transcription of antioxidant genes in the response to OxS [34, 36, 37].

The evidence of a similar oxidative and inflammatory [38] pattern in MCI and LOAD strengthen the widely supported concept of a biochemical equivalence between pre- and clinical conditions [39] which, in turn, might explain the lack of differences between MCI/MCI and MCI/dementia shown in our study.

In our opinion, our data adds to clinical practise, especially as it regards the use of antioxidant supplementation in the treatment of MCI and LOAD patients. Indeed, if confirmed on larger samples, the finding that OxS level might not be crucial for the progression from MCI to LOAD might explain the ineffectiveness of antioxidant therapy in MCI patients [40]. On the contrary, this approach would be possibly beneficial in healthy subjects that still do not present the signs of an altered oxidative balance.

Finally, we would like also to underline some limitations and strengths of this study. First, the full assessment of nutritional status was not performed in the subjects of this study. For this reason, it is difficult to establish, with a high degree of certainty, whether the decrease of RAP observed in MCI and LOAD patients is linked to a ROS-dependent depletion or to a scarce dietary intake of antioxidants. Second, we are aware that other markers of OxS might be more helpful than those we used in this study, for the understanding of the mechanism underlying the relationship between OxS and LOAD. In particular, the measurement of 4-hydroxynonenal (4HNE)-protein adducts could be used to address this aim, because of their proved ability to modulate signaling pathway [41]. Third, to the best of our knowledge, the sample MCI subjects enrolled for longitudinal study ($n = 111$), as well the size of the whole cross-sectional sample ($n = 422$), are by far the largest among human studies on this specific topic.

5. Conclusion

Taken together our data suggest that OxS might be precociously involved in LOAD pathogenesis. However, further investigations are needed to determine the appropriate OxS indicators to be measured in the progression from MCI to LOAD needs.

Conflict of Interests

The authors declare that there is no conflict of interests regarding the publication of this paper.

Acknowledgments

This work was partly supported by "Ministero della Salute," IRCCS Research Program, Ricerca Corrente 2012–2014, Linea n. 2 "Malattie complesse" and by the "5 × 1000" voluntary contribution.

References

[1] W. R. Markesbery, F. A. Schmitt, R. J. Kryscio, D. G. Davis, C. D. Smith, and D. R. Wekstein, "Neuropathologic substrate of mild cognitive impairment," *Archives of Neurology*, vol. 63, no. 1, pp. 38–46, 2006.

[2] R. C. Petersen, R. Doody, A. Kurz et al., "Current concepts in mild cognitive impairment," *Archives of Neurology*, vol. 58, no. 12, pp. 1985–1992, 2001.

[3] D. Anchisi, B. Borroni, M. Franceschi et al., "Heterogeneity of brain glucose metabolism in mild cognitive impairment and clinical progression to Alzheimer disease," *Archives of Neurology*, vol. 62, no. 11, pp. 1728–1733, 2005.

[4] M. A. Lovell and W. R. Markesbery, "Oxidative damage in mild cognitive impairment and early Alzheimer's disease," *Journal of Neuroscience Research*, vol. 85, no. 14, pp. 3036–3040, 2007.

[5] P. Rinaldi, M. C. Polidori, A. Metastasio et al., "Plasma antioxidants are similarly depleted in mild cognitive impairment and in Alzheimer's disease," *Neurobiology of Aging*, vol. 24, no. 7, pp. 915–919, 2003.

[6] G. Valacchi, C. Sticozzi, A. Pecorelli et al., "Cutaneous responses to environmental stressors," *Annals of the New York Academy of Science*, vol. 1271, pp. 75–81, 2012.

[7] I. Dalle-Donne, R. Rossi, R. Colombo, D. Giustarini, and A. Milzani, "Biomarkers of oxidative damage in human disease," *Clinical Chemistry*, vol. 52, no. 4, pp. 601–623, 2006.

[8] C. M. Bergamini, S. Gambetti, A. Dondi, and C. Cervellati, "Oxygen, reactive oxygen species and tissue damage," *Current Pharmaceutical Design*, vol. 10, no. 14, pp. 1611–1626, 2004.

[9] D. Boyd-Kimball, R. Sultana, H. F. Poon et al., "Proteomic identification of proteins specifically oxidized by intracerebral injection of amyloid β-peptide (1–42) into rat brain: implications for Alzheimer's disease," *Neuroscience*, vol. 132, no. 2, pp. 313–324, 2005.

[10] Y. Matsuoka, M. Picciano, J. la Francois, and K. Duff, "Fibrillar β-amyloid evokes oxidative damage in a transgenic mouse model of Alzheimer's disease," *Neuroscience*, vol. 104, no. 3, pp. 609–613, 2001.

[11] D. Praticò, K. Uryu, S. Leight, J. Q. Trojanoswki, and V. M.-Y. Lee, "Increased lipid peroxidation precedes amyloid plaque formation in an animal model of Azheimer amyloidosis," *Journal of Neuroscience*, vol. 21, no. 12, pp. 4183–4187, 2001.

[12] M. Valko, D. Leibfritz, J. Moncol, M. T. D. Cronin, M. Mazur, and J. Telser, "Free radicals and antioxidants in normal physiological functions and human disease," *International Journal of Biochemistry and Cell Biology*, vol. 39, no. 1, pp. 44–84, 2007.

[13] K. J. Barnham, C. L. Masters, and A. I. Bush, "Neurodegenerative diseases and oxidatives stress," *Nature Reviews Drug Discovery*, vol. 3, no. 3, pp. 205–214, 2004.

[14] P. Mao and P. H. Reddy, "Aging and amyloid beta-induced oxidative DNA damage and mitochondrial dysfunction in Alzheimer's disease: implications for early intervention and therapeutics," *Biochimica et Biophysica Acta*, vol. 1812, no. 11, pp. 1359–1370, 2011.

[15] C. Cervellati, E. Cremonini, C. Bosi et al., "Systemic oxidative stress in older patients with mild cognitive impairment or late onset Alzheimer's disease," *Current Alzheimer Research*, vol. 10, no. 4, pp. 365–372, 2013.

[16] M. C. Irizarry, Y. Yao, B. T. Hyman, J. H. Growdon, and D. Praticò, "Plasma F2A isoprostane levels in Alzheimer's and Parkinson's disease," *Neurodegenerative Diseases*, vol. 4, no. 6, pp. 403–405, 2007.

[17] I. Guidi, D. Galimberti, S. Lonati et al., "Oxidative imbalance in patients with mild cognitive impairment and Alzheimer's disease," *Neurobiology of Aging*, vol. 27, no. 2, pp. 262–269, 2006.

[18] G. Zuliani, M. Ranzini, G. Guerra et al., "Plasma cytokines profile in older subjects with late onset Alzheimer's disease or vascular dementia," *Journal of Psychiatric Research*, vol. 41, no. 8, pp. 686–693, 2007.

[19] G. McKhann, D. Drachman, and M. Folstein, "Clinical diagnosis of Alzheimer's disease: report of the NINCDS-ADRDA work group under the auspices of Department of Health and Human Services Task Force on Alzheimer's disease," *Neurology*, vol. 34, no. 7, pp. 939–944, 1984.

[20] A. Alberti, L. Bolognini, D. Macciantelli, and M. Caratelli, "The radical cation of N,N-diethl-para-phenylendiamine: a possible indicator of oxidative stress in biological samples," *Research on Chemical Intermediates*, vol. 26, no. 3, pp. 253–267, 2000.

[21] C. Cervellati, F. S. Pansini, G. Bonaccorsi et al., "17β-estradiol levels and oxidative balance in a population of pre-, peri-, and post-menopausal women," *Gynecological Endocrinology*, vol. 27, no. 12, pp. 1028–1032, 2011.

[22] I. F. F. Benzie and J. J. Strain, "Ferric reducing/antioxidant power assay: direct measure of total antioxidant activity of biological fluids and modified version for simultaneous measurement of total antioxidant power and ascorbic acid concentration," *Methods in Enzymology*, vol. 299, pp. 15–27, 1998.

[23] E. Cremonini, G. Bonaccorsi, C. M. Bergamini et al., "Metabolic transitions at menopause: in post-menopausal women the increase in serum uric acid correlates with abdominal adiposity as assessed by DXA," *Maturitas*, vol. 75, no. 1, pp. 62–66, 2013.

[24] D. Duplancic, L. Kukoc-Modun, D. Modun, and N. Radic, "Simple and rapid method for the determination of uric acid-independent antioxidant capacity," *Molecules*, vol. 16, no. 8, pp. 7058–7067, 2011.

[25] M. A. Smith, P. L. Richey Harris, L. M. Sayre, J. S. Beckman, and G. Perry, "Widespread peroxynitrite-mediated damage in Alzheimer's disease," *Journal of Neuroscience*, vol. 17, no. 8, pp. 2653–2657, 1997.

[26] D. Praticò, "Evidence of oxidative stress in Alzheimer's disease brain and antioxidant therapy: lights and shadows," *Annals of the New York Academy of Sciences*, vol. 1147, pp. 70–78, 2008.

[27] M. A. Smith, X. Zhu, M. Tabaton et al., "Increased iron and free radical generation in preclinical Alzheimer disease and mild cognitive impairment," *Journal of Alzheimer's Disease*, vol. 19, no. 1, pp. 363–372, 2010.

[28] T. J. Montine, J. F. Quinn, D. Milatovic et al., "Peripheral F2-isoprostanes and F4-neuroprostanes are not increased in Alzheimer's disease," *Annals of Neurology*, vol. 52, no. 2, pp. 175–179, 2002.

[29] F. Sinem, K. Dildar, E. Gökhan, B. Melda, Y. Orhan, and M. Filiz, "The serum protein and lipid oxidation marker levels in Alzheimer's disease and effects of cholinesterase inhibitors and antipsychotic drugs therapy," *Current Alzheimer Research*, vol. 7, no. 5, pp. 463–469, 2010.

[30] I. Baldeiras, I. Santana, M. T. Proença et al., "Oxidative damage and progression to Alzheimer's disease in patients with mild cognitive impairment," *Journal of Alzheimer's Disease*, vol. 21, no. 4, pp. 1165–1177, 2010.

[31] M. Brys, E. Pirraglia, K. Rich et al., "Prediction and longitudinal study of CSF biomarkers in mild cognitive impairment," *Neurobiology of Aging*, vol. 30, no. 5, pp. 682–690, 2009.

[32] D. F. Silva, I. Santana, A. R. Esteves et al., "Prodromal metabolic phenotype in MCI cybrids: implications for Alzheimer's disease," *Current Alzheimer Research*, vol. 10, no. 2, pp. 180–190, 2013.

[33] E. Barone, F. di Domenico, G. Cenini et al., "Oxidative and nitrosative modifications of biliverdin reductase-a in the brain of subjects with Alzheimer's disease and amnestic mild cognitive impairment," *Journal of Alzheimer's Disease*, vol. 25, no. 4, pp. 623–633, 2011.

[34] R. von Bernhardi and J. Eugenín, "Alzheimer's disease: redox dysregulation as a common denominator for diverse pathogenic mechanisms," *Antioxidants and Redox Signaling*, vol. 16, no. 9, pp. 974–1031, 2012.

[35] R. Sultana, M. Perluigi, and D. A. Butterfield, "Protein oxidation and lipid peroxidation in brain of subjects with Alzheimer's disease: insights into mechanism of neurodegeneration from redox proteomics," *Antioxidants and Redox Signaling*, vol. 8, no. 11-12, pp. 2021–2037, 2006.

[36] A. Tarozzi, C. Angeloni, M. Malaguti et al., "Sulforaphane as a potential protective phytochemical against neurodegenerative diseases," *Oxidative Medicine and Cellular Longevity*, vol. 2013, Article ID 415078, 10 pages, 2013.

[37] V. Bocci and G. Valacchi, "Free radicals and antioxidants: how to reestablish redox homeostasis in chronic diseases?" *Current Medicinal Chemistry*, vol. 20, no. 27, pp. 3397–3415, 2013.

[38] P. Bermejo, S. Martín-Aragón, J. Benedí et al., "Differences of peripheral inflammatory markers between mild cognitive impairment and Alzheimer's disease," *Immunology Letters*, vol. 117, no. 2, pp. 198–202, 2008.

[39] S. Martín-Aragón, P. Bermejo-Bescós, J. Benedí et al., "Metalloproteinase's activity and oxidative stress in mild cognitive impairment and Alzheimer's disease," *Neurochemical Research*, vol. 35, no. 2, pp. 373–378, 2008.

[40] R. C. Petersen, R. G. Thomas, M. Grundman et al., "Vitamin E and donepezil for the treatment of mild cognitive impairment," *The New England Journal of Medicine*, vol. 352, no. 23, pp. 2379–2388, 2005.

[41] A. Pecorelli, L. Ciccoli, C. Signorini et al., "Increased levels of 4HNE-protein plasma adducts in Rett syndrome," *Clinical Biochemistry*, vol. 44, no. 5-6, pp. 368–371, 2011.

Hindawi Publishing Corporation
BioMed Research International
Volume 2013, Article ID 942431, 9 pages
http://dx.doi.org/10.1155/2013/942431

Research Article

Depletion of Luminal Pyridine Nucleotides in the Endoplasmic Reticulum Activates Autophagy with the Involvement of mTOR Pathway

Orsolya Kapuy and Gábor Bánhegyi

Department of Medical Chemistry, Molecular Biology and Pathobiochemistry, Semmelweis University, Tűzoltó utca 37-47, Budapest 1094, Hungary

Correspondence should be addressed to Gábor Bánhegyi; banhegyi@eok.sote.hu

Received 6 July 2013; Revised 3 October 2013; Accepted 7 October 2013

Academic Editor: Cristina Angeloni

It has been recently shown that redox imbalance of luminal pyridine nucleotides in the endoplasmic reticulum (ER) together with oxidative stress results in the activation of autophagy. In the present study we demonstrated that decrease of luminal NADPH/$NADP^+$ ratio alone by metyrapone was sufficient to promote the mechanism of "self-eating" detected by the activation of LC3. Depletion of luminal NADPH had also significant effect on the key proteins of mTOR pathway, which got inactivated by dephosphorylation. These findings were also confirmed by silencing the proteins (glucose-6-phosphate transporter and hexose-6-phosphate dehydrogenase) responsible for NADPH generation in the ER lumen. However, silencing the key components and addition of metyrapone had different effects on downstream substrates 4EBP1 and p70S6K of mTOR. The applied treatments did not compromise the viability of the cells. Our data suggest that ER stress caused by luminal NADPH depletion activates a pro-survival autophagic mechanism firmly coupled to the activation of mTOR pathway.

1. Introduction

The endoplasmic reticulum (ER) is a eukaryotic cellular component that acts as an essential integrator of external and internal stimuli by keeping the balance of protein level (so called proteostasis) [1, 2]. ER has a crucial role in folding and secretion of secreted and membrane proteins, calcium storage, and lipid biosynthesis [2, 3]. Recent experimental data have shown that for the proper function of the ER, a high luminal NADPH/$NADP^+$ ratio is essential [4, 5]. The reduced luminal NADPH is required for the prereceptorial activation of glucocorticoids (such as cortisol), for some reactions of biotransformation and presumably for local antioxidant defense. NADPH level is primarily sustained by the coordinated action of the ER glucose-6-phosphate transporter (G6PT) and the luminal hexose-6-phosphate dehydrogenase (H6PDH), while NADPH can be consumed by different luminal reductases (such as carbonyl reductases) [6–8].

The imbalance of NADPH/$NADP^+$ ratio or depletion of luminal NADPH level sensitizes the ER to different oxidative injuries [5]. Starvation has been reported to cause a shift in the redox state of luminal pyridine nucleotides toward the oxidized direction [9]. Experimentally, addition of G6PT blockers S3483 or chlorogenic acid or the ROS generating menadione results in the decrease of luminal NADPH [5, 10]. Metyrapone decreases luminal NADPH level by the stimulation of carbonyl reductases and by carbonyl reductase independent mechanisms [4, 11]. Interestingly, combined treatment of NADPH depleting agents (e.g., inhibition or silencing G6PT, silencing H6PDH, and oxidation of ER luminal pyridine nucleotides) and oxidative stress induced by menadione results in the induction of autophagy markers [5].

It has been also proved that autophagosome formation gets immediately induced in the presence of ER stressors (such as thapsigargin and tunicamycin) [12, 13]. This observation is confirmed by increasing autophagic function. Any disturbance of autophagy accelerates cell death claiming that

autophagy plays important roles in cell survival during ER stress [12, 13].

The autophagy plays an important role to "digest" the damaged cytoplasmic components of cells at physiological conditions [14]. In addition autophagy has an essential role in promoting cellular-survival during starvation by "self-eating" of parts of the cytoplasm and intracellular organelles [14, 15]. Autophagy induced by nutrient deprivation can be mimicked by addition of drug rapamycin [16].

Mammalian target of rapamycin (mTOR) alias FKBP-rapamycin associated protein (FRAP) is an evolutionally conserved serine/threonine kinase of mTOR pathway that is a major effector of cell growth and proliferation by controlling protein synthesis [17, 18]. The phosphorylated form of mTOR/FRAP is active, while the kinase becomes immediately inactive and dephosphorylated upon nutrient depletion [18]. Some of the targets of mTOR/FRAP are phosphorylated directly, such as Eukaryotic translation initiation factor 4E-binding protein 1 (4EBP1) and Ribosomal protein S6 kinase 1 (p70S6K). Both 4EBP1 and p70S6K become dephosphorylated in response to starvation resulting in block of protein translation [18, 19]. Some new results have shown that DNA damage and ER stress-related Gadd34 is also required for autophagy induction under nutrient-depleted conditions [20]. The Gadd34 knock-downed mice cannot promote starvation-dependent mTOR/FRAP kinase dephosphorylation [21]. However, beside CHOP/Gadd153, Gadd34 is also a crucial member of unfolded protein response (UPR) [13]. UPR is a complex network of signalling pathways measuring both the not properly folded protein level and the precise balance between production and consumption of folded proteins [13, 22].

In this study we reexamined the role of metyrapone in autophagy induction claiming that NADPH depletion without combination of oxidative agent can be sufficient to enhance autophagic process. Treatment with NADPH depleting agents results in dephosphorylation of the key molecules of mTOR pathway confirming that the imbalance of ER luminal pyridine nucleotides induces a starvation phenotype.

2. Materials and Methods

2.1. Materials. Metyrapone, rapamycin, 3-methyladenine, Wortmannin, and trypan blue were purchased from Sigma. All other chemicals were of reagent grade.

2.2. Cell Culture and Maintenance. As model system, human liver carcinoma (HepG2) cell line was used. Due to the relatively large dimension of ER in HepG2 cells they offer an excellently suitable *in vitro* model system for studying the effect of addition of different type of ER stressors. HepG2 cells were maintained in DMEM medium supplemented with 10% fetal bovine serum and 1% antibiotics/antimycotics. Culture dishes and cell treatment plates were kept in a humidified incubator at 37°C in 95% air and 5% CO_2.

2.3. RNA Interference. The silencing of G6PT and H6PDH was managed by transfection with siG6PT and/or siH6PDH, respectively. The corresponding RNA interference was performed using Lipofectamine RNAi Max (Invitrogen) in GIBCOTM Opti-MEM I (GlutaMAXTM-I) Reduced-Serum Medium liquid (Invitrogen) and 20 pmol/mL siRNA. Interfering RNAs for human G6PT (gene ID: NM 001467) and H6PD were constructed by Invitrogen. The used oligonucleotide for human G6PT: 5′-CGAAACAUCCGCACC-AAGAdTdT-3′ (sense) and 5′-UCUUGGUGCGGAUGU-UUCGdTdT-3′ (antisense) [23]. The used oligonucleotide for human H6PD was 5′-UUAUGGAGACAUGUCCCUGGA-GCUC-3′ (sense) and 5′-GAGCUCAGGGACAUGUCU-CCAUAA-3′ (antisense). Interfering materials were annealed duplexes in both cases [5].

2.4. SDS-PAGE and Western Blot Analysis. HepG2 cells were harvested and lysed with 20 mM Tris, 135 mM NaCl, 10% glycerol, and 1% NP40 at pH 6.8. Protein content of cell lysates was measured using Pierce BCA Protein Assay. Equal amounts of protein were used in each procedure. SDS-PAGE was performed by using Hoefer miniVE (Amersham). The protein patterns were transferred onto Millipore 0.45 μm PVDF membrane. Immunoblotting was accomplished with TBS Tween (0.1%), containing 5% nonfat dry milk for blocking membrane and for antibody solutions. The correct loading was controlled by staining with Ponceau S in each experiment. The following antibodies were used: antiGADD153, antiLC3B, antiGADD34, antimTOR/FRAP, antimTOR/FRAP-P, antip70S6K, antip70S6K-P, antiprocaspase 3, antiGAPDH (SantaCruz), anti4EBP1, anti4EBP1-P, antiPARP, antieIF2alpha-P, antieIF2alpha (Cell Signaling), and HRP conjugated secondary antibodies (SantaCruz).

2.5. Cell Viability Assays. The number of viable cells was detected using a trypan blue exclusion assay. Cells were incubated with isotonic solution of trypan blue 0.6% and both permeabilized and nonpermeabilized cells were counted. In case of each experiment at least three parallels were measured. Cell viability was also determined by CellTiter-Blue Assay from Promega. 20 μL of reagent was added to each 100 μL of medium in a 96-well plate. In this method the viable cells are able to reduce the indicator dye resazurin into resorufin, while the nonviable cells lose their metabolic capacity. The absorbance was read at 570 nm using 600 nm as a reference wavelength.

2.6. HPLC Detection of Metyrapone. The uptake of drug metyrapone was measured via HPLC. Cell cultures were incubated for 0, 10, 20, 30, 40, and 120 min, then cells and media were separated, and cells were lysed with 20 mM Tris, 135 mM NaCl, 10% glycerol, and 1% NP40 at pH 6.8. 150 μL media of each sample was directly added to 150 μL ice-cold methanol. The protein concentration of each sample was set to 0.075 mg/mL with MOPS buffer. Then 150 μL of these samples were added to 150 μL ice-cold methanol. Samples were stored at −20°C until analysis. After sedimentation of the precipitates by centrifugation (20 000 ×g for 10 min at 4°C), the metyrapone content of the supernatants was measured by HPLC (Alliance 2690; Waters Corp., Milford,

MA, USA) using a Nucleosil 100 C18 column (5 μm 25 × 0.46) (Teknokroma). The eluent was 58% methanol, samples were eluted for 30 min and the absorbance was detected at 245 nm wavelength (Dual l Absorbance Detector 2487). The retention times of metyrapone (approx. 15 min) was determined by injecting standards.

3. Results

3.1. NADPH Depletion in the ER Lumen by Metyrapone Results in Autophagy Activation and Downregulation of mTOR Pathway. We have shown previously that combination of depletion of ER luminal NADPH and menadione-induced oxidative stress injury results in autophagy and decreased viability in HepG2 cells [5]. However, under experimental conditions performed in those experiments imbalance of NADPH level caused by metyrapone alone was not sufficient to induce autophagic events or viability alterations. Here we found that prolonged incubation was not sufficient to induce autophagy (data not shown), but the increased concentration of metyrapone (75–100 μM) was able to promote formation of autophagy marker, LC3II; however, the apoptosis markers, such as cleavage of PARP and procaspase 3, did not show any apoptotic event suggesting that an autophagy-dependent process switches on during metyrapone treatment (Figure 1(a)).

To investigate further the general effect of luminal NADPH depletion, a viability assay was carried out and the viable cells were also counted (Figures 1(b) and 1(c)). These analyses showed—in accordance with previous findings [5]—that no cumulative cell death was present during the treatment at either metyrapone concentration for 1 hour (Figures 1(b) and 1(c)). These results suggest that high concentration of metyrapone results in drug-induced autophagy; however, this mechanism does not enhance "self-eating"-dependent cell death. To confirm the positive effect of metyrapone on autophagy induction a combined treatment was established with various autophagy inhibitors, such as 3-methyladenine and Wortmannin (Figure 2). Autophagy was less evident in both simultaneous treatments (metyrapone + 3-methyladenine and metyrapone + Wortmannin) and relative cell viability was also decreased (Figure 2). Cleaved PARP indicates apoptotic cell death at addition of Wortmannin even at combined treatment. Thus, NADPH depletion-induced autophagy showed similar characteristic to rapamycin treatment (Figure 2).

Beside autophagy activation, a remarkable induction of Gadd34 and the slight but delayed activation of proapoptotic CHOP/Gadd153 could also be observed upon metyrapone addition (at concentrations >50 μM) confirming ER stress (Figure 3(a)). eIF2α phosphorylation could not be observed after 1-hour treatment in accordance with the phosphatase activity of induced Gadd34 (Figure 3(a)).

As Gadd34 acts on mTOR/FRAP pathway negatively by dephosphorylating and activates the inhibitor TSC2 of mTOR/FRAP directly [20] we are interested in whether this starvation-controlled pathway is active or not during metyrapone treatment. Therefore, the phosphorylation of mTOR/FRAP kinase and its two well-known downstream targets (4EBP1 and p70S6K) was also followed by Western blotting (Figure 3(b)). Although Gadd34 gets activated and mTOR/FRAP becomes dephosphorylated at drug concentration >50 μM, 4EBP1 is not shown any dephosphorylation after 1- hour treatment. These data suggest that mTOR pathway could not be fully inactived during redox imbalance of ER luminal pyridine nucleotides. Interestingly p70S6K kinase, the other target of mTOR/FRAP becomes almost completely dephosphorylated even after 1 hour treatment with 10 μM metyrapone (Figure 3(b)) supposing that drug-induced luminal NADPH depletion of ER has actually some negative effect on mTOR/FRAP-dependent starvation pathway.

3.2. The kinetic Profile of Metyrapone-Induced mTOR Inactivation. To get the time course of metyrapone treatment (100 μM), its effects were followed in time. The level of LC3II was already elevated at 1 h and further increased at 2 h of incubation with 100 μM metyrapone assuming autophagic process after 1-hour treatment (Figure 4(a)). Interestingly eIF2α phosphorylation and activity of both Gadd34 and CHOP/Gadd153 show only a transient peak (Figure 4(b)). Metyrapone treatment resulted in a stress-dependent UPR activation; however, the UPR elements completely disappeared after 120 min. These data also support the idea that autophagy activated by NADPH depletion promotes a cell survival process by adapting the cells to a tolerable stress condition. We claim that the metyrapone-induced ER stress is not severe enough to induce cell death. No PARP cleavage was observed during treatment supposing that apoptotic process remained inactive (Figure 4(a)). These results were also confirmed by carrying a viability assay, which did not show any cumulative cell death even after 2-hour long luminal redox imbalance (Figure 4(c)).

The time course of the phosphorylation of the key components of mTOR pathway was also examined. mTOR/FRAP gets dephosphorylated after 50–60 min, and this dephosphorylation became completed after 2 hours supposing the turning off of mTOR/FRAP pathway during treatment (Figure 5). While mTOR/FRAP getS dephosphorylated relatively late, the inactivation of p70S6K was observed after 15 min. Although both mTOR/FRAP and p70S6K kinase get dephosphorylated, mTOR/FRAP target 4EBP1 remains active and phosphorylated (Figure 5). This various activation profile of downstream targets of mTOR/FRAP suggests kinetic differences between them. It can also be possible that metyrapone treatment has an mTOR-independent effect on 4EBP1 and/or p70S6K phosphorylation/dephosphorylation.

To rule out the possibility that cells are able to adapt to metyrapone by pumping the drug out, its uptake was measured by HPLC. The increase of metyrapone concentration in the cells shows hyperbolic characteristic reaching a maximum level after 30 min and it was maintained on this level even after 120 min (Figures 6(a) and 6(b)). This picture shows that a constant metyrapone level was reached after 30 min in the cell, which was in agreement with the time course of metyrapone induced effects.

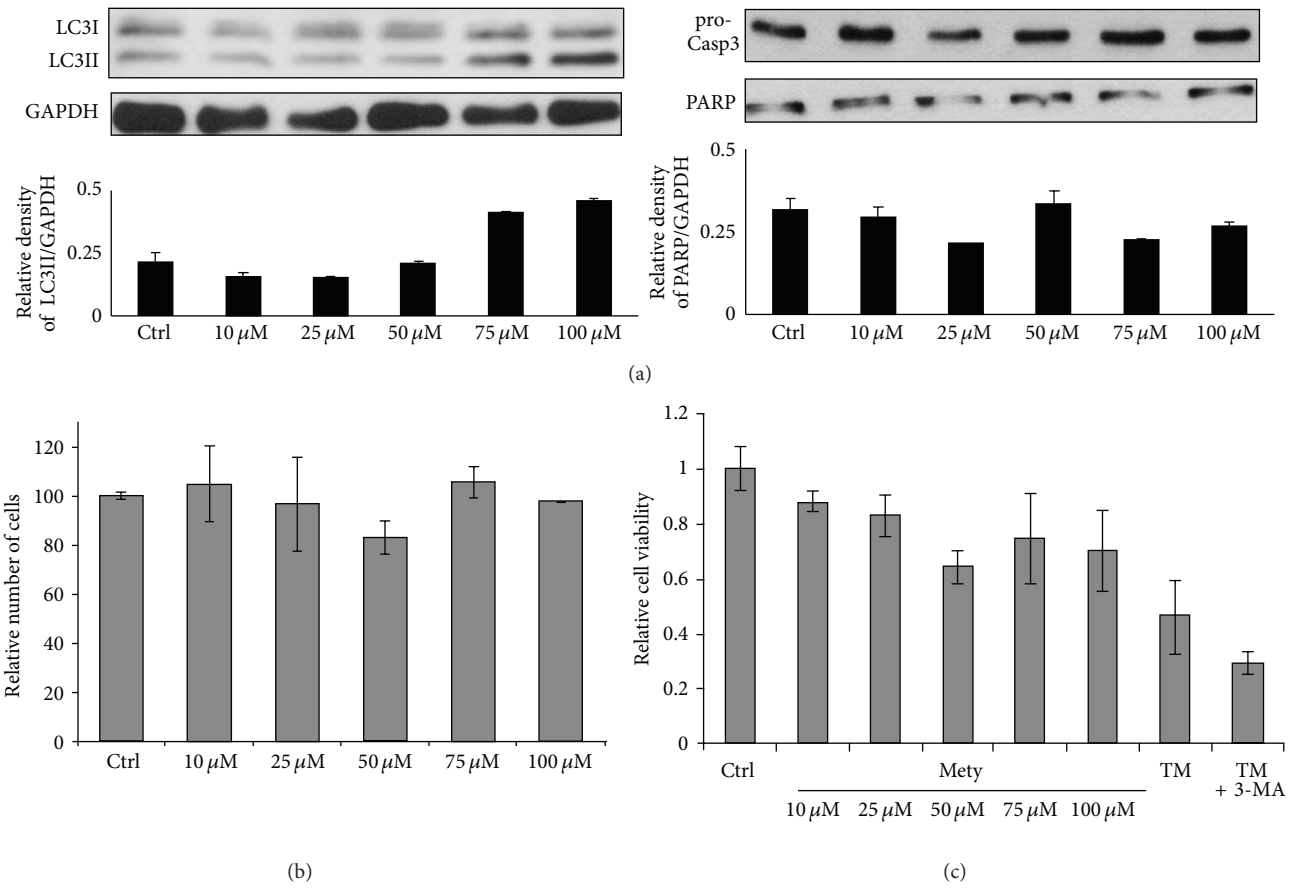

Figure 1: NADPH depletion induced by metyrapone is sufficient to promote autophagy. HepG2 cells were treated with different amount of metyrapone (10 μM–100 μM) for 1 h at 37°C. (a) Cell lysates were analysed by Western blot by immunoreacting with antibodies against LC3, procaspase 3, PARP, and GAPDH, respectively. The relative density of both the lower band of LC3/GAPDH and PARP/GAPDH were plotted. (b) Cell viability was assessed by counting the cells both permeable and nonpermeable for trypan blue. About 95% of the cells were nonpermeable for trypan blue. (c) Cell viability was followed by using Cell Titer-Blue Assay and the relative cell viability was represented after 1-hour long metyrapone treatment. As positive controls cells were treated with tunicamycin (TM—25 μM) for 2 hours combined with/without 2-hour long 3-methyladenine pretreatment (3-MA—10 mM).

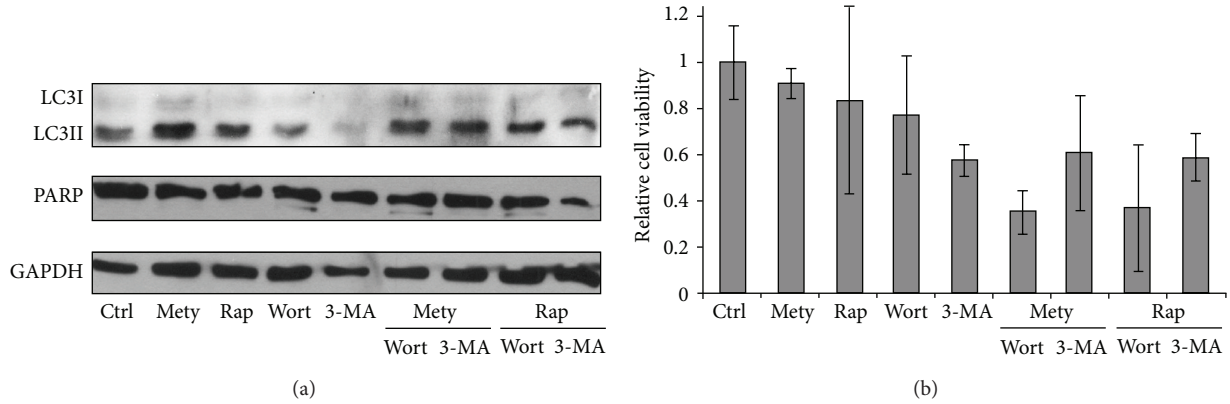

Figure 2: NADPH depletion and autophagy inhibition together promote cell death. HepG2 cells were treated with metyrapone (Mety—100 μM), rapamycin (Rap—100 nM), Wortmannin (Wort—1 μM), and 3-methyladenine (3-MA—10 mM) for 2 h at 37°C. Cells were also pretreated with Wort/3-MA for 2 h; then Mety/Rap was added for another 2 h. (a) Cell lysates were analysed by Western blot by immunoreacting with antibodies against LC3, PARP, and GAPDH, respectively. (b) Cell viability was followed by using Cell Titer-Blue Assay and the relative cell viability was represented after treatment.

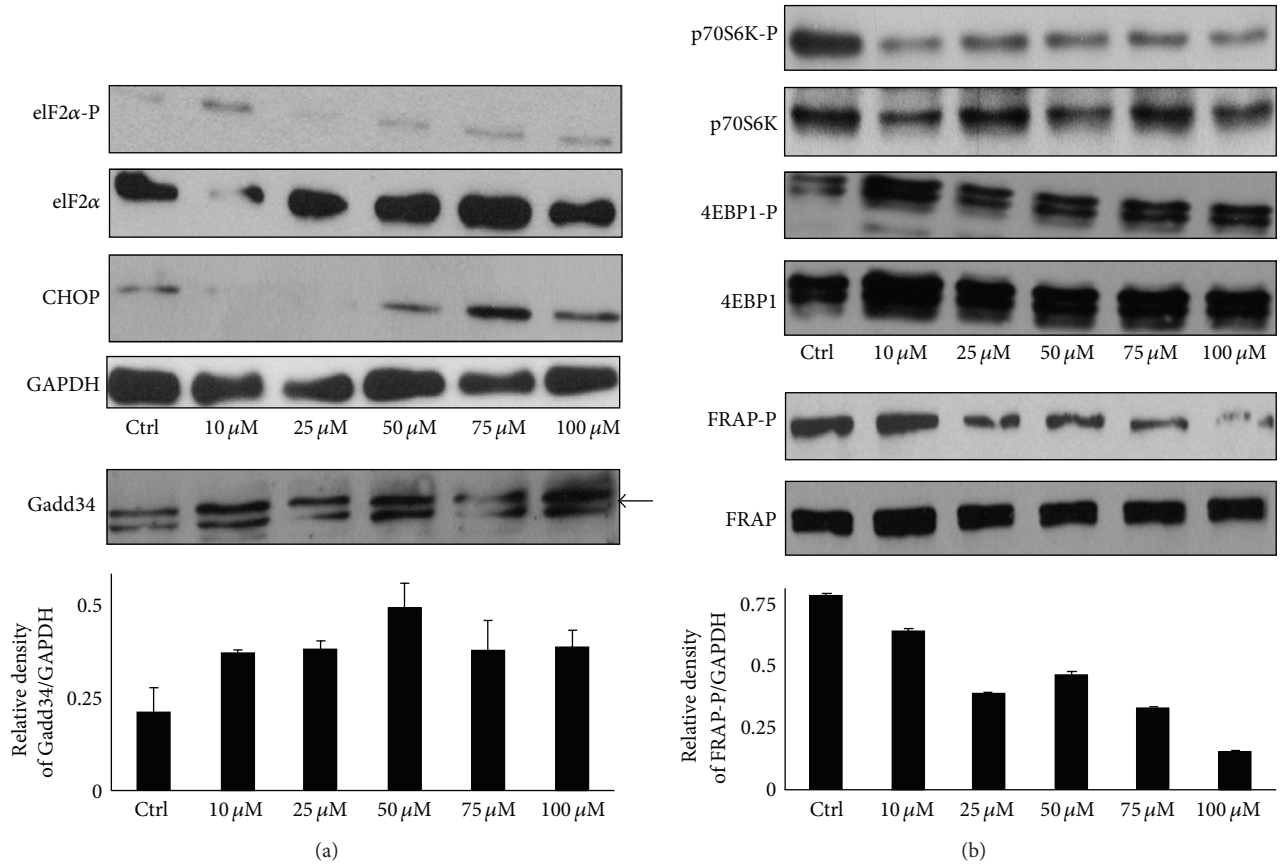

Figure 3: NADPH depletion induced by metyrapone enhances ER stress and influences the phosphorylation status of mTOR pathway proteins. HepG2 cells were treated with different amount of metyrapone (10 μM–100 μM) for 1 h at 37°C. (a) Cell lysates were analysed by Western blot by immunoreacting with antibodies against eIF2α-P, eIF2α, CHOP/Gadd153, GAPDH, and Gadd34, respectively. The relative density of Gadd34/GAPDH was plotted. (b) Cell lysates were analysed by Western blot by immunoreacting with antibodies against mTOR/FRAP-P, mTOR/FRAP, 4EBP1-P, 4EBP1, p70S6K-P, and p70S6K, respectively. The relative density of phosphorylated FRAP/GAPDH was represented.

3.3. Imbalance of ER Luminal NADPH/NADP$^+$ Ratio and mTOR Inactivation by Silencing of G6PT and/or H6PDH. Although the role of metyrapone was already proved by imbalance the pyridine nucleotide level in luminal ER, the exact way of its action, and its targets have been not explored yet. We had to confirm that metyrapone is not able to act directly on one of the steps of mTOR pathway besides inducing the depletion of ER luminal NADPH. Therefore, the two key proteins of maintaining luminal NADPH level, G6PT, and H6PDH were silenced in HepG2 cells by transfection with the corresponding siRNA. G6PT is needed for glucose-6-phosphate uptake of the ER, while H6PDH transforms glucose-6-phosphate to 6-phosphogluconate by generating NADPH [24]. This transformation requires NADP$^+$; therefore, silencing the expression of these two genes results in serious NADPH depletion in the ER lumen.

Transfection of HepG2 cells with siG6PT and/or siH6PDH reduced the level of G6PT and/or H6PDH dramatically (Figure 7). Both siG6PT and siH6PDH resulted in activation of autophagic event (Figure 7). This was demonstrated by the remarkable increase of LC3II level and intensive Gadd34 expression, while the cleavage of procaspase 3 and PARP was not observed. These data show that similarly to autophagy induced by metyrapone treatment, the survival process switches on during silencing of G6PT and/or H6PDH. Interestingly, the mTOR/FRAP target 4EBP1 gets fully dephosphorylated after silencing G6PT and/or H6PDH suggesting that imbalance of luminal NADPH/NADP$^+$ ratio affects the mTOR/FRAP pathway negatively (Figure 7). Silencing of either G6PT or H6PDH, in agreement with our previous results [5], did not compromise the viability of the cells (data not shown).

4. Discussion

The present results show that depletion of ER NADPH either by the pharmacological agent metyrapone or by silencing of the key proteins of luminal NADPH generation switched on an autophagic mechanism with the incomplete inactivation of the mTOR pathway.

We observed that high concentration of metyrapone was able to enhance the autophagy marker LC3II even after 1 h, suggesting that the imbalance of ER luminal pyridine

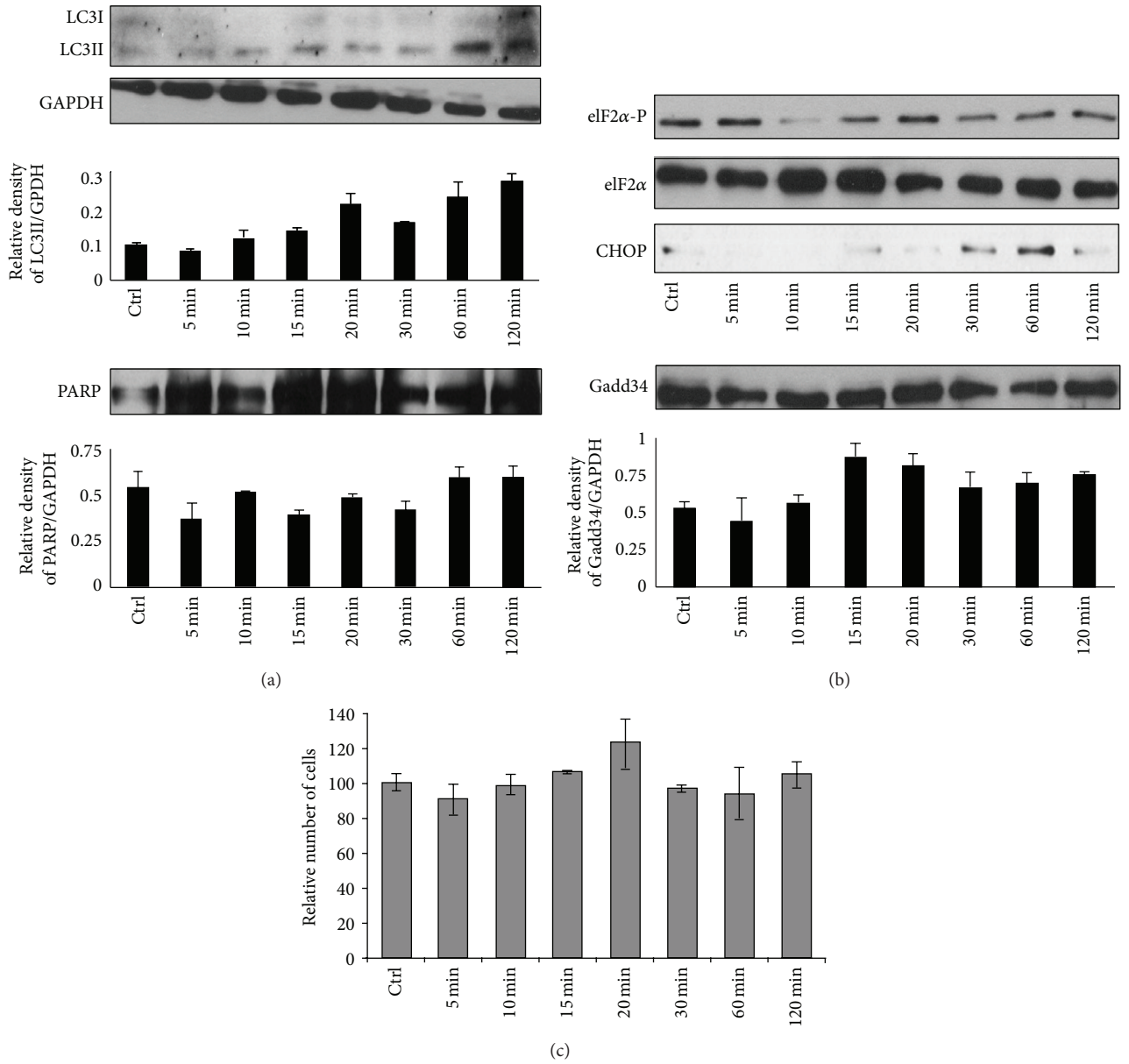

Figure 4: Time course of the effect of high concentration metyrapone on ER stress. HepG2 cells were treated with 100 μM metyrapone for 5–120 min at 37°C. (a) Cell lysates were analysed by Western blot by immunoreacting with antibodies against LC3, PARP, and GAPDH, respectively. The relative density of both the lower band of LC3/GAPDH and PARP/GAPDH were represented. (b) Cell lysates were analysed by Western blot by immunoreacting with antibodies against ER stress markers, such as eIF2α-P, eIF2α, CHOP/Gadd153, and Gadd34, respectively. The relative density of Gadd34/GAPDH was represented. (c) Cell viability was assessed by counting the cells both permeable and non-permeable to trypan blue. About 5% of the cells were nonpermeable for trypan blue.

nucleotides is alone sufficient to induce the "self-eating" mechanism (Figure 1). The ER-stress related autophagy inducer Gadd34 became active at relatively low concentration of metyrapone, while increased expression of the pro-apoptotic transcription factor CHOP/Gadd153 was detected only at high amount of drug (Figure 3(a)). Since this induction of CHOP/Gadd153 did not result in a decrease of cell viability in our experimental system (Figure 1), we suggested that autophagic response induced by NADPH depletion might have a role in cell survival. This observation was also confirmed by using autophagy inhibitors together with metyrapone (Figure 2). Interestingly, metyrapone after a short exposure (30 min) transiently increased the expression of transcription factor CHOP/Gadd153 following Gadd34 induction (Figure 4(b)), but cells remained viable (Figures 4(a) and 4(c)). These results suggest that first autophagy gets activated to turn on the "self-eating" mechanism to heal damages. Later apoptosis via CHOP tries to switch on but the stress level induced by NAPDH depletion is not high enough to develop the self-killing mechanism; therefore,

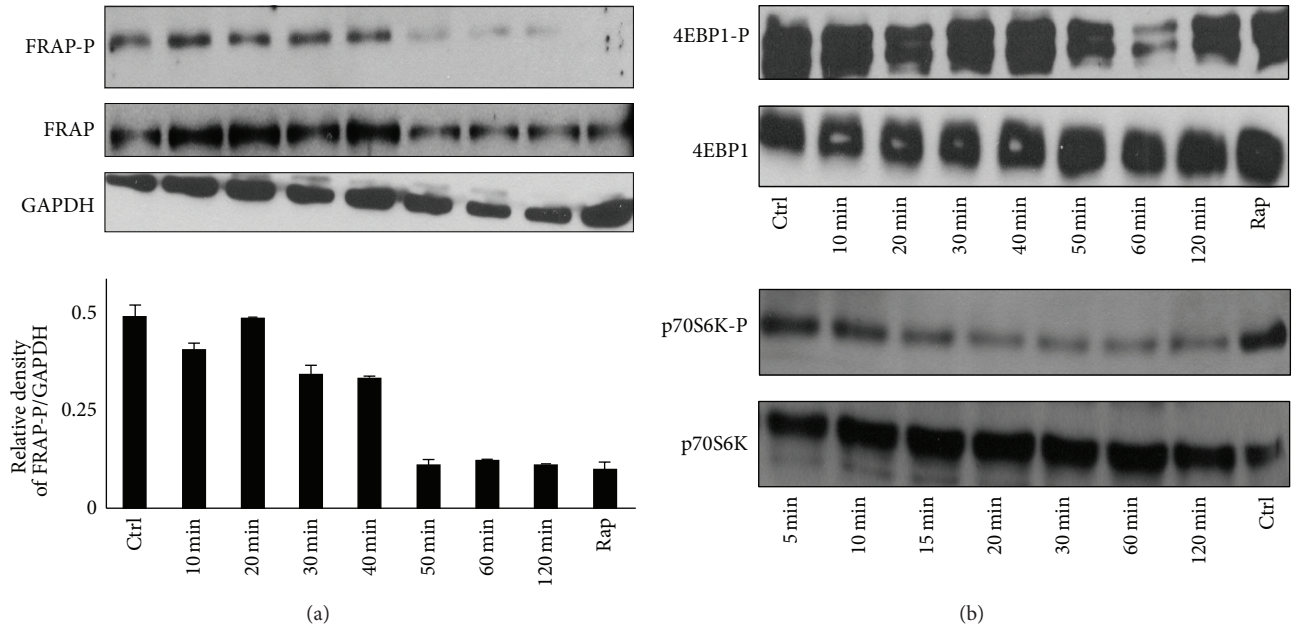

Figure 5: Time course of the effect of high concentration metyrapone on phosphorylation status of mTOR pathway proteins. HepG2 cells were treated with 100 μM metyrapone for 5–120 min at 37°C. Each sample was analysed by Western blot by immunoreacting with antibodies against mTOR/FRAP-P, mTOR/FRAP, 4EBP1-P, 4EBP1, p70S6K-P, and p70S6K, respectively. The relative density of phosphorylated FRAP/GAPDH was represented. As positive control of autophagy cells were treated with 100 nM rapamycin for 1 hour at 37°C.

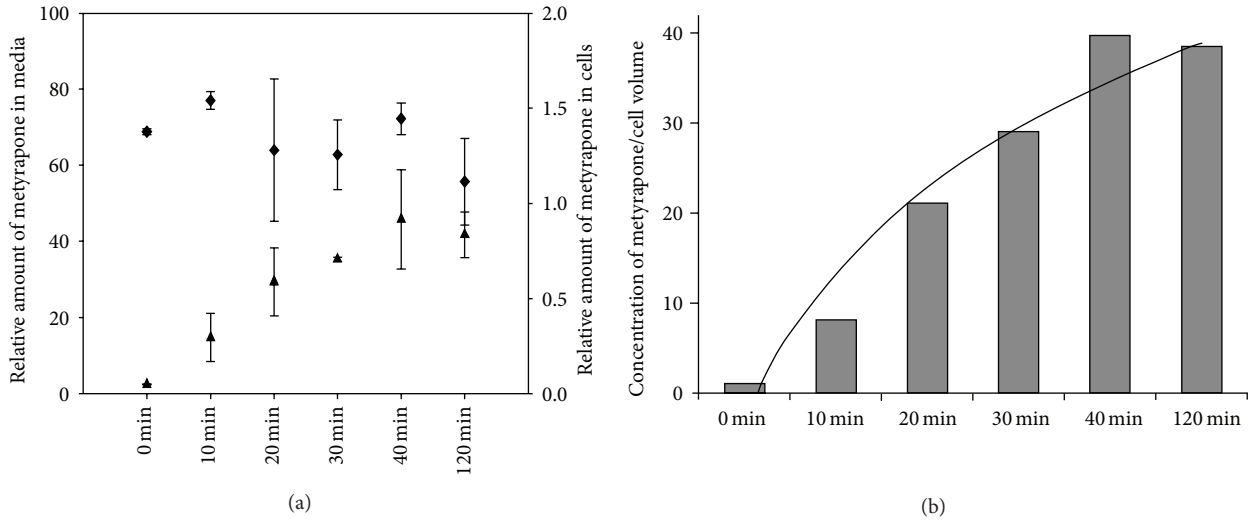

Figure 6: Metyrapone uptake of HepG2 cells. HepG2 cells were treated with 100 μM metyrapone for 0–120 min at 37°C. (a) After cell lysis, cells metyrapone concentrations were measured by HPLC till 120 min upon the addition of metyrapone, and their relative amounts were calculated both in the media (black diamond) and the cells (black triangle). (b) Metyrapone concentration in cells referring to cell volume is plotted at each time point and a trend line was fitted (black hyperbolic line). For detailed description of HPLC method see Section 2.

CHOP/Gadd153 has only a transient peak. These results correspond to our recently published data where we claim that cellular stress induces autophagy-dependent survival immediately, while the stress level has to reach a critical threshold to promote apoptotic cell death [25].

Gadd34 has been shown to induce autophagy via the dephosphorylation of TSC2, which leads to the suppression of the mTOR pathway, a potent inhibitor of autophagy [21]. In agreement with the supposed role of Gadd34 in the regulation of mTOR pathway, a decreased phosphorylation of mTOR and p70S6K was also observed after longer incubations. However, the mTOR target 4EBP1 remains phosphorylated (Figure 5). This various activation profile of downstream targets of mTOR suggests kinetic differences between them.

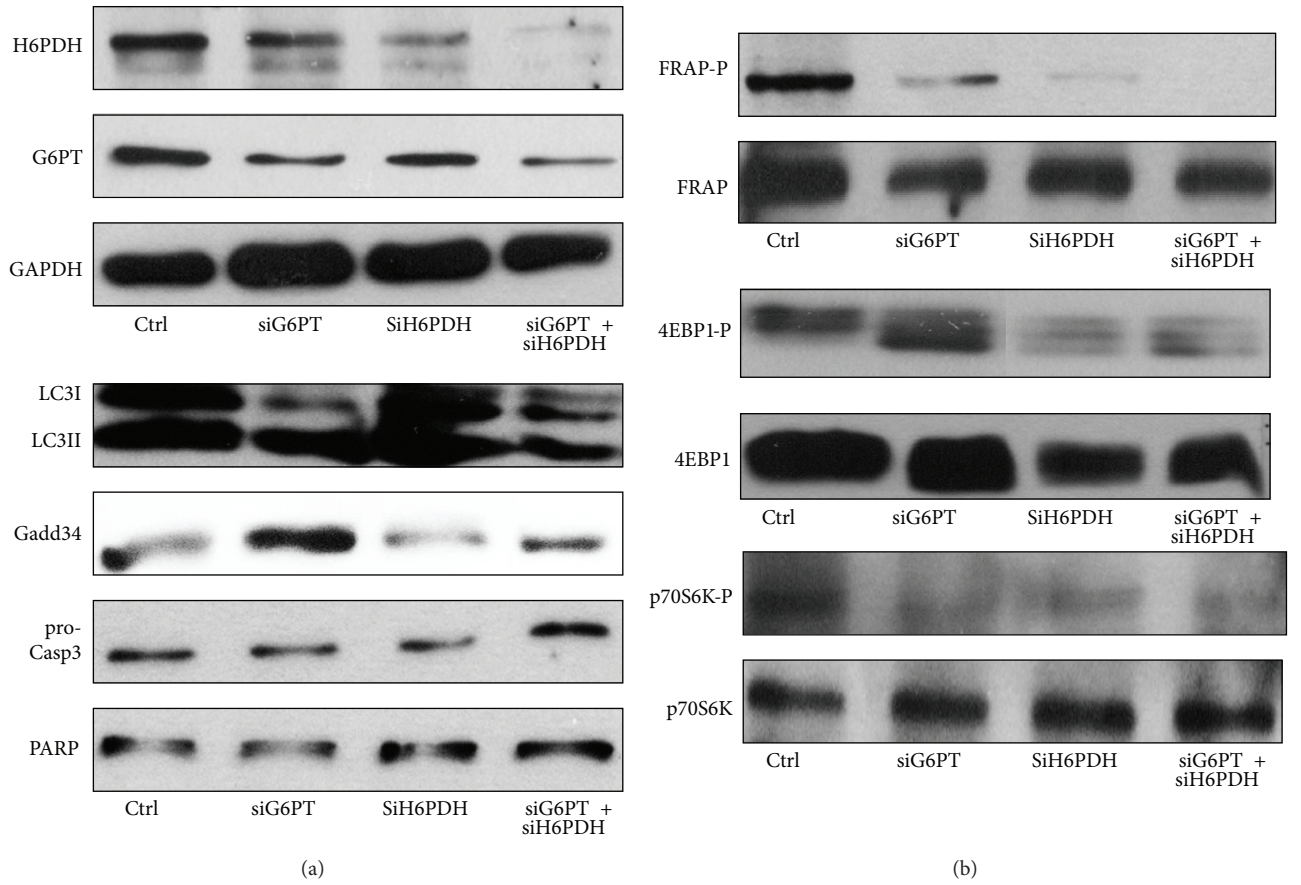

Figure 7: Transient knockdown of G6PT and/or H6PDH by siRNAs induces autophagy. HepG2 cells were treated with siRNA construct for G6PT and/or H6PDH. For description of this method see Section 2. Cells were lysed after 24 hours of silencing and samples were analysed by Western blot by immunoreacting with antibodies against G6PT, H6PDH, GAPDH, LC3, procaspase 3, PARP, Gadd34, mTOR/FRAP-P, mTOR/FRAP, 4EBP1-P, 4EBP1, p70S6K-P and p70S6K, respectively.

It can also be possible that metyrapone treatment has an mTOR-independent effect on 4EBP1 and/or p70S6K phosphorylation/dephosphorylation. These considerations are also supported by the observations that p70S6K dephosphorylation precedes that of mTOR (Figure 5) and requires lower metyrapone concentration (Figure 3(b)). Moreover, 4EBP1 dephosphorylation was evident upon silencing-based consumption of the luminal NADPH pool (Figure 7). It should be noted that although the downstream targets of mTOR (i.e., p70S6K and 4EBP1) are supposed to be regulated in line with each other, in some cases they are inhibited differently [26, 27].

The results gained by metyrapone were confirmed by silencing of the proteins responsible for generation ER luminal NADPH. Activation of the autophagic machinery was indicated by increased Gadd34 expression, LC3II formation, and dephosphorylation of 4EBP1 (Figure 7).

In conclusion, the depletion of luminal NADPH in the ER (and/or the decreased NADPH/$NADP^+$ ratio) results in ER stress followed by the activation of autophagic response. The scenario consists of the temporary increase of CHOP/Gadd153 without the alteration of cell viability. Thus, the NADPH depletion dependent ER stress unequivocally results in a physiological prosurvival response. Although the elements of mTOR pathway respond differently to imbalance of luminal pyridine nucleotides, these data suggested that the NADPH depletion-induced autophagosome formation has starvation-related phenotype. The findings underline the role of the redox state of ER luminal pyridine nucleotides (and the metabolic pathways affecting it) in the nutrient sensing of the cell [24].

Acknowledgments

This work was supported by Grants from the Hungarian Scientific Research Fund (OTKA PD 104110 to Orsolya Kapuy, K 100293 to Gábor Bánhegyi). Orsolya Kapuy is grateful to Éva Margittai and Beáta Lizák for their valuable comments and advices. Orsolya Kapuy is a fellow of Bolyai Research Scholarship of the Hungarian Academy of Sciences.

References

[1] M. Csala, G. Bánhegyi, and A. Benedetti, "Endoplasmic reticulum: a metabolic compartment," *FEBS Letters*, vol. 580, no. 9, pp. 2160–2165, 2006.

[2] A. Görlach, P. Klappa, and T. Kietzmann, "The endoplasmic reticulum: folding, calcium homeostasis, signaling, and redox control," *Antioxidants and Redox Signaling*, vol. 8, no. 9-10, pp. 1391–1418, 2006.

[3] H. Malhi and R. J. Kaufman, "Endoplasmic reticulum stress in liver disease," *Journal of Hepatology*, vol. 54, no. 4, pp. 795–809, 2011.

[4] P. Marcolongo, S. Senesi, B. Gava et al., "Metyrapone prevents cortisone-induced preadipocyte differentiation by depleting luminal NADPH of the endoplasmic reticulum," *Biochemical Pharmacology*, vol. 76, no. 3, pp. 382–390, 2008.

[5] P. Száraz, G. Bánhegyi, and A. Benedetti, "Altered redox state of luminal pyridine nucleotides facilitates the sensitivity towards oxidative injury and leads to endoplasmic reticulum stress dependent autophagy in HepG2 cells," *International Journal of Biochemistry and Cell Biology*, vol. 42, no. 1, pp. 157–166, 2010.

[6] P. Marcolongo, S. Piccirella, S. Senesi et al., "The glucose-6-phosphate transporter-hexose-6-phosphate dehydrogenase-11β-hydroxysteroid dehydrogenase type 1 system of the adipose tissue," *Endocrinology*, vol. 148, no. 5, pp. 2487–2495, 2007.

[7] E. A. Walker, A. Ahmed, G. G. Lavery et al., "11β-Hydroxysteroid dehydrogenase type 1 regulation by intracellular glucose 6-phosphate provides evidence for a novel link between glucose metabolism and hypothalamo-pituitary-adrenal axis function," *The Journal of Biological Chemistry*, vol. 282, no. 37, pp. 27030–27036, 2007.

[8] G. Bánhegyi, M. Csala, and A. Benedetti, "Hexose-6-phosphate dehydrogenase: linking endocrinology and metabolism in the endoplasmic reticulum," *Journal of Molecular Endocrinology*, vol. 42, no. 4, pp. 283–289, 2009.

[9] É. Kereszturi, F. S. Kálmán, T. Kardon, M. Csala, and G. Bánhegyi, "Decreased prereceptorial glucocorticoid activating capacity in starvation due to an oxidative shift of pyridine nucleotides in the endoplasmic reticulum," *FEBS Letters*, vol. 584, no. 22, pp. 4703–4708, 2010.

[10] G. Bánhegyi, A. Benedetti, R. Fulceri, and S. Senesi, "Cooperativity between 11β-hydroxysteroid dehydrogenase type 1 and hexose-6-phosphate dehydrogenase in the lumen of the endoplasmic reticulum," *The Journal of Biological Chemistry*, vol. 279, no. 26, pp. 27017–27021, 2004.

[11] E. Maser and K. J. Netter, "Purification and properties of a metyrapone-reducing enzyme from mouse liver microsomes—this ketone is reduced by an aldehyde reductase," *Biochemical Pharmacology*, vol. 38, no. 18, pp. 3049–3054, 1989.

[12] M. Ogata, S.-I. Hino, A. Saito et al., "Autophagy is activated for cell survival after endoplasmic reticulum stress," *Mol Cell Biol*, vol. 26, no. 24, pp. 9220–9231, 2006.

[13] P. Walter and D. Ron, "The unfolded protein response: from stress pathway to homeostatic regulation," *Science*, vol. 334, no. 6059, pp. 1081–1086, 2011.

[14] B. Levine and G. Kroemer, "Autophagy in the pathogenesis of disease," *Cell*, vol. 132, no. 1, pp. 27–42, 2008.

[15] B. Ravikumar, S. Sarkar, J. E. Davies et al., "Regulation of mammalian autophagy in physiology and pathophysiology," *Physiological Reviews*, vol. 90, no. 4, pp. 1383–1435, 2010.

[16] T. Noda and Y. Ohsumi, "Tor, a phosphatidylinositol kinase homologue, controls autophagy in yeast," *The Journal of Biological Chemistry*, vol. 273, no. 7, pp. 3963–3966, 1998.

[17] R. Watanabe, L. Wei, and J. Huang, "mTOR signaling, function, novel inhibitors, and therapeutic targets," *Journal of Nuclear Medicine*, vol. 52, no. 4, pp. 497–500, 2011.

[18] N. Hay and N. Sonenberg, "Upstream and downstream of mTOR," *Genes and Development*, vol. 18, no. 16, pp. 1926–1945, 2004.

[19] R. Zoncu, A. Efeyan, and D. M. Sabatini, "mTOR: from growth signal integration to cancer, diabetes and ageing," *Nature Reviews Molecular Cell Biology*, vol. 12, no. 1, pp. 21–35, 2011.

[20] R. Watanabe, Y. Tambe, H. Inoue et al., "GADD34 inhibits mammalian target of rapamycin signaling via tuberous sclerosis complex and controls cell survival under bioenergetic stress," *International Journal of Molecular Medicine*, vol. 19, no. 3, pp. 475–483, 2007.

[21] M. N. Uddin, S. Ito, N. Nishio, T. Suganya, and K.-I. Isobe, "Gadd34 induces autophagy through the suppression of the mTOR pathway during starvation," *Biochemical and Biophysical Research Communications*, vol. 407, no. 4, pp. 692–698, 2011.

[22] S. Y. Wang and R. J. Kaufman, "The impact of the unfolded protein response on human disease," *Journal of Cell Biology*, vol. 197, no. 7, pp. 857–867, 2012.

[23] A. Belkaid, I. B. Copland, D. Massillon, and B. Annabi, "Silencing of the human microsomal glucose-6-phosphate translocase induces glioma cell death: potential new anticancer target for curcumin," *FEBS Letters*, vol. 580, no. 15, pp. 3746–3752, 2006.

[24] G. Bánhegyi, M. Csala, and A. Benedetti, "Hexose-6-phosphate dehydrogenase: linking endocrinology and metabolism in the endoplasmic reticulum," *Journal of Molecular Endocrinology*, vol. 42, no. 4, pp. 283–289, 2009.

[25] O. Kapuy, P. K. Vinod, J. Mandl, and G. B*l*nhegyi, "A cellular stress-directed bistable switch controls the crosstalk between autophagy and apoptosis," *Molecular Biosystems*, vol. 9, no. 2, pp. 296–306, 2013.

[26] A. Y. Choo and J. Blenis, "Not all substrates are treated equally Implications for mTOR, rapamycin-resistance and cancer therapy," *Cell Cycle*, vol. 8, no. 4, pp. 567–572, 2009.

[27] R. Nawroth, F. Stellwagen, W. A. Schulz et al., "S6k1 and 4E-BP1 are independent regulated and control cellular growth in bladder cancer," *PLoS ONE*, vol. 6, no. 11, Article ID e27509, 2011.